

Phenylacetylene oligomers as synthetic information molecules

by

Jonathan Swain
Clare College

Department of Chemistry
University of Cambridge

This dissertation is submitted for the degree of Doctor of Philosophy

March 2018

Phenylacetylene oligomers as synthetic information molecules

Summary:

Nucleic acids store genetic information in the sequence of nucleobases. Through duplex formation and template directed synthesis, the information stored in nucleic acids determines their three-dimensional structure and function. Nucleic acids are essential molecules for biological processes and have been used in nanotechnology. Modified nucleic acids have been synthesised that still form duplexes and can be tolerated by enzymes, suggesting that it is possible to construct a synthetic system comparable to nucleic acids, orthogonal to nucleic acids. This thesis describes the synthesis of a new class of synthetic information molecule, characterisation of the duplex forming properties, and attempts at templated oligomerisation reactions.

The new synthetic information molecule is based on the phenylacetylene oligomer framework developed by Moore and co-workers. Recognition was achieved via a base-pair that is made from a single point high affinity H-bond, with phenol as the H-bond donor (D) and phosphine oxide as the H-bond acceptor (A). The Sonogashira coupling was used to construct the phenylacetylene oligomer backbone.

The AA, DD and AD 2-mers were synthesised and complementary 2-mers showed cooperative duplex formation. No intramolecular H-bonding due to folding was observed in the AD mixed 2-mer. Longer oligomers were synthesised using a method of oligomerisation and chromatographic separation by reverse-phase preparatory HPLC. Homo-oligomers up to the 7-mer were isolated and binding studies between complementary all donor, all acceptor homo-oligomers showed increasing duplex stability with each additional recognition unit in the oligomer chain. Oligomers containing both acceptor and donor recognition modules in the same chain were synthesised and NMR dilution studies were used to investigate their ability to fold.

Preliminary experiments were carried out to evaluate the ability of these information molecules to template oligomerisation reactions, but when reactions were carried out at concentrations low enough for a significant template effect, no coupling reactions were observed.

Declaration

This dissertation is the result of my own work carried out at the University of Cambridge from October 2014 to February 2018 and includes nothing which is the outcome of work done in collaboration except as declared in the Preface and specified in the text.

It is not substantially the same as any that I have submitted, or, is being concurrently submitted for a degree or diploma or other qualification at the University of Cambridge or any other University or similar institution except as declared in the Preface and specified in the text. I further state that no substantial part of my dissertation has already been submitted, or, is being concurrently submitted for any such degree, diploma or other qualification at the University of Cambridge or any other University or similar institution except as declared in the Preface and specified in the text

It does not exceed the prescribed word limit for the relevant Degree Committee.

Jon Swain

Contents

Chapter 1 Introduction: Natural and synthetic information molecules	1
1.1 Natural information molecules	2
1.2 Synthetic modifications to nucleic acids	7
1.3 Information transfer via template reactions	13
1.3.1 Biological template polymerisation	14
1.3.2 Template ligation using oligonucleotides	15
1.4 Template polymerisation	20
1.5 Synthetic information molecules	22
1.6 Phenylacetylene oligomers	34
1.7 Conclusions	39
1.8 References	40
Chapter 2 Aims	47
Chapter 3 Modular design of an information molecule	51
3.1 Introduction	52
3.2 Design of system	54
3.2.1 Recognition groups	55
3.2.2 Backbone	56
3.2.3 Coupling chemistry	57
3.2.4 Solubility	58
3.3 Results and discussion	59
3.3.1 Synthesis of building blocks	59
3.3.2 Synthesis of 1-mer and 2-mer	60
3.3.3 NMR binding studies	62
3.3.3 Crystal structure of AD 2-mer	67
3.4 Conclusions	69
3.5 Experimental	70
3.5.1 Synthesis	70

3.5.2	Binding studies	96
3.5.3	X-ray crystal structure of 3.24	97
3.6	References	98
Chapter 4	Homo-oligomers	101
4.1	Introduction	102
4.2	Approach: Oligomer synthesis	103
4.3	Results and discussion	104
4.3.1	Synthesis of building blocks	104
4.3.2	Oligomer synthesis	106
4.3.3	Oligomer characterisation	110
4.3.4	NMR titration experiments	114
4.3.5	NMR denaturation experiments	115
4.4	Conclusions	127
4.5	Experimental	128
4.5.1	Synthesis	128
4.5.2	HPLC	148
4.5.3	Binding studies	150
4.6	References	153
Chapter 5	Mixed sequence oligomers	155
5.1	Introduction	156
5.2	Approach	157
5.3	Results and discussion	158
5.3.1	Oligomer synthesis	158
5.3.2	Oligomer characterisation	162
5.3.2	Binding studies	165
5.3.3	Crystal structure of DAD 3-mer	168
5.3.4	Modelling of DA _n D oligomers	169
5.4	Conclusions	171
5.5	Experimental	172
5.5.1	Synthesis	172
5.5.2	HPLC	184

5.5.3	Binding studies	186
5.5.4	X-ray crystal structure of 5.6	187
5.5.5	Molecular Mechanics	188
5.6	References	189
5.7	Acknowledgements	190
Chapter 6	Template oligomerisation	191
6.1	Introduction	192
6.2	Approach	196
6.3	Results and Discussion	198
6.3.1	Template reaction using mixed sequence oligomers	198
6.3.2	Template reaction using homo-oligomers	203
6.4	Conclusions	209
6.5	Experimental	210
6.5.1	Synthesis	210
6.6	References	216
Appendix	Fitting of NMR titrations, dilutions and denaturation experiments	217

Abbreviations

3D	Three dimensional
A	Adenine (when referring to DNA nucleobases)
A	Acceptor (when referring to H-bonding)
ATR	Attenuated Total Reflectance
<i>c</i>	Experimental concentration
C	Cytosine
CD	Circular dichroism
d	Doublet
D	Donor (when referring to H-bonding)
DCC	Dicyclohexylcarbodiimide
DMAP	N,N-dimethylaminopyridine
DMF	Dimethylformamide
DMSO	Dimethyl sulfoxide
DNA	Deoxyribonucleic acid
E. Coli	Escherichia coli
EDC	1-Ethyl-3-(3-dimethylaminopropyl)carbodiimide
EM	Effective molarity
FRET	Fluorescence resonance energy transfer
FT-IR	Fourier transform infrared spectroscopy
G	Guanine
GNA	Glycol Nucleic Acid
H-bond(ing)	Hydrogen bond(ing)
HPLC	High Performance Liquid Chromatography
HRMS	High Resolution Mass Spectrometry
<i>J</i>	J-coupling constant
<i>K</i>	Association constant
L	Ligand

LCMS	Liquid Chromatography and Mass Spectrometry
LNA	Locked nucleic acid
m	Multiplet
mRNA	Messenger RNA
MS	Mass spectrometry
NMR	Nuclear magnetic resonance
PCR	Polymerase chain reaction
Ph	Phenyl
PNA	Peptide nucleic acid
ppm	Parts per million
RNA	Ribonucleic acid
s	Singlet
T	Thymine
TBAF	Tetra- <i>n</i> -butylammonium fluoride
TEM	Transmission Electron Microscopy
TFA	Trifluoroacetic acid
THF	Tetrahydrofuran
TMS	Trimethylsilyl
TMSA	Trimethylsilyl acetylene
TNA	Threose nucleic acid
tRNA	Transfer RNA
U	Uracil
X-mer	An oligomer of X monomer units
•	Used to denote complex formation

Chapter 1

Introduction: Natural and synthetic information molecules

1.1 Natural information molecules

Information molecules are molecules that have the ability to encode information in their structure and communicate that information to other molecules. Nucleic acids are the only known information molecules and their structure was famously determined in 1953 by Watson and Crick.¹ Deoxyribonucleic acid (DNA) is a polymer that stores information in the sequence of monomer units, called nucleobases (**Figure 1.1a**). Each nucleobase contains a deoxyribose sugar, and these are joined to form a polymer by phosphodiester bonds. Attached to each nucleobase is a moiety called a nucleobase, one of adenine (A), thymine (T), guanine (G), or cytosine (C), each with a specific arrangement of H-bond donors and acceptors.²⁻⁴ The most energetically favourable interactions between nucleobases are when A pairs with T by forming two H-bonds, and G pairs with C forming three H-bonds (**Figure 1.1b**). This H-bonding specificity is important as it means a strand of DNA will selectively assemble with a strand containing a complementary sequence. Ribonucleic acid (RNA) is very similar to DNA with the deoxyribose replaced by ribose, and uracil (U) instead of thymine (T).

DNA forms a duplex with a double helix structure in aqueous media (**Figure 1.1c**). The double helix formation is driven by multiple factors: the hydrophobic effect of the non-polar bases in water, π-stacking between the aromatic nucleobases and minimisation of the repulsive electrostatic interactions between phosphate groups.^{5,6} The sequence specificity is down to the base pairing interactions.

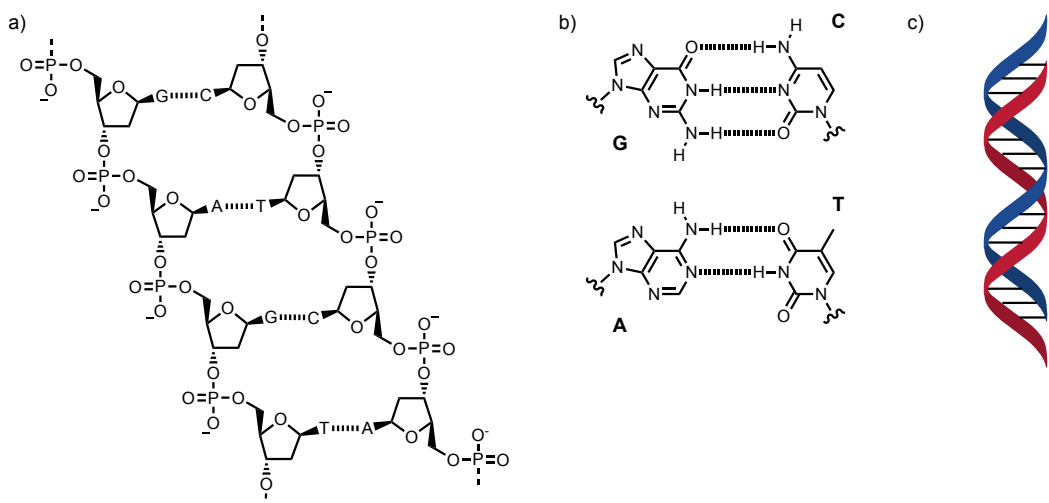
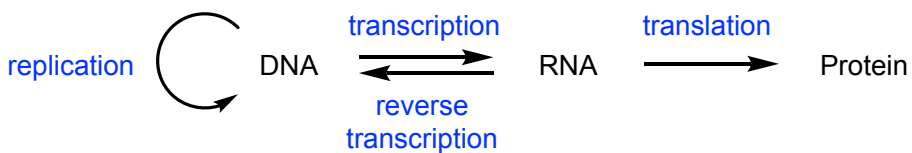


Figure 1.1: a) Detailed chemical structure of DNA forming a duplex, b) Watson-Crick base pairing between complementary nucleobases, c) Double helix formed by double stranded DNA.

The genetic information is stored in the sequence of monomers. During duplex formation the stored information is read, and the information can be copied by biological processes: replication, transcription and translation (**Scheme 1.1**).⁷ In DNA replication, a new molecule of DNA is synthesised that is identical to the original. In transcription, a molecule of RNA is synthesised that is complementary to a template DNA molecule, and in translation a polypeptide is synthesised with the sequence of amino acids determined by the sequence of nucleic acids. Information stored in the sequence of monomer units in DNA leads to the three-dimensional structure and function of DNA, RNA and the proteins synthesised. Therefore, the genetic information encoded in DNA is required for all biological processes and forms the basis of all life.



Scheme 1.1: The central dogma of molecular biology. Genetic information is copied to produce more DNA through DNA replication or to produce RNA through transcription. The information is read in translation to produce proteins. Reverse transcriptase enzymes can produce complementary DNA from an RNA template.

The sequence of monomer units (the primary structure) defines the pattern of H-bonds (the secondary structure) and three-dimensional shape (the tertiary structure) of single stranded DNA and RNA. RNA molecules have been discovered that are capable of catalysing biochemical reactions, these are known as ribozymes. Ribozymes can catalyse a variety of reactions, for example RNA polymerisation (**Figure 1.2**).⁸

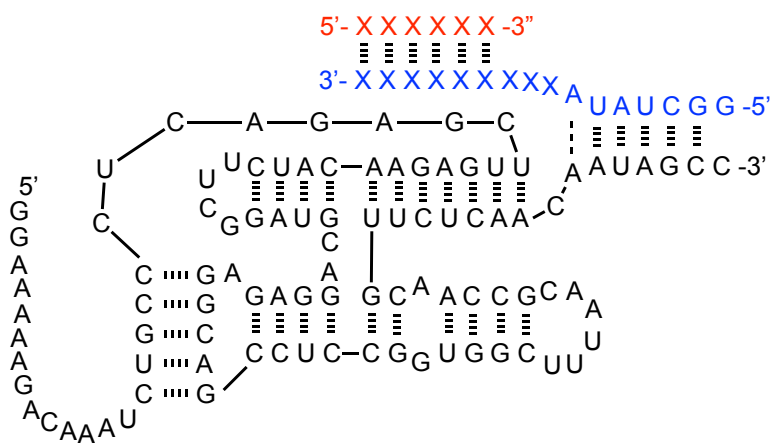


Figure 1.2: Secondary structure of a ribozyme (black) capable of promoting RNA polymerisation by extending an RNA primer (red) using nucleotide triphosphates and an appropriate RNA template (blue). The information encoded in the primary structure determines the secondary structure, tertiary structure, and function of the molecule.

Sequence selective duplex formation of DNA has led to its use as a programmable material for the designed assembly of nanoscale structures. The concept was first described by Seeman in 1982, who proposed using the molecular recognition properties of DNA to build molecular junctions and three-dimensional shapes.⁹ In 2006 Rothemund developed “DNA origami”, a method of producing nanoscale shapes from DNA.¹⁰ Structures were made from a 7,000 base pair “scaffold” DNA strand and multiple 200 base pair “staple” stands. The staple strands were complementary to sections of the scaffold strand and would induce the scaffold to fold into the desired shape. It is possible to predict the tertiary structure of a given sequence of nucleotides using computer aided design. This has allowed production of specific DNA structures,¹¹⁻¹⁶ as well as other functional DNA, such as nanomachines,¹⁶⁻²¹ and ion channels.²³

Yin and co-workers developed a method for construction of three-dimensional structures using short DNA strands called DNA bricks (**Figure 1.3**).²⁴ This modular design uses 32-mer oligonucleotide building blocks which can hybridise selectively with four neighbours using complementary sections of eight nucleotides. Blocks were used to construct specific shapes, which were characterised by transmission electron microscopy (TEM).

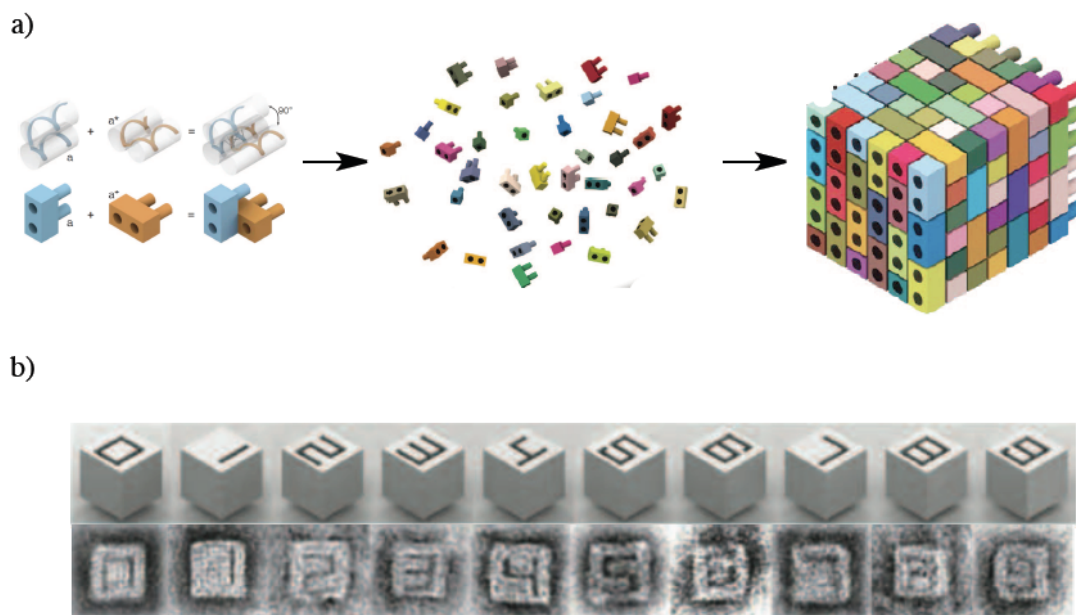


Figure 1.3: a) Short oligonucleotides with specific sequences assemble into 3D cuboids, b) Computer designed structures (top) compared with TEM images (bottom) for cuboids obtained through programmed assembly of DNA oligomers. Reprinted with permission from The American Association for the Advancement of Science.

Wang and co-workers reported a DNA walker, which moved along a track made of DNA (**Figure 1.4**).¹⁹ A bipedal walker containing two sections of single stranded DNA binds two DNA footholds in the track. The forward walking motion is activated by Hg^{2+} and H^+ , and the reverse walking motion is activated by cysteine and OH^- . The walking motion was observed by fluorescence resonance energy transfer (FRET), by labelling the footholds with fluorescent groups, and the walker with a quencher.

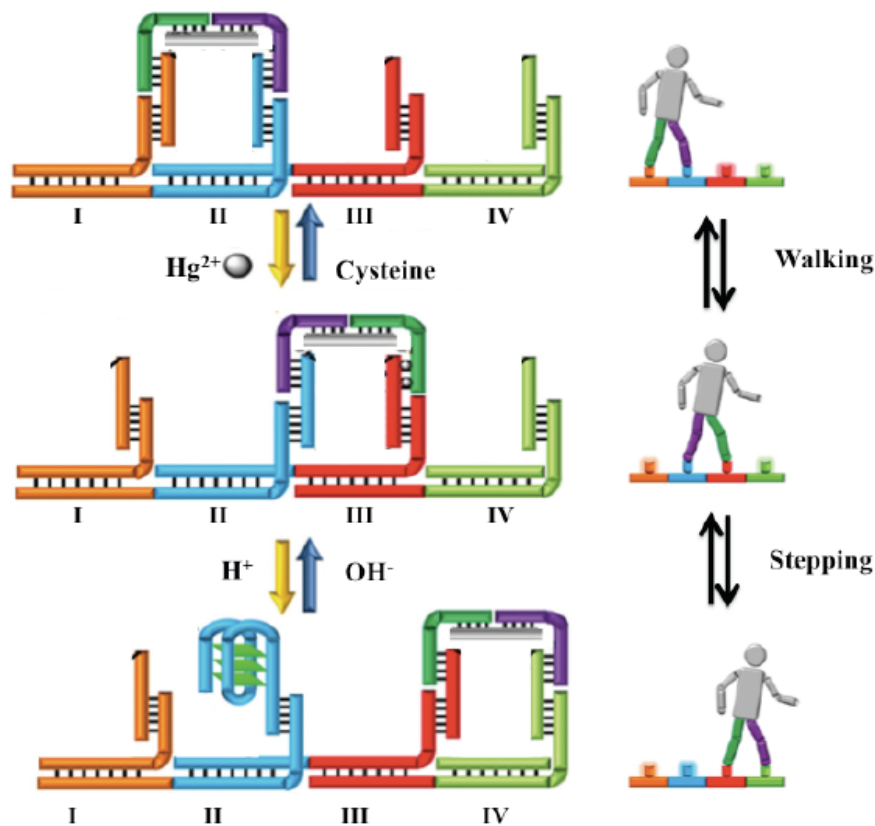


Figure 1.4: Schematic representation of a bipedal DNA walker along a track consisting of four DNA footholds. The walker consists of two DNA strands and the walking is triggered by $\text{Hg}^{2+}/\text{Cysteine}$ and H^+/OH^- . Reprinted with permission from Nano Letters.¹⁹ Copyright (2010) American Chemical Society.

DNA has been proposed as possible long-term data storage mechanism.²⁵ Due to its extremely high information density, it is predicted that it would only require 1 kg of DNA to satisfy current worldwide data storage requirements.²⁶ Erlich and Zielinski encoded 2.14×10^6 bytes of data in DNA, including a full computer operating system.²⁷

Nucleic acids have such a wide variety of functions and applications. Research into new information molecules would open the possibility of more useful molecules and more functions.

1.2 Synthetic modifications to nucleic acids

The ability of nucleic acids to store, read and copy information is not observed in any other natural molecules. The reason for this is not known and is an active area of research. Current research focuses on whether the structure of DNA evolved due to it being the only molecule capable of satisfying the requirements of a functional information molecule, or whether the structure was determined by the available building blocks during its evolution. If different building blocks were available, another information molecule may have evolved. To study if other molecules can perform the same functions as DNA, numerous examples of modified nucleic acids have been synthesised. These artificial genetic systems also offer the opportunity to study the relationship between nucleic acids and the origin of life. These modifications can be sorted into three groups, modification of the sugar, backbone coupling chemistry, and nucleobases.

The furanose ribose or deoxyribose in nucleic acids has been modified or replaced with different sugars to yield unnatural nucleic acids (**Figure 1.5**). Addition of a 2-methoxyethyl group to the 2' hydroxyl group in RNA (**Figure 1.5c**) was found to improve RNA affinity, showing higher thermal stability of 2-methoxyethyl RNA•RNA duplexes when compared to DNA•RNA duplexes.²⁸ In addition to this, increased nuclease resistance as well as a reduction in toxicity were observed, suggesting possible therapeutic use.²⁹ The furanose ribose was replaced with a pyranose ribose (**Figure 1.5d**) resulting in stronger base pairing and higher selectivity compared to DNA and RNA.³⁰ These pyranosyl-RNA molecules could be chemically replicated with retention of sequence information. Eschenmoser and co-workers developed threose nucleic acid (TNA) (**Figure 1.5e**). Threose is a simpler sugar to synthesise, leading to some to suggest it may have been a pre-RNA information molecule, on the evolutionary pathway to RNA.³¹ This hypothesis is supported by the fact TNA can form stable duplexes with both RNA and DNA, allowing information reading and transfer between information systems.³² TNA also forms stable duplexes by self-association, with a duplex structure closely resembling the A-form of RNA.³³ Polymerase enzymes can reverse transcribe TNA to DNA, and transcribe DNA information into

TNA.^{34–36} Coupled with PCR and *in vitro* selection this can be used to force Darwinian evolution of TNA, producing TNA aptamers that bind targets with high affinity and specificity.³⁷ Addition of a methylene link between the 2'-carbon and the 4'-oxygen in RNA produced the bicyclic “locked” nucleic acid (LNA) (**Figure 1.5f**).³⁸ The methylene bridge locks the sugar in a 3'-endo conformation, which is favourable for duplex formation, and leads to increased thermal stability when forming duplexes with DNA or RNA. A tricyclic nucleic acid was synthesised and again found to have increased thermal stability when forming duplexes with native DNA or RNA (**Figure 1.5g**).³⁹ DNA analogues using acyclic sugars have been made, such as glycol nucleic acid (GNA) (**Figure 1.5h**).^{40,41} Using enantiopure (*S*)- or (*R*)-glycidol, Meggers and co-workers synthesised a nucleic acid with a propylene glycol phosphodiester backbone. (*S*)-GNA•(*S*)-GNA and (*R*)-GNA•(*R*)-GNA duplexes exhibit similar thermal stabilities as native DNA and RNA duplexes, but (*S*)-GNA and (*R*)-GNA will not form duplexes with each other. GNA will not form duplexes with DNA, and can only form duplexes with RNA if the sequence has a low CG content.⁴²

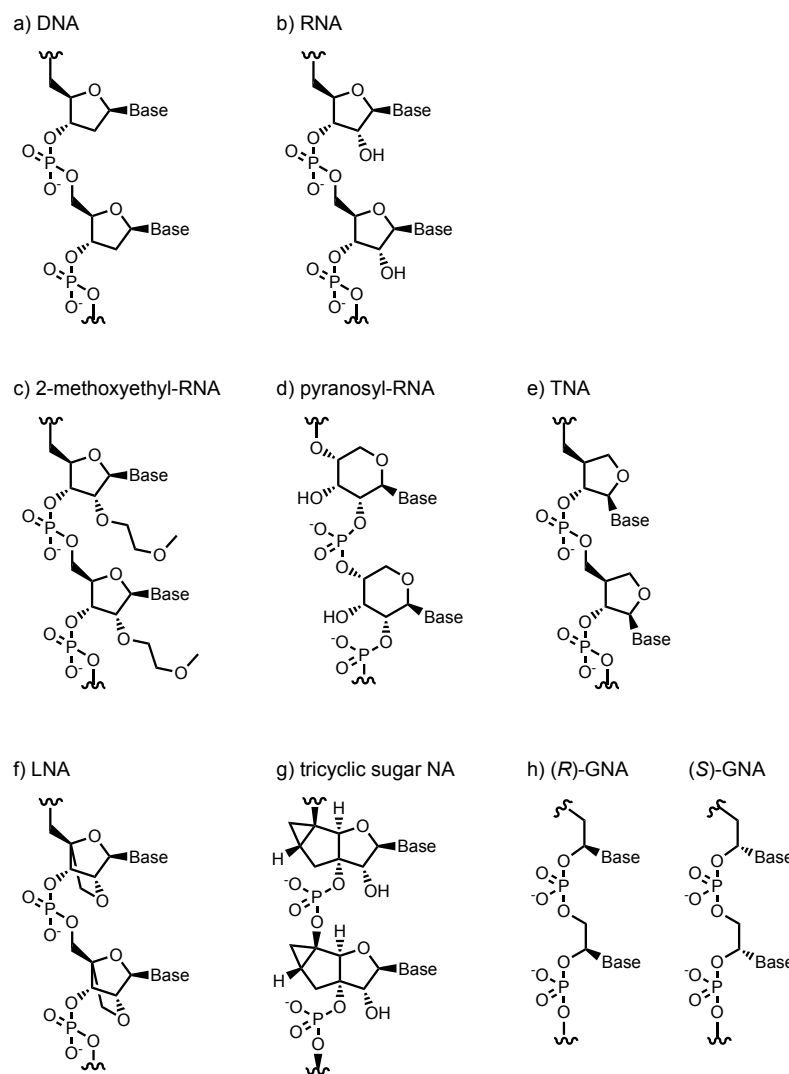


Figure 1.5: Natural nucleic acids (a, b) and synthetic nucleic acids with modified sugars (c-h).

Modification of the phosphate groups or entire backbone has been completed to produce synthetic nucleic acid systems (**Figure 1.6**). Modification of the phosphodiester linkage to a phosphoramide linkage produced a new class of nucleic acids (**Figure 1.6a**) capable of forming stable duplexes with themselves, DNA, and RNA.⁴³ Replacement with an amide linkage produced an uncharged nucleic acid (**Figure 1.6b**) which formed duplexes with RNA with higher thermal stability than the corresponding RNA•RNA duplex.⁴⁴ When the phosphodiester linkage was replaced with an uncharged sulfone group (**Figure 1.6c**), the lack of repulsion between charged groups in the backbone lead to collapse of chains longer than seven units.^{45,46} Triazole-linked nucleic acids (**Figure 1.6d**) were synthesised and found to form stable duplexes with complementary strands of

DNA.⁴⁷ Nielson and co-workers replaced the sugar phosphate backbone of DNA with a peptide-linked backbone, known as peptide nucleic acid (PNA) (**Figure 1.6e**).⁴⁸ PNA forms duplexes with itself that closely resemble DNA double helices, as well as forming stable duplexes with DNA and RNA.⁴⁹ The duplexes formed have higher thermal stability than native nucleic acid duplexes due to the lack of repulsion between charged groups in the backbone.^{50,51} PNA•DNA duplexes are more destabilised by a base pair mismatch than native DNA duplexes, showing greater sequence specificity. PNA is resistant to enzyme action and stable over a wide pH range, leading to uses in molecular biology, diagnostic assays and therapeutic uses.⁵² Due to its simplicity and spontaneous polymerisation at 100 °C it has been suggested that PNA was an early nucleic acid in the evolution of life.^{53,54} This hypothesis is supported by the fact that some cyanobacteria produce the backbone for PNA.^{55,56} The structure of PNA can tolerate some modifications without loss of function, such as thioester PNA (**Figure 1.6f**).⁵⁷

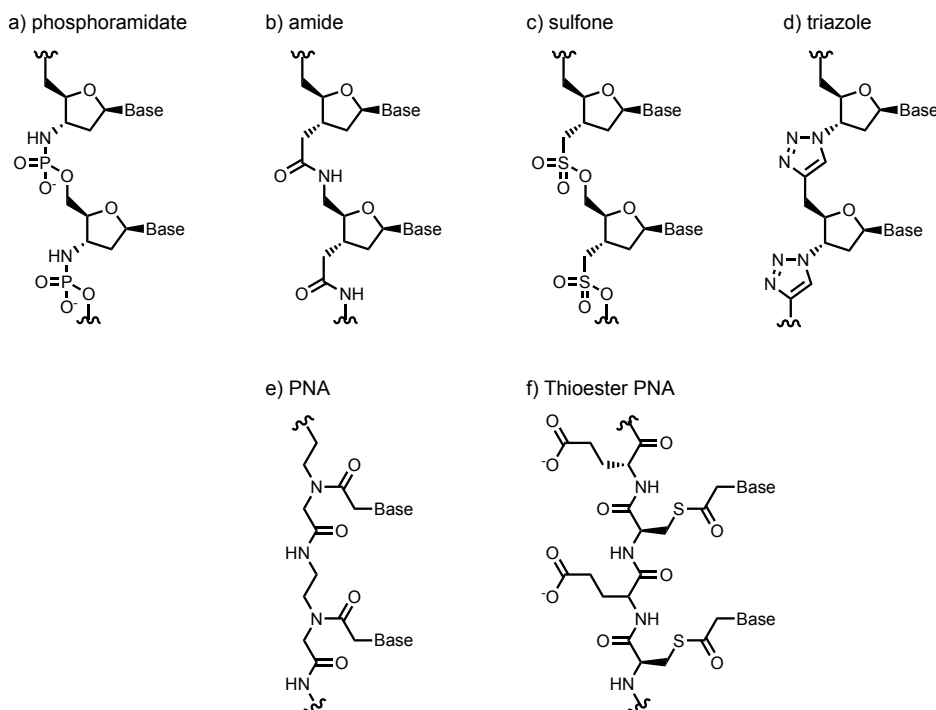


Figure 1.6: Synthetic nucleic acids with modified backbone coupling chemistry.

Modification of the nucleobases has yielded an expanded genetic alphabet, going beyond the natural A-T and G-C base pairs (**Figure 1.7**). Benner and co-workers reported the synthesis and enzymatic incorporation in both RNA and

DNA of two new nucleotides, bearing isoC and isoG nucleobases (**Figure 1.7a**).⁵⁸ Further bases K and X (**Figure 1.7b**) were synthesised which were again incorporated into RNA and DNA by enzyme action, leading to RNAs with greater diversity in structure and potential catalytic activity.⁵⁹ In 2006 Benner and co-workers developed two new nucleotides Z and P to add to the expanded genetic alphabet (**Figure 1.7c**).⁶⁰ The GACTZP library of oligonucleotides was used in *in vitro* evolution experiments to produce aptamers that bind liver cancer cells with high selectivity.⁶¹ Kool and co-workers developed a new genetic alphabet that has the nucleotides replaced by larger bases through the addition of a benzene ring, expanding the nucleobases by 2.4 Å (**Figure 1.7d-e**).⁶² The helices formed are more thermodynamically stable than native DNA, due to enhanced base stacking. Replication of these nucleic acids has been completed enzymatically in *E. Coli* cells.⁶³ Addition of a benzene ring to only the adenosine nucleobases still formed duplexes with T containing oligonucleotides, showing that different binding geometries can be tolerated (**Figure 1.7f**).⁶⁴ Inouye and co-workers synthesised artificial DNA replacing the natural nucleobases. The nucleobases used were inspired by natural bases and attached by acetylene bonds to the sugar phosphate backbone (**Figure 1.7g**).⁶⁵ These molecules form sequence selective duplexes with complementary DNA with thermal stabilities similar to natural duplexes. Matsuda and co-workers synthesised a set of nucleobases capable of forming four H-bonds (**Figure 1.7h**), which formed extremely strong duplexes.⁶⁶ Kool and co-workers also replaced nucleobases with a range of non-polar groups (**Figure 1.7i**).⁶⁷ When incorporated into DNA molecules they can act as reporter molecules with potential uses in biology and biochemical applications.⁶⁸

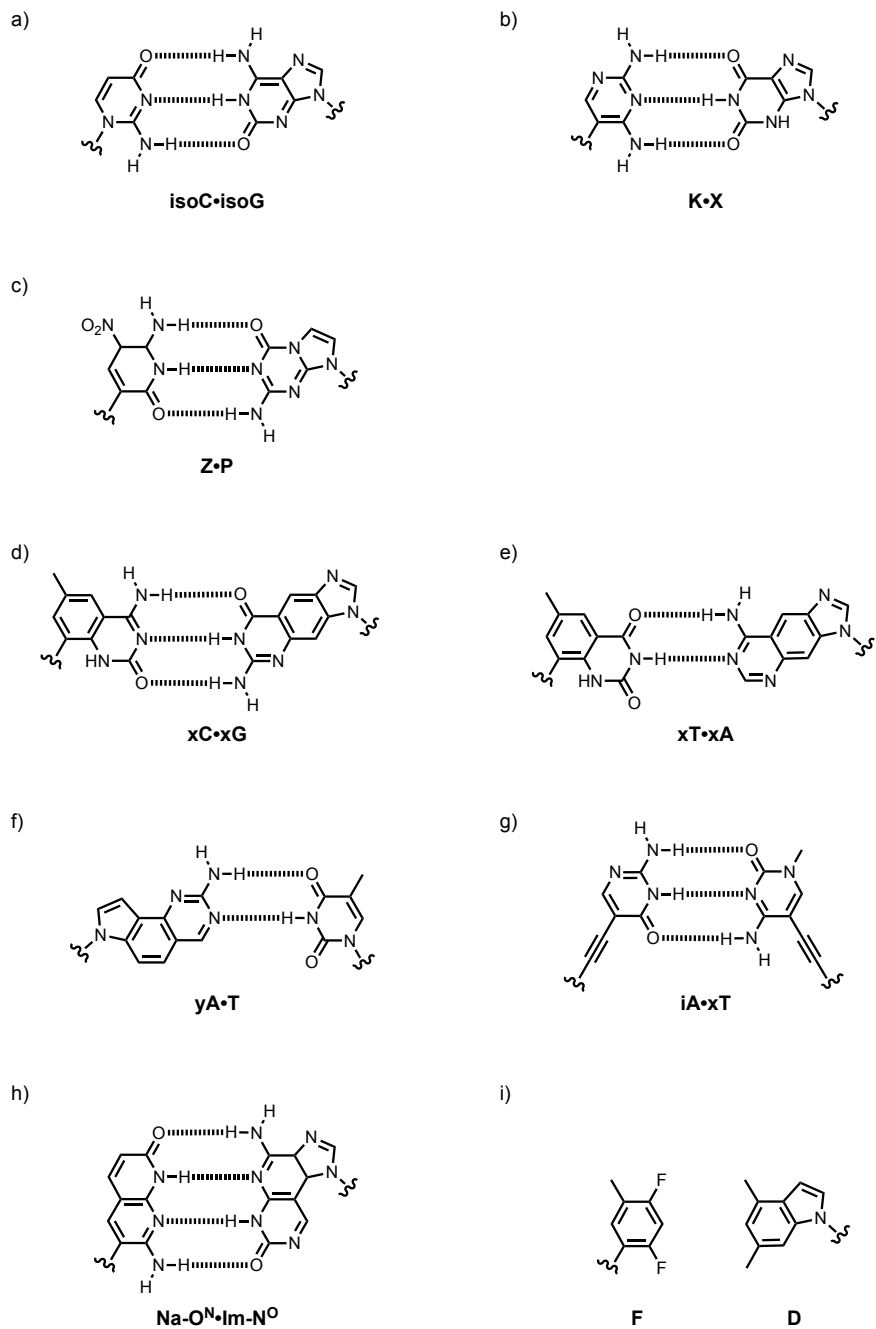


Figure 1.7: Synthetic nucleic acids with modified nucleobases.

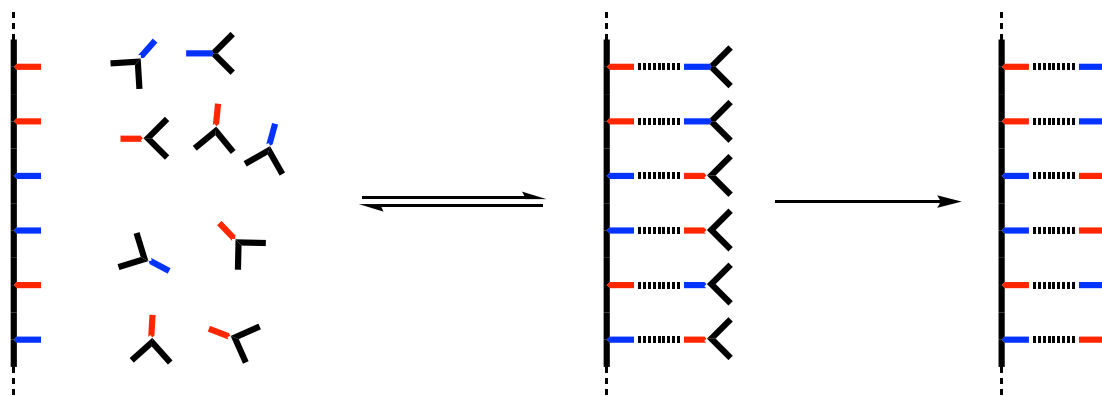
It has been shown that modifications to the structure of DNA are tolerated and can result in new molecules that retain some of the functions of DNA, suggesting that the structure of DNA is not required for its key properties.

1.3 Information transfer via template reactions

Template reactions are widely used for production of information molecules in nature. Template synthesis utilises non-covalent interactions to change the reaction rate or distribution of products of a covalent chemical reaction. Synthesis of a polymer by template synthesis (template polymerisation) utilises interactions between a pre-formed macromolecule (the template) and a growing polymer chain (daughter polymer). The interactions can affect the structure of the product formed, and the kinetics of the process.⁶⁹ Template polymerisation is observed in biological synthesis of macromolecules such as nucleic acids and polypeptides. Templated reactions can achieve high selectivity and efficiency, making them a useful synthetic technique. Templates can have a range of effects:

1. A kinetic effect, an enhancement in reaction rate (in this case the template's role is a catalyst).
2. A molecular weight distribution effect, influencing the molecular weight of the product and polydispersity.
3. A sequence distribution effect, defining the sequence of monomer units in the daughter polymer (important in biological processes).

A simplified description of template polymerisation is shown in **Scheme 1.2**. A polymer template bearing either acceptor (red) or donor (blue) recognition sites is mixed in solution with monomer units also bearing one of the recognition sites. Through specific non-covalent interactions, the monomer units align with the template, leaving covalent reaction sites exposed. Through enzymatic or chemical coupling reactions, the monomer units react forming a new daughter polymer with complementary sequence to the template.



Scheme 1.2: Schematic representation of template polymerisation. Monomers align via non-covalent interactions with the template, followed by chemical or enzymatic covalent reactions to form the backbone.

1.3.1 Biological template polymerisation

Template polymerisation is used for natural synthesis of biological macromolecules, and it therefore essential to all life. **Figure 1.8** shows a simple representation of the biological template synthesis used in a) DNA replication and b) translation.

In DNA replication (**Figure 1.8a**) a DNA duplex is separated into two molecules of DNA by the action of helicase enzymes.⁷⁰ Free DNA nucleotide triphosphates align with the exposed nucleobases and through the action of DNA polymerase enzymes two new duplexes are produced that are identical to the original DNA duplex. DNA is used to template the formation of RNA in an analogous process. After separation of the DNA duplex, RNA nucleotide triphosphates align with one strand of DNA (the non-coding strand) and RNA polymerase enzymes catalyse the production of a molecule of RNA that is identical in sequence to the coding strand (with thymine replaced by uracil). Messenger RNA (mRNA) strands can be used to template the formation of polypeptides (**Figure 1.8b**). Transfer RNA (tRNA) bearing three exposed nucleobases (known as an anti-codon) can bind to the mRNA at a sequence complementary to the anti-codon (a codon). Attached to the tRNA is an amino acid, which can react with the growing polypeptide chain attached to the previous tRNA, increasing the polypeptide by one amino acid. The sequence of amino acids in the polypeptide

determines its function and is coded for in the sequence of nucleotides in the mRNA. The sequence of monomer units in the RNA was encoded for by the genetic information stored in the DNA.

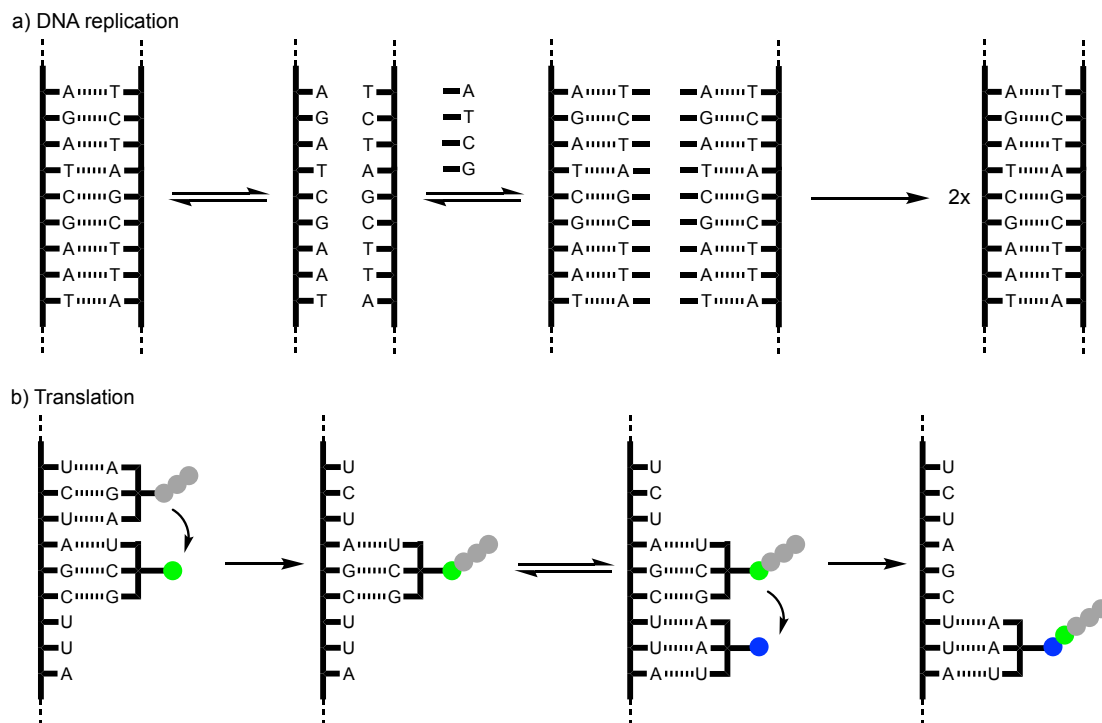
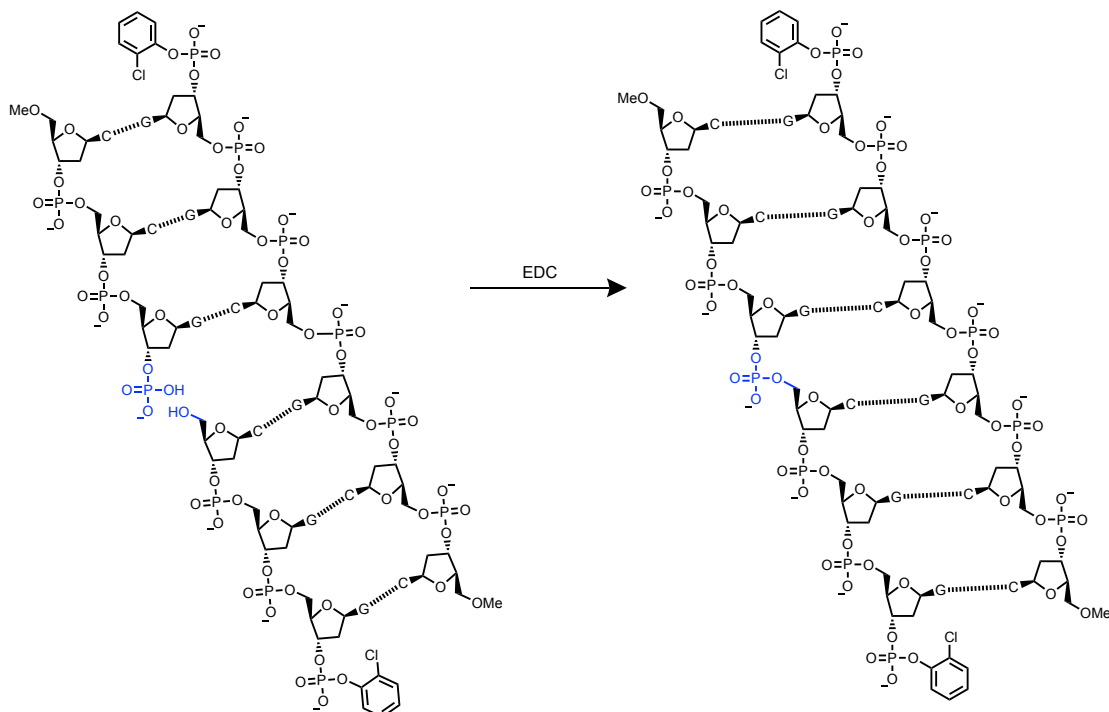


Figure 1.8: Schematic representation of biological enzyme-catalysed template synthesis. a) DNA replication producing two identical DNA duplexes from the template, b) Translation, producing a polypeptide from mRNA and tRNA.

1.3.2 Template ligation using oligonucleotides

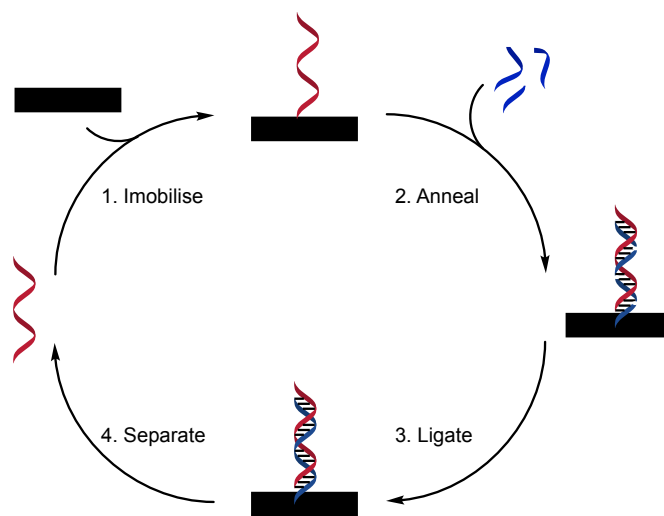
Nucleic acids have been used as templates for synthesising a range natural and non-natural nucleic acids.⁷¹ Non-enzymatic template synthesis of oligonucleotides was first reported by Naylor and Gilham in 1966.⁷² Using a poly A nucleotide, they were able to template the reaction between two poly T hexanucleotides to synthesise the dodecanucleotide. In 1986 von Kiedrowski developed the first non-enzymatic self-replicating molecule (**Scheme 1.3**).⁷³ A 5'-CCGCGG-3' hexanucleotide was used to complete a condensation reaction between two trinucleotides (5'-CCG-3' and 5'-CGG-3') each complementary to half of the template hexanucleotide. Using a 1-(3-dimethylaminopropyl)-3-ethylcarbodiimide (EDC) coupling replicated the template in 12% yield.

Autocatalysis of the condensation reaction was observed, but the effect was small due to the high stability of the duplex produced.



Scheme 1.3: Synthetic DNA replication using EDC mediated condensation, replicating a hexanucleotide template from trinucleotides complementary to the template.

To remove the problem of product inhibition due to the stability of the duplex formed, Von Kiedrowski and co-workers used an iterative, stepwise process (**Scheme 1.4**).⁷⁴ Two complementary 14-mer oligonucleotides were immobilised to a solid support using disulphide exchange reactions, and complementary fragments of each sequence were hybridised to the immobilised oligonucleotides. The fragments had 5'-NH modifications which were used for ligation using EDC. Denaturation and cleavage from the solid support using sodium hydroxide yielded free oligonucleotides on which the cycle could be repeated. The process was called Surface Promoted Replication and Exponential Amplification of DNA analogues (SPREAD) and is very similar to the enzymatic process used in the Polymerase Chain Reaction (PCR).



Scheme 1.4: General scheme of SPREAD. 1. Template is immobilised to a solid support. 2. Template binds complementary fragments from solution. 3. Fragments are linked by chemical ligation. 4. Copy is released by thermal denaturation; this copy is immobilised and the cycled repeated.

Lynn and co-workers used a DNA hexanucleotide to template the reaction between two trinucleotides modified with reductive amination capable functional groups (**Figure 1.9a**).⁷⁵ Eschenmoser and co-workers studied condensation reactions between TNA oligonucleotides using a TNA template, and found that replacement of adenine with 2,6-diaminopurine, an unnatural nucleobase, resulted in an increase in duplex stability and template effect (**Figure 1.9b**).⁷⁶ Nielson and Orgel have shown that it is possible to use RNA nucleotides to template the synthesis of complementary PNA strands and vice-versa, translating sequences between different systems without loss of information (**Figure 1.9c**).⁷⁷ With a RNA oligo-C 10-mer as a template, they reacted five PNA G 2-mers to synthesise the complementary strand.

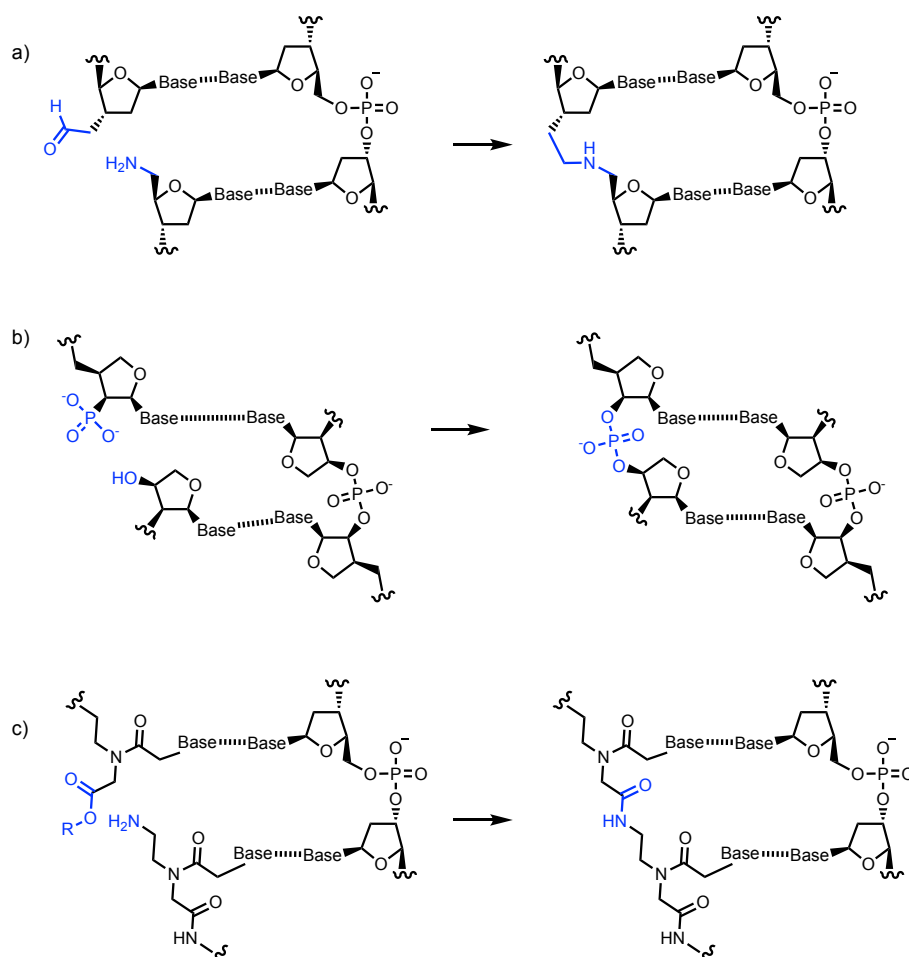


Figure 1.9: Ligation reactions using nucleic acids as a template: a) reductive amination using DNA as a template, b) phosphodiester formation using TNA template, c) ligation of PNA using a DNA template.

Tavasoli and co-workers used the supramolecular assembly of 5'-azide, 3'-alkyne oligonucleotides to synthesise the 335 base gene for the green fluorescent protein iLOV by click-ligation, which was then replicated by polymerases in vitro and encoded for a functional protein in E. Coli (**Figure 1.10**).⁷⁸ Synthesis of long oligonucleotides is problematic due to high error rates and low yields. This method utilises ten short, modified oligonucleotides with complementary sections to form a supramolecular assembly resembling the DNA duplex of the iLOV gene. Reaction of the 5'-azide and 3'-alkyne end groups using a copper-catalysed azide-alkyne cycloaddition produced the ligated gene. The chemical “scar” formed at the ligation site (in place of a phosphodiester bond) is tolerated by enzymes and did not significantly perturb the DNA helix formed.

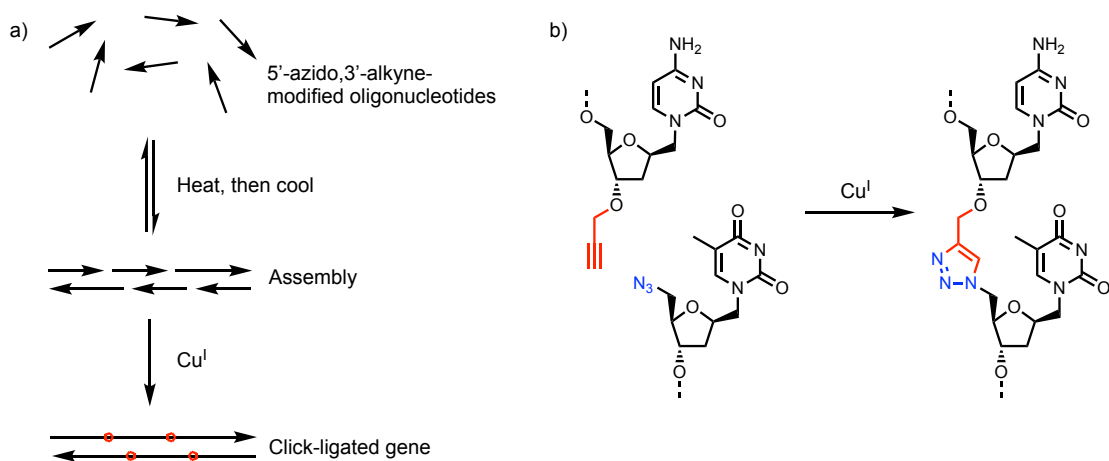


Figure 1.10: One-pot gene synthesis by click-DNA ligation. a) Schematic representation of a one-pot click-ligation strategy, b) Copper catalysed click-reaction between a 3'-alkyne and 5'-azido modified oligonucleotides forming a 1,4-linked 1,2,3-triazole linked oligonucleotide.

1.4 Template polymerisation

Template polymerisation is widely used in materials chemistry. Non-covalent interactions are used to increase rate (a kinetic effect) or to influence the molecular weight and polydispersity of the product (product distribution effects). No sequence information is copied in these reactions. The non-covalent interactions used are H-bonding or electrostatics.^{79,80} The coupling chemistry used is largely radical chemistry (**Figure 1.11a**), although there are other examples such as ring-opening metathesis polymerisation (ROMP).^{69,81} The most studied example is the polymerisation of acrylic acid or methylacrylic acid, with a variety of templates used. **Figure 1.11b** shows the polymerisation of acrylic or methylacrylic acid in the presence of polyvinylpyrrolidone which is acting as a H-bonding template.⁷⁹ The addition of a template lead to an increase in reaction rate, and the extent of this increase was determined by the pH, through the extent of deprotonation.

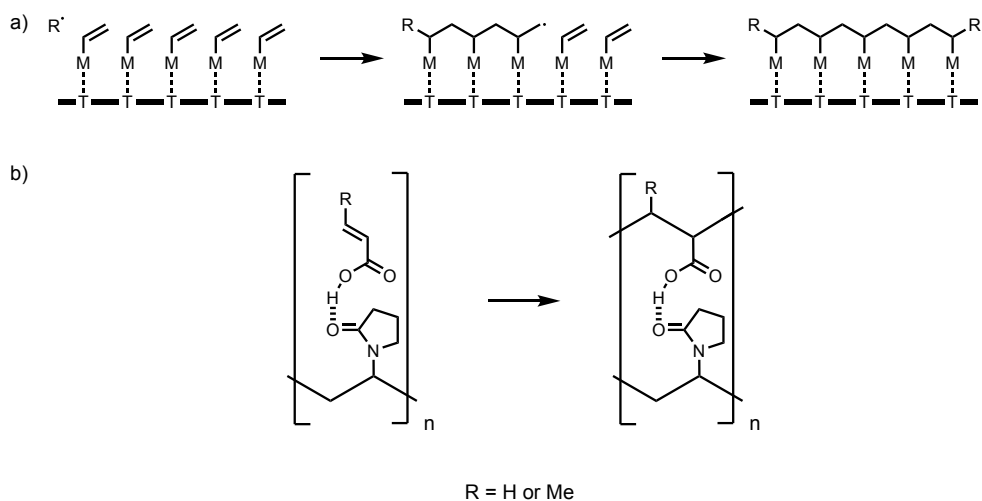
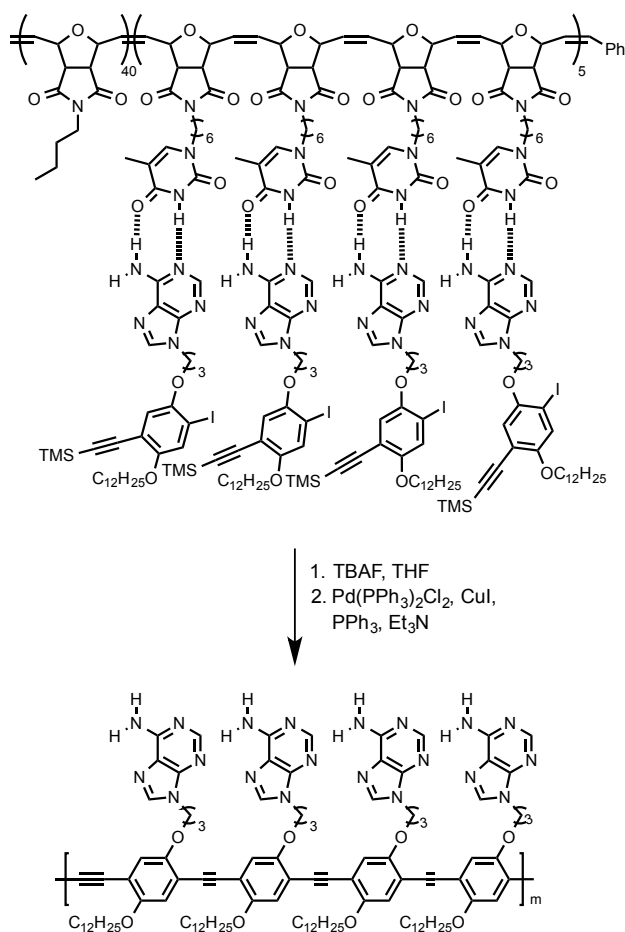


Figure 1.11: a) Schematic representation of template radical polymerisation, b) Template radical polymerisation of acrylic or methylacrylic acid with polyvinylpyrrolidone as a H-bonding template.

Nucleic acid analogues have been used in template polymerisation.^{71,82,83} Sleiman and co-workers synthesised a template of narrow molecular weight distribution using ROMP (**Scheme 1.5**). This template contained thymine nucleotides which were used to align complementary adenine-containing

monomers through H-bonding interactions.⁸⁴ A Sonogashira polymerisation lead to templated synthesis of a conjugated polymer, which had a narrow molecular weight distribution and a chain length similar to the template. When the same reaction was completed without the template, the degree of polymerisation was much lower, and the molecular weight distribution was considerably higher than the templated polymerisation.



Scheme 1.5: Template polymerisation using Sonogashira coupling chemistry and nucleobase pairing between monomer units and the template.

1.5 Synthetic information molecules

Many groups have attempted to synthesize chemical systems capable of storing and reading information. Gong and co-workers developed a class of fully programmable information storing oligomers.⁸⁵ Using a convergent and sequence selective synthesis, they produced a series of oligomers with aromatic amide backbones, with the information stored in the sequence of H-bond acceptors (A) and H-bond donors (D). Adjustment of the configuration of amide groups defined the sequence in 2-mer units (AA, AD or DD) (**Figure 1.12a**). The structure is stabilized by intramolecular H-bonds between N-alkylbenzamide groups and phenoxyalkyl groups, as well as steric effects of bulky solubilizing groups. Using amide coupling and specific building blocks the sequence of H-bonding groups on the oligomers could be controlled (**Figure 1.12b**).

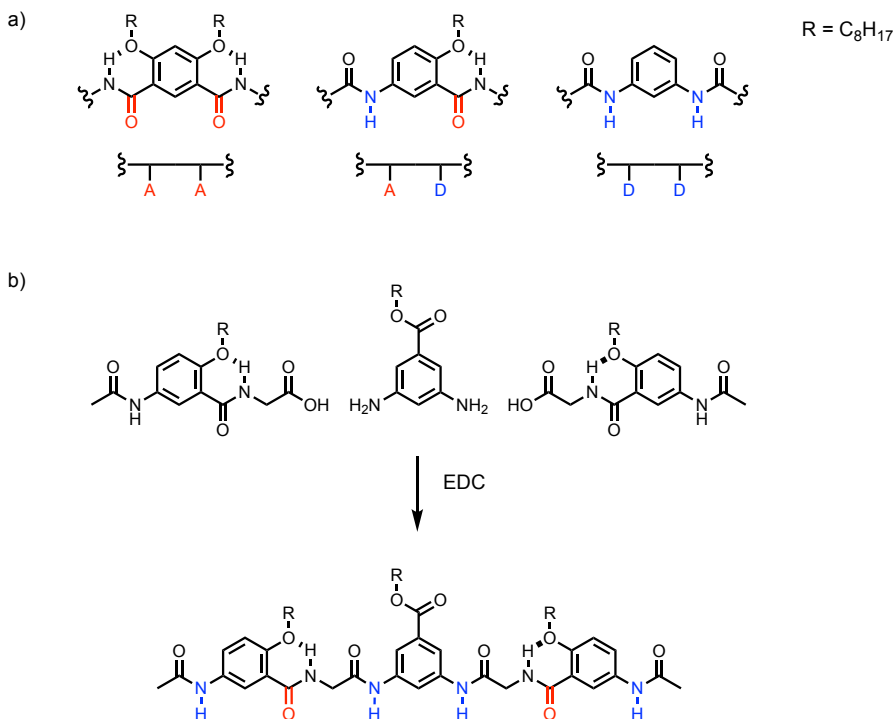


Figure 1.12: a) Different amide configurations leads to AA, AD and DD units for oligomer synthesis, b) example of coupling reaction to produce DADDAD 6-mer. A represents a H-bond acceptor (red), D represents a H-bond donor (blue).

Oligomers of the system (2-mers, 4-mers and 6-mers) of different sequences were synthesised (**Figure 1.13**).⁸⁶ These oligomers were found to form

duplexes in chloroform. The association constants for duplex formation were measured by ^1H NMR titrations and isothermal titration calorimetry. An increase in association constant from 25 M^{-1} for the 2-mer to greater than 10^9 M^{-1} for the 6-mer at 25°C shows cooperative duplex formation, and stability was found to be independent of sequence.

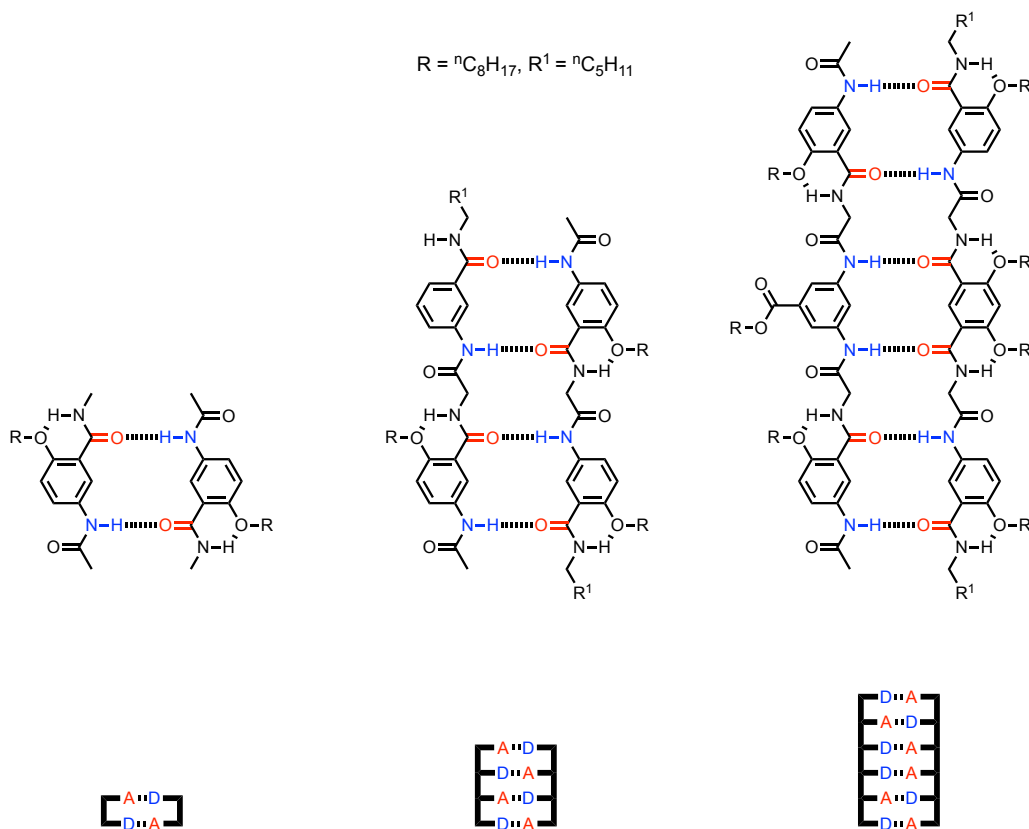


Figure 1.13: 2-mer, 4-mer and 6-mer H-bonded duplexes.

Duplexes were formed with a mismatch in sequence at one site (**Figure 1.14**), either acceptor to acceptor, or donor to donor.⁸⁷ Addition of the correct sequence easily displaced the mismatched oligomer. Isothermal titration calorimetry in chloroform and 5% DMSO indicated that the mismatched duplexes were 40 times less stable than the corresponding matched duplexes.

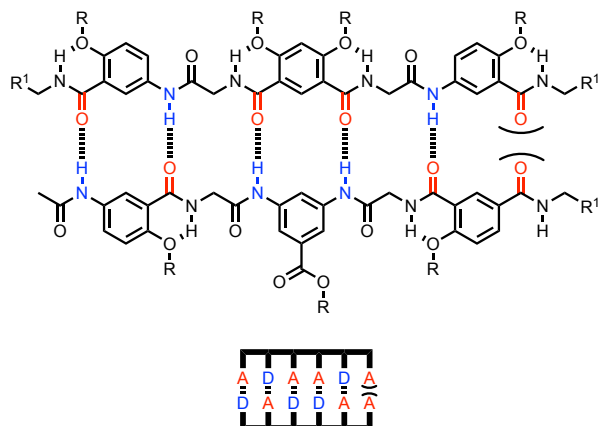
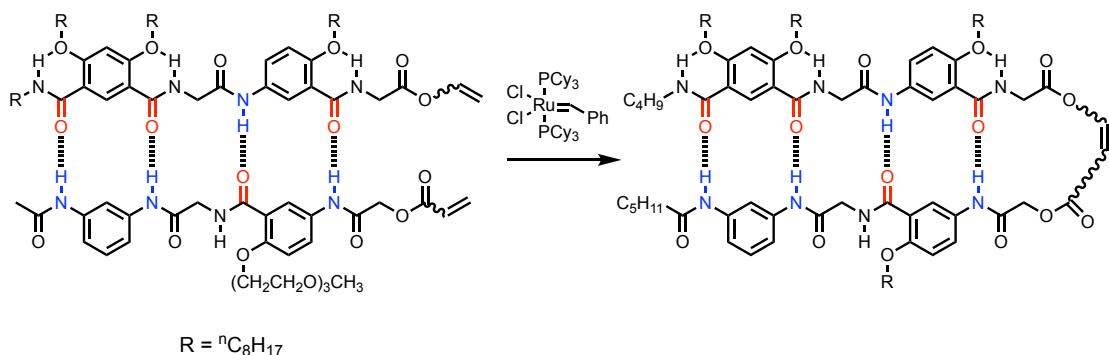


Figure 1.14: Sequence mismatched duplexes were found to have significantly lower association constants than analogous matched duplexes.

The sequence specificity of these duplexes could be exploited to direct chemical reactions (**Scheme 1.5**).⁸⁸ Alkenes attached to the same end of a duplex template should be brought into close proximity upon duplex formation in solution. This greatly increased the effective molarity of the alkenes and allowed metathesis using Grubbs' catalyst, trapping the duplex. The alkene formed could be removed by hydrolysis. High selectivity was observed, with no cross-metathesis products observed. If the sequence of one oligomer was reversed to hold the alkenes apart, no reaction was observed.



Scheme 1.5: Trapping of 4-mer duplex using alkene metathesis.

Yashima and co-workers synthesised a class of crescent-shaped *m*-terphenyl derivatives that form intertwined supramolecular complexes held together with charge-assisted H-bonding between carboxylate and amidinium

groups (**Figure 1.15**). Chiral groups added to the amidinium groups allowed control of the chirality of the helices formed.^{89,90}

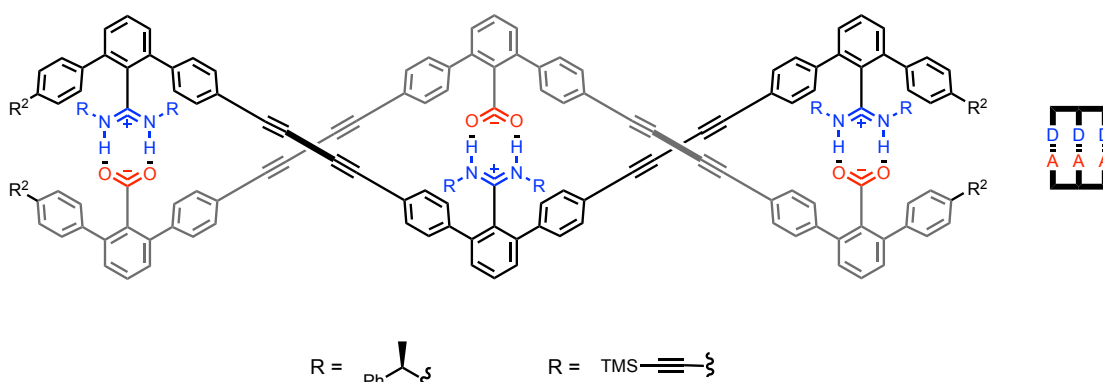


Figure 1.15: 3-mer salt bridge bonded heteroduplex formed of oligomers developed by Yashima and co-workers.

Oligomers of two, three or four *m*-terphenyl groups linked by diacetylene groups were synthesised using sequential TBAF deprotection and Glaser coupling (**Figure 1.16a**).⁹⁰ TBAF mediated deprotection of 1-mers and oligomers yielded a statistical mixture of starting material, mono-deprotected products and di-deprotected products, which were separated by flash chromatography. All possible sequences for 2-mers (DD, DA, AA) and 3-mers (DDD, DDA, DAD, AAD, ADA, AAA) were synthesised in addition to the homo-4-mers (DDDD, AAAA). The duplexes formed by complementary pairs were characterized by circular dichroism (CD) and ¹H NMR. The duplexes formed are stable under high performance liquid chromatography (HPLC) analysis allowing characterization by retention time matching. When the 2-mer species were mixed in CDCl₃, the CD and ¹H NMR spectra quickly changed to the summation of the individual helices spectra, suggesting self-sorting lead to the formation of only the complementary helices (**Figure 1.16b**). The same result was observed for a mixture of the 3-mers, and these were separated by HPLC to confirm the results. A mixture of the 1-mers and homo-oligomers (DD, AA, DDD, AAA, DDDD, AAAA) in CDCl₃ also quickly self-sorted into the complementary pairs, showing chain-length specificity in addition to the sequence-specificity already observed (**Figure 1.16c**).

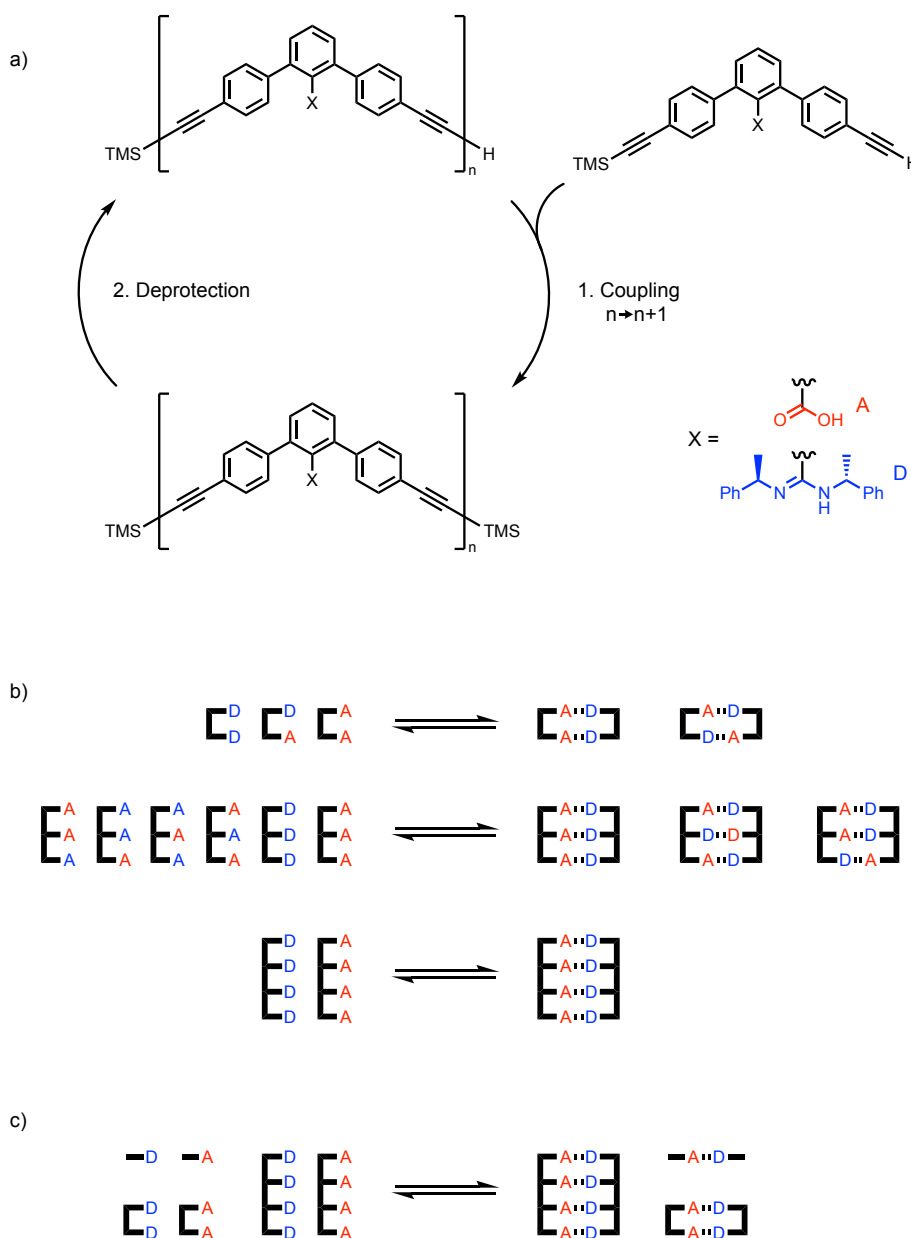
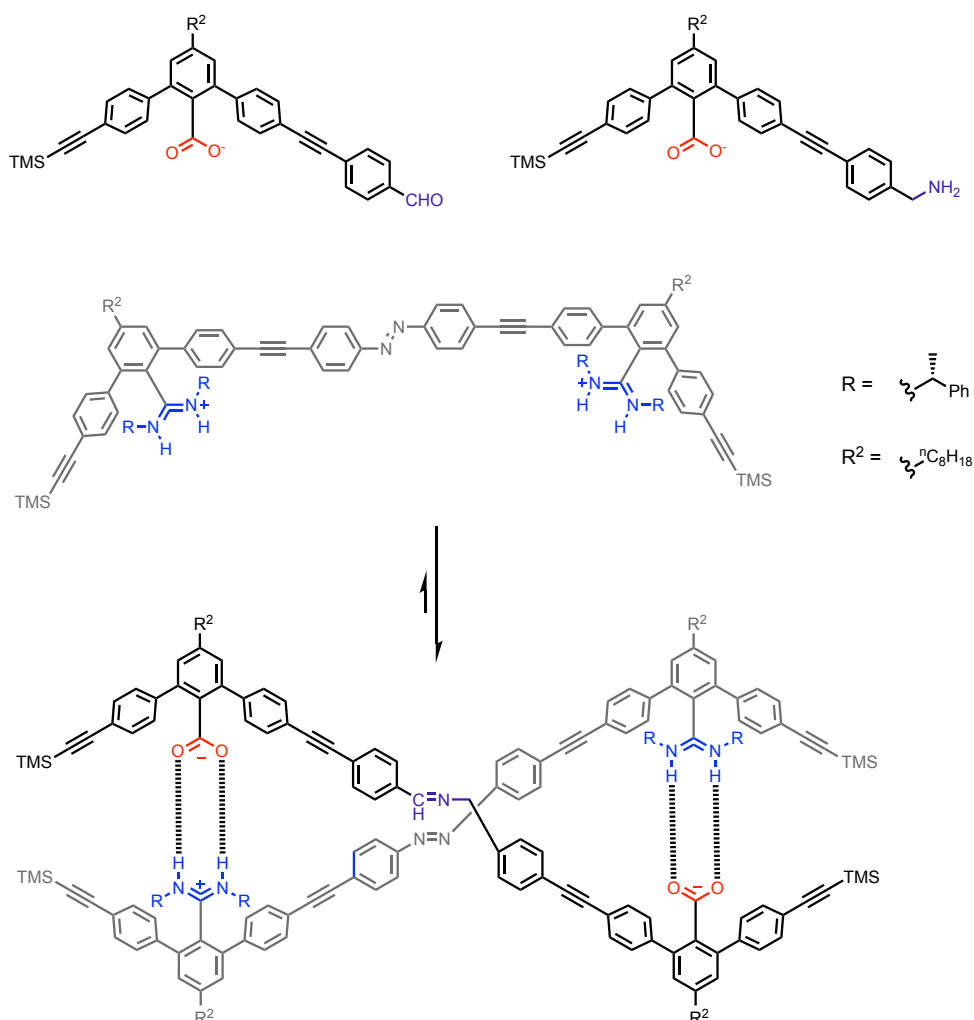


Figure 1.16: a) Synthesis of salt bridge oligomers with sequence and length control by sequential coupling and deprotection reactions (1) $\text{PdCl}_2(\text{PPh}_3)_2$, CuI , Et_3N , chloroform (2) TBAF , THF.

b and c) Sorting experiments showing duplex formation was length and sequence specific.

The reaction of two carboxylate 1-mers with either amino or formyl groups at one end was completed with and without a complementary amidinium 2-mer (**Scheme 1.6**).⁹¹ The reaction was carried out in benzene and monitored by ^1H NMR and CD over 72 hours. Addition of the template was found to increase

reaction rate by a factor of six. These oligomers were also found to have further uses as chiral catalysts.^{92,93}



Scheme 1.6: Template synthesis of a 2-mer using complementary 1-mers bearing aldehyde and amine functional groups.

Hunter and co-workers developed a poly-aniline information molecule with a modular design (**Figure 1.17**).⁹⁴ Information could be stored in the sequence of H-bonding recognition groups. Recognition sites at the aniline nitrogen were either H-bond donor (phenol), or H-bond acceptor (pyridine, pyridine N-oxide or phosphine oxide). These oligomers were designed to be soluble in organic solvents. Homo-sequence oligomers from 2-mers to 4-mers were synthesised with each of the three recognition groups using reductive amination as the coupling chemistry (**Figure 1.17b**).

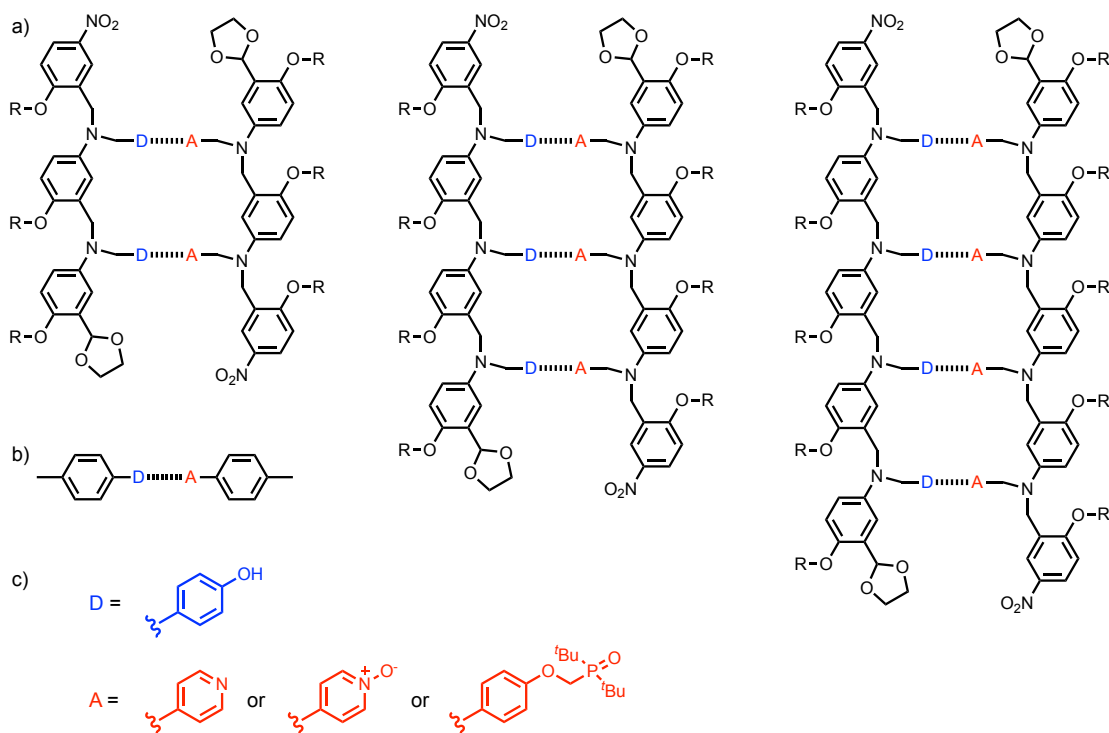


Figure 1.17: Duplexes formed by 2-mers, 3-mers and 4-mers. These were titrated along with representative a 1-mer system (b).

The association constants for duplex formation between complementary oligomers (K) were measured by NMR titration. All three combinations of donors and acceptors formed stable duplexes in toluene- d_8 . The stability of the 1:1 duplex formed increased with the number of recognition modules showing cooperative duplex formation, where the formation of the initial H-bond assists in the formation of further H-bonds (Figure 1.18). The effective molarity (EM) was found to increase with decreasing flexibility in the geometry of backbone between the H-bonding interactions and the recognition modules: 14 mM for the phosphine oxides, 40 mM pyridine N-oxides, and 80 mM for the pyridines. The H-bond formed between the pyridine and phenol was the weakest leading to the lowest association constants.

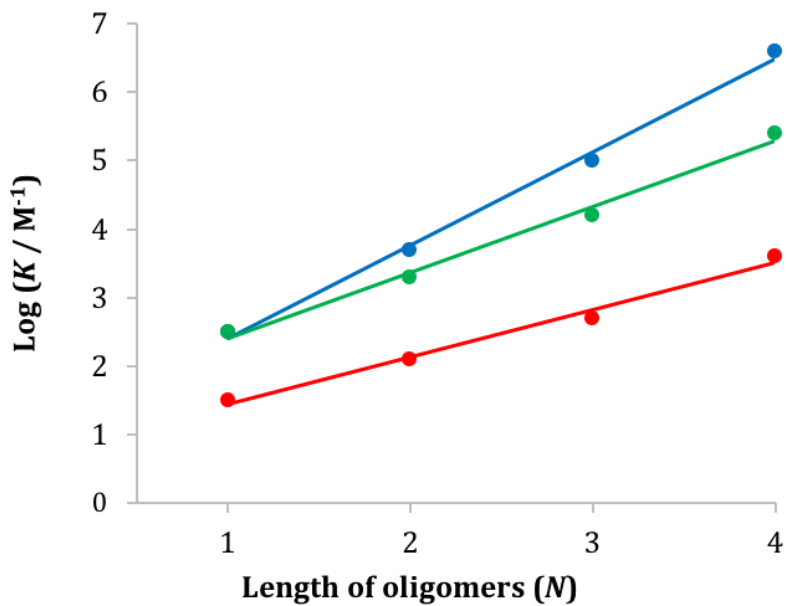


Figure 1.18: Plot of Log K against oligomer length for the formation of 1:1 duplexes shown in **Figure 1.17**: pyridine (red), phosphine oxide (green) and pyridine N-oxide (blue).

Due to the modular design of the information molecule it was possible to change the backbone without having to make any other changes to the molecule (**Figure 1.19**).⁹⁵ DD (phenol) and AA (phosphine oxide) 2-mers were synthesised with three different backbones with different geometries and flexibilities.

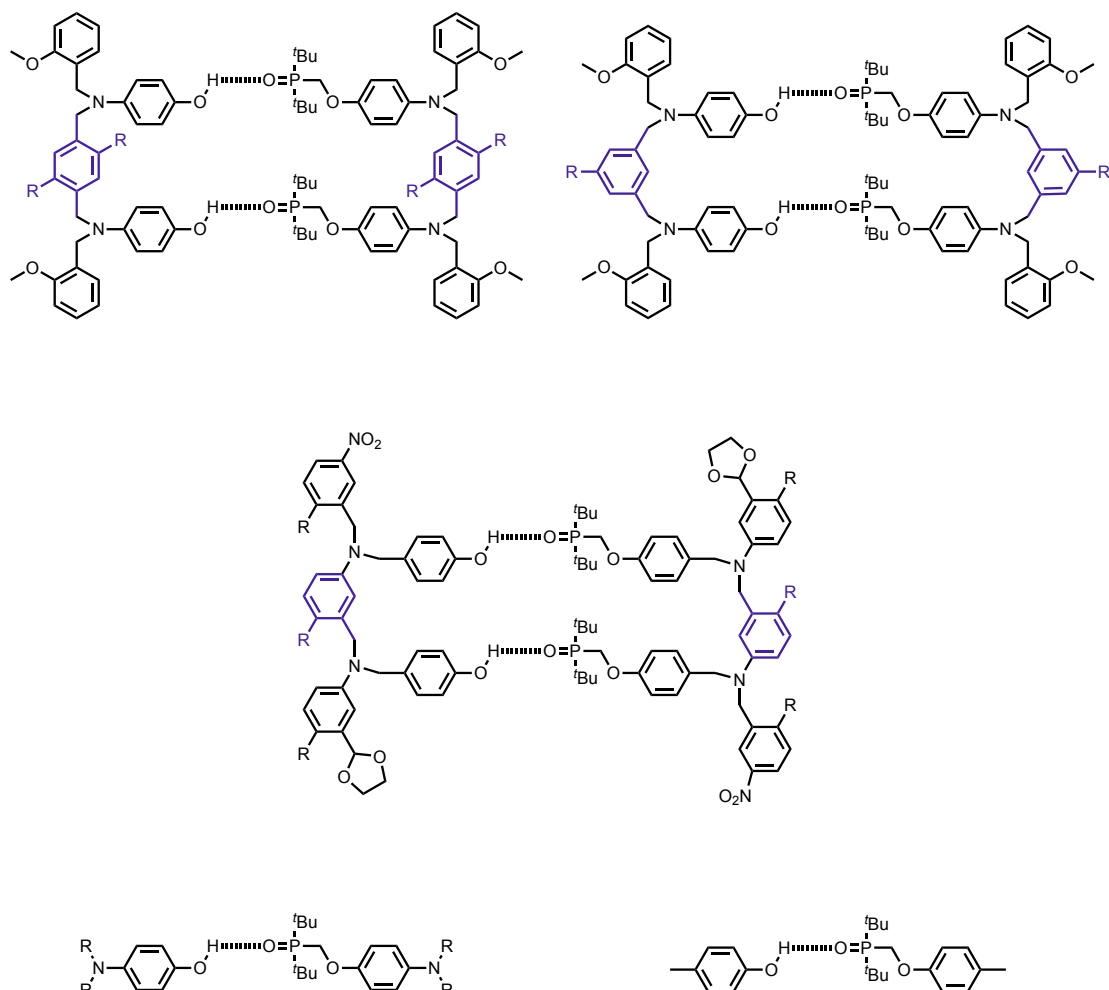


Figure 1.19: Duplexes formed by 2-mers of systems with three different backbones with varying conformational flexibility, and representative 1-mer systems for NMR titrations.

In toluene- d_8 , duplexes were formed for all combinations of 2-mers, with the EM for duplex formation remaining fairly constant (7-20 mM). Provided there is some flexibility, strict complementarity and a high degree of pre-organization is not required for duplex formation.

All possible 3-mers of the pyridine N-oxide system (**Figure 1.17**) were synthesised (AAA, DDD, AAD, DDA, ADA, DAD, ADD, DAA) and NMR binding studies performed in toluene- d_8 .⁹⁶ The pairwise interactions were investigated and association constants measured. Good sequence selectivity was observed, so that in mixtures that contain all eight sequences, the complementary duplexes are expected to dominate (**Figure 1.20**).

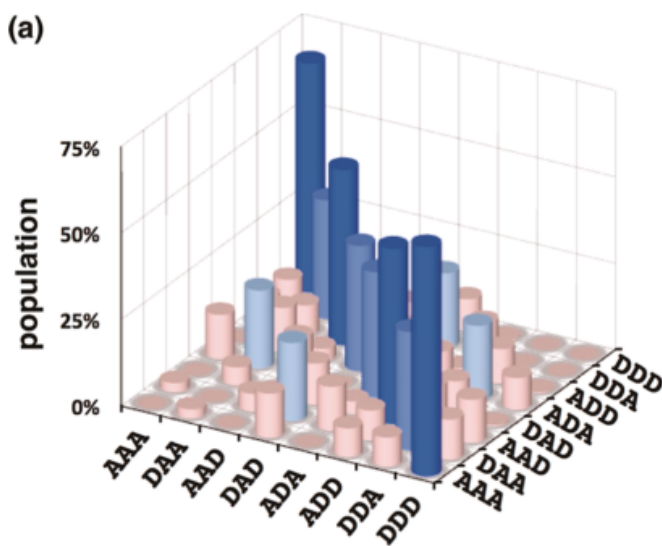


Figure 1.20: Calculated populations of duplexes formed by an equimolar mixture (100 mM) of all possible pyridine N-oxide 3-mers of the system shown in **Figure 1.17**, in toluene-*d*₈ (>50% dark blue, <20% pink). Reprinted with permission from the American Chemical Society.

Hunter and co-workers used building blocks bearing a thiol and an alkene functional group at either end to synthesize oligomers containing either phosphine oxide (acceptors) or phenol (donors) recognition sites (**Figure 1.21**).⁹⁷ NMR titration experiments showed an increase in association constant of an order of magnitude for each additional H-bonding unit. The effective molarity for this highly flexible system was found to be 18 mM, higher than the 14 mM for the more rigid reductive amination coupled system previously reported, showing highly flexible molecules can still form very stable duplexes.

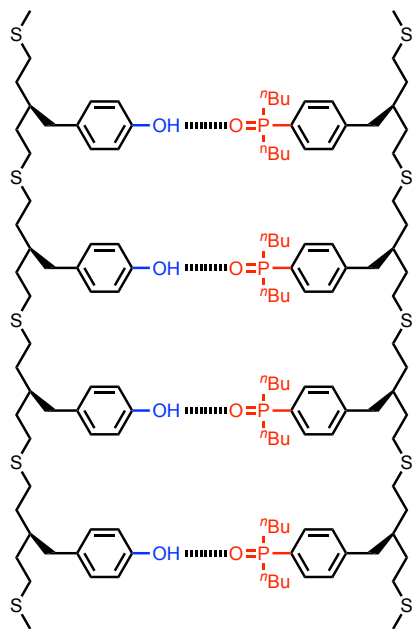


Figure 1.21: Duplex formed between 4-mer homo oligomers with highly flexible backbones synthesised using thiol-ene coupling.

For systems with a highly flexible backbone bearing both acceptor and donor recognition groups there are competing equilibria between intermolecular H-bond formation to form duplexes and folding to form an intramolecular H-bond (**Figure 1.22**).⁹⁸ NMR titration and dilution experiments were used to determine the extent of folding in a variety of systems. In systems with five or more rotatable bonds separating recognition sites, intramolecular H-bond formation is favoured, with the folded state highly populated. For more rigid systems (fewer than five rotatable bonds) intramolecular interactions are not observed, and folding does not complete with duplex formation. Folding to form H-bonds between adjacent recognition units would prevent duplex formation as there is no enthalpic advantage for duplex formation, and a larger entropic penalty.

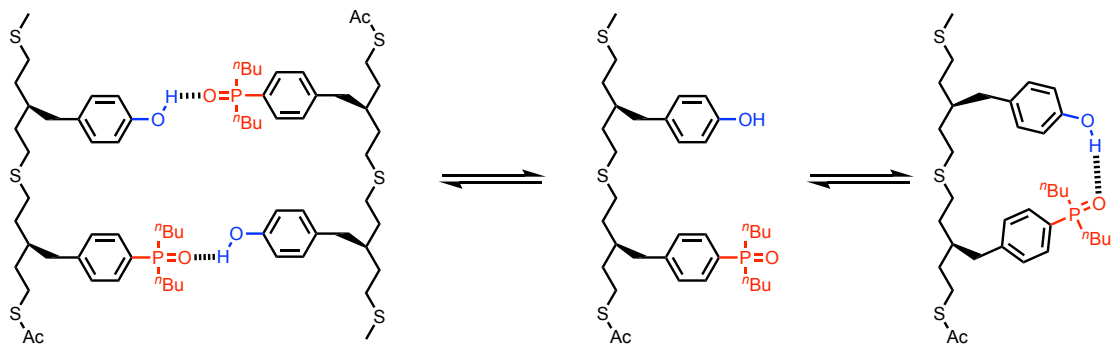
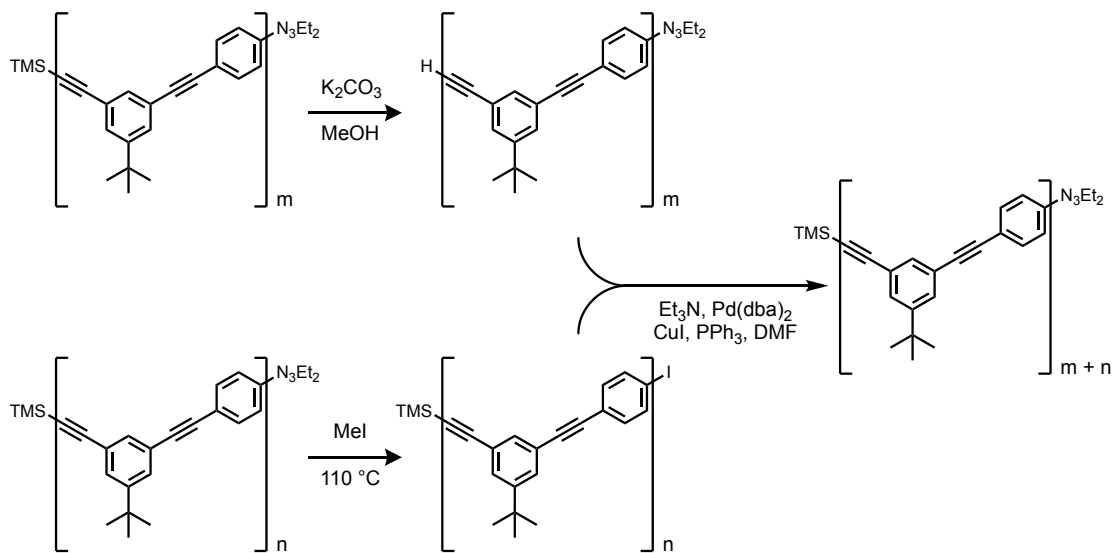


Figure 1.22: Competing equilibria between duplex formation and 1,2-intramolecular folding in information molecules with flexible backbones.

1.7 Phenylacetylene oligomers

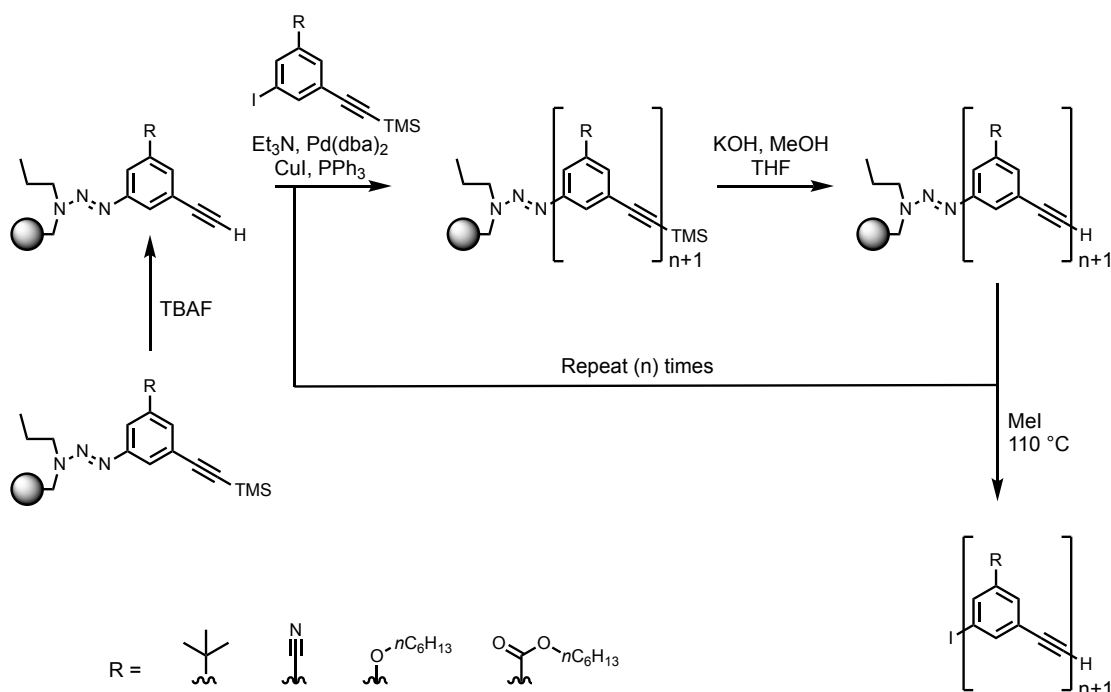
Moore and co-workers developed a class of phenylacetylene-based macromolecules, synthesised using Sonogashira coupling (**Scheme 1.7**).⁹⁹ These macromolecules could be used as molecular scaffolds to produce a variety of oligomers, dendrimers and macrocycles.^{99–104} To produce oligomers, monomer units were synthesised with trimethylsilyl (TMS) protected alkynes at one end, and aryl-3,3-dialkyltriazines as iodide masking groups at the other end. Selective deprotection of one end with either potassium carbonate to deprotect the alkyne, or methyl iodide to reveal the iodide yielded mono-functional intermediates. Sonogashira coupling of these intermediates yielded the protected dimer, which could be deprotected in the same way as the monomer units. Chains of up to 16 units were synthesised using this method. For oligomers bearing periodic or large sections of periodic sequences, this method is more efficient than traditional stepwise addition of monomer units, and was performed on a solid support to produce the 64-mer.¹⁰⁰



Scheme 1.7: Stepwise synthesis of phenylacetylene oligomers using orthogonal protecting groups to produce discrete length oligomers.

A *n*-propylamino-modified Merrifield resin supported monomer linked by a 1-aryl-3-propyl-3-(benzyl-support) triazine was synthesised, which allowed for solid phase synthesis of phenylacetylene oligomers with complete sequence

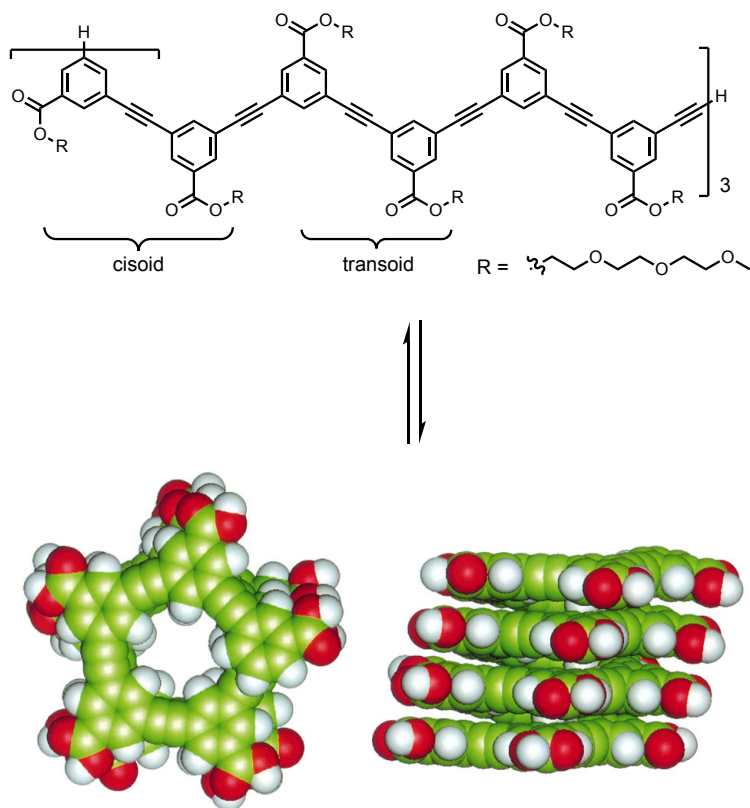
control on the gram scale (**Scheme 1.8**).¹⁰¹ Deprotection of the TMS-alkyne yielded the terminal alkyne, which was reacted with a TMS protected monomer bearing an iodide *via* Sonogashira coupling. Further deprotection and coupling yielded monodisperse oligomers with sequence control. Four different monomer units were used: hexyl benzoate, hexyl phenyl ether, benzonitrile or tert-butyl phenyl.



Scheme 1.8: Solid phase synthesis of phenylacetylene oligomers with complete length and sequence control

Chains of more than eight phenyl rings exhibit fluorescence quenching associated with π -stacking in polar solvents such as acetonitrile. Fluorescence at 350 nm is observed for oligomers in non-polar solvents and short oligomers in polar solvents. For longer oligomers in polar solvents this emission is quenched, and a red-shifted emission is observed at 420 nm, as expected with π -stacking. This is consistent with chains long enough to form supramolecular macrocycles folding back on themselves and is driven by solvophobic interactions (**Scheme 1.9**).^{105,106} Titration experiments with substitution of the polar solvent for a non-polar solvent resulted in sigmoidal curves that could be approximated by a two-state cooperative helix-coil transition. The stability of the helix formed was found

to increase linearly with oligomer length by around 0.7 kcal mol⁻¹ per monomer at 23 °C in acetonitrile. The UV/vis absorption spectra agreed with these results. The ratio of absorptions at 305 nm and 289 nm decreases with a higher proportion of diphenylacetylene units in a cisoid arrangement, as opposed to a transoid arrangement. The changes in this ratio during titration match the fluorescence results.



Scheme 1.9: In highly polar solvents, phenylacetylene oligomers of length greater than 7 units were found to fold into helical conformations. Example shown is octadecamer (molecular mechanics model, side chains omitted for clarity). Reprinted with permission from the Journal of the American Chemical Society.¹⁰⁷ Copyright (2000) American Chemical Society.

Helix formation leads to an 8 Å cavity in the centre of the molecule which can be used to bind guests (**Figure 1.23**).¹⁰⁷⁻¹¹⁰ Inwardly pointing ligation groups can be used to bind metal ions such as Ag^+ and an unsubstituted dodecamer was found to yield an internal binding pocket for non-polar molecules such as α -pinene. Binding of chiral, non-polar molecules by an achiral phenylacetylene

dodecamer resulted in a helical twist sense bias, the direction of which could be determined by CD.

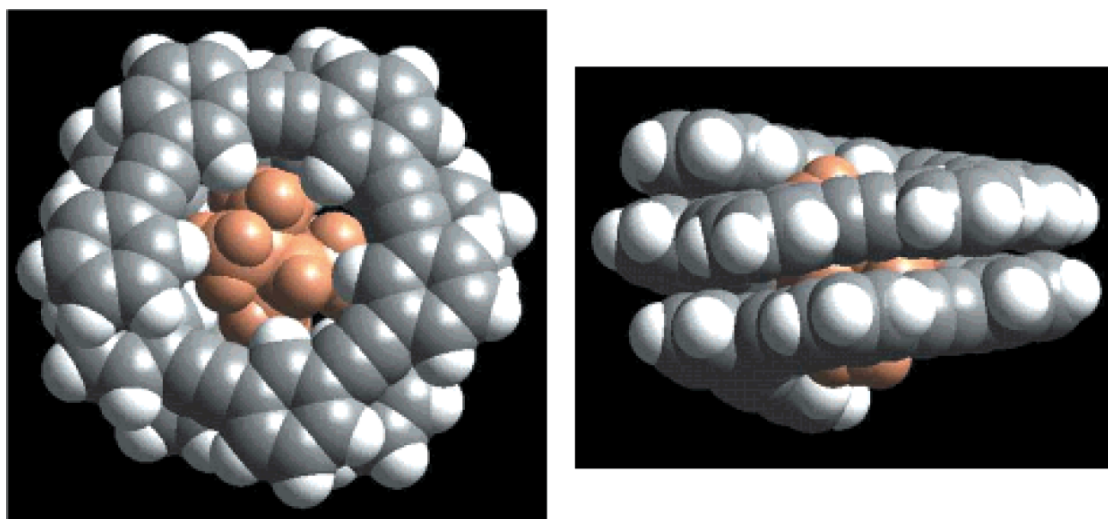


Figure 1.23: Phenylacetylene oligomers in helical conformation have been found to bind small, non-polar molecules in the cavity formed by folding. Shown is space filling model of the 1:1 complex of α -pinene and a phenylene acetylene dodecamer viewed from top and side (molecular mechanics model, side chains omitted for clarity). Reprinted with permission from the Journal of the American Chemical Society.¹⁰⁷ Copyright (2000) American Chemical Society.

Addition of chiral groups to the solubilising chains was found to induce a twist sense bias in the helix formed by phenylacetylene oligomers in polar solvents.¹¹¹ Oligomers of different lengths were synthesised with a mix of chiral and achiral solubilising groups. Tetradecamers with one or two chiral monomers, a hexadecamer with four chiral monomers and an octadecamer with six chiral monomers were all synthesised. The chiral monomers were located at the end of the oligomers (**Figure 1.24**).¹¹² All oligomers existed as random coils in chloroform, and in acetonitrile formed helices. CD measurements showed a strong helical twist sense bias with no sign of “fraying” at the end of the oligomer furthest from the chiral monomers. The chirality of the helix is passed on to the achiral monomers through the “Sergeants and soldiers” principle.¹¹³ Intermolecular aggregation of these oligomers in aqueous solutions showed that the twist sense

bias could be passed from chiral oligomers to achiral oligomers through aggregation.

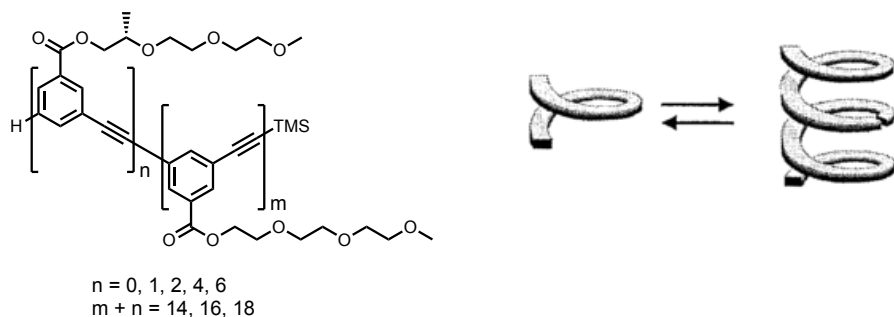


Figure 1.24: Phenylacetylene oligomers bearing a mix of chiral and achiral solubilising groups fold into helices and aggregate by stacking with transfer of chiral information *via* the Sergeants and Soldiers principle

Moore and co-workers synthesised a phenylacetylene oligomer with an intramolecular H-bond as a β -sheet mimic.¹¹⁴ This intramolecular H-bond held one diphenylacetylene unit in a cisoid conformation, and resulted in an increase in helix stability of 1.2 kcal mol⁻¹. Gong and co-workers synthesised phenylacetylene oligomers with intramolecular H-bonds stabilising every turn giving much higher stability helices (**Figure 1.25**).¹¹⁵

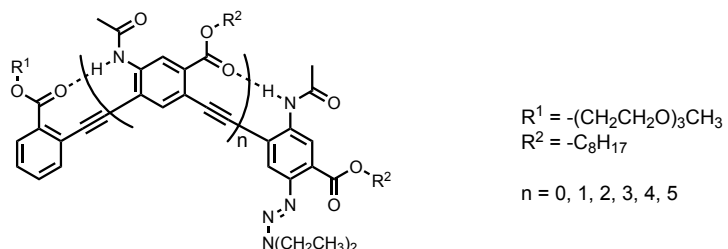


Figure 1.25: Phenylacetylene oligomers with a H-bond rigidified backbone to increase folding.

1.8 Conclusions

The ability of nucleic acids to store, read and copy information is unique in nature. Sequence selective duplex formation and template polymerisation, as well as the catalytic and substrate binding abilities of these molecules are made possible by the information encoded within their primary structure. Modified nucleic acids have been synthesised that retain some of these functions, suggesting the exact structure of DNA is not required to obtain useful properties. Attempts at new duplex forming oligomers have used a range of molecular architectures and recognition groups, with some success in encoding sequences and forming sequence and length selective duplexes. One problem for highly flexible information molecules is intramolecular H-bond formation causing folding, preventing duplex formation. Phenylacetylene oligomers are a useful molecular architecture which have been extensively studied and could form the backbone of a new class of synthetic information molecules with a rigid backbone.

1.9 References

- (1) Watson, J.; Crick, F. H. F. *Nature* **1953**, *171* (4356), 737–738.
- (2) Kyogoku, Y.; Lord, R. C.; Rich, A. *Science* **1966**, *154* (748), 518–520.
- (3) Kyogoku, Y.; Lord, R. C.; Rich, A. *J. Am. Chem. Soc.* **1967**, *89* (3), 496–504.
- (4) Newmark, R. A.; Cantor, C. R. *J. Am. Chem. Soc.* **1968**, *90* (16), 5010–5017.
- (5) Porschke, D. *Biopolymers* **1971**, *10* (10), 1989–2013.
- (6) Chan, S. I.; Schweizer, M. P.; Ts'o, P. O. P.; Helmkamp, G. K. *J. Am. Chem. Soc.* **1964**, *86* (19), 4182–4188.
- (7) Crick, F. *Nature* **1970**, *227* (5258), 561–563.
- (8) Johnston, W. K.; Unrau, P. J.; Lawrence, M. S.; Glasner, M. E.; Bartel, D. P. *Science* **2001**, *292* (5520), 1319–1325.
- (9) Seeman, N. C. *J. Theor. Biol.* **1982**, *99* (2), 237–247.
- (10) Rothemund, P. W. K. *Nature* **2006**, *440* (7082), 297–302.
- (11) Gothelf, K. V. *Science* **2012**, *338* (6111), 1159–1160.
- (12) Morse, M.; Barkai, A.; Tubul, S.; Alduino, A.; Gill, M.; Pang, S. *Nature* **2004**, *427*, 260–261.
- (13) Yin, P.; Hariadi, R. F.; Sahu, S.; Choi, H. M. T.; Sung, H. P.; LaBean, T. H.; Reif, J. H. *Science* **2008**, *321* (5890), 824–826.
- (14) Yan, H.; LaBean, T. H.; Feng, L.; Reif, J. H. *Proc. Natl. Acad. Sci. U. S. A* **2003**, *100* (14), 8103–8108.
- (15) Douglas, S. M.; Marblestone, A. H.; Teerapittayanon, S.; Vazquez, A.; Church, G. M.; Shih, W. M. *Nucleic Acids Res.* **2009**, *37* (15), 5001–5006.
- (16) Douglas, S. M.; Dietz, H.; Liedl, T.; Höglberg, B.; Graf, F.; Shih, W. M. *Nature* **2009**, *459* (7245), 414–418.
- (17) You, M.; Chen, Y.; Zhang, X.; Liu, H.; Wang, R.; Wang, K.; Williams, K. R.; Tan, W. *Angew. Chem. Int. Ed.* **2012**, *51* (10), 2457–2460.
- (18) Song, C.; Wang, Z. G.; Ding, B. *Small* **2013**, *9* (14), 2382–2392.
- (19) Wang, Z. G.; Elbaz, J.; Willner, I. *Nano Lett.* **2011**, *11* (1), 304–309.
- (20) Andersen, E. S.; Dong, M.; Nielsen, M. M.; Jahn, K.; Subramani, R.; Mamdouh, W.; Golas, M. M.; Sander, B.; Stark, H.; Oliveira, C. L. P.; et al. *Nature* **2009**, *459* (7243), 73–76.

- (21) Chhabra, R.; Sharma, J.; Liu, Y.; Yan, H. *Nano Lett.* **2006**, *6* (5), 978–983.
- (22) Zhang, X.; Ding, X.; Zou, J.; Gu, H. *Nature* **2010**, *465*, 202–206.
- (23) Langecker, M.; Arnaut, V.; Martin, T. G.; List, J.; Renner, S.; Mayer, M.; Dietz, H.; Simmel, F. C. *Science* **2012**, *338* (6109), 932–936.
- (24) Ke, Y.; Ong, L. L.; Shih, W. M.; Yin, P. *Science* **2012**, *338* (6111), 1177–1183.
- (25) Goldman, N.; Bertone, P.; Chen, S.; Dessimoz, C.; LeProust, E. M.; Sipos, B.; Birney, E. *Nature* **2013**, *494* (7435), 77–80.
- (26) Extance, A. *Nature* **2016**, *537*, 22–24.
- (27) Erlich, Y.; Zielinski, D. *Science* **2017**, *355* (6328), 950–954.
- (28) Tereshko, V.; Portmann, S.; Tay, E. C.; Martin, P.; Natt, F.; Altmann, K. H.; Egli, M. *Biochemistry* **1998**, *37* (30), 10626–10634.
- (29) Teplova, M.; Minasov, G.; Tereshko, V.; Inamati, G. B.; Cook, P. D.; Manoharan, M.; Egli, M. *Nat. Struct. Biol.* **1999**, *6* (6), 535–539.
- (30) Pitsch, S.; Krishnamurthy, R.; Bolli, M.; Wendeborn, S.; Holzner, A.; Minton, M.; Lesueur, C.; Schlönvogt, I.; Jaun, B.; Eschenmoser, A. *Helv. Chim. Acta* **1995**, *78* (7), 1621–1635.
- (31) Orgel, L. E. *Science* **2000**, *290* (5495), 1306.
- (32) Schöning, K.; Scholz, P.; Guntha, S.; Wu, X.; Krishnamurthy, R.; Eschenmoser, A. *Science* **2000**, *290* (5495), 1347.
- (33) Ebert, M. O.; Mang, C.; Krishnamurthy, R.; Eschenmoser, A.; Jaun, B. *J. Am. Chem. Soc.* **2008**, *130* (15), 15105–15115.
- (34) Chaput, J. C.; Ichida, J. K.; Szostak, J. W. *J. Am. Chem. Soc.* **2003**, *125* (4), 856–857.
- (35) Horhota, A.; Zou, K.; Ichida, J. K.; Yu, B.; McLaughlin, L. W.; Szostak, J. W.; Chaput, J. C. *J. Am. Chem. Soc.* **2005**, *127* (20), 7427–7434.
- (36) Ichida, J. K.; Zou, K.; Horhota, A.; Yu, B.; McLaughlin, L. W.; Szostak, J. W. *J. Am. Chem. Soc.* **2005**, *127* (9), 2802–2803.
- (37) Yu, H.; Zhang, S.; Chaput, J. C. *Nat. Chem.* **2012**, *4* (3), 183–187.
- (38) Singh, S. K.; Nielsen, P.; Koshkin, A. A.; Wengel, J. *Chem. Commun.* **1998**, 455–456.
- (39) Renneberg, D.; Leumann, C. J. *J. Am. Chem. Soc.* **2002**, No. 14, 5993–6002.
- (40) Zhang, L.; Peritz, A.; Meggers, E. *J. Am. Chem. Soc.* **2005**, *127* (12), 4174–4175.

- (41) Meggers, E.; Zhang, L. *Acc. Chem. Res.* **2010**, *43* (8), 1092–1102.
- (42) Schlegel, M. K.; Peritz, A. E.; Kittigowittana, K.; Zhang, L.; Meggers, E. *ChemBioChem* **2007**, *8* (8), 927–932.
- (43) Gryaznov, S. M.; Lloyd, D. H.; Chen, J.; Schultz, R. G.; Dedionisio, L. A.; Ratmeyert, L.; Wilsont, W. D. *Proc. Natl. Acad. Sci. U. S. A.* **1995**, *92*, 5798–5802.
- (44) De Mesmaeker, A.; Lesueur, C.; Bévière, M. O.; Waldner, A.; Fritsch, V.; Wolf, R. M. *Angew. Chemie Int. Ed. English* **1996**, *35* (23/24), 2790–2794.
- (45) Roughton, A. L.; Portmann, S.; Benner, S. A.; Egli, M. *J. Am. Chem. Soc.* **1995**, *117* (27), 7249–7250.
- (46) Richert, C.; Roughton, A. L.; Benner, S. A. *J. Am. Chem. Soc.* **1996**, *118* (19), 4518–4531.
- (47) Isobe, H.; Fujino, T.; Yamazaki, N.; Guillot-Nieckowski, M.; Nakamura, E. *Org. Lett.* **2008**, *10* (17), 3729–3732.
- (48) Nielsen, P. E.; Egholm, M.; Berg, R. H.; Buchardt, O. *Science* **1991**, *254* (5037), 1497–1500.
- (49) Kiliszek, A.; Banaszak, K.; Dauter, Z.; Rypniewski, W. *Nucleic Acids Res.* **2015**, *44* (4), 1937–1943.
- (50) Sen, A.; Nielsen, P. E. *Nucleic Acids Res.* **2007**, *35* (10), 3367–3374.
- (51) Sen, A.; Nielsen, P. E. *Biophys. Chem.* **2009**, *141* (1), 29–33.
- (52) Anstaett, P.; Gasser, G. *Chim. Int. J. Chem.* **2014**, *68* (4), 264–268.
- (53) Wittung, P.; Nielsen, P. E.; Buchardt, O.; Egholm, M.; Norde'n, B. *Nature* **1994**, *368* (6471), 561–563.
- (54) Nelson, K. E.; Levy, M.; Miller, S. L. *Proc. Natl. Acad. Sci. U. S. A.* **2000**, *97* (8), 3868–3871.
- (55) Banack, S. A.; Metcalf, J. S.; Jiang, L.; Craighead, D.; Ilag, L. L.; Cox, P. A. *PLoS One* **2012**, *7* (11), 1–4.
- (56) Brudno, Y.; Birnbaum, M. E.; Kleiner, R. E.; Liu, D. R. *Nat. Chem. Biol.* **2010**, *6* (2), 148–155.
- (57) Ura, Y.; Beierle, J. M.; Leman, L. J.; Orgel, L. E.; Ghadiri, M. R. *Science* **2009**, *325* (5936), 73–77.
- (58) Switzer, C.; Moronev, S. E.; Benner, S. A. *J. Am. Chem. Soc.* **1989**, *111* (21), 8322–8323.
- (59) Piccifilli, J.; Krauch, T.; Moroney, S. E.; Benner, S. A. *Nature* **1990**, *343*, 33–

- 37.
- (60) Yang, Z.; Hutter, D.; Sheng, P.; Sismour, A. M.; Benner, S. A. *Nucleic Acids Res.* **2006**, *34* (21), 6095–6101.
- (61) Zhang, L.; Yang, Z.; Sefah, K.; Bradley, K. M.; Hoshika, S.; Kim, M. J.; Kim, H. J.; Zhu, G.; Jiménez, E.; Cansiz, S.; et al. *J. Am. Chem. Soc.* **2015**, *137* (21), 6734–6737.
- (62) Liu, H.; Gao, J.; Lynch, S. R.; Saito, Y. D. *Science* **2003**, *302*, 868–871.
- (63) Delaney, J. C.; Gao, J.; Liu, H.; Shrivastav, N.; Essigmann, J. M.; Kool, E. T. *Angew. Chem. Int. Ed.* **2009**, *48* (25), 4524–4527.
- (64) Lu, H.; He, K.; Kool, E. T. *Angew. Chem. Int. Ed.* **2004**, *43* (43), 5834–5836.
- (65) Doi, Y.; Chiba, J.; Morikawa, T.; Inouye, M. *J. Am. Chem. Soc.* **2008**, *130* (27), 8762–8768.
- (66) Hikishima, S.; Minakawa, N.; Kuramoto, K.; Fujisawa, Y.; Ogawa, M.; Matsuda, A. *Angew. Chem. Int. Ed.* **2005**, *44* (4), 596–598.
- (67) Kool, E. T. *Acc. Chem. Res.* **2002**, *35* (11), 936–943.
- (68) Wilson, J. N.; Kool, E. T. *Org. Biomol. Chem.* **2006**, *4* (23), 4265.
- (69) Połowiński, S. *Prog. Polym. Sci.* **2002**, *27* (3), 537–577.
- (70) Lodish, H.; Berk, A.; Matsudaira, P.; Kaiser, C.; Krieger, M. 5th Ed.; Freeman, W. H. & Company, 2003.
- (71) Li, X.; Liu, D. R. *Angew. Chem. Int. Ed.* **2004**, *43* (37), 4848–4870.
- (72) Naylor, R.; Gilham, P. T. *Biochemistry* **1966**, *5* (8), 2722–2728.
- (73) Kiedrowski, G. Von. *Angew. Chem. Int. Ed.* **1986**, *119* (10), 932–935.
- (74) Luther, A.; Brandsch, R.; Von Kiedrowski, G. *Nature* **1998**, *396* (6708), 245–248.
- (75) Zhan, Z. Y. J.; Lynn, D. G. *J. Am. Chem. Soc.* **1997**, *119* (50), 12420–12421.
- (76) Wu, X.; Delgado, G.; Krishnamurthy, R.; Eschenmoser, A. *Org. Lett.* **2002**, *4* (9), 1283–1286.
- (77) Böhler, C.; Nielsen, P. E.; Orgel, L. E. *Nature*, **1995**, *376*, 578–581.
- (78) Kukwikila, M.; Gale, N.; El-Sagheer, A. H.; Brown, T.; Tavassoli, A. *Nat. Chem.* **2017**, *9* (11), 1089–1098.
- (79) Ferguson, J. S.; Shah, S. A. O. *Eur. Polym. J.* **1968**, *4*, 343–354.
- (80) Tsuchida, E.; Osada, Y. *J. Polym. Sci.* **1975**, *13*, 559–569.
- (81) Higashi, F.; Nakano, Y. *J. Polym. Sci. Polym. Chem. Ed.* **1980**, *18*, 851–856.

- (82) Li, X.; Zhan, Z. Y. J.; Knipe, R.; Lynn, D. G. *J. Am. Chem. Soc.* **2002**, *124* (5), 746–747.
- (83) Khan, A.; Haddleton, D. M.; Hannon, M. J.; Kukulj, D.; Marsh, A. *Macromolecules* **1999**, *32* (20), 6560–6564.
- (84) Lo, P. K.; Sleiman, H. F. *J. Am. Chem. Soc.* **2009**, *131* (12), 4182–4183.
- (85) Gong, B.; Yan, Y.; Zeng, H.; Skrzypczak-Jankunn, E.; Kim, Y. W.; Zhu, J.; Ickes, H. *J. Am. Chem. Soc.* **1999**, *121* (23), 5607–5608.
- (86) Zeng, H.; Miller, R. S.; Flowers, R. A.; Gong, B. *J. Am. Chem. Soc.* **2000**, *122* (11), 2635–2644.
- (87) Zeng, H.; Ickes, H.; Flowers, R. A.; Gong, B. *J. Org. Chem.* **2001**, *66* (10), 3574–3583.
- (88) Yang, X.; Gong, B. *Angew. Chem. Int. Ed.* **2005**, *44*, 1352–1356.
- (89) Tanaka, Y.; Katagiri, H.; Furusho, Y.; Yashima, E. *Angew. Chem. Int. Ed.* **2005**, *44* (25), 3867–3870.
- (90) Ito, H.; Furusho, Y.; Hasegawa, T.; Yashima, E. *J. Am. Chem. Soc.* **2008**, *130* (42), 14008–14015.
- (91) Yamada, H.; Furusho, Y.; Ito, H.; Yashima, E. *Chem. Commun.* **2010**, *46* (20), 3487–3489.
- (92) Hasegawa, T.; Furusho, Y.; Katagiri, H.; Yashima, E. *Angew. Chem. Int. Ed.* **2007**, *46* (31), 5885–5888.
- (93) Yamada, H.; Furusho, Y.; Yashima, E. *J. Am. Chem. Soc.* **2012**, *134* (17), 7250–7253.
- (94) Iadevaia, G.; Stross, A. E.; Neumann, A.; Hunter, C. A. *Chem. Sci.* **2016**, *7* (3), 5686–5691.
- (95) Iadevaia, G.; Stross, A. E.; Neumann, A.; Hunter, C. A. *Chem. Sci.* **2016**, *7* (3), 1760–1767.
- (96) Stross, A. E.; Iadevaia, G.; Núñez-Villanueva, D.; Hunter, C. A. *J. Am. Chem. Soc.* **2017**, *139* (36), 12655–12663.
- (97) Núñez-Villanueva, D.; Hunter, C. A. *Chem. Sci.* **2017**, *8* (1), 206–213.
- (98) Núñez-Villanueva, D.; Iadevaia, G.; Stross, A. E.; Jinks, M. A.; Swain, J. A.; Hunter, C. A. *J. Am. Chem. Soc.* **2017**, *139* (19), 6654–6662.
- (99) Zhang, J.; Moore, J. S.; Xu, Z.; Aguirre, R. A. *J. Am. Chem. Soc.* **1992**, *114* (6), 2273–2274.
- (100) Young, J. K.; Nelson, J. C.; Moore, J. S. *J. Am. Chem. Soc.* **1994**, *116* (23),

- 10841–10842.
- (101) Nelson, J. C.; Young, J. K.; Moore, J. S. *J. Org. Chem.* **1996**, *61* (23), 8160–8168.
- (102) Xu, Z.; Kahr, M.; Walker, K. L.; Wilkins, C. L.; Moore, J. S. *J. Am. Chem. Soc.* **1994**, *116* (11), 4537–4550.
- (103) Wu, Z.; Lee, S.; Moore, J. S. *J. Am. Chem. Soc.* **1992**, *114*, 8730–8732.
- (104) Zhao, D.; Moore, J. S. *Chem. Commun.* **2003**, No. 7, 807–818.
- (105) Prince, R. B.; Saven, J. G.; Wolynes, P. G.; Moore, J. S.; Pennsyl, V. *J. Am. Chem. Soc.* **1999**, *121* (9), 3114–3121.
- (106) Lahiri, S.; Thompson, J. L.; Moore, J. S. *J. Am. Chem. Soc.* **2000**, *122*, 11315–11319.
- (107) Prince, R. B.; Barnes, S. A.; Moore, J. S. *J. Am. Chem. Soc.* **2000**, *122*, 2758–2762.
- (108) Prince, R. B.; Okada, T.; Moore, J. S. *Angew. Chem. Int. Ed.* **1999**, *38* (1/2), 233–236.
- (109) Tanatani, A.; Mio, M. J.; Moore, J. S. *J. Am. Chem. Soc.* **2001**, *123* (8), 1792–1793.
- (110) Stone, M. T.; Moore, J. S. *Org. Lett.* **2003**, *6* (4), 469.
- (111) Prince, R. B.; Brunsved, L.; Meijer, E. W.; Moore, J. S. *Angew. Chem. Int. Ed.* **2000**, *39* (1), 228–230.
- (112) Prince, R. B.; Moore, J. S.; Brunsved, L.; Meijer, E. W. *Chem. Eur. J.* **2001**, *7* (19), 4150–4154.
- (113) Brunsved, L.; Meijer, E. W.; Prince, R. B.; Moore, J. S. *J. Am. Chem. Soc.* **2001**, *123* (33), 7978–7984.
- (114) Cary, J. M.; Moore, J. S. *Org. Lett.* **2002**, *4* (26), 4663–4666.
- (115) Yang, X.; Yuan, L.; Yamato, K.; Brown, A. L.; Feng, W.; Furukawa, M.; Zeng, X. C.; Gong, B. *J. Am. Chem. Soc.* **2004**, *126* (7), 3148–3162.

Chapter 2

Aims

2 Aims

The aims of this work involve developing a synthetic information molecule with the same functions as nucleic acids but containing no elements of nucleic acid structure. This orthogonal structure will allow use of the information molecule in different solvents and allow the information molecule to interact with different substrates. Using DNA as inspiration, a new information molecule will be designed consisting of monomer units bearing H-bonding recognition groups. The sequence of these monomer units will define the tertiary structure and function of the information molecule.

The first aim is to synthesise monomers and to develop an efficient coupling chemistry for synthesis of oligomers bearing single point H-bonding binding sites that can be used to store information (**Figure 2.1a**). The second aim is to investigate sequence selective, cooperative duplex formation through NMR titrations of the oligomers synthesised (**Figure 2.1b**). Oligomers bearing both H-bond donors and H-bond acceptors will be synthesised and NMR dilutions used to investigate folding of the backbone caused by intramolecular H-bonding. Finally, template oligomerisation reactions will be investigated using homo-oligomers of a known length to template oligomer length of daughter strands (**Figure 2.1c**).

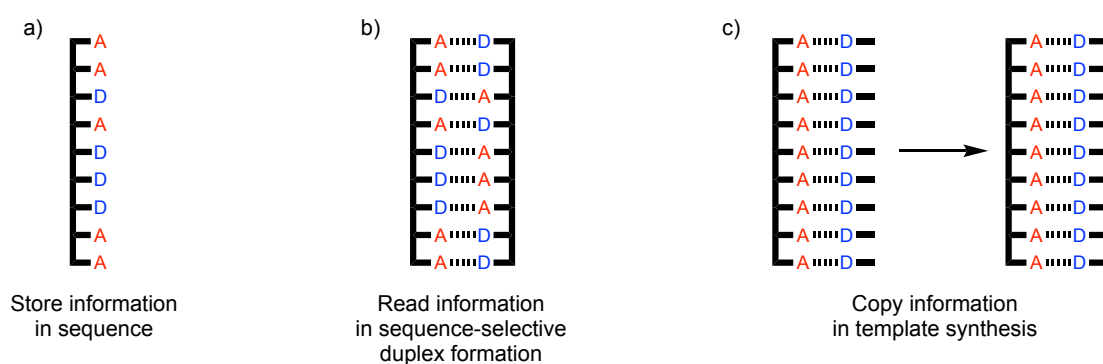


Figure 2.1: a) Information can be stored in the sequence of monomer units, b) information can be read by sequence-selective duplex formation, c) information can be copied in template synthesis.

The designed information molecule is based around a rigid phenylacetylene oligomer backbone (**Figure 2.2**) to prevent 1,2-folding that has prevented duplex formation in previous synthetic information molecules. A single point H-bond is used for recognition, for ease of synthesis and to prevent problems of mismatching associated with more complex recognition systems.

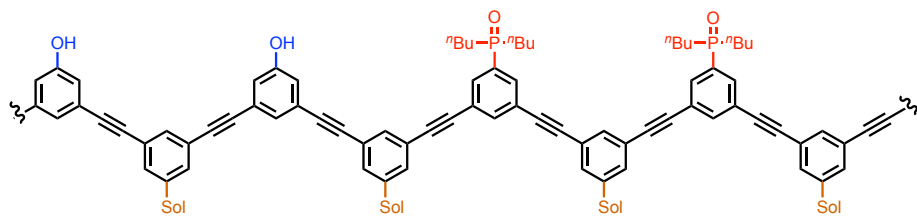


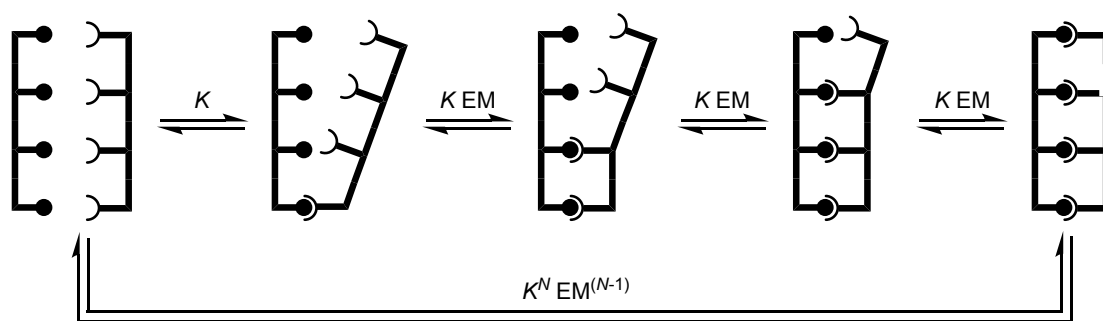
Figure 2.2: Phenylacetylene based synthetic information oligomer with single point H-bonds as a recognition system.

Chapter 3

Modular design of an information molecule

3.1 Introduction

The first two checkpoints in making a functional information molecule are storage of information through oligomer synthesis and reading of the information stored through sequence selective duplex formation.¹ In non-covalent duplex formation between two oligomers with multiple binding sites, the formation of the first interaction is an intermolecular process described by association constant K (**Scheme 3.1**).² Assuming identical binding sites, each subsequent interaction has an association constant of K multiplied by the effective molarity (EM). The EM is defined as the ratio between the equilibrium constants for an intramolecular process and an intermolecular process.^{2,3} Each of these subsequent interactions is effectively an intramolecular process, and the increase in association constant is due to the reduced entropic penalty. This is known as the chelate cooperativity. The product K EM is a measure of the cooperativity in a system that makes multiple interactions and is determined by the structure of the molecule. In highly cooperative systems where K EM $\gg 1$, duplex formation is favoured and the formation of the first interaction leads to a “zipping up” producing the fully bound duplex.⁴ These systems display all-or-nothing behaviour with partially bound states not significantly populated, therefore K EM is a useful parameter for assessing duplex formation in potential information molecule systems.



Scheme 3.1: Stepwise cooperative duplex formation. The initial interaction has an association constant of K , and all subsequent interactions have equilibrium constants of K EM. The overall association constant between the two oligomers is K^N EM $^{(N-1)}$ where N is the number of recognition units. The equilibrium constants have additional statistical factors that are not shown.

For an oligomer with N binding sites the overall association constant (K_N) is the product of the individual stepwise association constants.⁵ Assuming the effective molarity is a feature of the backbone and does not change during assembly, the overall association constant $K_N = \sigma K^N \text{EM}^{(N-1)}$. σ is a statistical factor with the value of 2 for these oligomers, due to the possibility of parallel and antiparallel structure, assuming each are equally populated. Measurement of this association constant can be used to experimentally determine the EM associated with an architecture using equation 3.1.

$$\text{EM} = \left(\frac{K_N}{2(K)^N}\right)^{\left(\frac{1}{N-1}\right)} \quad (3.1)$$

At all stages in the stepwise formation of the duplex, there is an off-pathway equilibrium with higher order aggregates that are not shown in **Scheme 3.1**. The probability of forming these off-pathway intermolecular complexes relative to zipping up of the duplex is the ratio c/EM (c is the concentration of the oligomers). At the low working concentration of the oligomers in this chapter these states will not be significantly populated. The stabilities of the fully assembled duplexes will increase proportionally to $(K \text{EM})^N$. The number of possible competing complexes also increases with N , but the stability of these complexes will not increase with N , so off-pathway complexes will become increasingly less significant as N increases.

This chapter describes the process of designing a synthetic information molecule, synthesis of short oligomers to determine if the system was synthetically accessible, and binding studies to determine EM to assess if the design has potential to be used as an information molecule.

3.2 Design of system

As is the case in many areas of research, nature was used for inspiration. Nature's information molecules are nucleic acids (DNA and RNA), which can be described as comprising of four modules (**Figure 3.1**):

1. The recognition system. Each monomer unit contains a nucleobase that has a specific array of H-bond acceptors and donors. These can interact with a complementary nucleobase in sequence selective duplex formation. The duplex formation is driven by the hydrophobicity of the nucleobases.^{6,7}
2. A polymeric backbone. The flexible sugar-phosphate backbone in DNA allows the recognition sites to reach each other.
3. Chemistry for covalent synthesis of the backbone. The backbone of DNA is formed by synthesis of strong phosphodiester bonds.
4. Groups to control solubility. The charged phosphate groups in the backbone increase the solubility of DNA in water.

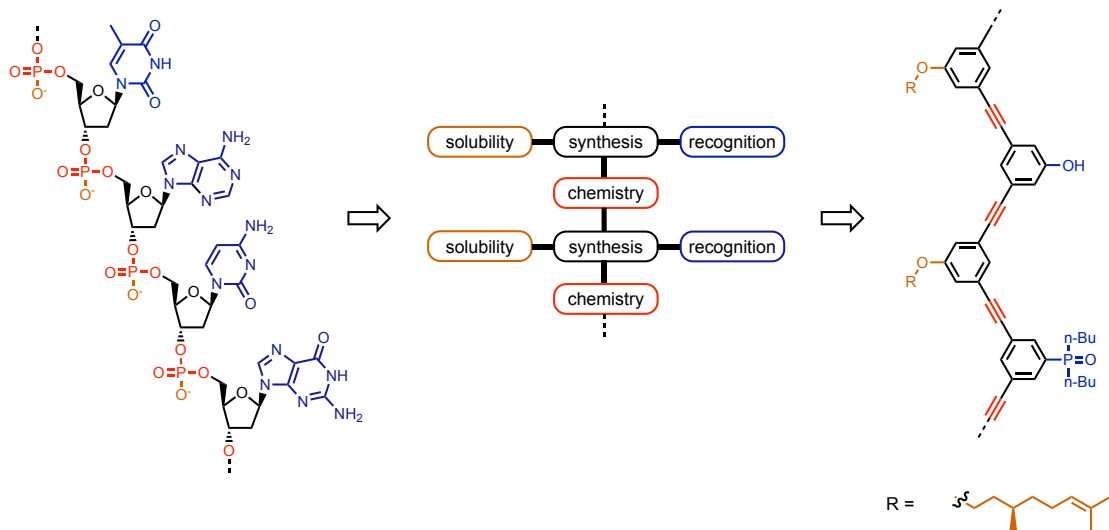


Figure 3.1: Modular design of a new information molecule using DNA as inspiration. DNA can be described as containing 4 modules: recognition (blue), backbone (black), coupling chemistry (red) and solubility (orange). This modular description has been used to design a new synthetic information molecule.

This basic description of DNA provided the starting point for designing a new information molecule that could function in the same way as nucleic acids.

Multiple DNA analogues have been synthesised with one or more of these modules replaced by unnatural structures, with the systems retaining some of the functionality of DNA.⁸⁻¹⁹ Molecular architectures with the potential to become functional information molecules have been described by Hunter *et al.*²⁰⁻²⁴ This demonstrates the specific structure of DNA is not required for a functional information molecule and that a synthetic information molecule containing none of the structural elements of DNA is possible. This modular design will allow optimisation of the individual components of the system to produce a functional synthetic information molecule. The designed information molecule is shown in **Figure 3.1**, and the choice of modules discussed below.

3.2.1 Recognition groups

The recognition system used was a high affinity single point H-bond, giving rise to a two-letter alphabet. The H-bond donor is a phenol, and the H-bond acceptor is an aryl phosphine oxide (**Figure 3.2**). In non-polar solvents, these functional groups form a strong hydrogen bond. This two-letter alphabet can be used to store information in binary form. A simple binary system to store information was chosen to try to reduce mismatching associated with more complex recognition systems such as nucleobases.²⁵

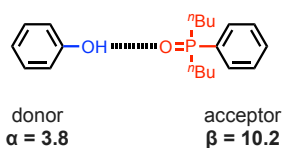


Figure 3.2: Recognition using a single point H-bond between phenol (H-bond donor, blue) and aryl phosphine oxide (H-bond acceptor, red). α and β values are H-bonding parameters of the functional groups.^{26,27}

The free energy gain on duplex formation and therefore the association constant between these groups can be estimated using equation 3.2 where α and β are H-bond donor and acceptor parameters of the functional groups.²⁸ The H-bonding properties of the solvent are given by α_s and β_s and the value of 6 kJ mol⁻¹ is the standard molar free energy cost of the bimolecular association in

solution. In toluene ($\alpha_s = 1.0$ and $\beta_s = 2.1$)²⁹ the estimated association constant is 840 M^{-1} , and in chloroform ($\alpha_s = 2.2$ and $\beta_s = 0.8$)²⁸ the estimated association constant is 38 M^{-1} . Previous work has shown typical supramolecular effective molarities to be in the range of $10\text{-}1000 \text{ mM}$.^{2,5,30,31} Provided the EM associated with the molecular architecture is greater than 100 mM , the predicted value of K EM will be greater than 1 in both solvents, leading to cooperative duplex formation.

$$\Delta G^\circ(\text{kJ mol}^{-1}) = -RT \ln K = -(\alpha - \alpha_s)(\beta - \beta_s) + 6 \quad (3.2)$$

3.2.2 Backbone

The backbone used was a *m*-phenylacetylene oligomer. Phenylacetylene oligomers contain no H-bonding functionalities to interfere with the recognition groups. The recognition groups are located on alternate phenyl rings, and the solubilising groups are attached at the other phenyl rings (**Figure 3.3**). Qualitatively EM increases with geometric complementarity and decreases with conformational flexibility.³² The oligo-*m*-phenylacetylene backbone is rigid, with only two rotors between recognition groups. This rigidity was designed to fix the recognition groups in the correct position for duplex formation, leading to a high EM and cooperative duplex formation, whilst preventing 1,2 H-bond formation between adjacent recognition groups. As explained earlier, the rotation can lead to some conformational change, which may be necessary to allow recognition groups to reach each other. The folding of single strands of phenylacetylene oligomers can result in helices with cavities in the centre, which could result in functionality in the proposed phenylacetylene oligomers.³³

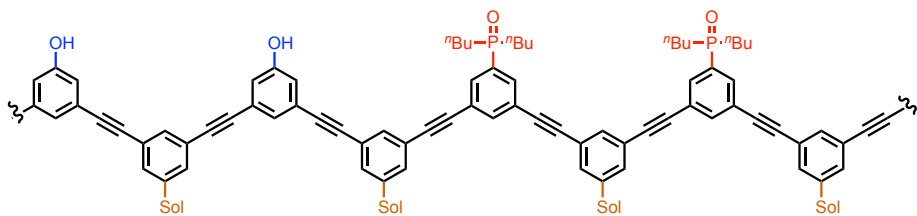
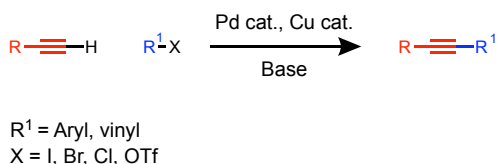


Figure 3.3: Phenylacetylene oligomer as a backbone for a synthetic information molecule, alternating aromatic rings bear recognition (red/blue) or solubility modules (orange).

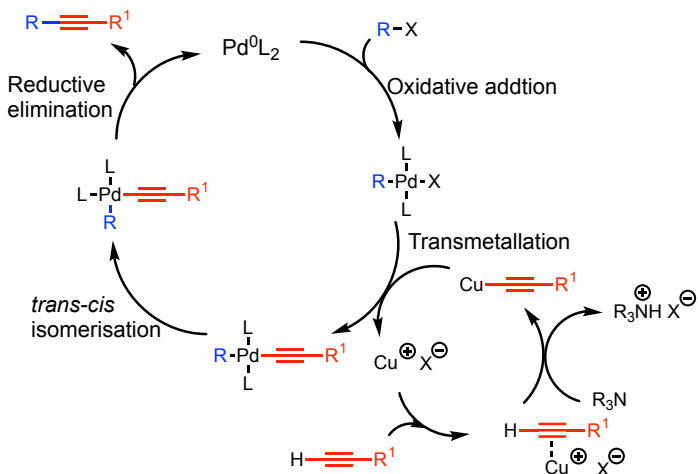
3.2.3 Coupling chemistry

To produce phenylacetylene oligomers, Sonogashira coupling was used. This is a palladium catalysed reaction between a terminal alkyne and an aryl or vinyl halide to produce a di-substituted alkyne (**Scheme 3.2**).³⁴ It has been found to be high yielding, irreversible and tolerant of many functional groups, making it ideal for this synthesis. The yields are high in non-polar solvents and under mild conditions where the recognition groups will have the strongest interactions, making the Sonogashira coupling ideal for template synthesis.



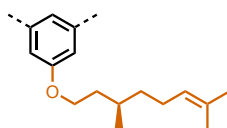
Scheme 3.2: The Sonogashira coupling.

The Sonogashira coupling involves two catalytic cycles, using palladium and copper (**Scheme 3.3**).³⁴ The palladium inserts into the carbon-halogen bond through an oxidative addition. This is followed by a transmetalation step with the copper acetylidyde formed in the copper cycle. The final step is a reductive elimination producing the product. The reaction must be performed in anaerobic conditions to suppress the copper catalysed Glaser coupling between terminal alkynes and prevent oxidation of the palladium catalyst. The reactivity of the aryl or vinyl halide used increases with increasing size of halide, iodides often react at room temperature, whereas bromides require heating.

**Scheme 3.3:** The Sonogashira coupling catalytic cycle.

3.2.4 Solubility

DNA experiments are primarily completed in water. A modular design allows replacement of the solubilising group to give solubility in any solvent desired. To maximise the strength of the recognition H-bond non-polar, organic solvents will be used for the new information molecule. Phenylacetylene oligomers have been found to have poor solubility in organic solvents.³⁵ Ether linked alkyl chains are synthetically accessible, and unlikely to interfere with recognition H-bonding (ether $\beta = 3.3$).²⁷ A (*S*)-(-)- β -citronellyl chain was attached to the phenylacetylene oligomers *via* an ether linkage (**Figure 3.4**). This is a branched alkyl chain with good solubility in organic solvents, available cheaply in high enantiomeric excess. The chirality of the solubilising group may lead to interesting folding as seen in Moore's previous work, and could be exploited at a later date.³⁶

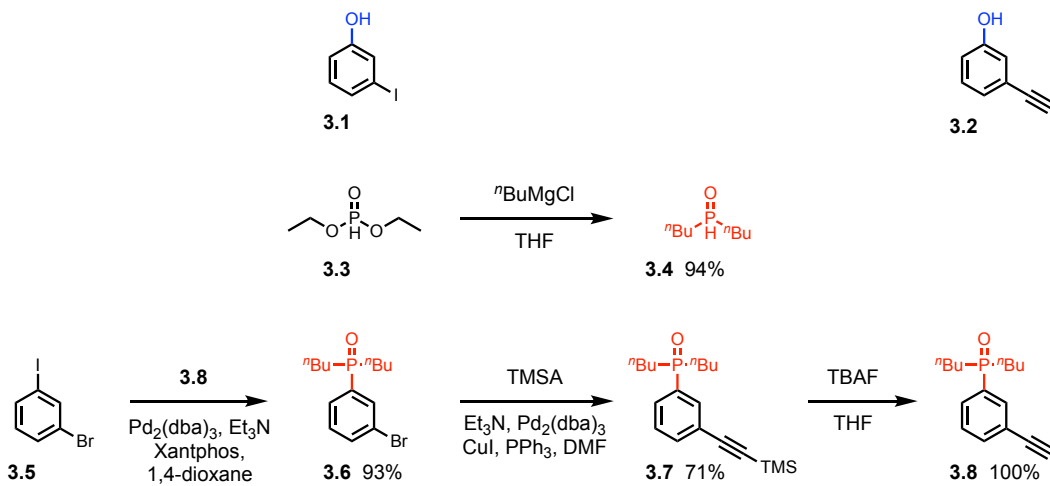
**Figure 3.4:** The citronellyl solubilising group used to increase solubility in organic solvents.

3.3 Results and discussion

To determine if the designed system was a viable synthetic information molecule, 1-mers and 2-mers were synthesised and their binding properties studied using NMR titration and dilution experiments.

3.3.1 Synthesis of building blocks

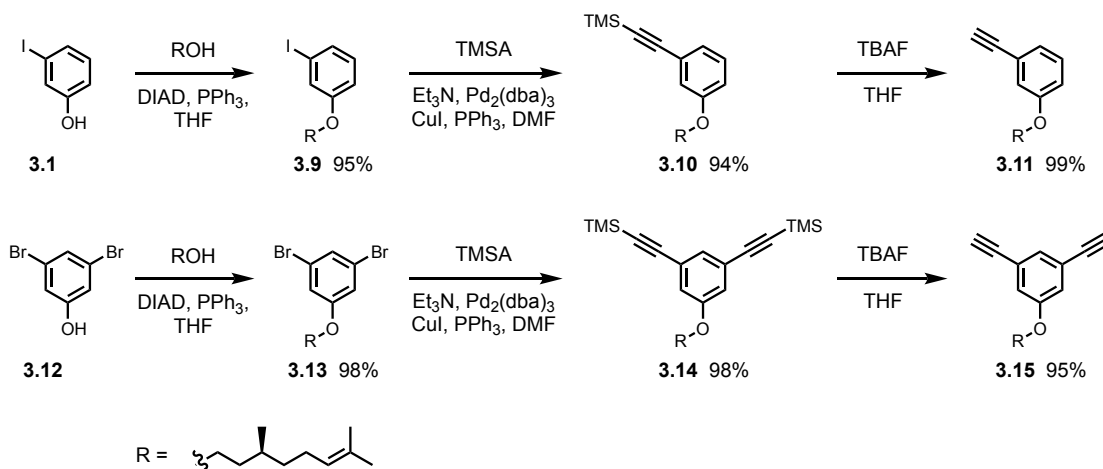
Recognition modules bearing single Sonogashira coupling functionalities were synthesised for the ends of short oligomers (**Scheme 3.4**). 3-iodophenol (**3.1**) and 3-hydroxyphenylacetylene (**3.2**) were commercially available as the donor modules. Palladium mediated P-arylation of 3-bromo iodobenzene (**3.5**) with di-*n*-butylphosphine oxide afforded **3.6**. Sonogashira coupling with trimethylsilylacetylene (TMSA) yielded **3.7**, and tetrabutylammonium fluoride-(TBAF) mediated deprotection yielded the final module (**3.8**). Both the alkyne (**3.8**) and bromide (**3.6**) can be used as acceptor modules.



Scheme 3.4: Synthesis of mono-functional recognition modules used as oligomer end groups.

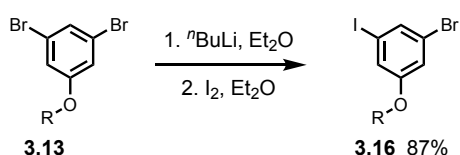
Mono- and di-functional solubilising modules were also synthesised (**Scheme 3.5**). A Mitsunobu reaction between 3-iodo phenol (**3.1**) and *S*-(*-*)- β -citronellol yielded **3.9**. Subsequent Sonogashira coupling with TMSA produced **3.10** and TBAF deprotection produced the mono-functional solubilising module

(**3.11**). The same Mitsunobu, Sonogashira and TBAF deprotection starting with 3,5-dibromophenol (**3.12**) afforded the di-functional solubilising module (**3.15**).



Scheme 3.5: Synthesis of solubilising modules required for synthesis.

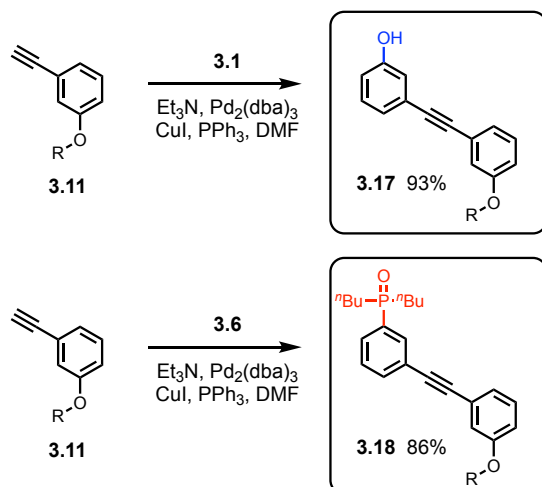
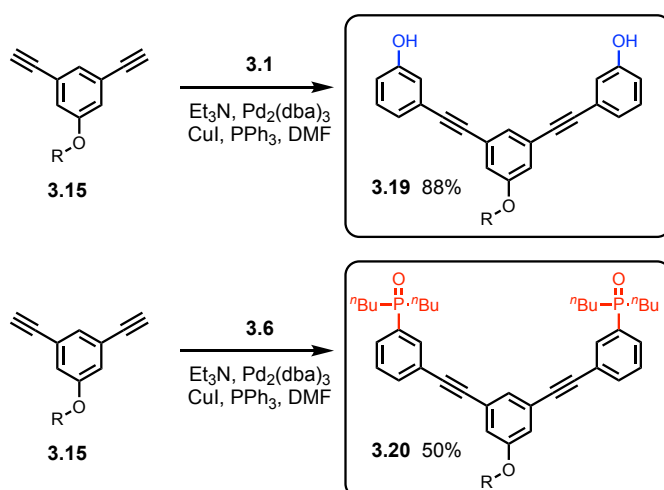
For synthesis of a mixed acceptor-donor (AD) 2-mer, an unsymmetrically substituted solubilising module was synthesised with the differing reactivity of the halides to be used for regioselectivity in synthesis (**Scheme 3.6**). Lithium-halogen exchange with **3.13** using *n*BuLi followed by reaction with iodine gave the bromoiodobenzene derivative **3.16**.



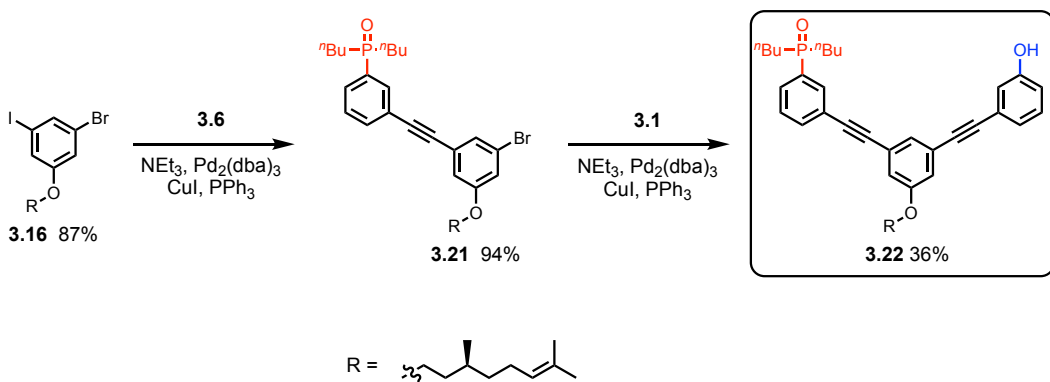
Scheme 3.6: Synthesis of an unsymmetrical solubilising module.

3.3.2 Synthesis of 1-mer and 2-mer

Sonogashira coupling of **3.2** with **3.1** afforded the donor (D) 1-mer (**3.17**), and reaction of **3.11** with **3.6** afforded the acceptor (A) 1-mer (**3.18**, **Scheme 3.7**). Double Sonogashira coupling of **3.15** with **3.1** or **3.6** gave the 2-mers DD and AA (**3.19** and **3.20**, **Scheme 3.8**).

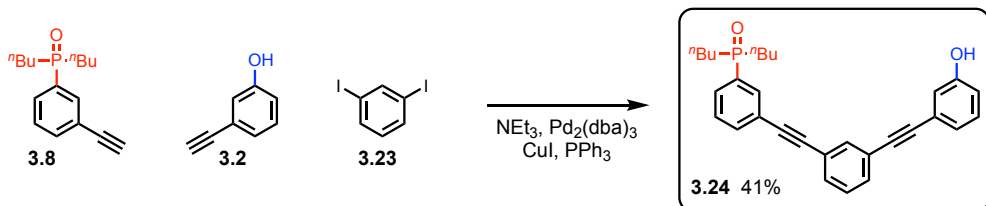
**Scheme 3.7:** Synthesis of D and A 1-mers.**Scheme 3.8:** Synthesis of DD and AA 2-mers.

Two versions of the AD 2-mer were prepared: one with the *S*-(*-*)- β -citronelloxy solubilising group for binding studies (**Scheme 3.9**), and one with no solubilising group for X-ray crystallography (**Scheme 3.10**). Di-halide **3.16** was coupled to **3.6** at the more reactive iodo-position to produce **3.21** in good yield. Reaction of the resulting bromide with **3.1** afforded the AD 2-mer (**3.22**).



Scheme 3.9: Synthesis of AD 2-mer with solubilising group for NMR binding studies.

The AD 2-mer without a solubilising group (**3.24**) was synthesised from a statistical Sonogashira coupling of an equimolar mixture of **3.8**, **3.2** and 1,3-diiodobenzene (**3.23**) followed by separation using column chromatography (**Scheme 3.10**).



Scheme 3.10: Synthesis of AD 2-mer without solubilising group by a statistical Sonogashira coupling. All three possible products were formed and the desired product isolated by column chromatography.

3.3.3 NMR binding studies

NMR titration and dilution experiments were performed to measure the association constants for the A•D, AA•DD and AD•AD complexes in CDCl_3 . For the titrations, the acceptor phosphine oxide was used as the host and the donor phenol as the guest following the change in ^{31}P phosphine oxide signal. A large increase in the chemical shift of the phosphine oxide signal was observed indicating H-bond formation. For the A•D and AA•DD complexes, association constants were determined by fitting ^{31}P NMR titration data to a 1:1 binding

isotherm. Self-association constants for the AD•AD complexes were determined by fitting ^{31}P NMR dilution data to a dimerization isotherm.

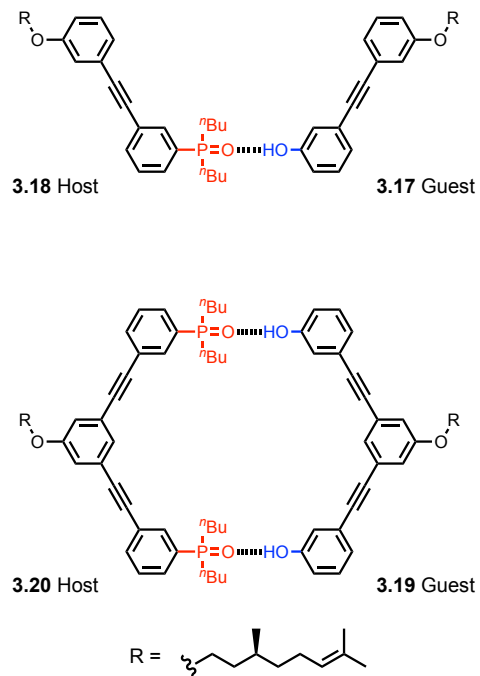


Figure 3.5: A•D and AA•DD complexes for which association constants K were measured by ^{31}P NMR titrations.

The value of K_{ref} was determined by the titration of **3.17** into **3.18** in CDCl_3 (**Figure 3.6**). **Figures 3.6** and **3.7** show the ^{31}P NMR spectra of titrations of duplexes **3.18•3.17** and **3.20•3.19** and the fitting of the complexation induced changes in chemical shift to a 1:1 binding isotherm in CDCl_3 .

In CDCl_3 the free 1-mer phosphine oxide (**3.18**) had a chemical shift of 40.3 ppm, and a predicted limiting bound chemical shift of 45.8 ppm (**Figure 3.6**). The average association constant determined for the A•D complex in CDCl_3 was $30 \pm 1 \text{ M}^{-1}$.

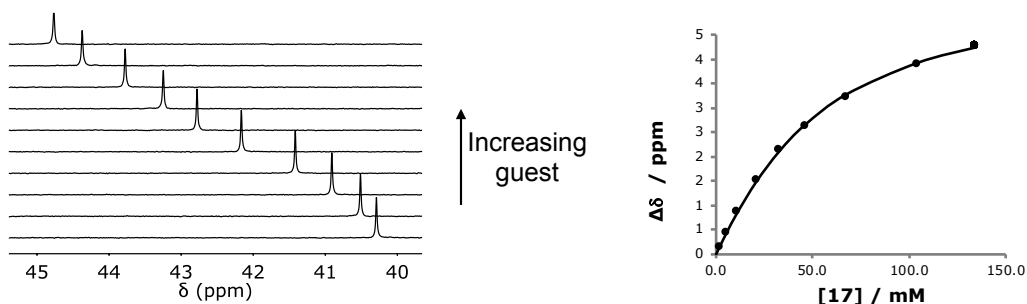


Figure 3.6: ^{31}P NMR data (202 MHz) for titration of **3.17** (D) into **3.18** (A) ($[\text{A}] = 31.9 \text{ mM}$) at 298 K in CDCl_3 . Representative titration spectra and plot of complexation-induced change in chemical shift versus guest concentration (the line represents the best fit to a 1:1 binding isotherm).

In CDCl_3 the free 2-mer phosphine oxide (**3.20**) had a chemical shift of 40.2 ppm, and a predicted limiting bound chemical shift of 44.4 ppm (**Figure 3.7**). The average association constant determined for the AA•DD complex in CDCl_3 was $240 \pm 80 \text{ M}^{-1}$.

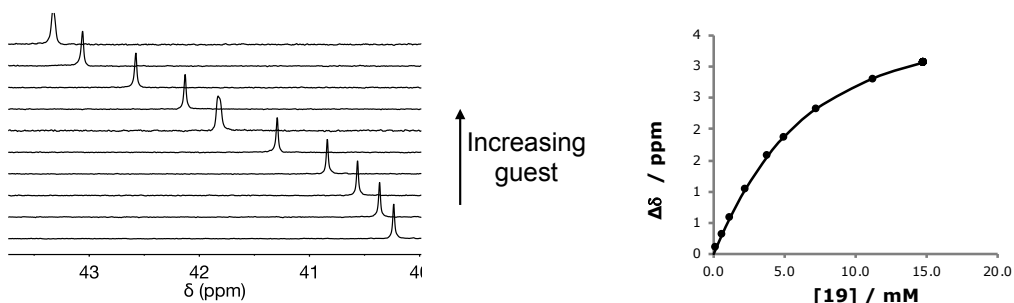
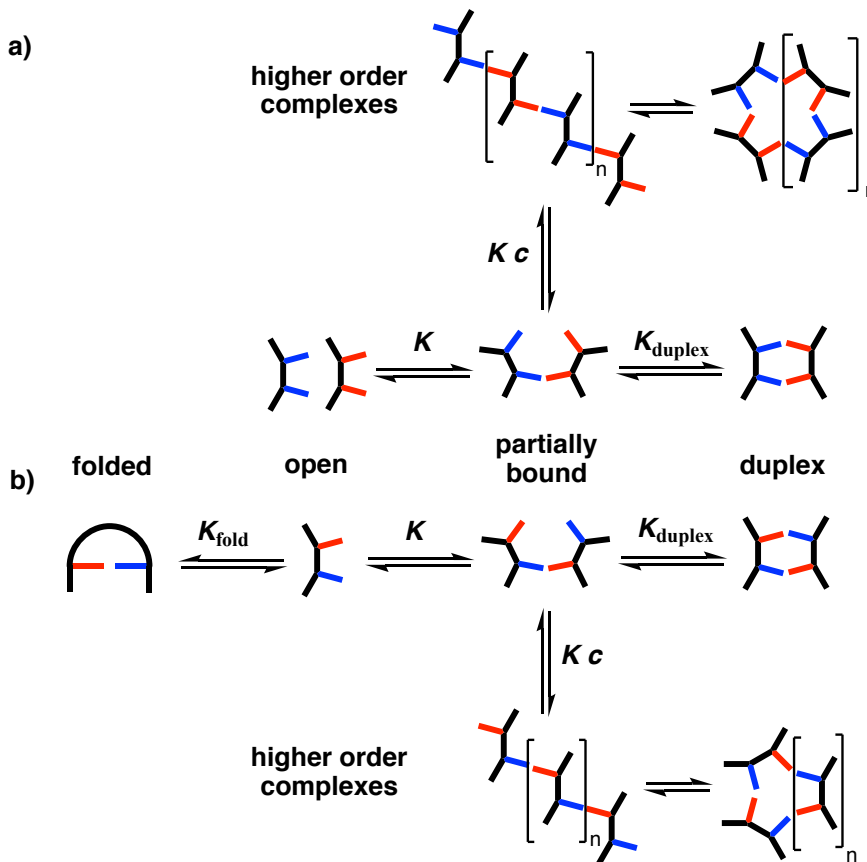


Figure 3.7: ^{31}P NMR data (202 MHz) for titration of **3.19** (DD) into **3.20** (AA) ($[\text{A}] = 3.68 \text{ mM}$) at 298 K in CDCl_3 . Representative titration spectra and plot of complexation-induced change in chemical shift versus guest concentration (the line represents the best fit to a 1:1 binding isotherm).

A 1:1 binding isotherm fit well to the titration data and the association constants, EM and important chemical shifts are reported in **Table 3.1**. The ^{31}P chemical shifts of the free and bound phosphine oxides are almost identical for the 1-mer and 2-mer in CDCl_3 . A large positive change in ^{31}P NMR chemical shift is indicative of H-bond formation, and the results in **Table 3.1** imply that all phosphine oxides are fully bound. The large increase in association constant going

from 1-mer to 2-mer shows strong cooperative duplex formation. EM can be calculated from equation 3.2 and is 134 ± 44 mM in chloroform. The chelate cooperativity associated with duplex assembly (K_{EM}) is 4 ± 1 . A value greater than 1 shows that the duplex is the most populated state. The cooperativity of duplex formation implies that it should be possible to propagate the assembly of longer oligomers using this information oligomer design.

Scheme 3.11 shows the equilibria that are possible for the 2-mer duplexes. Under dilute conditions, the higher order complexes are not expected to be significantly populated. K and K_{duplex} were measured in the 1-mer and 2-mer titrations described above. For the AA•DD complexes, the product KEM_d is greater than 1, which means that the duplex shown in **Scheme 3.11a** is the most populated species for concentrations lower than EM_d . The value of K_{duplex} in **Scheme 3.11** is expected to be similar for the AA•DD and the corresponding AD•AD duplexes. If there are no competing equilibria, then the observed self-association constant for the AD system would be similar to the to the association constant measured for the formation of the corresponding AA•DD duplex. Previous work has found backbone folding and 1,2 H-bond formation between adjacent phenol and phosphine oxide recognition units to be a major problem for other synthetic information molecules.²⁰ 1,2 folding would be fatal for duplex formation as there is no enthalpic advantage over folding, and a larger entropic penalty.



Scheme 3.11: Competing equilibria in the assembly of (a) AA•DD complexes and (b) AD•AD complexes. The equilibrium constants have additional statistical factors that are not shown.

The association constant of unimolecular folding K_{fold} cannot be measured directly but can be calculated from the AD•AD dimerization constant and the association constant for the AA•DD duplex. The dimerization association constant for **3.22** was determined by an NMR dilution experiment. In CDCl_3 the free AD 2-mer phosphine oxide (**3.22**) had a limiting free chemical shift of 40.2 ppm and a predicted limiting bound chemical shift of 44.1 ppm, both extrapolated from the fitting (**Figure 3.8**). These chemical shifts match with the free and bound shifts for the AA 2-mer, showing there is no H-bond formation due to folding in the free state. The dimerization constant for the formation of the AD•AD complex in CDCl_3 was determined to be $130 \pm 30 \text{ M}^{-1}$. The dimerization constant for the formation of the AD•AD complex is the same order of magnitude as the association constant for the AA•AD complex, showing that there is no folding occurring. Folding would cause a decrease in dimerization constant due to competing equilibria. This

structure has a rigid backbone that holds the recognition groups apart, so this result is not unexpected.²⁰

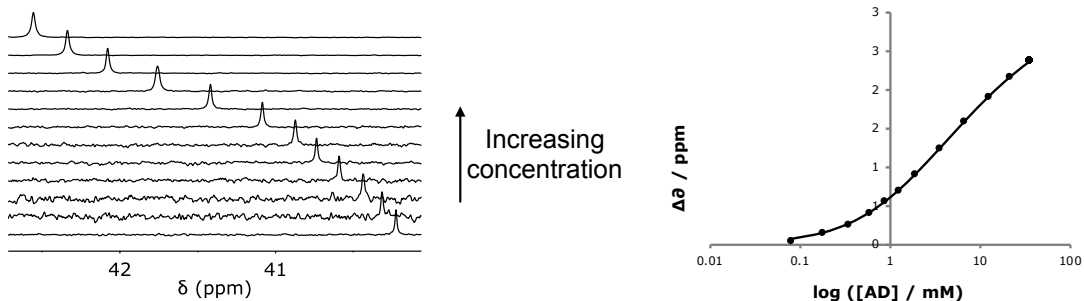


Figure 3.8: ^{31}P NMR data (202 MHz) for dilution of AD 2-mer, **3.22** ($[\text{AD}] = 0.08 - 35.8 \text{ mM}$) at 298 K in CDCl_3 . Representative dilution spectra and plot of complexation-induced change in chemical shift as a log function of guest concentration (the line represents the best fit to a dimerization isotherm).

Table 3.1: Association constants (K_{obs}), effective molarities (EM) and ^{31}P chemical shifts (δ) measured by NMR titrations and dilutions in CDCl_3 at 298 K.

Complex	$K_{\text{obs}} / \text{M}^{-1}$	δ_{free}	δ_{bound}	$\Delta\delta / \text{PPM}$	K_{fold}	$EM_{\text{fold}} / \text{mM}$	$EM_{\text{duplex}} / \text{mM}$
A●D	30 ± 1	40.3	45.8	5.5	-	-	-
AA●DD	240 ± 80	40.2	44.4	4.2	-	-	133 ± 44
AD●AD	130 ± 30	40.2	44.1	3.9	n.d.	n.d.	-

n.d. = not detected. Errors were calculated as two times the standard deviation from the average value (95% confidence limit).

3.3.3 Crystal structure of AD 2-mer

The 2-mer **3.24** was crystallised by slow evaporation from toluene and chloroform. In the crystal structure (**Figure 3.9**) there is no intramolecular H-bonding in the solid state, in agreement with the solution phase NMR results, but a duplex is not observed. Instead, **3.24** crystallises as a linear H-bonded polymer, the state that the AD 2-mers are likely to populate at high concentrations ($c > EM_d$).

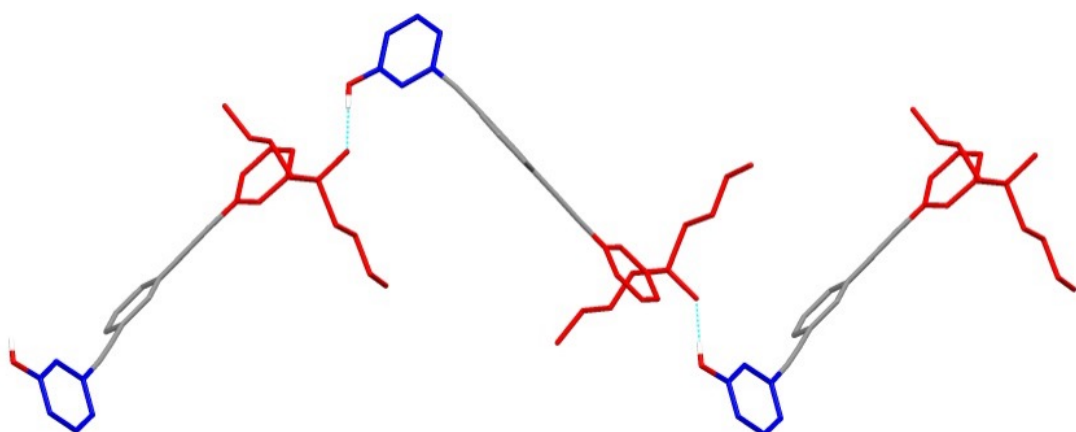


Figure 3.9: Single-crystal X-ray structure of AD 2-mer (**3.24**), which forms a linear H-bonded polymer in the solid state. Three adjacent unit cells with a total of three molecules of **3.24** are shown. Hydrogen atoms have been omitted for clarity. The backbones are shown in grey, the H-bond donor recognition units in dark blue, the H-bond acceptor units in red, and H-bonds in light blue.

3.4 Conclusions

Using a modular description of information molecules inspired by DNA, a new class of information molecule has been designed. Synthesis of appropriate building blocks was completed successfully, and these were used to prepare 1-mers and 2-mers. The coupling chemistry was found to be reliable suggesting synthesis of longer oligomers should be possible.

Binding studies on the A•D, AA•DD and AD•AD duplexes using NMR titrations and dilution experiments found highly cooperative duplex formation in CDCl₃. The increase in binding constant from the 1-mer to 2-mer was found to be an order of magnitude. The effective molarity (EM) for the formation of the second intramolecular H-bond in the 2-mer duplex in CDCl₃ was 133 ± 44 mM. Due to the strong H-bonding between the phosphine oxide and phenol (30 ± 1 M⁻¹ in CDCl₃) the value of K_{EM} was 4 ± 1 in CDCl₃, showing that the fully bound doubly H-bonded duplex is significantly populated. NMR dilution experiments were used to determine the extent of any intramolecular folding in the AD 2-mer, but none was observed. The X-ray crystal structure was obtained for the AD 2-mer analogue lacking a solubilising group, which confirmed the absence of intramolecular folding. The system presented in this chapter appears to be a promising design for a new type of information oligomer.

3.5 Experimental

3.5.1 Synthesis

All the reagents were obtained from commercial sources (Sigma-Aldrich, Alfa Aesar, Fisher Scientific and Fluorochem) and were used without further purification. Thin layer chromatography was carried out using silica gel 60F (Merck) on aluminium. Flash chromatography was carried out on an automated system (Combiflash Rf+ or Combiflash Rf Lumen) using prepacked cartridges of silica (25 μ or 50 μ PuriFlash® Columns). ^1H and ^{13}C NMR spectra were recorded on either a Bruker AV3400 or AV3500 spectrometer at 298 K unless specifically stated otherwise. Residual solvent was used as an internal standard. All chemical shifts are quoted in ppm on the δ scale and the coupling constants expressed in Hz. Signal splitting patterns are described as follows: s (singlet), d (doublet), t (triplet), q (quartet), m (multiplet). ES+ mass spectra were obtained on a Waters LCT premier mass spectrometer. FTIR spectra were recorded on a PerkinElmer Spectrum One FT-IR spectrometer. Melting points were recorded on a Mettler Toledo MP90 melting point apparatus and are reported as an uncorrected range of three repeats. Optical rotations were measured on an Anton-Paar MCP 100 digital polarimeter with a sodium lamp (589 nm). ES+ was carried out on a Waters LCT-TOF spectrometer or a Waters Xevo G2-S bench top QTOF machine.

Dibutylphosphine oxide (**3.4**)

A flask, evacuated and filled with nitrogen (x3) was charged with nBuMgCl (2M in Et_2O , 23.3 mL, 46.5 mmol) and the solution cooled to 0 °C. A solution of diethylphosphite (2.00 mL, 15.5 mmol) in THF (24 mL) was added dropwise over 15 min. The reaction was stirred at 0 °C for 15 min then at room temperature for 2 hr. Reaction was cooled to 0 °C and 0.1 M HCl (30 mL) added over 15 min. CH_2Cl_2 (30 mL) was added and mixture stirred for 10 min. The reaction was filtered under vacuum through celite and layers separated. The organic layer was dried (MgSO_4) and solvent removed by rotary evaporation under reduced pressure. Azeotrope with hexane (2x 30 mL) yielded **3.4** as an amorphous white solid (2.36 g, 14.5 mmol, 94% yield).

TLC R_f : 0.00 (EtOAc:40-60 pet. ether 1:1);

Melting Point: 56.5-59.2 °C;

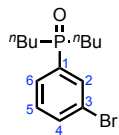
$^1\text{H NMR}$ (400 MHz, CDCl_3): δ 6.86 (d, J = 446.5 Hz, 1H, PH), 1.89-1.69 (m, 4H, nBu), 1.69-1.52 (m, 4H, nBu), 1.52-1.38 (m, 4H, nBu), 0.94 (t, J = 8.0 Hz, 6H, nBu);

$^{13}\text{C NMR}$ (101 MHz, CDCl_3): δ 28.7 (d, J = 93.0 Hz, nBu), 24.0 (d, J = 15.0 Hz, nBu), 23.6 (d, J = 4.0 Hz, nBu), 13.6 (nBu);

$^{31}\text{P NMR}$ (162 MHz, CDCl_3): δ 35.0 (phosphine oxide);

FT-IR (ATR): 3323 (br), 1635 (br) $\nu_{\text{max}}/\text{cm}^{-1}$.

Matches previously reported spectral data³⁷

(3-bromophenyl)dibutylphosphine oxide (**3.6**)

3.5 (250 mg, 1.55 mmol) was added to a dried flask and the flask evacuated and back-filled with nitrogen (x3). m-bromoiodobenzene (0.217 mL, 1.71 mmol) was added and 1,4-dioxane (deoxygenated by freeze-pump-thaw, 4 mL) was added. In a separate flask, Pd₂(dba)₃ (31.0 mg, 34.2 µmol) and Xantphos (20.0 mg, 34.2 µmol) were placed in a flask and evacuated and back-filled with nitrogen (x3). These were dissolved in 1,4-dioxane (3 mL) and the solution transferred to the initial flask. Et₃N (0.230 mL, 1.55 mmol) was added and the reaction stirred at room temperature for 2 hr. CH₂Cl₂ (20 mL) was added and the reaction washed with NaHCO₃ (25 mL). The aqueous layer was extracted with CH₂Cl₂ (3x 10 mL), combined organics dried (MgSO₄) and solvent removed by rotary evaporation under reduced pressure yielding a brown solid (680 mg). This solid was separated by flash chromatography (MeOH:CH₂Cl₂, 1:19) to yield the desired compound **3.6** as a yellow oil (459 mg, 1.45 mmol, 93% yield).

TLC R_f: 0.37 (MeOH:CH₂Cl₂ 1:9);

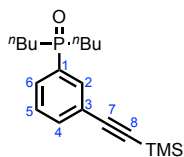
¹H NMR (400 MHz, CDCl₃): δ 7.83 (dt, *J* = 10.5, 1.5 Hz, 1H, 2-H), 7.67-7.63 (m, 1H, 4-H), 7.63-7.57 (m, 1H, 6-H), 7.36 (td, *J* = 8.0, 3.0 Hz, 1H, 5-H), 2.04-1.75 (m, 4H, *n*Bu), 1.69-1.30 (m, 8H, *n*Bu), 0.87 (t, *J* = 8.0 Hz, 6H, *n*Bu);

¹³C NMR (101 MHz, CDCl₃): δ 135.6 (d, *J* = 89.0 Hz, 1-C), 134.5 (d, *J* = 3.0 Hz, 4-C), 133.2 (d, *J* = 9.0 Hz, 2-C), 130.3 (d, *J* = 12.0 Hz, 5-C), 128.9 (d, *J* = 9.0 Hz 6-C), 123.3 (d, *J* = 14.0 Hz, 3-C), 29.7 (d, *J* = 65.0 Hz, *n*Bu), 24.1 (d, *J* = 14.0 Hz, *n*Bu), 23.5 (d, *J* = 4.0 Hz, *n*Bu), 13.6 (*n*Bu);

³¹P NMR (162 MHz, CDCl₃): δ 39.8 (phosphine oxide);

FT-IR (ATR): 2956, 2932, 2871, 1465, 1398, 1169 $\nu_{\text{max}}/\text{cm}^{-1}$;

HRMS (ES+): C₁₄H₂₃⁷⁹BrOP calcd. 317.0670 found 317.0668, Δ = -0.6 ppm.

Dibutyl(3-((trimethylsilyl)ethynyl)phenyl)phosphine oxide (**3.7**)

3.6 (317 mg, 1.00 mmol), Pd₂(dba)₃ (18.0 mg, 20.0 μmol), CuI (4.00 mg, 20.0 μmol) and PPh₃ (26.0 mg, 0.100 mmol) were added to a flask of Et₃N (5 mL) and DMF (5 mL). N₂ was bubbled through the reaction for 15 min. TMSA (0.170 mL, 1.20 mmol) was added and the reaction stirred at 50 °C for 4 hr in the dark under N₂. The reaction was filtered through celite and washed through with EtOAc (30 mL). The solution was washed with 1 M HCl (3x 30 mL) and 5% LiCl solution (2x 30mL). The solution was dried (MgSO₄) and solvent was removed by rotary evaporation under reduced pressure yielding a brown oil (280 mg). This solid was separated by flash chromatography (MeOH:CH₂Cl₂ 1:19) to yield the desired compound **3.7** as a brown oil (268 mg, 0.80 mmol, 80% yield).

TLC R_f: 0.28 (MeOH:CH₂Cl₂ 1:19);

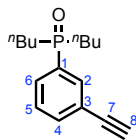
¹H NMR (400 MHz, CDCl₃): δ 7.74 (dt, *J* = 11.0, 1.5 Hz, 1H, 2-H), 7.63 (ddt, *J* = 10.5, 7.5, 1.5 Hz, 1H, 6-H), 7.57 (dd, *J* = 8.0, 1.5 Hz, 1H, 4-H), 7.40 (td, *J* = 8.0, 2.5 Hz, 1H, 5-H), 2.06 – 1.75 (m, 4H, ⁿBu), 1.70 – 1.44 (m, 2H, ⁿBu), 1.45 – 1.27 (m, 6H, ⁿBu), 0.84 (t, *J* = 7.0 Hz, 6H, ⁿBu), 0.23 (s, 9H, TMS);

¹³C NMR (101 MHz, CDCl₃): δ 134.7 (d, *J* = 3.0 Hz, 4-C), 133.6 (d, *J* = 10.0 Hz, 2-C), 132.8 (d, *J* = 91.0 Hz, 1-C), 130.2 (d, *J* = 8.0 Hz, 6-C), 128.5 (d, *J* = 12 Hz, 5-C), 123.8 (d, *J* = 12 Hz, 3-C), 103.8 (7-C), 95.9 (8-C), 29.5 (d, *J* = 69.0 Hz, ⁿBu), 24.0 (d, *J* = 14.0 Hz, ⁿBu), 23.4 (d, *J* = 4.0 Hz, ⁿBu), 13.5 (ⁿBu), -0.17 (TMS);

³¹P NMR (162 MHz, CDCl₃): δ 41.3 (phosphine oxide);

FT-IR (ATR): 2958, 2930, 2163, 1467, 1400, 1164, 842, 759, 693 $\nu_{\text{max}}/\text{cm}^{-1}$;

HRMS (ES+): C₁₉H₃₂OPSi calcd. 335.1960 found 335.1956, Δ = -1.2 ppm.

Dibutyl(3-ethynylphenyl)phosphine oxide (**3.8**)

3.7 (365 mg, 0.859 mmol) was dissolved in dry THF (29 mL) and reaction purged with nitrogen. Reaction was cooled to 0 °C and TBAF (1M in THF, 1.89 mL, 1.89 mmol) added. Reaction was stirred for 10 min, then diluted with EtOAc (50 mL). This solution was washed with 1M HCl (3x 50 mL), dried (MgSO_4), and the solvent was removed by rotary evaporation under reduced pressure yielding **3.8** as a brown oil (230 mg, 0.820 mmol, 95% yield).

TLC R_f : 0.28 (MeOH:CH₂Cl₂ 1:19);

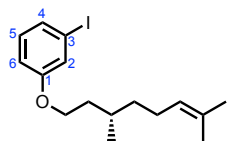
¹H NMR (400 MHz, CDCl₃): δ 7.80 (dt, J = 11.0, 1.5 Hz, 1H, 2-H), 7.73 (ddt, J = 10.5, 7.5, 1.5 Hz, 1H, 6-H), 7.65 (dd, J = 8.0, 1.5 Hz, 1H, 4-H), 7.48 (td, J = 8.0, 2.5 Hz, 1H, 5-H), 3.17 (s, 1H, 8-H), 2.06 – 1.78 (m, 4H, ⁿBu), 1.61 – 1.55 (m, 2H, ⁿBu), 1.48 – 1.33 (m, 6H, ⁿBu), 0.89 (t, J = 7.0 Hz, 6H, ⁿBu);

¹³C NMR (101 MHz, CDCl₃): δ 134.9 (d, J = 3.0 Hz, 4-C), 133.7 (d, J = 10.0 Hz, 2-C), 133.3 (d, J = 91.0 Hz, 1-C), 133.7 (d, J = 8.0 Hz, 6-C), 128.7 (d, J = 12.0 Hz, 5-C), 125.0 (d, J = 12.0 Hz, 3-C), 122.9 (7-C), 78.5 (6-C), 29.6 (d, J = 69.0 Hz, ⁿBu), 24.1 (d, J = 14.0 Hz, ⁿBu), 23.5 (d, J = 4.0 Hz, ⁿBu), 13.6 (ⁿBu);

³¹P NMR (162 MHz, CDCl₃): δ 40.2 (phosphine oxide);

FT-IR (ATR): 2958, 2930, 2163, 1467, 1400, 1164, 842, 759, 693 $\nu_{\text{max}}/\text{cm}^{-1}$;

HRMS (ES+): C₁₆H₂₄OP calcd. 263.1565 found 263.1563, Δ = -0.8 ppm.

(S)-1-(3,7-dimethyloct-6-en-1-yl)oxy)-3-iodobenzene (3.9)

3-iodophenol (1.00 g, 4.55 mmol), *S*-(*-*)- β -citronellol (1.66 mL, 9.09 mmol) and PPh₃ (1.55 g, 5.91 mmol) were dissolved in dry THF (30 mL) under N₂. Diisopropyl azodicarboxylate (1.17 mL, 5.91 mmol) was added slowly at 0 °C. The reaction was allowed to warm to room temperature and was stirred overnight under N₂. The solvent was removed by rotary evaporation under reduced pressure yielding a brown solid (3.12 g). This solid was separated by flash chromatography (40-60 pet. ether) to yield the desired compound **3.9** as a light-yellow oil (1.55 g, 4.33 mmol, 95% yield).

TLC R_f: 0.58 (40-60 pet. ether);

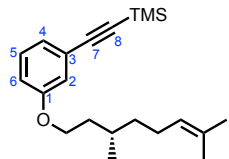
[α]_D²⁰ = -4.27 (*c* 1.02, CHCl₃);

¹H NMR (400 MHz, CDCl₃): δ 7.27 (d, *J* = 8.0 Hz, 1H, 4-H), 7.26 (s, 1H, 2-H), 6.99 (t, *J* = 8.0 Hz, 1H, 5-H), 6.86 (m, 1H, 6-H), 5.14 – 5.06 (m, 1H, Sol), 4.00 – 3.89 (m, 2H, Sol), 2.08 – 1.92 (m, 2H, Sol), 1.85 – 1.76 (m, 1H, Sol), 1.69 (s, 3H, Sol), 1.68 – 1.63 (m, 1H, Sol), 1.61 (s, 3H, Sol), 1.60 – 1.55 (m, 1H, Sol), 1.42 – 1.33 (m, 1H, Sol), 1.28 – 1.18 (m, 1H, Sol), 0.95 (d, *J* = 6.5 Hz, 3H, Sol);

¹³C NMR (101 MHz, CDCl₃): δ 159.7 (1-C), 131.4 (Sol), 130.7 (H 5-C), 129.6 (4-C), 124.6 (Sol), 123.6 (2-C), 114.2 (6-C), 94.4 (3-C), 66.5 (Sol), 37.1 (Sol), 36.0 (Sol), 29.5 (Sol), 25.8 (Sol), 25.5 (Sol), 19.6 (Sol), 17.7 (Sol);

FT-IR (ATR): 2958, 2923, 2873, 1584, 1567, 1467, 1241, 1224 $\nu_{\text{max}}/\text{cm}^{-1}$;

HRMS (ES+): C₁₆H₂₄IO calcd. 359.0872 found 359.0861, Δ = -3.1 ppm.

(S)-((3-(3,7-dimethyloct-6-en-1-yl)oxy)phenyl)ethynyl)trimethylsilane (3.10**)**

3.9 (1.00 g, 2.79 mmol), Pd₂(dba)₃ (51.0 mg, 55.8 µmol), CuI (10.0 mg, 55.8 µmol) and PPh₃ (73.0 mg, 0.279 mmol) were added to a flask of Et₃N (18 mL) and N₂ bubbled through the reaction for 15 min. TMSA (0.440 mL, 3.07 mmol) was added and the reaction stirred at room temperature for 4 hr in the dark under N₂. The reaction was filtered through celite and washed through with EtOAc (50 mL). The solution was washed with 1 M HCl (3x 50 mL). The solution was dried (MgSO₄) and solvent was removed by rotary evaporation under reduced pressure yielding a brown solid (1.13 g). This solid was separated by flash chromatography (40-60 pet. ether) to yield the desired compound **3.10** as a light-yellow oil (860 mg, 2.62 mmol, 94% yield).

TLC R_f: 0.32 (40-60 pet. ether);

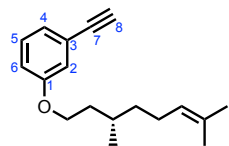
[α]_D²⁰ = -5.48 (c 0.91, CHCl₃);

¹H NMR (400 MHz, CDCl₃): δ 7.18 (t, *J* = 8.0 Hz, 1H, 5-H), 7.04 (dt, *J* = 8.0, 1.0 Hz, 4-H), 6.99 (dd, *J* = 2.5, 1.0 Hz, 2-H), 6.86 (ddd, *J* = 8.0, 2.5, 1.0 Hz, 6-H), 5.15 – 5.07 (m, 1H, Sol), 4.01 – 3.93 (m, 2H, Sol), 2.10 – 1.92 (m, 2H, Sol), 1.88 – 1.76 (m, 1H, Sol), 1.69 (s, 3H, Sol), 1.68 – 1.63 (m, 1H, Sol), 1.61 (s, 3H, Sol), 1.60 – 1.55 (m, 1H, Sol), 1.42 – 1.33 (m, 1H, Sol), 1.28 – 1.18 (m, 1H, Sol), 0.95 (d, *J* = 6.5 Hz, 3H, Sol), 0.25 (s, 9H, TMS);

¹³C NMR (101 MHz, CDCl₃): δ 158.8 (1-C), 131.3 (Sol), 129.2 (5-C), 124.6 (Sol), 124.3 (4-C), 124.0 (3-C), 117.2 (2-C), 115.9 (6-C), 105.1 (7-C), 93.8 (8-C), 66.3 (Sol), 37.1 (Sol), 36.1 (Sol), 29.5 (Sol), 25.7 (Sol), 25.5 (Sol), 19.6 (Sol), 17.7 (Sol), -0.01 (TMS);

FT-IR (ATR): 2959, 2925, 1596, 1574, 1249, 1156, 934 $\nu_{\text{max}}/\text{cm}^{-1}$;

HRMS (ES+): C₂₁H₃₃OSi calcd. 329.2301 found 329.2301, Δ = 0.00 ppm.

(S)-1-((3,7-dimethyloct-6-en-1-yl)oxy)-3-ethynylbenzene (3.11)

3.10 (350 mg, 1.07 mmol) was dissolved in dry THF (30 mL) and reaction purged with nitrogen. Reaction was cooled to 0 °C and TBAF (1M in THF, 2.13 mL, 2.13 mmol) added. Reaction was stirred for 10 min and filtered through a plug of silica, washing through EtOAc:pet. ether (1:49). The solvent was removed by rotary evaporation under reduced pressure yielding **3.11** as a yellow oil (270 mg, 1.05 mmol, 99% yield).

TLC R_f : 0.17 (40-60 pet. ether);

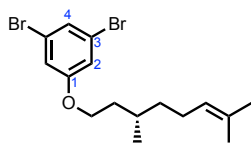
[α]_D²⁰ = -5.98 (*c* 0.93, CHCl₃);

¹H NMR (400 MHz, CDCl₃): δ 7.21 (t, *J* = 8.0 Hz, 1H, 5-H), 7.07 (dt, *J* = 8.0, 1.0 Hz 1H, 4-H), 7.01 (dd, *J* = 2.5, 1.0 Hz, 1H, 2-H), 6.90 (ddd, *J* = 8.0, 2.5, 1.0 Hz, 1H, 6-H), 5.14 – 5.07 (m, 1H, Sol), 4.03 – 3.93 (m, 2H, Sol) 3.05 (s, 1H, 8-H), 2.10 – 1.92 (m, 2H, Sol), 1.88 – 1.76 (m, 1H, Sol), 1.69 (s, 3H, Sol), 1.68 – 1.63 (m, 1H, Sol), 1.61 (s, 3H, Sol), 1.60 – 1.55 (m, 1H, Sol), 1.42 – 1.33 (m, 1H, Sol), 1.28 – 1.18 (m, 1H, Sol), 0.95 (d, *J* = 6.5 Hz, 3H, Sol);

¹³C NMR (101 MHz, CDCl₃): δ 158.8 (1-C), 131.3 (Sol), 129.3 (5-C), 124.6 (Sol), 124.4 (4-C), 123.0 (3-C), 117.6 (2-C), 116.0 (6-C), 83.7 (7-C), 76.8 (8-C), 66.5 (Sol), 37.1 (Sol), 36.1 (Sol), 29.5 (Sol), 25.7 (Sol), 25.5 (Sol), 19.5 (Sol), 17.7 (Sol);

FT-IR (ATR): 3299, 2961, 2915, 1975, 1575, 1474, 1257, 1145 ν_{max} /cm⁻¹;

HRMS (ES+): C₁₈H₂₅O calcd. 257.1905 found 257.1905, Δ = 0.00 ppm.

(*S*)-((1,3-dibromo-5-(3,7-dimethyloct-6-en-1-yl)oxy)benzene (3.13**)**

3,5-dibromophenol (3.00 g, 11.9 mmol), *S*-(-)- β -citronellol (4.34 mL, 23.8 mmol) and PPh₃ (4.14 mg, 15.8 mmol) were dissolved in dry THF (90 mL) under N₂. Diisopropyl azodicarboxylate (3.11 mL, 15.8 mmol) was added slowly at 0 °C. The reaction was allowed to warm to room temperature and was stirred overnight under N₂. The solvent was removed by rotary evaporation under reduced pressure yielding a brown solid (6.10 g). This solid was separated by flash chromatography (40-60 pet. ether) to yield the desired compound **3.13** as a yellow oil (4.55 g, 11.7 mmol, 98% yield).

TLC R_f: 0.60 (40-60 pet. ether);

[α]_D²⁰ = -4.11 (c 1.31, CHCl₃);

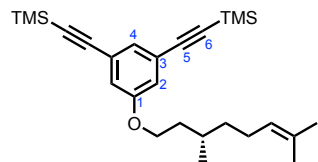
¹H NMR (400 MHz, CDCl₃): δ 7.23 (t, *J* = 1.5 Hz, 1H, 4-H), 6.98 (d, *J* = 1.5 Hz, 2H, 2-H), 5.14 – 5.06 (m, 1H, Sol), 4.00 – 3.89 (m, 2H, Sol), 2.08 – 1.92 (m, 2H, Sol), 1.85 – 1.76 (m, 1H, Sol), 1.69 (s, 3H, Sol), 1.68 – 1.63 (m, 1H, Sol), 1.61 (s, 3H, Sol), 1.60 – 1.55 (m, 1H, Sol), 1.42 – 1.33 (m, 1H, Sol), 1.28 – 1.18 (m, 1H, Sol), 0.95 (d, *J* = 6.5 Hz, 3H, Sol);

¹³C NMR (101 MHz, CDCl₃): δ 160.3 (1-C), 131.4 (Sol), 126.2 (4-C), 124.5 (Sol), 123.1 (3-C), 116.9 (2-C), 66.9 (Sol), 37.0 (Sol), 35.9 (Sol), 29.4 (Sol), 25.7 (Sol), 25.4 (Sol), 19.5 (Sol), 17.7 (Sol);

FT-IR (ATR): 2955, 2913, 1583, 1557, 1437, 1254, 828 $\nu_{\text{max}}/\text{cm}^{-1}$;

HRMS (ES+): C₁₆H₂₂⁷⁹Br₂O calcd. 386.9954 found 386.9960, Δ = 1.59 ppm.

(*S*)-((5-((3,7-dimethyloct-6-en-1-yl)oxy)1,3-phenylene)bis(ethyne-2,1-diyl))bis(trimethylsilane) (**3.14**)



3.13 (1.00 g, 2.56 mmol), Pd₂(dba)₃ (94.0 mg, 0.103 mmol), CuI (20.0 mg, 0.103 mmol) and PPh₃ (134 mg, 0.513 mmol) were added to a flask of Et₃N (17 mL) and N₂ bubbled through the reaction for 15 min. TMSA (0.870 mL, 6.15 mmol) was added and the reaction heated to 95 °C for 15 min by microwave. The reaction was filtered through celite and washed through with EtOAc (80 mL). The solution was washed with 1 M HCl (3x 50 mL). The solution was dried (MgSO₄) and the solvent was removed by rotary evaporation under reduced pressure yielding a yellow liquid (1.26 g). This solid was separated by flash chromatography (40-60 pet. ether) to yield the desired compound **3.14** as a light-yellow oil (1.07 g, 2.51 mmol, 98% yield).

TLC R_f: 0.57 (40-60 pet. ether);

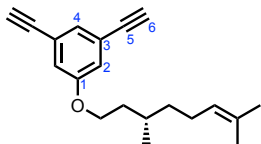
[α]_D = -3.51 (*c* 1.03, CHCl₃);

¹H NMR (400 MHz, CDCl₃): δ 7.18 (t, *J* = 1.5, Hz, 1H, 4-H), 6.93 (d, *J* = 1.5 Hz, 2H, 2-H), 5.13 – 5.07 (m, 1H, Sol), 3.99 – 3.92 (m, 2H, Sol), 2.09 – 1.92 (m, 2H, Sol), 1.85 – 1.76 (m, 1H, Sol), 1.69 (s, 3H, Sol), 1.68 – 1.63 (m, 1H, Sol), 1.61 (s, 3H, Sol), 1.60 – 1.55 (m, 1H, Sol), 1.42 – 1.33 (m, 1H, Sol), 1.28 – 1.18 (m, 1H, Sol), 0.95 (d, *J* = 6.5 Hz, 3H, Sol), 0.24 (s, 18H, TMS);

¹³C NMR (101 MHz, CDCl₃): δ 158.6 (1-C), 131.3 (Sol), 128.0 (4-C), 124.6 (Sol), 124.2 (3-C), 118.3 (2-C), 104.1 (5-C), 94.5 (6-C), 66.7 (Sol), 37.0 (Sol), 35.9 (Sol), 29.7 (Sol), 25.7 (Sol), 25.4 (Sol), 19.5 (Sol), 17.7 (Sol), -0.09 (TMS);

FT-IR (ATR): 2961, 2929, 1578, 1249, 1156, 837, 758 $\nu_{\text{max}}/\text{cm}^{-1}$;

HRMS (ES+): C₂₆H₄₁OSi₂ calcd. 425.2696 found 425.2698, Δ = 0.5 ppm.

(S)-1-((3,7-dimethyloct-6-en-1-yl)oxy)-3,5-diethynylbenzene (3.15)

3.14 (365 mg, 0.859 mmol) was dissolved in dry THF (29 mL) and reaction purged with nitrogen. Reaction was cooled to 0 °C and TBAF (1M in THF, 1.89 mL, 1.89 mmol) added. Reaction was stirred for 10 min and filtered through a plug of silica, washing through with pet. ether. The solvent was removed by rotary evaporation under reduced pressure yielding **3.15** as a brown oil (230 mg, 0.820 mmol, 95% yield).

TLC R_f : 0.40 (40-60 pet. ether);

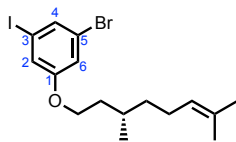
[α]D = -4.44 (c 0.70, CHCl3);

1H NMR (400 MHz, CDCl3): δ 7.20 (t, J = 1.5, Hz, 1H, 4-H), 7.00 (d, J = 1.5 Hz, 2H, 2-H), 5.13 – 5.07 (m, 1H, Sol), 3.99 – 3.92 (m, 2H, Sol) 3.05 (s, 2H, 6-H), 2.09 – 1.92 (m, 2H, Sol), 1.85 – 1.76 (m, 1H, Sol), 1.69 (s, 3H, Sol), 1.68 – 1.63 (m, 1H, Sol), 1.61 (s, 3H, Sol), 1.60 – 1.55 (m, 1H, Sol), 1.42 – 1.33 (m, 1H, Sol), 1.28 – 1.18 (m, 1H, Sol), 0.95 (d, J = 6.5 Hz, 3H, Sol);

13C NMR (101 MHz, CDCl3): δ 158.7 (1-C), 131.4 (Sol), 128.1 (4-C), 124.6 (Sol), 123.3 (3-C), 118.9 (2-C), 82.64 (5-C), 77.52 (6-C), 66.6 (Sol), 37.1 (Sol), 35.9 (Sol), 29.5 (Sol), 25.7 (Sol), 25.4 (Sol), 19.5 (Sol), 17.7 (Sol);

FT-IR (ATR): 3297, 2960, 2925, 1579, 1420, 1321, 1294, 1158 ν_{max} /cm⁻¹;

HRMS (ES+): C₂₀H₂₅O calcd. 281.1905 found 281.1905, Δ = 3.6 ppm.

(S)-1-bromo -3-(3,7-dimethyloct-6-en-1-yl)oxy)-5-iodobenzene (3.16)

3.13 (1.00 g, 2.56 mmol) was dissolved in dry Et₂O (30 mL) in a dried flask. The reaction was cooled to -78 °C. ⁿBuLi (1.6 M in hexanes, 1.76 mL, 2.82 mmol) was added slowly over 1 hr, and the reaction was stirred for 1 hr at -78 °C. A solution of I₂ (1.30 g, 5.13 mmol) in dry Et₂O (5 mL) was added and reaction stirred at -78 °C for 1 hr before being allowed to warm to room temperature over 1 hr. Saturated Na₂S₂O₃ (30 mL) solution was added and reaction stirred until colourless. The organic phase was separated and washed with water (2x 30 mL) and brine (30 mL). The solution was dried (MgSO₄) and the solvent was removed by rotary evaporation under reduced pressure yielding crude product (1.08 g). This oil was separated by flash chromatography (40-60 pet. ether) to yield the desired compound **3.16** as a light-yellow oil (972 mg, 2.22 mmol, 87% yield).

TLC R_f: 0.55 (40-60 Pet. Ether);

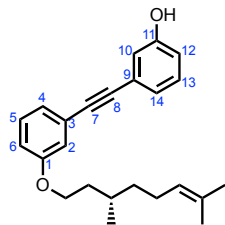
[α]_D²⁰ = -3.72 (*c* 1.26, CHCl₃);

¹H NMR (400 MHz, CDCl₃): δ 7.42 (dd, *J* = 1.5, 1.5 Hz, 1H, 4-H), 7.17 (dd, *J* = 2.0, 1.5 Hz, 1H, 2-H), 7.01 (dd, *J* = 2.0, 1.5 Hz, 1H, 6-H), 5.15 – 5.04 (m, 1H, Sol), 3.99 – 3.88 (m, 2H, Sol), 2.10 – 1.90 (m, 2H, Sol), 1.87 – 1.75 (m, 1H, Sol), 1.69 (s, 3H, Sol), 1.68 – 1.63 (m, 1H, Sol), 1.61 (s, 3H, Sol), 1.60 – 1.55 (m, 1H, Sol), 1.42 – 1.33 (m, 1H, Sol), 1.28 – 1.18 (m, 1H, Sol), 0.95 (d, *J* = 6.5 Hz, 3H, Sol), 0.24 (s, 9H, Sol);

¹³C NMR (101 MHz, CDCl₃): δ 160.1 (1-C), 131.8 (4-C), 131.4 (Sol), 124.5 (Sol), 123.1 (5-C), 122.8 (2-C), 117.6 (6-C), 94.2 (3-C), 66.9 (Sol), 37.0 (Sol), 35.9 (Sol), 29.4 (Sol), 25.8 (Sol), 25.4 (Sol), 19.5 (Sol), 17.7 (Sol);

FT-IR (ATR): 2962, 2914, 1577, 1550, 1433, 1228, 829 $\nu_{\text{max}}/\text{cm}^{-1}$;

HRMS (ES+): C₁₆H₂₂BrIO calcd. 436.9977 found 436.9971, Δ = -1.4 ppm.

(S)-3-((3-((3,7-dimethyloct-6-en-1-yl)oxy)phenyl)ethynyl)phenol (3.17)

3.11 (350 mg, 1.37 mmol), 3-iodophenol (301 mg, 1.37 mmol), $\text{Pd}_2(\text{dba})_3$ (25 mg, 27.0 μmol), CuI (5 mg, 27.0 μmol) and PPh_3 (36.0 mg, 0.137 mmol) were added to a flask of Et_3N (9 mL) and N_2 bubbled through the reaction for 15 min. The reaction was stirred at room temperature for 4 hr in the dark under N_2 . The reaction was filtered through celite and washed through with EtOAc (30 mL). The solution was washed with 1 M HCl (3x 30 mL). The solution was dried (MgSO_4) and the solvent was removed by rotary evaporation under reduced pressure yielding a brown solid (680 mg). This solid was separated by flash chromatography ($\text{EtOAc}:40\text{-}60$ pet. ether, 1:4) to yield the desired compound **3.17** as a brown solid (442 mg, 1.27 mmol, 93% yield).

TLC R_f : 0.17 ($\text{EtOAc}:40\text{-}60$ pet. ether 1:9);

Melting Point: 40.4-43.1 °C;

$[\alpha]_D = -4.54$ (*c* 0.48, CHCl_3);

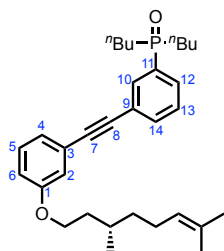
$^1\text{H NMR}$ (400 MHz, CDCl_3): δ 7.27 – 7.17 (m, 2H, 5, 13-H), 7.14 – 7.09 (m, 2H, 4, 14-H), 7.06 (dd, 1H, J = 2.5, 1.5 Hz, 2-H), 7.00 (dd, 1H, J = 2.5, 1.5 Hz, 10-H), 6.90 (ddd, 1H, J = 8.5, 2.5, 1.0 Hz, 6-H), 6.82 (ddd, 1H, J = 8.0, 2.5, 1.0 Hz, 12-H), 5.13 – 5.07 (m, 1H, Sol), 4.99 (bs, 1H, OH), 4.01 – 3.91 (m, 2H, Sol), 2.09 – 1.92 (m, 2H, Sol), 1.85 – 1.76 (m, 1H, Sol), 1.70 (s, 3H, Sol), 1.60 – 1.63 (m, 1H, Sol), 1.62 (s, 3H, Sol), 1.60 – 1.55 (m, 1H, Sol), 1.42 – 1.33 (m, 1H, Sol), 1.28 – 1.18 (m, 1H, Sol), 0.96 (d, J = 6.5 Hz, 3H, Sol);

$^{13}\text{C NMR}$ (101 MHz, CDCl_3): δ 158.9 (1-C), 155.3 (11-C), 131.4 (Sol), 129.7 (5-C), 129.4 (13-C), 124.7 (Sol), 124.5 (3-C), 124.4 (9-C), 124.1 (4-C), 124.0 (14-C), 118.2 (10-C), 117.0 (2-C), 115.8 (12-C), 115.6 (6-C), 89.5 (7-C), 88.7 (8-C), 66.4 (Sol), 37.1 (Sol), 36.1 (Sol), 29.5 (Sol), 25.8 (Sol), 25.5 (Sol), 19.6 (Sol), 17.7 (Sol);

FT-IR (ATR): 3365 (br), 2911, 1612, 1574, 1496, 1324, 1189 $\nu_{\text{max}}/\text{cm}^{-1}$;

HRMS (ES+): C₂₄H₂₈O₂ calcd. 349.2155 found 349.2162, $\Delta = -2.08$ ppm.

(*S*)-dibutyl(3-((3-((3,7-dimethyloct-6-en-1-yl)oxy)phenyl)ethynyl)phenyl)phosphine oxide (**3.18**)



3.11 (103 mg, 0.400 mmol), **3.4** (152 mg, 0.480 mmol), Pd₂(dba)₃ (7.30 mg, 8.00 μmol), CuI (1.50 mg, μmol) and PPh₃ (10.5 mg, 40.0 μmol) were added to a flask of Et₃N (4 mL) and N₂ bubbled through the reaction for 15 min. The reaction was heated to 95 °C by microwave irradiation for 10 min. The reaction was filtered through celite and washed through with EtOAc (10 mL). The solution was washed with 1 M HCl (3x 10 mL). The solution was dried (MgSO₄) and the solvent was removed by rotary evaporation under reduced pressure yielding a brown solid (201 mg). This solid was separated by flash chromatography (MeOH;CH₂Cl₂ 1:19) to yield the desired compound **3.18** as a brown solid (169 mg, 0.343 mmol, 86% yield).

TLC R_f: 0.50 (MeOH:CH₂Cl₂ 1:9);

[α]_D = -4.48 (c 0.96, CHCl₃);

¹H NMR (400 MHz, CDCl₃): δ 7.81 (d, *J* = 10.0 Hz, 1H, 10-H), 7.67 – 7.59 (m, 2H, 12, 14-H), 7.44 (t, *J* = 8.0 Hz, 1H, 13-H), 7.21 (t, *J* = 8.0 Hz, 1H, 5-H), 7.08 (d, *J* = 8.0 Hz, 1H, 4-H), 7.03 (t, *J* = 2.0 Hz, 1H, 2-H), 6.87 (dd, *J* = 8.0, 2 Hz, 6-C), 5.11 – 5.04 (m, 1H, Sol), 4.01 – 3.91 (m, 2H, Sol), 2.04 – 1.73 (m, 7H, Sol, *n*Bu), 1.71 – 1.49 (m, 12H, Sol, *n*Bu), 1.46 – 1.27 (m, 5H, Sol, *n*Bu), 0.92 (d, *J* = 6.5 Hz, 3H, Sol), 0.84 (t, *J* = 7 Hz, 6H, *n*Bu);

¹³C NMR (101 MHz, CDCl₃): δ 158.9 (1-C), 134.3 (14-C), 133.6 (d, *J* = 84.0 Hz, 11-C), 133.4 (d, *J* = 9.0 Hz, 10-C), 131.2 (Sol), 130.0 (d, *J* = 7.5 Hz, 12-C), 129.4 (5-C), 128.7 (d, *J* = 10.0 Hz, 13-C), 124.6 (Sol), 124.0 (3-C), 123.9 (d, *J* = 10 Hz, 9-C), 123.9 (4-C), 117.0 (2-C), 115.9 (6-C), 90.8 (8-C), 88.1 (7-C), 66.4 (Sol), 37.1 (Sol), 36.1

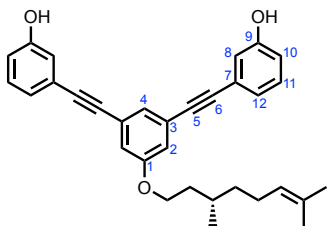
(Sol), 29.6 (d, $J = 69.0$ Hz, ^nBu), 29.5 (Sol), 25.7 (Sol), 25.4 (Sol), 24.1 (d, $J = 15.0$ Hz, ^nBu), 23.4 (d, $J = 2.0$ Hz, ^nBu), 19.6 (Sol), 17.7 (Sol), 13.5 (d, $J = 1.0$ Hz, ^nBu);

^{31}P NMR (162 MHz, CDCl₃): δ 40.3 (phosphine oxide);

FT-IR (ATR): 2957, 2929, 1596, 1574, 1466, 1222, 1170, 686 $\nu_{\text{max}}/\text{cm}^{-1}$;

HRMS (ES+): C₃₂H₄₆O₂P₁ calcd. 493.3230 found 493.3222, $\Delta = -1.69$ ppm.

(*S*)-3,3'-(5-((3,7-dimethyloct-6-en-1-yl)oxy)-1,3-phenylene)bis(ethyne-2,1-diyl)diphenol (**3.19**)



3.15 (75 mg, 0.268 mmol), 3-iodophenol (118 mg, 0.536 mmol), $\text{Pd}_2(\text{dba})_3$ (5.00 mg, 5.50 μmol), CuI (1 mg, 5.50 μmol) and PPh_3 (7.00 mg, 26.8 μmol) were added to a flask of Et_3N (2 mL) and N_2 bubbled through the reaction for 15 min. The reaction was stirred at room temperature for 4 hr in the dark under N_2 . The reaction was filtered through celite and washed through with EtOAc (10 mL). The solution was washed with 1 M HCl (3x 10 mL). The solution was dried (MgSO_4) and the solvent was removed by rotary evaporation under reduced pressure yielding a brown solid (201 mg). This solid was separated by flash chromatography ($\text{EtOAc}:40\text{-}60$ pet. Ether, 1:4) to yield the desired compound **3.19** as a brown solid (110 mg, 0.237 mmol, 88% yield).

TLC R_f : 0.15 ($\text{EtOAc}/40\text{-}60$ pet. ether 1:9);

Melting Point: 65.2-68.5 °C;

[α]_D = -2.519 (*c* 0.68, CHCl_3);

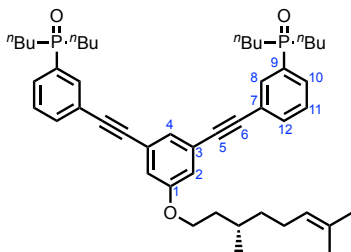
$^1\text{H NMR}$ (400 MHz, CDCl_3): δ 7.28 (t, J = 1.5 Hz, 1H, 4-H), 7.22 (t, J = 8 Hz, 2H, 11-H), 7.13-7.09 (m, 2H, 12-H), 7.03, (d, J = 1.5 Hz, 2H, 2-H), 7.02-6.96 (m, 2H, 8-H), 6.84 (ddd, J = 8.0, 2.5, 1.0 Hz, 2H, 10-H), 5.17 – 5.09 (m, 1H, Sol), 5.06 (br, 2H, OH), 4.07 – 3.96 (m, 2H), 2.09 – 1.92 (m, 2H), 1.85 – 1.76 (m, 1H), 1.70 (s, 3H), 1.60 – 1.63 (m, 1H), 1.62 (s, 3H), 1.60 – 1.55 (m, 1H), 1.42 – 1.33 (m, 1H), 1.28 – 1.18 (m, 1H), 0.96 (d, J = 6.5 Hz, 3H);

$^{13}\text{C NMR}$ (101 MHz, CDCl_3): δ 158.8 (1-C), 155.3 (9-C), 131.4 (Sol), 129.7 (11-C), 127.3 (4-C), 124.6 (Sol), 124.4 (12-C), 124.3 (3-C), 124.2 (7-C), 118.3 (2-C), 117.9 (8-C), 116.0 (10-C), 89.2 (7-C), 88.6 (6-C), 66.6 (Sol), 37.1 (Sol), 36.0 (Sol), 29.5 (Sol), 25.8 (Sol), 25.5 (Sol), 19.6 (Sol), 17.7 (Sol);

FT-IR (ATR): 3390 (br), 1577, 1184, 864, 781, 735 $\nu_{\text{max}}/\text{cm}^{-1}$;

HRMS (ES+): C₃₂H₃₂O₃ calcd. 465.2417 found 465.2424, $\Delta = -1.49$ ppm.

(*S*)-(((5-((3,7-dimethyloct-6-en-1-yl)oxy)-1,3-phenylene)bis(ethyne-2,1-diyl))bis(3,1-phenylene))bis(dibutylphosphine oxide) (**3.20**)



3.15 (80.0 mg, 0.285 mmol), **3.4** (217 mg, 0.685 mmol), $\text{Pd}_2(\text{dba})_3$ (12.5 mg, 13.7 μmol), CuI (3.00 mg, 13.7 μmol) and PPh_3 (18 mg, 68.5 μmol) were added to a flask of Et_3N (4 mL) and N_2 bubbled through the reaction for 15 min. The reaction was heated to 95 °C by microwave irradiation for 10 min. The reaction was filtered through celite and washed through with EtOAc (10 mL). The solution was washed with 1 M HCl (3x 10 mL). The solution was dried (MgSO_4) and the solvent was removed by rotary evaporation under reduced pressure yielding a brown solid (201 mg). This solid was separated by flash chromatography ($\text{MeOH}:\text{CH}_2\text{Cl}_2$ 1:19) to yield the desired compound **3.20** as a brown oil (107 mg, 0.141 mmol, 50% yield).

TLC R_f : 0.40 ($\text{MeOH}:\text{CH}_2\text{Cl}_2$ 1:9);

Melting Point: 40.4–43.1 °C;

$[\alpha]_D = -1.16$ (c 1.3, CHCl_3);

$^1\text{H NMR}$ (400 MHz, CDCl_3): δ 7.83 (d, $J = 11.0$ Hz, 2H, 8-H), 7.70 – 7.62 (m, 4H, 10, 12-H), 7.44 (td, $J = 8.0, 2.5$ Hz, 2H, 11-H), 7.29 (t, $J = 1.5$ Hz, 1H, 4-H), 7.04 (d, $J = 2.5$ Hz, 2H, 2-H), 5.11 – 5.04 (m, 1H, Sol), 4.01 – 3.91 (m, 2H, Sol), 2.04 – 1.73 (m, 7H, Sol, $n\text{Bu}$), 1.71 – 1.49 (m, 12H, Sol, $n\text{Bu}$), 1.46 – 1.27 (m, 5H, Sol, $n\text{Bu}$), 0.92 (d, $J = 6.5$ Hz, 3H, Sol), 0.84 (t, $J = 7$ Hz, 6H, $n\text{Bu}$);

$^{13}\text{C NMR}$ (101 MHz, CDCl_3): δ 158.9 (1-C), 134.3 (d, $J = 2.5$ Hz, 12-C), 133.8 (d, $J = 86.0$ Hz, 9-C), 133.5 (d, $J = 9.5$ Hz, 8-C), 131.3 (Sol), 130.2 (d, $J = 6.0$ Hz, 10-C), 128.7 (d, $J = 10.0$ Hz, 11-C), 127.2 (4-C), 124.6 (Sol), 124.1 (3-C), 123.6 (7-C) 118.1 (2-C), 89.8 (5-C), 88.7 (6-C), 66.4 (Sol), 37.1 (Sol), 36.1 (Sol), 29.6 (d, $J = 69.0$ Hz, $n\text{Bu}$),

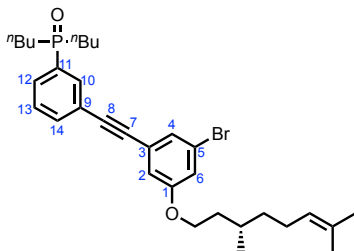
29.5 (Sol), 25.7 (Sol), 25.4 (Sol), 24.1 (d, $J = 15.0$ Hz, ^nBu), 23.4 (d, $J = 2.0$ Hz, ^nBu), 19.6 (Sol), 17.7 (Sol), 13.5 (d, $J = 1.0$ Hz, ^nBu);

^{31}P NMR (162 MHz, CDCl₃): δ 35.3 (phosphine oxide);

FT-IR (ATR): 2958, 2929, 1578, 1221, 1170, 1046, 793, 692 $\nu_{\text{max}}/\text{cm}^{-1}$;

HRMS (ES+): C₄₈H₆₇O₃P₂ calcd. 753.4560 found 753.4545, $\Delta = -2.00$ ppm.

(S)-(3-((3-bromo-5-((3,7-dimethyloct-6-en-1-yl)oxy)phenyl)ethynyl)phenyl)dibutylphosphine oxide (3.21)



3.6 (226 mg, 0.860 mmol), **3.16** (343 mg, 0.780 mmol), Pd₂(dba)₃ (15.0 mg, 16.0 µmol), CuI (3.00 mg, 16.0 µmol) and PPh₃ (21.0 mg, 79.0 µmol) were added to a flask under N₂. Et₃N (5 mL) and DMF (5 mL) were added and the reaction purged with N₂ for 20 min, then stirred at room temperature overnight in the dark. The reaction was washed through celite with EtOAc (30 mL) and washed with 1M HCl (3x 30 mL) and 5% LiCl solution (2x 30 mL). The solution was dried (MgSO₄) and the solvent was removed by rotary evaporation under reduced pressure to yield a brown oil (572 mg). This oil was separated by flash chromatography (MeOH:CH₂Cl₂, 1:19) to yield the desired compound **3.21** as a light brown oil (420 mg, 0.730 mmol, 94% yield).

TLC R_f: 0.25 (MeOH:CH₂Cl₂ 1:9)

[α]_D²⁰ = -3.31 (*c* 0.90, CHCl₃)

¹H NMR (400 MHz, CDCl₃): δ 7.82 (dt, *J* = 11.0, 1.5 Hz, 1H, 10-H), 7.68 (ddt, *J* = 10.5, 7.5, 1.5 Hz, 1H, 12-H), 7.65 (dd, *J* = 8.0, 1.5 Hz, 1H, 14-H), 7.49 (td, *J* = 8.0, 2.5 Hz, 1H, 13-H), 7.26 (t, *J* = 1.5 Hz, 1H, 4-H), 7.05 (t, *J* = 1.5 Hz, 1H, 6-H), 6.98 (dd, *J* = 1.5 Hz, 1H, 2-H), 5.13 – 5.06 (m, 1H, Sol), 4.03 – 3.95 (m, 2H, Sol), 2.08 – 1.89 (m, 4H, Sol, *n*Bu), 1.91 – 1.77 (m, 3H, Sol), 1.70 – 1.44 (m, 10H, Sol, *n*Bu), 1.47 – 1.34 (m, 7H, Sol, *n*Bu), 1.32 – 1.20 (m, 1H, Sol), 0.95 (d, *J* = 6.5 Hz, 3H, Sol), 0.88 (t, *J* = 7.0 Hz, 6H, *n*Bu);

¹³C NMR (101 MHz, CDCl₃): δ 159.6 (1-C), 134.3 (d, *J* = 3.0 Hz, 14-C), 133.5 (d, *J* = 9.0 Hz, 10-C), 133.4 (d, *J* = 91.0 Hz, 11-C), 131.4 (Sol), 130.4 (d, *J* = 8.0 Hz, 12-C), 128.7 (d, *J* = 11.5 Hz, 13-C), 126.6 (4-C), 125.1 (3-C), 124.6 (Sol), 123.5 (d, *J* = 12.0 Hz, 9-C), 122.6 (5-C), 118.9 (6-C), 116.2 (2-C), 89.2 (7-C), 89.2 (8-C), 66.8 (Sol),

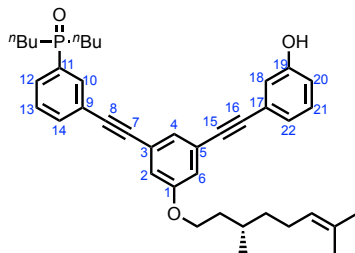
37.1 (Sol), 35.9 (Sol), 29.6 (d, $J = 69.0$ Hz, ^nBu), 29.5 (Sol), 25.7 (Sol), 25.4 (Sol),

24.1 (d, $J = 14.0$ Hz, ^nBu), 23.5 (d, $J = 4.0$ Hz, ^nBu), 19.5 (Sol), 17.7 (Sol), 13.6 (^nBu);

FT-IR (ATR): 2957, 2929, 2110, 1593, 1558, 1424, 1173, 796 $\nu_{\text{max}}/\text{cm}^{-1}$

HRMS (ES+): $\text{C}_{32}\text{H}_{45}\text{O}_2\text{BrP}$ calcd. 571.2341 found 571.2331, $\Delta = -1.8$ ppm.

(*S*)-dibutyl(3-((3-((3,7-dimethyloct-6-en-1-yl)oxy)-5-((3-hydroxyphenyl)ethynyl)phenyl)ethynyl)phenyl)phosphine oxide (**3.22**)



3.21 (390 mg, 0.680 mmol), 3-hydroxylphenylacetlyene (0.373 mL, 3.41 mmol), $\text{Pd}_2(\text{dba})_3$ (13.0 mg, 14.0 μmol), CuI (2.70 mg, 14.0 μmol), and PPh_3 (19.0 mg, 71.0 μmol) were placed in a flask under N_2 . Degassed DMF (5 mL) and Et_3N (5 mL) were added and reaction stirred overnight at 50 °C in the dark. The reaction was washed through celite with EtOAc (30 mL) and washed with 1M HCl (3x 30 mL) and 5% LiCl solution (2x 30mL). The solution was dried (MgSO_4) and the solvent was removed by rotary evaporation under reduced pressure to yield a brown oil (502 mg). This solid was separated by flash chromatography ($\text{MeOH}:\text{CH}_2\text{Cl}_2$ 1:19) to yield the desired compound **3.22** as a brown oil (76.0 mg, 0.120 mmol, 19% yield).

TLC R_f : 0.23 ($\text{MeOH}:\text{CH}_2\text{Cl}_2$ 1:9)

[α]_D²⁰ = -3.94 (*c* 1.10, CHCl_3);

¹H NMR (400 MHz, CDCl_3): δ 8.72 (bs, 1H, OH), 7.83 (dt, *J* = 11.5, 1.5 Hz, 1H, 10-H), 7.75 – 7.63 (m, 2H, 12, 14-H), 7.50 (td, *J* = 7.5, 2.5 Hz, 1H, 13-H), 7.25 (t, *J* = 1.5 Hz, 1H, 4-H, 20-H), 7.19 (t, *J* = 8.0 Hz, 1H, 21-H), 7.13 (dd, *J* = 2.5, 1.5 Hz, 1H, 18-H), 7.04 (dt, *J* = 7.5, 1.0 Hz, 1H), 7.01 (qd, *J* = 2.5, 1.5 Hz, 2H, 2, 6-H), 6.93 (ddd, *J* = 8.0, 2.5, 1.0 Hz, 1H, 22-H), 5.14 – 5.07 (m, 1H, Sol), 4.05 – 3.95 (m, 2H, Sol), 2.10 – 1.77 (m, 7H, Sol, *n*Bu), 1.73 – 1.54 (m, 8H, Sol, *n*Bu), 1.50 – 1.33 (m, 6H, Sol, *n*Bu), 1.28 – 1.16 (m, 1H, Sol), 0.96 (d, *J* = 6.5 Hz, 3H, Sol), 0.87 (t, *J* = 7.0 Hz, 6H, *n*Bu);

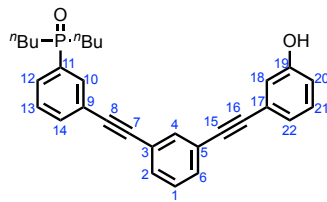
¹³C NMR (101 MHz, CDCl_3): δ 158.8 (1-C), 157.1 (19-C), 134.6 (d, *J* = 2.0 Hz, 14-C), 133.3 (d, *J* = 10.0 Hz, 10-C), 133.0 (d, *J* = 56.0 Hz, 11-C), 131.4 (Sol), 130.1 (d, *J* = 8.0. Hz, 12-C), 129.5 (21-C), 128.9 (d, *J* = 11.0 Hz, 13-C), 127.3 (4-C), 124.7 (17-C), 124.6 (Sol), 124.1 (5-C), 124.0 (3-C), 123.7 (d, *J* = 3.0 Hz, 9-C), 123.1 (22-C), 118.7 (18-C), 118.1 (6-C), 117.6 (2-C), 116.5 (20-C), 90.3 (16-C), 90.1 (15-C), 88.3

(8-C), 87.9 (7-C), 66.6 (Sol), 37.1 (Sol), 36.0 (Sol), 29.5 (Sol), 29.4 (d, $J = 51.0$ Hz, ^nBu), 25.7 (Sol), 25.5 (Sol), 24.1 (d, $J = 15.0$ Hz, ^nBu), 23.4 (d, $J = 4.0$ Hz, ^nBu), 19.5 (Sol), 17.7 (Sol), 13.6 (^nBu);

FT-IR (ATR): 2958, 2929, 2215, 1577, 1449, 1195, 1156 $\nu_{\text{max}}/\text{cm}^{-1}$;

HRMS (ES+): $\text{C}_{40}\text{H}_{50}\text{O}_3\text{P}$ calcd. 609.3498 found 609.3492, $\Delta = -1.0$ ppm.

Dibutyl(3-((3-((3-hydroxyphenyl)ethynyl)phenyl)ethynyl)phenyl)phosphine oxide (**3.24**)



3-hydroxyphenylacetylene (52.0 mg, 0.440 mmol), 1,3-diiodobenzene (145 mg, 0.440 mmol), **3.6** (115 mg, 0.440 mmol), Pd₂(dba)₃ (8.00 mg, 8.8 µmol), CuI (2.00 mg, 8.8 µmol) and PPh₃ (12.0 mg, 44.0 µmol) were added to a flask under N₂. Et₃N (4.4 mL) was added and the reaction stirred at room temperature overnight in the dark. The reaction was washed through celite with EtOAc (20 mL), and washed with 1M HCl (3x 20 mL) and 5% LiCl solution (2x 30mL). The solution was dried (MgSO₄) and the solvent was removed by rotary evaporation under reduced pressure to yield a brown solid (125 mg). This solid was purified by flash chromatography (MeOH:CH₂Cl₂ 1:19) to yield the desired compound **3.24** as a yellow crystalline solid (69.0 mg, 0.150 mmol, 35% yield).

TLC R_f: 0.21 (MeOH:CH₂Cl₂ 1:19);

Melting Point: 146.3-149.0 °C;

¹H NMR (400 MHz, CDCl₃): δ 8.40 (bs, 1H, OH), 7.85 (d, *J* = 11.0 Hz, 1H, 10-H), 7.74 – 7.60 (m, 3H, 4, 12, 14-H), 7.57 – 7.40 (m, 3H, 2, 6, 13-H), 7.31 (t, *J* = 7.8 Hz, 1H, 1-H), 7.19 (t, *J* = 7.9 Hz, 1H, 21-H), 7.12 (d, *J* = 1.0 Hz, 1H, 18-H), 7.05 (d, *J* = 7.6 Hz, 1H, 22-H), 6.92 (dd, *J* = 8.0, 1.5 Hz, 1H, 20-H), 2.10 – 1.97 (m, 2H, ⁿBu), 1.96 – 1.85 (m, 2H, ⁿBu), 1.70 – 1.56 (m, 2H, ⁿBu), 1.50 – 1.34 (m, 6H, ⁿBu), 0.87 (t, *J* = 7.0 Hz, 6H, ⁿBu);

¹³C NMR (101 MHz, CDCl₃): δ 156.9 (19-C), 134.7 (4-C), 134.6 (d, *J* = 3.0 Hz, 14-C), 133.4 (d, *J* = 10.0 Hz, 10-C), 132.2 (d, *J* = 4.0 Hz, 9-C), 132.1 (6-C), 132.1 (2-C), 132.0 (1-C), 131.4 (d, *J* = 52 Hz, 11-C), 130.1 (5-C), 130.0 (3-C), 129.5 (21-C), 128.9 (d, *J* = 12.0 Hz, 13-C), 128.6 (d, *J* = 17.0 Hz, 12-H), 123.2 (22-C), 122.9 (17-C), 118.6 (18-C), 116.5 (20-C), 90.4, 90.1, 88.7, 87.8, 29.4 (d, *J* = 70 Hz, ⁿBu), 24.0 (d, *J* = 15 Hz, ⁿBu), 23.4 (d, *J* = 4 Hz, ⁿBu), 13.6 (ⁿBu);

^{31}P NMR (162 MHz, CDCl_3): δ 43.3 (phosphine oxide);

FT-IR (ATR): 3073 (br), 2957, 2930, 2217, 1593, 1144, 791, 731, 687 $\nu_{\text{max}}/\text{cm}^{-1}$;

HRMS (ES+): $\text{C}_{30}\text{H}_{32}\text{O}_2\text{P}$ calcd. 455.2140 found 455.2144, $\Delta = 0.9$ ppm.

3.5.2 Binding studies

A•D and AA•DD complexes

Binding constants were measured by ^{31}P NMR titrations in a Bruker 500 MHz AVIII HD Smart Probe spectrometer at 298 K. The host (phosphine oxide derivatives **3.18** or **3.20**) was dissolved in CDCl_3 at a known concentration ($[\text{3.18}] = 20 - 30 \text{ mM}$, $[\text{3.20}] = 3.5 - 4.0 \text{ mM}$). The guest (phenol derivatives **3.17** or **3.19**) was dissolved in the host solution and made to a known concentration ($[\text{3.17}] = 230 - 240 \text{ mM}$, $[\text{3.19}] = 25 - 40 \text{ mM}$). A known volume of host was added to an NMR tube and the spectrum was recorded. Known volumes of guest in host solution were added to the NMR tube, and the spectra were recorded after each addition. The chemical shifts of the host spectra were monitored as a function of guest concentration and analysed using a purpose written software in Microsoft Excel. Errors were calculated as two times the standard deviation from the average value (95% confidence limit).

NMR dilutions of AD 2-mer

^{31}P NMR dilution experiments for **3.22** were performed in a Bruker 500 MHz AVIII HD Smart Probe spectrometer at 298 K. Known volumes of the AD 2-mer in solution at known concentrations were added to NMR tubes and the spectra were recorded ($[\text{3.22}] = 0.08 - 35.8 \text{ mM}$). The chemical shifts of the phosphine oxide peaks in the ^{31}P NMR spectra were monitored as a function of guest concentration and analysed using a purpose written software in Microsoft Excel. Errors were calculated as two times the standard deviation from the average value (95% confidence limit).

3.5.3 X-ray crystal structure of 3.24

Pure compound 3.24 (4 mg) was dissolved in toluene (0.5 mL), and the mixture was filtered to a vial and sealed with a plastic cap with a small hole, resulting in crystallization after 10 days at room temperature. Crystals suitable for X-ray crystallography were selected using an optical microscope and examined at 180 K on a Nonius KappaCCD diffractometer using Mo K α radiation ($\lambda = 0.7107 \text{ \AA}$). All non-hydrogen atoms were refined anisotropically. Hydrogen atoms were placed in idealized positions. The procedure was repeated with chloroform and the results were the same.

Formula	$C_{30}H_{31}O_2P$		
Temperature / K	180		
Space group	$P\bar{2}_1/n$		
Cell lengths / \AA	a 9.0540 (0.0004)	b 25.6599 (0.0011)	c 11.7725 (0.0005)
Cell angles / $^\circ$	α 90	β 111.578 (0.002)	γ 90
Cell volume / \AA^3	2543.37		
Z	4		
R factor	0.0686		

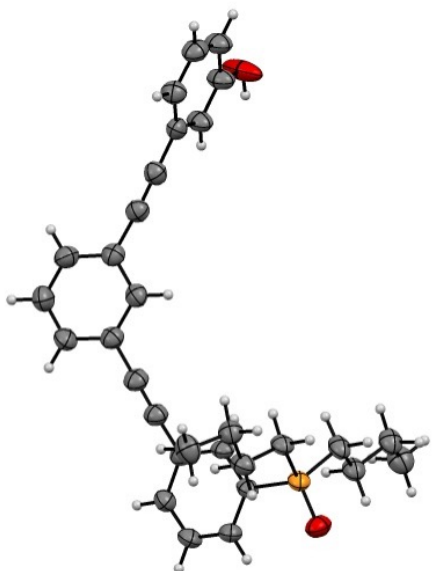


Figure 3.12: X-ray structure of 3.24 in ORTEP view (ellipsoids are drawn at 50% probability level).

3.6 References

- (1) Ito, H.; Furusho, Y.; Hasegawa, T.; Yashima, E. *J. Am. Chem. Soc.* **2008**, *130* (42), 14008–14015.
- (2) Hunter, C. A.; Anderson, H. L. *Angew. Chem. Int. Ed.* **2009**, *48* (41), 7488–7499.
- (3) Mulder, A.; Huskens, J.; Reinhoudt, D. N. *Org. Biomol. Chem.* **2004**, *2* (23), 3409.
- (4) Badjić, J. D.; Nelson, A.; Cantrill, S. J.; Turnbull, W. B.; Stoddart, J. F. *Acc. Chem. Res.* **2005**, *38* (9), 723–732.
- (5) Hogben, H. J.; Sprafke, J. K.; Hoffmann, M.; Pawlicki, M.; Anderson, H. L. *J. Am. Chem. Soc.* **2011**, *133* (51), 20962–20969.
- (6) Chan, S. I.; Schweizer, M. P.; Ts'o, P. O. P.; Helmkamp, G. K. *J. Am. Chem. Soc.* **1964**, *86* (19), 4182–4188.
- (7) Porschke, D. *Biopolymers* **1971**, *10* (10), 1989–2013.
- (8) Appella, D. H. *Curr. Opin. Chem. Biol.* **2009**, *13* (5–6), 687–696.
- (9) Wilson, C.; Keefe, A. D. *Curr. Opin. Chem. Biol.* **2006**, *10* (6), 607–614.
- (10) Pinheiro, V. B.; Holliger, P. *Curr. Opin. Chem. Biol.* **2012**, *16* (3–4), 245–252.
- (11) Eschenmoser, A.; Krishnamurthy, R. *Pure Appl. Chem.* **2000**, *72* (3), 343–345.
- (12) Eschenmoser, A. *Orig. Life Evol. Biosph.* **2004**, *34*, 277–306.
- (13) Chaput, J. C.; Yu, H.; Zhang, S. *Chem. Biol.* **2012**, *19* (11), 1360–1371.
- (14) Benner, S. A. *Acc. Chem. Res.* **2004**, *37* (10), 784–797.
- (15) Nguyen, H. V.; Zhao, Z.; Sallustrau, A.; Horswell, S. L.; Male, L.; Mulas, A.; Tucker, J. H. R. *Chem. Commun.* **2012**, *48*, 12165–12167.
- (16) Nielsen, P. E. *Acc. Chem. Res.* **1999**, *32* (7), 624–630.
- (17) Nielsen, P. E.; Egholm, M.; Berg, R. H.; Buchardt, O. *Science* **1991**, *254* (5037), 1497–1500.
- (18) Mittapalli, G. K.; Reddy, K. R.; Xiong, H.; Munoz, O.; Han, B.; De Riccardis, F.; Krishnamurthy, R.; Eschenmoser, A. *Angew. Chem. Int. Ed.* **2007**, *46*, 2470–2477.
- (19) Mittapalli, G. K.; Osornio, Y. M.; Guerrero, M. A.; Reddy, K. R.; Krishnamurthy, R.; Eschenmoser, A. *Angew. Chem. Int. Ed.* **2007**, *46*, 2478–

- 2484.
- (20) Núñez-Villanueva, D.; Iadevaia, G.; Stross, A. E.; Jinks, M. A.; Swain, J. A.; Hunter, C. A. *J. Am. Chem. Soc.* **2017**, *139* (19), 6654–6662.
- (21) Núñez-Villanueva, D.; Hunter, C. A. *Chem. Sci.* **2017**, *8* (1), 206–213.
- (22) Iadevaia, G.; Stross, A. E.; Neumann, A.; Hunter, C. A. *Chem. Sci.* **2016**, *7* (3), 1760–1767.
- (23) Stross, A. E.; Iadevaia, G.; Hunter, C. A. *Chem. Sci.* **2016**, *7* (1), 94–101.
- (24) Stross, A. E.; Iadevaia, G.; Núñez-Villanueva, D.; Hunter, C. A. *J. Am. Chem. Soc.* **2017**, *139* (36), 12655–12663.
- (25) Hoogsteen, K. *Acta Crystallogr.* **1963**, *16* (9), 907–916.
- (26) Abraham, M. H.; Chadha, H. S.; Whiting, G. S.; Mitchell, R. C. *J. Pharm. Sci.* **1994**, *83* (8), 1085–1100.
- (27) Calero, C. S.; Farwer, J.; Gardiner, E. J.; Hunter, C. A.; Mackey, M.; Scuderi, S.; Thompson, S.; Vinter, J. G. *Phys. Chem. Chem. Phys.* **2013**, *15* (41), 18262.
- (28) Hunter, C. A. *Angew. Chem. Int. Ed.* **2004**, *43* (40), 5310–5324.
- (29) Chekmeneva, E.; Hunter, C. A.; Misuraca, M. C.; Turega, S. M. *Org. Biomol. Chem.* **2012**, *10* (30), 6022.
- (30) Houk, K. N.; Leach, A. G.; Kim, S. P.; Zhang, X. *Angew. Chemie - Int. Ed.* **2003**, *42* (40), 4872–4897.
- (31) Page, M. I.; Jencks, W. P. *Proc. Natl. Acad. Sci.* **1971**, *68* (8), 1678–1683.
- (32) Misuraca, M. C.; Grecu, T.; Freixa, Z.; Garavini, V.; Hunter, C. A.; Van Leeuwen, P. W. N. M.; Segarra-Maset, M. D.; Turega, S. M. *J. Org. Chem.* **2011**, *76* (8), 2723–2732.
- (33) Stone, M. T.; Moore, J. S. *Org. Lett.* **2003**, *6* (4), 469.
- (34) Sonogashira, K. *J. Organomet. Chem.* **2002**, *653* (1–2), 46–49.
- (35) Zhang, J.; Moore, J. S.; Xu, Z.; Aguirre, R. A. *J. Am. Chem. Soc.* **1992**, *114* (6), 2273–2274.
- (36) Prince, R. B.; Okada, T.; Moore, J. S. *Angew. Chem. Int. Ed.* **1999**, *38* (1/2), 233–236.
- (37) Bloomfield, A. J.; Herzon, S. B. *Org. Lett.* **2012**, *14* (17), 4370–4373.

Chapter 4

Homo-oligomers

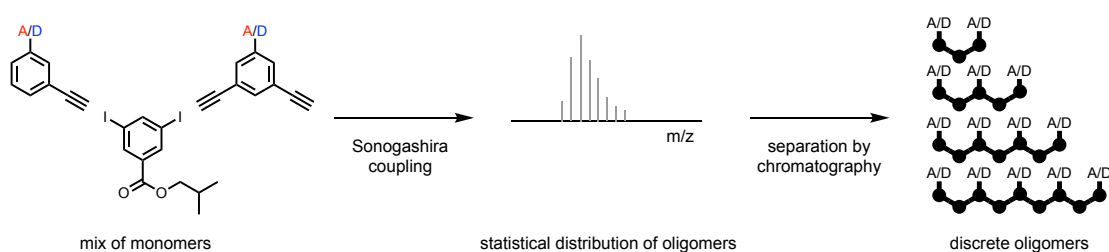
4.1 Introduction

The synthesis and binding studies in chapter 3 show that these information molecules form stable, cooperative duplexes in chloroform. The effective molarity for the formation of intramolecular H-bonds was found to be $133 \pm 44 \text{ mM}^{-1}$, and the chelate cooperativity associated with duplex assembly (K_{refEM}) is 4 ± 1 in chloroform. A value of K_{refEM} greater than one shows that the fully bound duplex is the most populated state. There was no sign of 1,2-folding in the mixed sequence 2-mer, so intramolecular H-bonding should not prevent duplex formation in longer oligomers.

This chapter describes the synthesis of additional building blocks and their use to synthesise longer oligomers. Homo-oligomers with either acceptor or donor recognition units were synthesised, and binding studies were used to characterise duplex formation between length complementary oligomers.

4.2 Approach: Oligomer synthesis

Traditional stepwise synthesis of oligomers using deprotection-coupling cycles is time-consuming. A method of oligomerisation followed by separation of the oligomeric product mixture by reverse phase preparative high-pressure liquid chromatography (HPLC) was used to rapidly access a family of homo-oligomers of varying length (**Scheme 4.1**). The average oligomer length can be controlled by adding mono-functional chain stoppers to the reaction mixture. For the internal recognition units in an oligomer, bis-acetylene modules were used, and the corresponding mono-acetylene modules were used for the terminal recognition units. A diiodo-solubilising module was used as the Sonogashira coupling partner for the oligomerisation reaction.

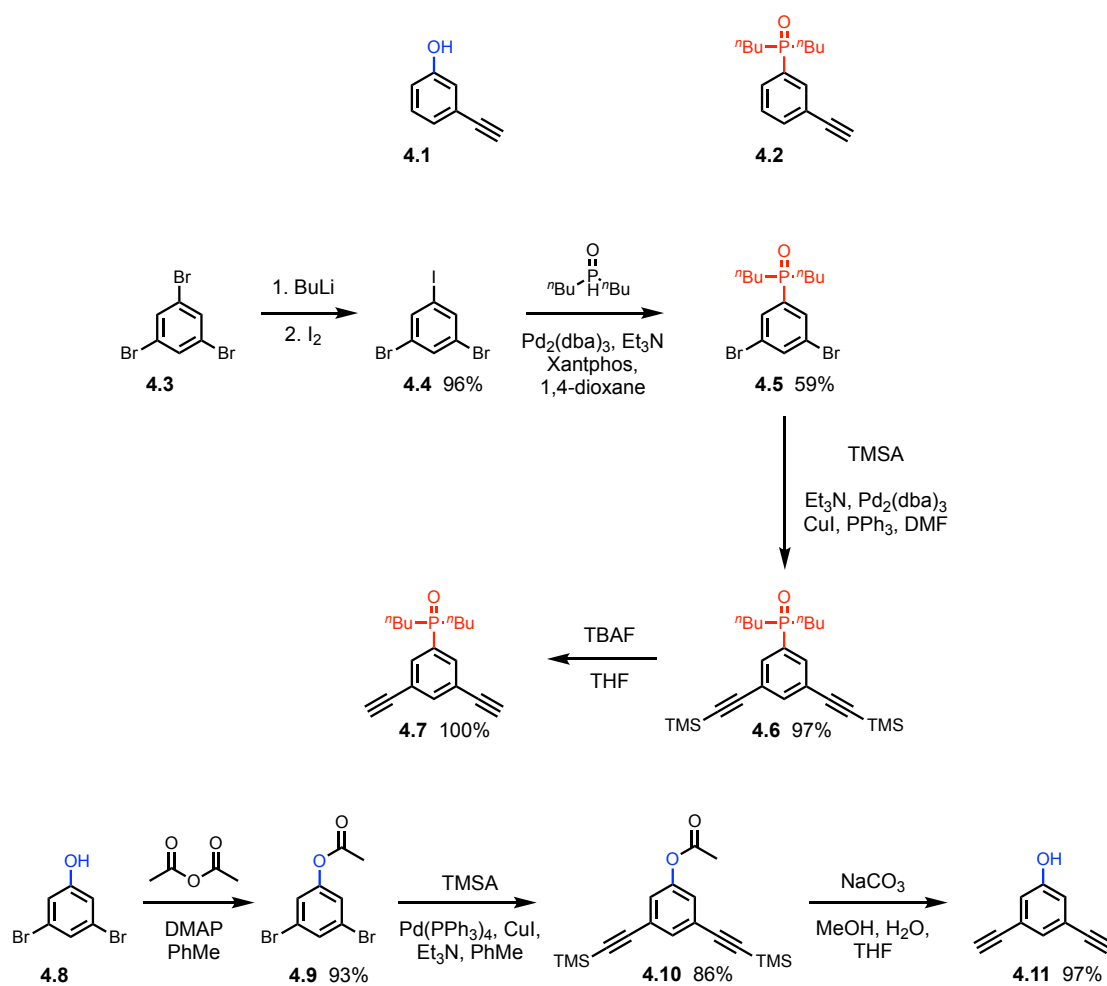


Scheme 4.1: Oligomerisation using a mix of modules to produce a mixture of oligomers of different lengths, followed by chromatographic separation to yield discrete oligomers.

4.3 Results and discussion

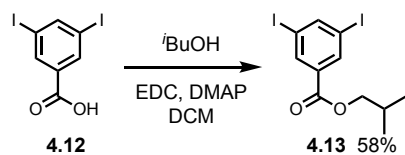
4.3.1 Synthesis of building blocks

Mono-acetylene donor recognition module (**4.1**) was commercially available, and mono-acetylene acceptor recognition module (**4.2**) was prepared as described in chapter 3. Recognition modules bearing two acetylene moieties were synthesised using the route shown in **Scheme 4.2**. Lithium halogen exchange with **4.3** using $^n\text{BuLi}$ followed by reaction with iodine gave dibromoiodobenzene (**4.4**). The difference in reactivity of halides allowed for selective P-arylation with di-*n*-butylphosphine oxide to yield **4.5**. Sonogashira coupling with TMSA yielded **4.6**, and TBAF mediated deprotection yielded the final module (**4.7**) (**Scheme 4.2**). Acetylation of 3,5-dibromophenol (**4.8**) with acetic anhydride yielded the acetate derivative (**4.9**). Acetylation increased reactivity for the subsequent Sonogashira coupling with TMSA yielding **4.10**. Simultaneous base-mediated deprotection of the phenol and acetylenes yielded the final bis-acetylene H-bond donor module (**4.11**) (**Scheme 4.2**).



Scheme 4.2: Mono-acetylene recognition modules and synthesis of bis-acetylene recognition modules.

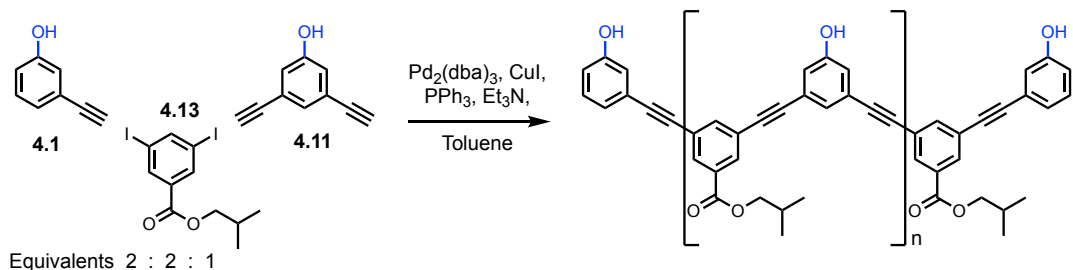
The diiodo-solubilising module (**4.13**) was synthesised by an EDC-mediated esterification of 3,5-diiodobenzoic acid (**4.12**) with *i*BuOH (**Scheme 4.3**).



Scheme 4.3: Synthesis of diiodo-solubilising module

4.3.2 Oligomer synthesis

Donor homo-oligomers were synthesised by oligomerisation of the phenol recognition modules (**4.1** and **4.11**) with the solubilising module (**4.13**) under Sonogashira conditions (**Scheme 4.4**). The ratio of starting materials was chosen to reflect the intended composition of the desired product, in this case the trimer. The resulting solution contained a large amount of insoluble particulates. The reaction mixture could be partially dissolved in ethanol but filtration and LCMS analysis showed only the 3-mer in significant amounts. The product mixture was much more soluble in dimethyl sulfoxide (DMSO) and LCMS analysis of the DMSO solution showed the presence of oligomers up to the 6-mer (**Figure 4.1a**). The LCMS method was transferred to preparative HPLC, and the oligomers were separated (**Figure 4.1b**). Donor homo-oligomers from the 3-mer (**4.14**) to 6-mer (**4.17**) were isolated (Table 4.1). A 2-mer with a different solubilising group was obtained previously by a stepwise synthesis (Chapter 3). The overall yield with respect to the solubilising module was 15%. The low yield is thought to be due to the solubility problems during chromatography. The most abundant oligomer was the 3-mer, matching the initial stoichiometry of the starting materials used in the reaction.



Scheme 4.4: Oligomerisation of phenol modules to yield donor homo-oligomers

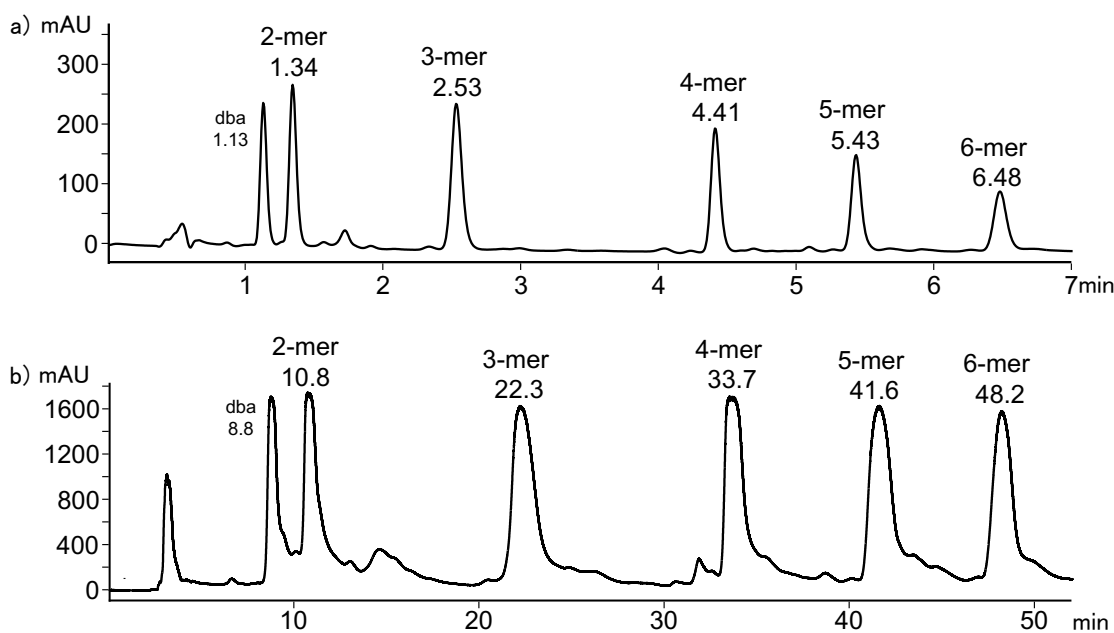


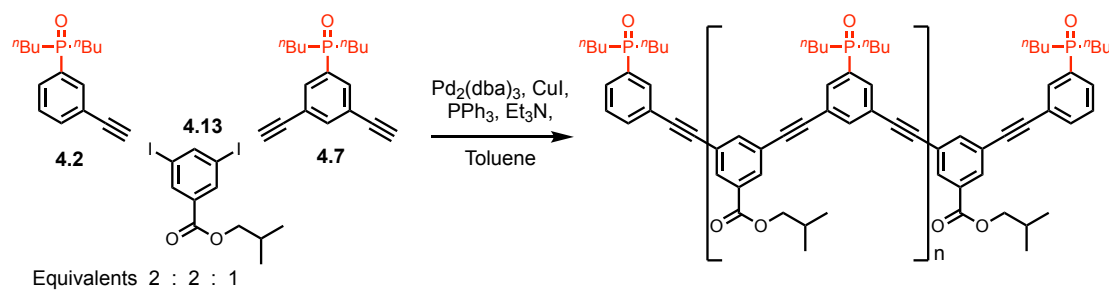
Figure 4.1: (a) LCMS analysis of donor oligomerisation mixture using a Hichrom C₈C₁₈ column (50 × 4.6 mm, 5 µm particle size) with a water/THF (0.1% formic acid) solvent system (THF: 58% for 3 min, 65% for 4 min) at a flow rate of 1 mL min⁻¹. (b) Preparative HPLC (bottom) separation of donor oligomerisation mixture using a HIRBP-6988 prep column (250 × 25 mm, 5 µm particle size) with a water/THF solvent system (THF: 58% for 21 min, 65% for 31 min) at 15 mL min⁻¹. Both samples were prepared in DMSO. UV/vis absorption was measured at 290 nm. Peaks identified by MS are labelled with retention time in minutes. dba = dibenzylideneacetone.

Table 4.1: Donor homo-oligomers isolated from phenol oligomerisation reaction.

Product	Oligomer sequence	Mass / mg	mol / µmol	% by mol fraction
4.14 (3-mer)	DDD	5.9	8.1	40
4.15 (4-mer)	DDDD	5.6	5.3	27
4.16 (5-mer)	DDDDD	5.6	4.2	21
4.17 (6-mer)	DDDDDD	4.2	2.5	12

Acceptor homo-oligomers were synthesised by oligomerisation of the phosphine oxide recognition modules (**4.2** and **4.7**) with the solubilising module (**4.13**) under Sonogashira conditions (**Scheme 4.5**). The ratio of starting materials was chosen to reflect the intended composition of the desired product, in this case

the trimer. The reaction mixture was dissolved in ethanol and analysed by LCMS (**Figure 4.2a**). Oligomers up to the 7-mer were observed. The LCMS method was transferred to preparative HPLC, and the oligomers were separated (**Figure 4.2b**). Acceptor homo-oligomers from the 3-mer (**4.18**) to 7-mer (**4.21**) were isolated (Table 4.2). A 2-mer with a different solubilising group was obtained previously by a stepwise synthesis (Chapter 3). The overall yield with respect to the solubilising module was 33%. The most abundant oligomer was again the 3-mer, matching the initial stoichiometry of the starting materials used in the reaction.



Scheme 4.5: Oligomerisation of phosphine oxide modules to yield acceptor homo-oligomers

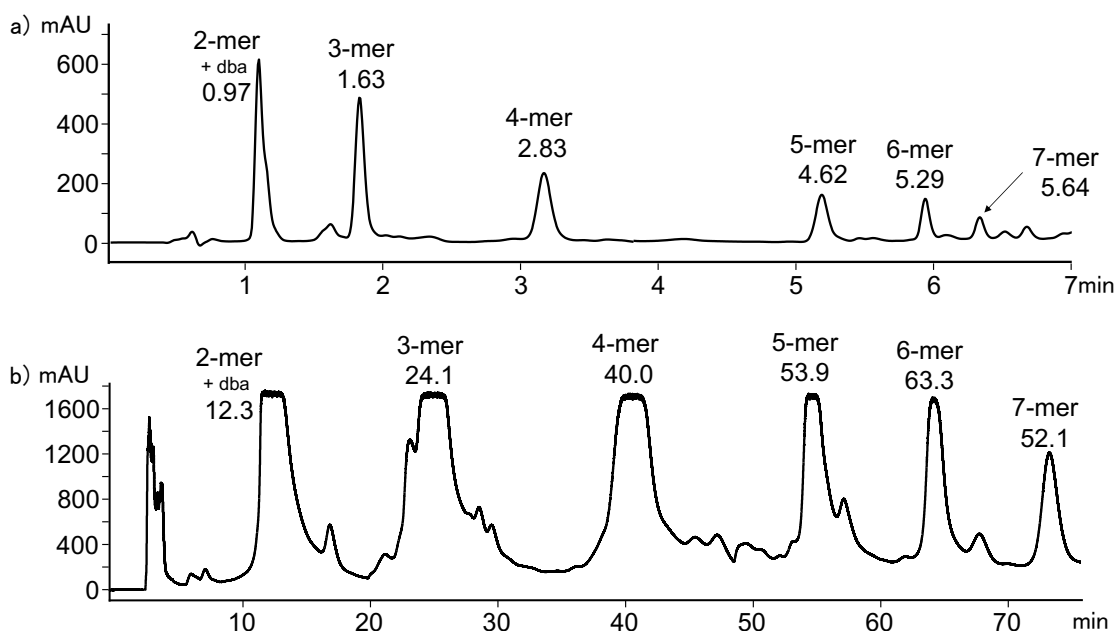


Figure 4.2: (a) LCMS analysis of acceptor oligomerisation mixture using a Hichrom C₈C₁₈ column (50 × 4.6 mm, 5 µm particle size) with a water/THF (0.1% formic acid) solvent system (THF: 60% for 3 min, 60-65% over 1 min, 65% for 3 min) at a flow rate of 1 mL min⁻¹. (b) Preparative HPLC (bottom) separation of donor oligomerisation mixture using a HIRBP-6988 prep column (250 × 25 mm, 5 µm particle size) with a water/THF solvent system (THF: 60% for 42 min, 65% for 33 min) at 15 mL min⁻¹. Both samples were prepared in EtOH. UV/vis absorption was measured at 290 nm. Peaks identified by MS are labelled with retention time in minutes. dba = dibenzylideneacetone.

Table 4.2: Acceptor homo-oligomers isolated from phosphine oxide oligomerisation reaction.

Product	Oligomer sequence	Mass / mg	mol / µmol	% by mol fraction
4.18 (3-mer)	AAA	27.8	24.0	58
4.19 (4-mer)	AAAA	18.4	11.4	27
4.20 (5-mer)	AAAAA	8.5	4.1	9.8
4.21 (6-mer)	AAAAAA	4.2	1.7	4.0
4.22 (7-mer)	AAAAAAA	1.5	0.5	1.2

4.3.3 Oligomer characterisation

The oligomers were initially identified by MS, and ^1H NMR spectroscopy was used to confirm the structures of the isolated products. The oligomers gave rise to distinct ^1H NMR signals which could be assigned to the terminal recognition modules, the internal recognition modules, and the solubilising modules. The ratios of integrals were used to confirm oligomer length. For the donor oligomers, the ratio of the integrals of the ^1H NMR signals due to the terminal solubilising groups (blue and orange) compared with the signals due to the internal solubilising groups (red and green) allowed quantification of number of solubilising groups and therefore oligomer length (**Figure 4.3**). Similarly, for the acceptor oligomers, the ratio of the integrals of the ^1H NMR signals due to the terminal solubilising groups (blue) compared with the signals due to the internal solubilising groups (red) allowed quantification of the number of solubilising groups and therefore oligomer length. These results were confirmed using the ratio of integrals of the ^{31}P NMR signals due to the terminal phosphine oxides (blue) compared with the signals due to the internal phosphine oxides (red) (**Figure 4.4**).

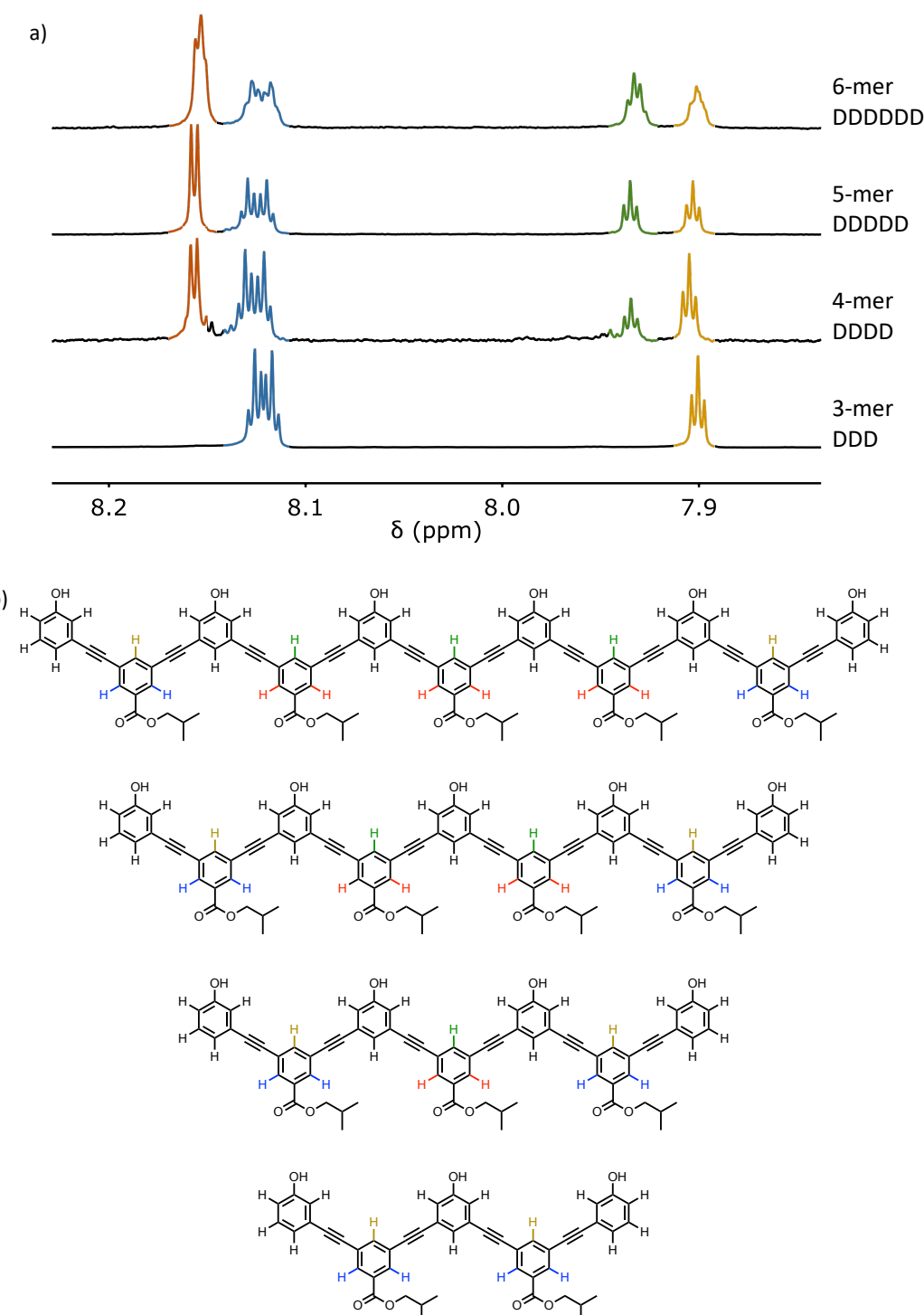
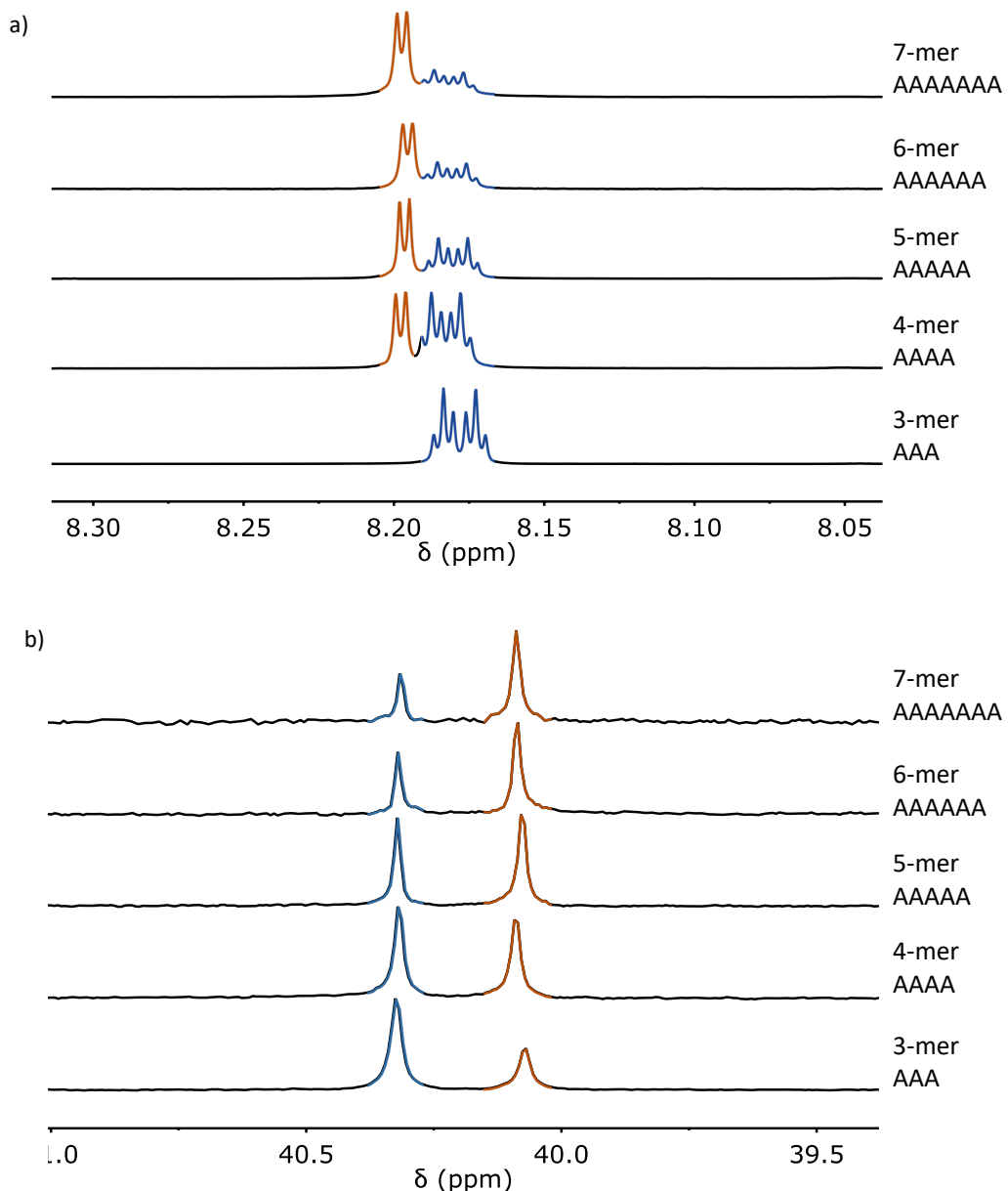


Figure 4.3: (a) Partial ^1H NMR spectra (500 MHz, $\text{THF}-d_8$) and (b) chemical structures of donor homo-oligomers. The signals in the ^1H NMR spectra are assigned to the chemical structures using colour coding. There is some contamination in the 4-mer spectrum that was not possible to remove by HPLC.



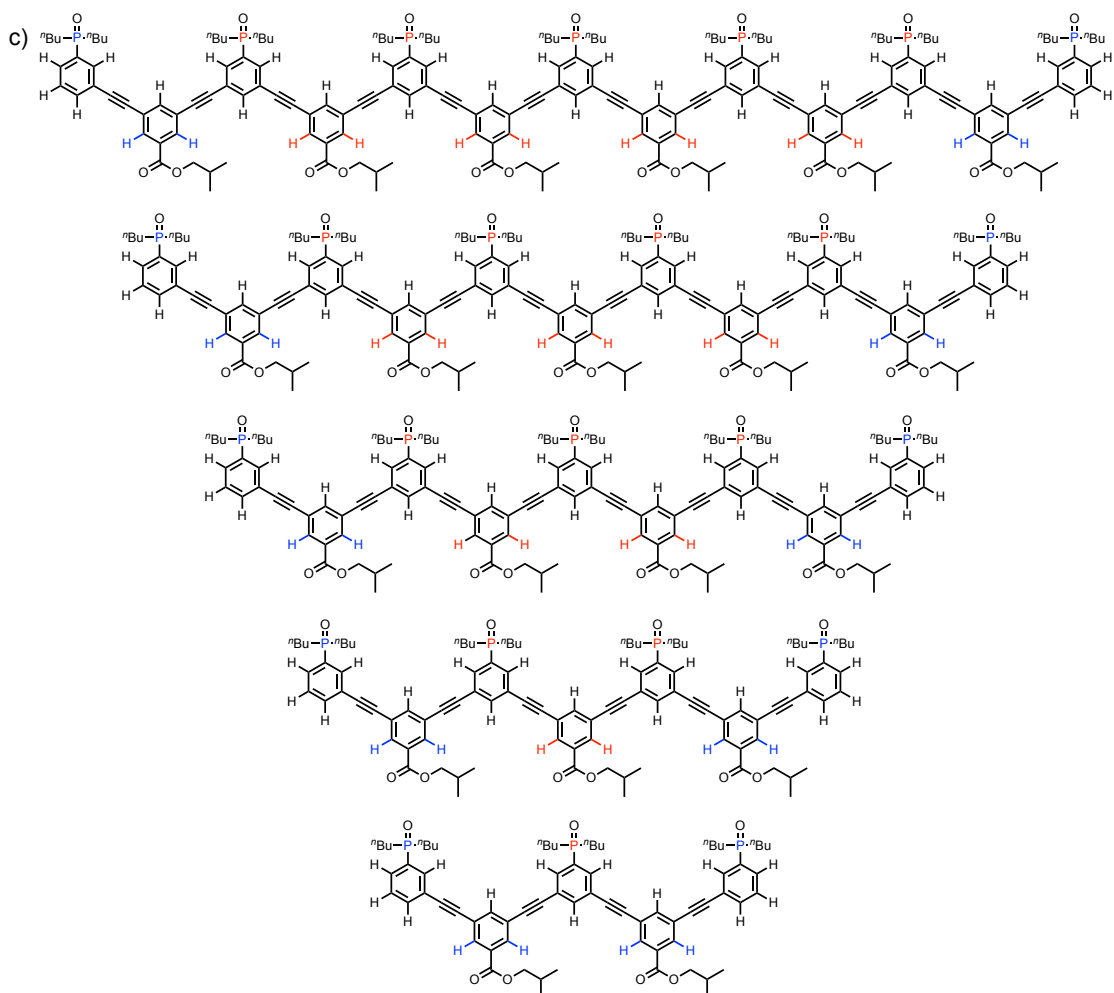


Figure 4.4: (a) Partial ^1H NMR spectra (500 MHz, CDCl_3), (b) ^{31}P NMR spectra (162 MHz, CDCl_3) and (c) chemical structures of acceptor homo-oligomers. The signals in the ^1H and ^{31}P NMR spectra are assigned to the chemical structures using colour coding.

For both the donor homo-oligomers in THF and the acceptor homo-oligomers in chloroform, the chemical shifts of the signals due to equivalent protons from equivalent building blocks do not change as the length of the oligomers increases. Moore and co-workers observed substantial upfield changes in chemical shift (0.5 ppm) for the signals due to the aromatic protons as the length of phenylacetylene oligomers increased in acetonitrile.¹ These chemical shift changes are indicative of folding into a helical conformation with stacking of the aromatic rings. It is clear that in chloroform and THF there is no folding of the oligomers described here.

4.3.4 NMR titration experiments

Donor and acceptor 1-mers and 2-mers bearing a citronellyl solubilising group were synthesised previously (**Figure 4.5**). Association constants for formation of the A•D and AA•DD complexes in toluene-*d*₈ were determined using ³¹P NMR titration experiments (**Figures 4.6**). The results are summarised in Table 4.4. The large downfield changes in ³¹P NMR chemical shift (+6-7 ppm) are indicative of H-bond formation. The association constants in toluene-*d*₈ are two orders of magnitude higher than the values previously measured in CDCl₃. The effective molarity in toluene is 38 ± 11 mM and the chelate cooperativity associated with duplex assembly (*K*_{refEM}) is 29 ± 8. The EM in toluene-*d*₈ is similar to the EM in CDCl₃ (134 ± 44 mM) but due to the much larger association constant, the chelate cooperativity associated with duplex assembly (*K*_{refEM}) is much higher than in CDCl₃ (4 ± 1).

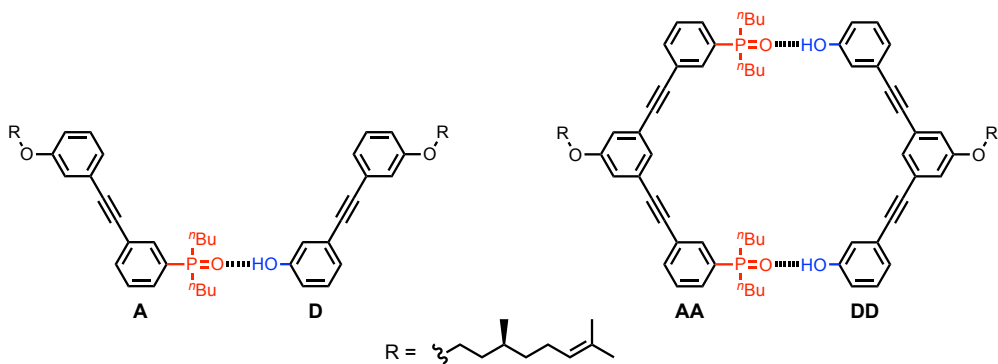


Figure 4.5: A•D and AA•DD complexes for which association constants (*K*) were measured.

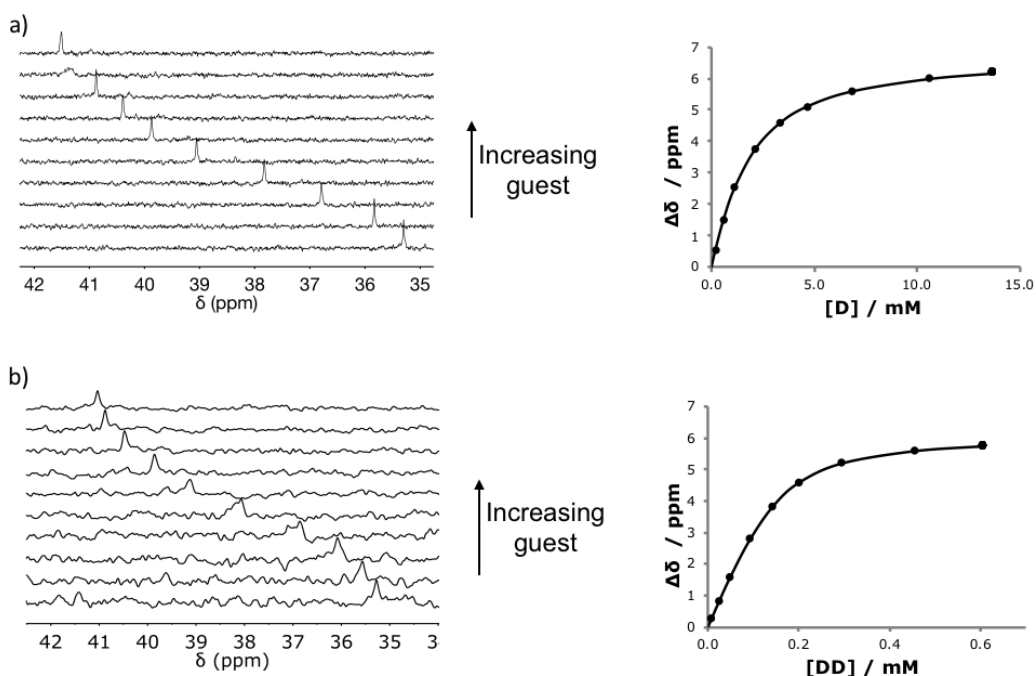
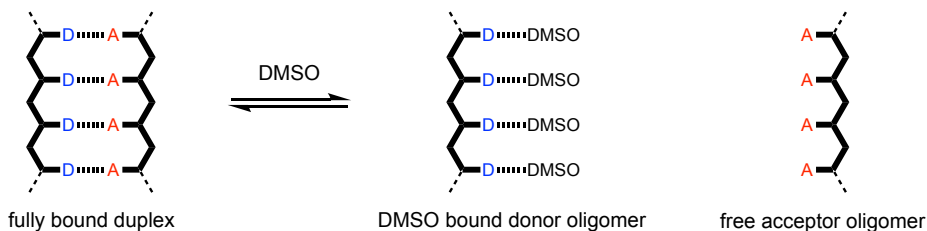


Figure 4.6: ^{31}P NMR data (202 MHz) for titration of a) **3.17** (D) into **3.18** (A) (1.02 mM), and b) **3.19** (DD) into **3.20** (AA) (0.15 mM) at 298 K in toluene- d_8 . Representative titration spectra and plots of complexation-induced change in chemical shift versus guest concentration (the line represents the best fit to a 1:1 binding isotherm).

4.3.5 NMR denaturation experiments

The poor solubility of the donor oligomers in toluene made it impossible to measure association constants for duplex formation for longer oligomers by titration experiments. In the presence of the complementary acceptor oligomer, both DDD and DDDD are soluble at mM concentrations in toluene. However, it proved impossible to solubilise the longer donor oligomers in toluene, even in the presence of the complementary acceptor oligomer. A method of denaturation of preassembled duplexes using a competing ligand was developed to determine the association constants (**Scheme 4.6**). Equimolar solutions of complementary 2-mers, 3-mers and 4-mers form fully bound duplexes at mM concentrations in toluene. Addition of DMSO- d_6 was used to denature the complex, which could be monitored by following the decrease in ^{31}P NMR chemical shift, due to the disruption of the H-bonding interactions (**Figure 4.7**).



Scheme 4.6: Denaturation of duplexes using DMSO as a competing ligand to bind the donor oligomer.

For the AA•DD duplex, the ^{31}P NMR spectrum contains only one peak, which moved upfield by 5 ppm on addition of DMSO, indicating complete denaturation of the duplex (**Figure 4.7b**). For the AAA•DDD duplex the ^{31}P NMR spectrum is more complicated due to the presence of two non-equivalent signals in a 2:1 ratio, and considerable broadening was observed, presumably due to slower exchange between free and bound states of the more stable duplex (**Figure 4.7c**). For the AAAA•DDDD duplex, the ^{31}P NMR spectrum contains two non-equivalent phosphine oxide signals in a 1:1 ratio (**Figure 4.7d**). In all three cases, the chemical shifts of the ^{31}P signals in toluene are 40-41 ppm in the absence of DMSO, which indicates that the duplexes are fully assembled with all of the phosphine oxides H-bonded to phenol groups on the complementary oligomers. At the end of all three denaturation experiments, the chemical shifts of the phosphine oxide signals increased again at very high concentrations of DMSO. This observation is presumably due to a change in the nature of the solvent. Similar changes were observed in a control experiment using a sample containing only the A 1-mer, where no H-bonding interactions are present (**Figure 4.7a**). The 1-mer data were used to correct the changes in chemical shift measured in the denaturation experiments for the change in solvent. The ^{31}P chemical shift of the A 1-mer was subtracted from the ^{31}P chemical shift of the duplex measured at the same concentration of DMSO-*d*₆. The corrected chemical shifts ($\delta_{\text{corrected}}$) were used in Equation 4.1 to fit the data to a denaturation isotherm (see experimental section for details).

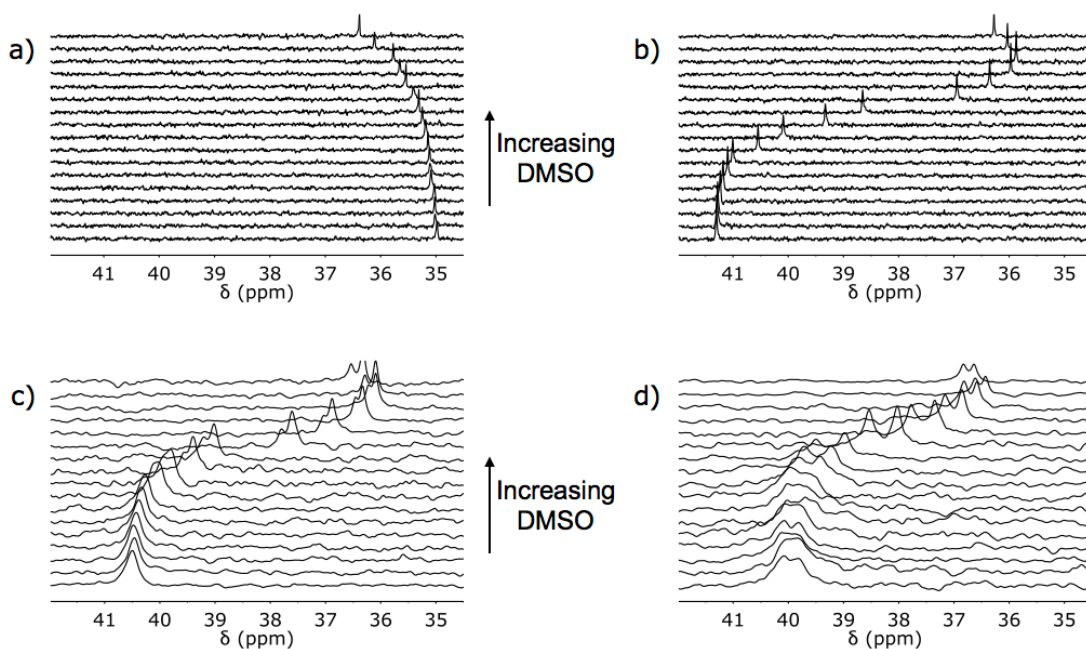


Figure 4.7: ^{31}P NMR spectra (202 MHz, toluene- d_8) for denaturation of equimolar solutions (1 mM) of a) **3.18** (A), b) **3.19** (DD) and **3.20** (AA), c) **4.14** (DDD) and **4.18** (AAA), and d) **4.15** (DDDD) and **4.19** (AAAA), with DMSO- d_6 (0.1 mM to 1 M) at 298 K. The concentration of oligomers starts at 1.0 mM and decreases to 0.7 mM from bottom to top.

$$\% \text{ duplex} = (\delta_{\text{corrected}} - \delta_{\text{free}})/(\delta_{\text{duplex}} - \delta_{\text{free}}) \quad 4.1$$

A simple two-state, all or nothing denaturation isotherm did not fit well to the data acquired from the denaturation experiments, so partially denatured species must also be considered (**Figure 4.11**). **Figures 4.8-4.10** show all possible complexes present in the denaturation experiments. For the 2-mer, both the fully bound duplex and unbound oligomers are present at the start of the experiment. Binding of one molecule of DMSO to the duplex leads to the partially denatured AA•DD•DMSO complex. It is possible to estimate the equilibrium constant for the formation of this complex as the product of K_d (the D•DMSO association constant) and K_1 (the A•D association constant), multiplied by a statistical factor of 4. The value of K_1 is reported in Table 4.4, and K_d was measured by ^1H NMR titration of DMSO into the D 1-mer in toluene ($K_d = 150 \text{ M}^{-1}$). The DD 2-mer can bind one or two molecules of DMSO, and the equilibrium constants for formation of the DD•DMSO and DD•(DMSO)₂ complexes can be estimated using the D•DMSO

association constant as $2K_d$ and K_d^2 respectively. The data for denaturation of the AA•DD duplex fit well to an isotherm allowing for all of these species, and this allowed determination of K_2 as the only unknown equilibrium constant. The results are shown in Table 4.4 and **Figure 4.11**. The value of K_2 determined in the denaturation experiment is comparable to the value determined in the corresponding titration experiment in toluene, which indicates that the denaturation methodology provides a robust method for determining duplex stability.

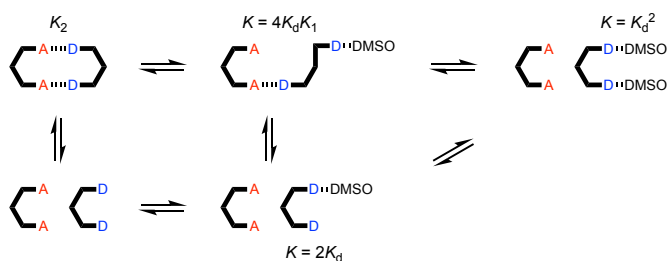


Figure 4.8: Equilibria involved in denaturation of AA•DD. K_d = D•DMSO association constant and K_n = association constant for duplex formation between homo-oligomers of length n in toluene- d_8 .

Denaturation of the AAA•DDD and AAAA•DDDD duplexes could involve a larger number of different species (**Figures 4.9** and **4.10**). The equilibrium constants for formation of most of these species can also be estimated from the values of K_d and K_1 , but some partially denatured duplexes have no direct analogues. For example, a number of different structures are possible for the AAA•DDD•DMSO complex, and we do not know whether complexes with DMSO bound to one of the terminal recognition units have similar stability to the complex with DMSO bound to the central recognition unit. By analogy with the AA•DD•DMSO complex, one might assume that the association constant for AAA•DDD•DMSO complex, K_p , will be the product of K_d and K_2 , multiplied by a statistical factor, but to avoid any bias in the fitting, K_p was optimised as a variable along with the K_3 in analysis of the AAA•DDD denaturation isotherm. The results are shown in Table 4.4 and **Figure 4.11**. The value of K_p is equal to $3.5 K_d K_2$. If the duplex preferentially denatures from the ends, so that the central H-bond is intact in the partially denatured AAA•DDD•DMSO complex, the statistical factor would

be 4, which is close to the optimised value of 3.5. The AAA•DDD duplex is an order of magnitude more stable than the AA•DD duplex, which confirms that the fully assembled triply H-bonded duplex is formed in toluene.

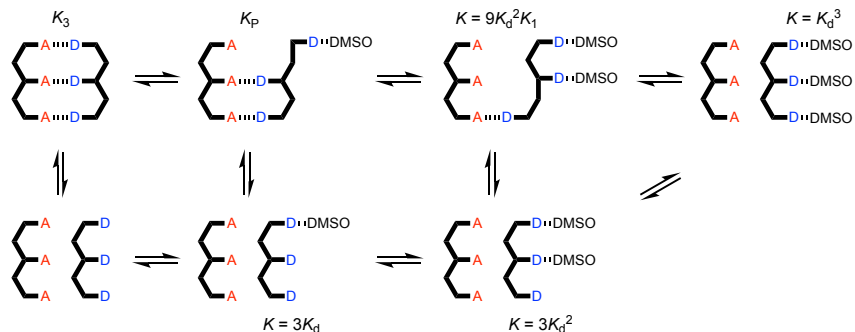


Figure 4.9: Equilibria involved in denaturation of AAA•DDD. K_d = D•DMSO association constant and K_n = association constant for duplex formation between homo-oligomers of length n in toluene- d_8

For denaturation of the AAAA•DDDD duplex, there are two partially denatured complexes with unknown stability, AAAA•DDDD•DMSO and AAAA•DDDD•(DMSO)₂ (**Figure 4.10**). Therefore, fitting of the denaturation data for this system involved optimisation of three equilibrium constants, K_4 , K_{P1} and K_{P2} . The results are shown in Table 4.4 and **Figure 4.11**. The AAAA•DDDD is more than an order of magnitude more stable than the AAA•DDD duplex, which confirms that the fully assembled duplex with all four H-bonds is formed in toluene. The value of K_{P1} is equal to 7.5 K_d K_3 . If the duplex preferentially denatures from the ends, so that the central H-bonds are both intact in the partially denatured AAAA•DDDD•DMSO complex, the statistical factor would be 4, which is smaller than the optimised value of 7.5. This result suggests that there are some additional partially denatured states where the central H-bonds are broken. The value of K_{P2} is equal to 8.0 K_d^2 K_2 . If the duplex preferentially denatures from the ends, the statistical factor would be 9, which is close to the optimised value.

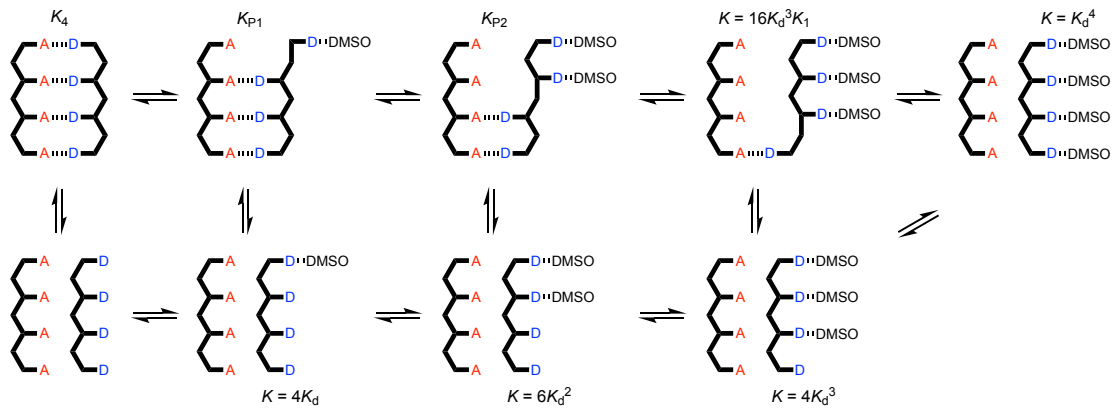


Figure 4.10: Equilibria involved in denaturation of AAAA•DDDD. $K_d = D \bullet DMSO$ association constant and K_n = association constant for duplex formation between homo-oligomers of length N in toluene- d_8 .

Figure 4.11 shows the data from each of the denaturation experiments. Lines of best fit representing a two-state, all or nothing fitting (**Figure 4.11a**) and the fitting considering partially denatured species (**Figure 4.11b**) are shown for each data set. By eye the second fit looks better, and this was confirmed by statistical analysis of the residuals. Equation 4.2 can be used to calculate S , the difference between the calculated line and the experimental data, normalised for the number of variables fitted.² For each data point, ε_i is the difference between the measured value and the line of best fit, n is number of data points, and m is number of parameters. The calculated values for S for each fit are collected in Table 4.3. For the AA•DD fitting the number of parameters is the same for both fits, for the AAA•DDD fitting there is one additional parameter in the new fitting (K_p), and for the AAAA•DDDD fitting there is two additional parameters (K_{p1} and K_{p2}). The value of S for the new fitting is an order of magnitude lower in all cases, indicating a much better fit.

$$S = \frac{\sum_{i=1}^n (\varepsilon_i)^2}{n - m} \quad 4.2$$

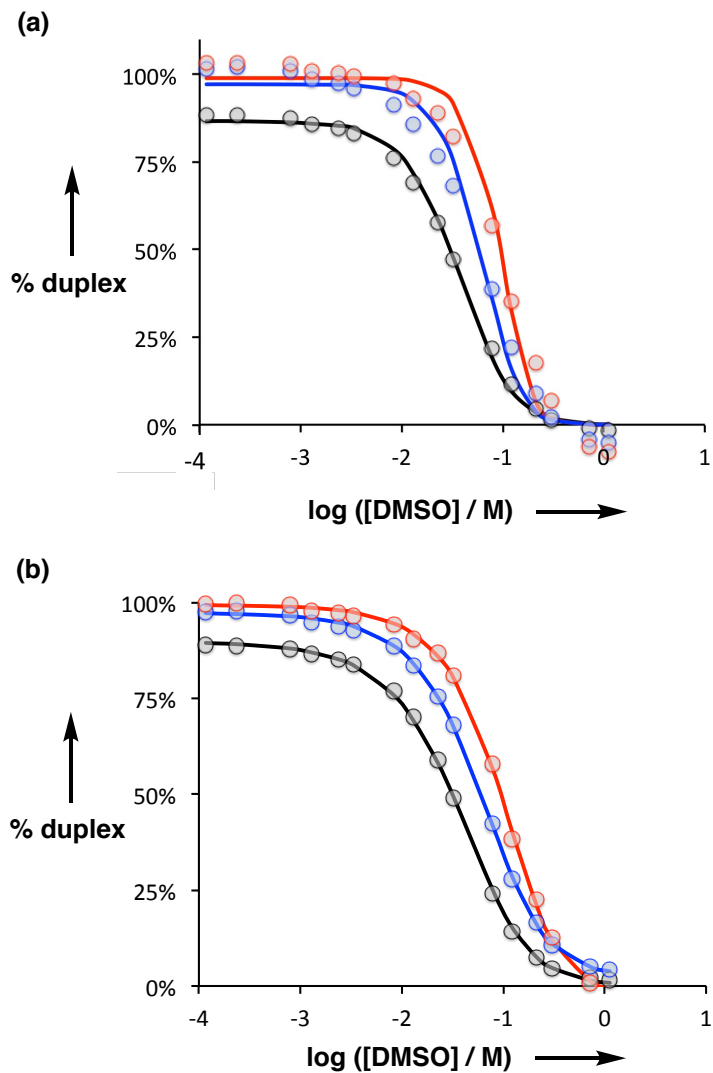


Figure 4.11: Duplex denaturation data in toluene- d_8 at 298 K plotted as a function of the log concentration of DMSO- d_6 in toluene- d_8 at 298 K, for **3.20•3.19** (AA•DD, black), **4.18•4.14** (AAA•DDD, blue) and **4.19•4.15** (AAAA•DDDD, red). The dots represent the experimental values obtained using equation 4.1 and the lines are the calculated denaturation isotherms using: (a) a two-state, all or nothing fitting, and (b) the fitting considering partially denatured species.

Table 4.3: Value of S for the 2-state, and new fitting considering partially denatured species for each duplex.

Complex	S	
	2-state	New
AA•DD	2.0×10^{-3}	8.3×10^{-4}
AAA•DDD	4.3×10^{-3}	7.8×10^{-4}
AAAA•DDDD	4.0×10^{-3}	8.9×10^{-4}

Figure 4.12 shows the speciation of different complexes calculated for the denaturation experiments. During the denaturation of all duplexes, the first step is breaking of one phenol-phosphine oxide H-bond forming a phenol-DMSO H-bond (**Figure 4.12**). For the AA•DD duplex this leaves only one phenol-phosphine oxide bond remaining. At 1 mM this bond is not energetically favourable, and the complex breaks to yield free AA and DD•DMSO (**Figure 4.12a**). As the concentration of DMSO increases the DD•(DMSO)₂ complex is formed. For the AAA•DDD and AAAA•DDDD duplexes, the major intermediate formed in the denaturation is the one DMSO partially denatured state (The blue lines in **Figure 4.12b** and **c**). As the concentration of DMSO increases the duplexes are fully denatured.

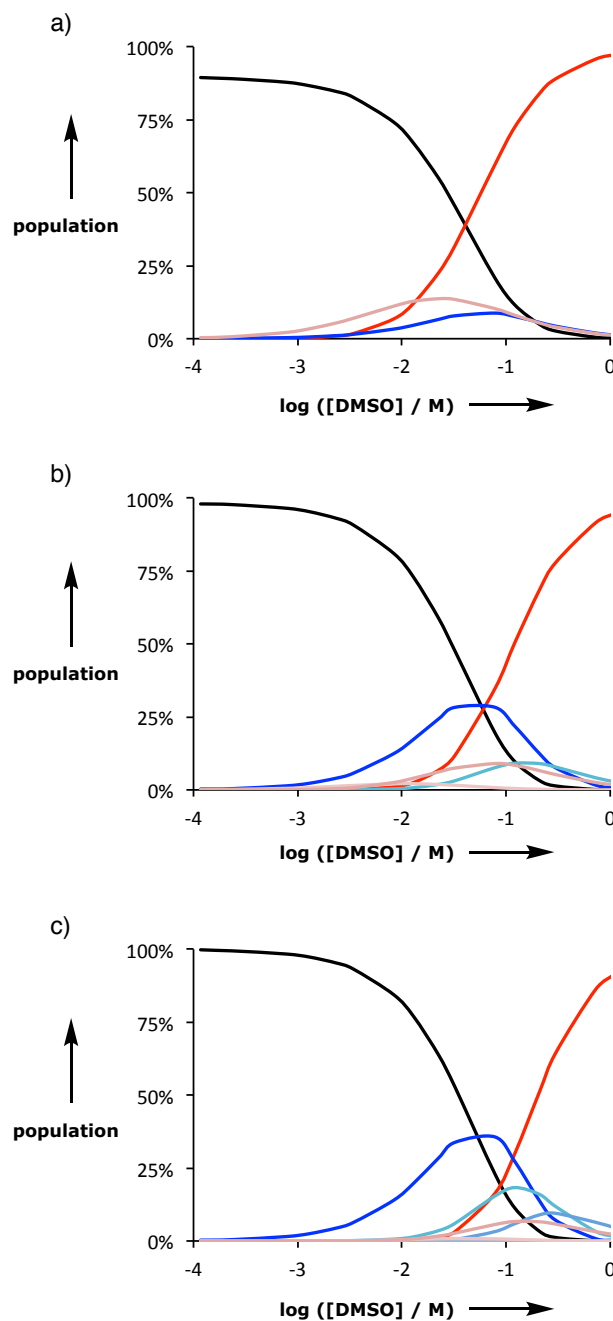


Figure 4.12: a) Population of species during denaturation of 2-mers: AA•DD (black), DD•DMSO (pink), AA•DD•DMSO (blue), and DD•(DMSO)₂ (red), b) Population of species during denaturation of 3-mers: AAA•DDD (black), AAA•DDD•DMSO (blue), DDD•(DMSO)₂ (pink), AAA•DDD•(DMSO)₂ (green), and DDD•(DMSO)₃ (red). Other possible species have very low populations, and c) Population of species during denaturation of 4-mers: AAAA•DDDD (black), AAAA•DDDD•DMSO (blue), AAAA•DDDD•(DMSO)₂ (cyan), DDDD•(DMSO)₃ (pink), and DDDD•(DMSO)₄ (red). Other possible species have very low populations.

The denaturation of the duplexes can also be observed by ^1H NMR spectroscopy (**Figure 4.13**). Aromatic peaks of the oligomers move by 0.1-0.6 ppm on denaturation. As observed for the ^{31}P data, there are differences at very high concentrations of DMSO- d_6 due to the change in the nature of the solvent. For the AA•DD duplex, the signal due to the OH proton starts at 6.2 ppm, suggesting that the duplex is not fully bound, and moves to 9.8 ppm when bound to DMSO (**Figure 4.13a**). For both the AAA•DDD and AAAA•DDDD duplexes, the signals due to the OH protons start at about 11 ppm, suggesting that the duplexes are fully bound, and move to about 10 ppm when bound to DMSO (**Figure 4.13b** and **c**).

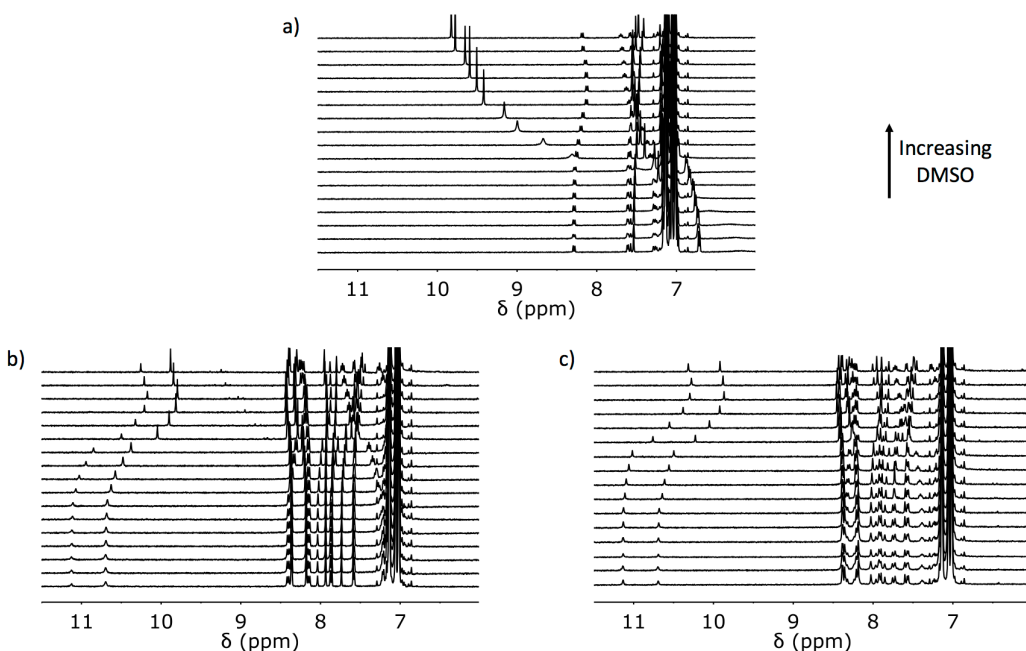


Figure 4.13: ^1H NMR spectra (500 MHz) for denaturation of a) AA•DD, b) AAA•DDD, and c) AAAA•DDDD with DMSO- d_6 at 298 K in toluene- d_8 . The concentration of oligomers starts at 1.0 mM and decreases to 0.7 mM from bottom to top.

The association constants determined by denaturation followed by ^{31}P NMR, calculated EM and chemical shifts are shown in Table 4.3. The association constant for AA•DD obtained from the denaturation experiment is within error of the value obtained through NMR titrations. For longer oligomers the association constants increase with each additional H-bond as expected, and the calculated EM for each step does not vary significantly. The chemical shifts for the free and

bound species do not vary significantly. The consistency of the results suggests that the values obtained from the denaturation experiments are accurate. In all cases the value of K_{refEM} is much greater than 1, showing that the duplex is the most populated state. A plot of Log K of duplex formation as a function of the number of recognition modules in the oligomers (N) gives a straight line (**Figure 4.14**). Each additional H-bond corresponds to an increase in stability of over an order of magnitude.

Table 4.4: Association constants (K), effective molarities (EM) and ^{31}P NMR chemical shifts (δ) measured by NMR titration and DMSO denaturation experiments in toluene- d_8 at 298 K.

Complex	K / M^{-1}	EM / mM	K_{refEM}	δ_{free}	δ_{bound}
A●D	760 ^a	-	-	35.3	42.1
AA●DD	44,000 ^a	38 ^a	29 ^a	35.3	41.3
	83,000 ^b	72	55	34.8	42.1
AAA●DDD	2,300,000 ^b	52	39	34.8	40.5
AAAA●DDDD	130,000,000 ^b	59	45	35.3	40.1

a) Determined by titration (errors are $\pm 30\%$), b) determined by denaturation

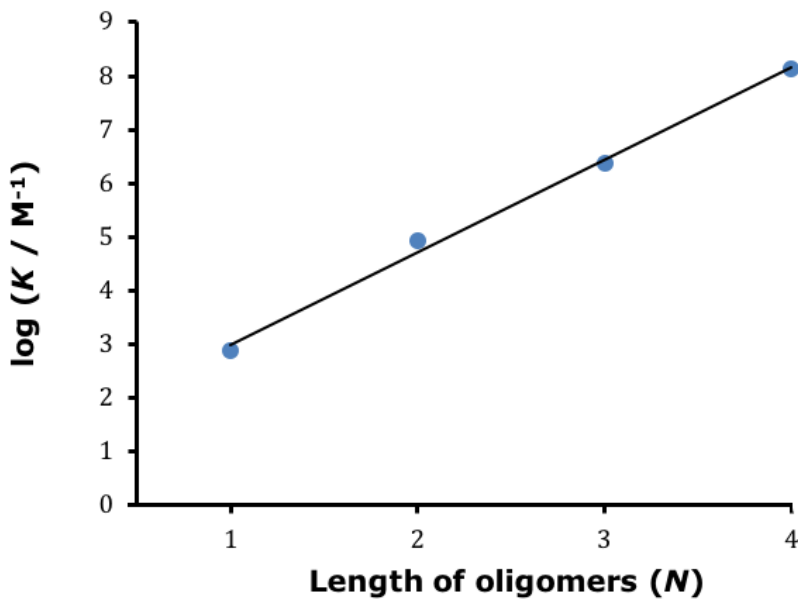


Figure 4.14: Log (K / M^{-1}) in toluene- d_8 duplex formation between length complementary oligomers plotted as a function of the number of recognition modules in an oligomer (N). The line of best fit is shown for the duplexes measured in this chapter, $\log K_N = 1.7N + 1.3$.

4.4 Conclusions

Building blocks for oligomerisations were synthesised and used to synthesise homo-oligomers. The mixtures of oligomeric products were separated by reverse-phase preparative HPLC. Mass spectrometry and NMR spectroscopy were used to identify the products. Donor oligomers up to the 6-mer and acceptor oligomers up to the 7-mer were synthesised, isolated and characterised.

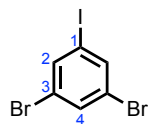
The association constants for duplexes formed by complementary homo-oligomers were measured using a method of denaturation with a competing ligand. In deuterated toluene, DMSO was used to denature the duplexes. These experiments required a more complex fitting than used previously due to the presence of partially bound states. The increase in association constant for each additional H-bond was greater than an order of magnitude, reaching 10^8 M^{-1} for the 4-mers. The effective molarity (EM) for the duplex formation remained fairly constant with an average value of 61 mM^{-1} . The average value of $K_{\text{ref}}\text{EM}$ was 51, showing the fully bound duplex was the major species for each oligomer length.

The system appears to be a promising design for a new type of information oligomer, with the synthesis of longer oligomers possible. These longer oligomers retain the ability of the dimers to form cooperative duplexes in organic solvents.

4.5 Experimental

4.5.1 Synthesis

All the reagents were obtained from commercial sources (Sigma-Aldrich, Alfa Aesar, Fisher Scientific and Fluorochem) and were used without further purification. Thin layer chromatography was carried out using silica gel 60F (Merck) on aluminium. Flash chromatography was carried out on an automated system (CombiFlash Rf+ or CombiFlash Rf Lumen) using prepacked cartridges of silica (25 μ or 50 μ PuriFlash® Columns). ^1H and ^{13}C NMR spectra were recorded on either a Bruker AV3400 or AV3500 spectrometer at 298 K unless specifically stated otherwise. Residual solvent was used as an internal standard. All chemical shifts are quoted in ppm on the δ scale and the coupling constants expressed in Hz. Signal splitting patterns are described as follows: s (singlet), d (doublet), t (triplet), quart (quartet), m (multiplet). ES+ mass spectra were obtained on a Waters LCT premier mass spectrometer. FTIR spectra were recorded on a PerkinElmer Spectrum One FT-IR spectrometer. Melting points were recorded on a Mettler Toledo MP90 melting point apparatus and are reported as an uncorrected range of three repeats. ES+ was carried out on a Waters LCT-TOF spectrometer or a Waters Xevo G2-S bench top QTOF machine. Compounds **3.17** (D), **3.18** (A), **3.19** (DD), **3.20** (AA) and **4.2** was synthesised in chapter 3.

3,5-dibromoiodobenzene (**4.4**)

1,3,5-tribromobenzene (2.00 g, 6.35 mmol) was dissolved in dry Et₂O (60 mL) in a dried flask. The reaction was cooled to -78 °C. *n*BuLi (1.6 M in hexanes, 4.37 mL, 6.99 mmol) was added slowly over 1 h, and the reaction was stirred for 1 h at -78 °C. A solution of I₂ (3.20 g, 12.7 mmol) in dry Et₂O (10 mL) was added and reaction stirred at -78 °C for 1 h before being allowed to warm to room temperature over 1 hr. Saturated Na₂S₂O₃ (50 mL) solution was added and reaction stirred until colourless. The organic phase was separated and washed with water (2 × 50 mL) and brine (50 mL). The solution was dried (MgSO₄) and the solvent was removed by rotary evaporation under reduced pressure yielding crude product (2.40 g). This solid was washed through a plug of silica by 40-60 pet. ether (300 mL), and the solvent was removed to yield the desired compound **4.4** as white needles (2.20 g, 6.08 mmol, 96% yield).

TLC *R*_f: 0.65 (40-60 pet. ether);

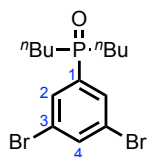
Melting Point: 120.0-122.0 °C;

¹H NMR (400 MHz, CDCl₃): δ 7.80 (d, *J* = 1.5 Hz, 2H, 2-H), 7.64 (t, *J* = 1.5 Hz, 1H, 4-H);

¹³C NMR (101 MHz, CDCl₃): δ 138.5 (2-C), 133.6 (4-C), 123.4 (3-C), 94.4 (1-C);

FT-IR (ATR): 3062, 1546, 1397, 1096 *v*_{max}/cm⁻¹;

Matches previously reported spectral data.³

Dibutyl(3,5-dibromophenyl)phosphine oxide (**4.5**)

*n*Butylphosphine oxide (693 mg, 4.27 mmol) was added to a dried flask and the flask evacuated and back-filled with nitrogen ($\times 3$). **4.4** (1.70 g, 4.70 mmol) was added and 1,4-dioxane (deoxygenated by freeze-pump-thaw, 5 mL) was added. In a separate flask, Pd₂(dba)₃ (108 mg, 0.118 mmol) and Xantphos (68.0 mg, 0.118 mmol) were placed in a flask and evacuated and back-filled with nitrogen ($\times 3$). These were dissolved in 1,4-dioxane (5 mL) and the solution transferred to the initial flask. Et₃N (600 μ L, 4.27 mmol) was added and the reaction stirred at room temperature for 2 h. CH₂Cl₂ (20 mL) was added and the reaction washed with saturated NaHCO₃ solution (25 mL). The aqueous layer was extracted with CH₂Cl₂ (3x 10 mL) combined organics dried (MgSO₄), and solvent removed yielding a brown solid (2.16 g). This solid was separated by flash chromatography (MeOH:CH₂Cl₂, 1:20) to yield the desired compound **4.5** as an orange crystalline solid (1.00 g, 2.52 mmol, 59% yield).

TLC R_f: 0.25 (MeOH:CH₂Cl₂ 1:20);

Melting Point: 90.3-92.2 °C;

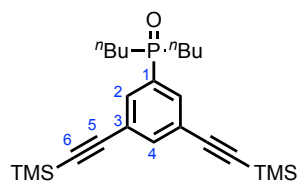
¹H NMR (400 MHz, CDCl₃): δ 7.83 (td, *J* = 2.0, 0.5 Hz, 1H, 4-H), 7.76 (dd, *J* = 10.5, 2.0 Hz, 2H, 2-H), 2.02-1.78 (m, 4H, *n*Bu), 1.70-1.54 (m, 2H, *n*Bu), 1.49-1.35 (m, 6H, *n*Bu), 0.91 (t, *J* = 7.0 Hz, 6H, *n*Bu);

¹³C NMR (101 MHz, CDCl₃): δ 137.2 (4-C), 137.0 (d, *J* = 2 Hz, 3-C), 131.8 (d, *J* = 9 Hz, 2-C), 123.8 (d, *J* = 14 Hz, 1-C), 29.7 (d, *J* = 69 Hz, *n*Bu), 24.0 (d, *J* = 15 Hz, *n*Bu), 23.4 (d, *J* = 4 Hz, *n*Bu), 13.6 (*n*Bu);

³¹P NMR (162 MHz, CDCl₃): δ 39.5 (Phosphine oxide);

FT-IR (ATR): 2956, 2928, 2869, 1546, 1397, 1169, 1130, 736 ν_{\max} /cm⁻¹;

HRMS (ES+): C₁₃H₂₂Br₂OP calcd. 394.9775 found 394.9769, Δ = -1.5 ppm.

(3,5-bis((trimethylsilyl)ethynyl)phenyl)dibutylphosphine oxide (**4.6**)

4.5 (300 mg, 0.757 mmol), Pd₂(dba)₃ (14.0 mg, 15.1 µmol), CuI (3.00 mg, 15.1 µmol) and PPh₃ (20.0 mg, 75.7 µmol) were added to a flask of Et₃N (5 mL) and N₂ bubbled through the reaction for 15 min. TMSA (260 µL, 1.82 mmol) was added and the reaction stirred at 50 °C overnight under N₂. The reaction was filtered through celite and washed through with EtOAc (10 mL). The solution was washed with 1 M HCl (3 × 10 mL). The solution was dried (MgSO₄) and solvent was removed by rotary evaporation under reduced pressure yielding a brown oil (420 mg). This solid was separated by flash chromatography (MeOH:CH₂Cl₂, 1:19) to yield the desired compound **4.6** as a brown oil (315 mg, 0.731 mmol, 97% yield).

TLC R_f: 0.25 (MeOH:CH₂Cl₂, 1:19);

Melting Point: 103.3-106.0 °C;

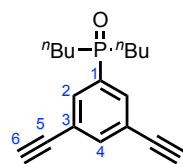
¹H NMR (400 MHz, CDCl₃): δ 7.71-7.68 (m, 3H, 2, 4-H), 2.01-1.70 (m, 4H, ⁿBu), 1.64-1.51 (m, 2H, ⁿBu), 1.45-1.30 (m, 6H, ⁿBu), 0.87 (t, *J* = 7.0 Hz, 6H, ⁿBu), -0.24 (s, 18H, TMS);

¹³C NMR (101 MHz, CDCl₃): δ 137.7 (d, *J* = 3 Hz, 4-C), 133.7 (d, *J* = 89 Hz, 1-C), 131.8 (d, *J* = 9 Hz, 3-C), 124.1 (d, *J* = 13 Hz, 2-C), 103.0 (5-C), 96.6 (6-C), 29.6 (d, *J* = 69 Hz, ⁿBu), 24.1 (d, *J* = 14 Hz, ⁿBu), 23.4 (d, *J* = 4 Hz, ⁿBu), 13.6 (ⁿBu), -0.2 (TMS);

³¹P NMR (162 MHz, CDCl₃): δ 40.2 (phosphine oxide);

FT-IR (ATR): 2956, 2928, 2869, 1546, 1397, 1169, 1130, 736 $\nu_{\text{max}}/\text{cm}^{-1}$;

HRMS (ES+): C₂₄H₄₀OPSi₂ calcd. 431.2355 found 431.2355, Δ = 0 ppm.

Dibutyl(3,5-diethylphenyl)phosphine oxide (**4.7**)

4.6 (100 mg, 0.232 mmol) was dissolved in dry THF (8 mL) and reaction purged with nitrogen. Reaction was cooled to 0 °C and TBAF (1M in THF, 0.510 mL, 0.510 mmol) added. Reaction was stirred for 10 min, diluted with EtOAc (25 mL) washed with 1M HCl (3 × 25 mL). The solution was dried (MgSO_4) and solvent was removed by rotary evaporation under reduced pressure yielding **4.7** as a brown oil (66.0 mg, 0.232 mmol, 100% yield).

TLC R_f : 0.20 (MeOH: CH_2Cl_2 , 1:19);

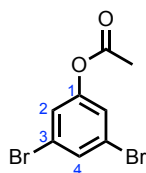
$^1\text{H NMR}$ (400 MHz, CDCl_3): δ 7.80 – 7.71 (m, 3H, 2, 4-H), 3.19 (s, 2H, 6-H), 2.11–1.80 (m, 4H, ^nBu), 1.67–1.53 (m, 2H, ^nBu), 1.45–1.30 (m, 6H, ^nBu), 0.88 (t, $J = 7.0$ Hz, 6H, ^nBu);

$^{13}\text{C NMR}$ (101 MHz, CDCl_3): δ 138.2 (d, $J = 3$ Hz, 4-C), 133.8 (d, $J = 9$ Hz, 3-C), 132.5 (d, $J = 89$ Hz, 1-C), 123.3 (d, $J = 13$ Hz, 2-C), 81.5 (5-C), 79.5 (6-C), 29.2 (d, $J = 69$ Hz, ^nBu), 24.0 (d, $J = 14$ Hz, ^nBu), 23.3 (d, $J = 4$ Hz, ^nBu), 13.5 (^nBu);

$^{31}\text{P NMR}$ (162 MHz, CDCl_3): 40.3 (phosphine oxide);

FT-IR (ATR): 2956, 2928, 2869, 1546, 1397, 1169, 1130, 736 $\nu_{\text{max}}/\text{cm}^{-1}$;

HRMS (ES+): $\text{C}_{18}\text{H}_{24}\text{OP}$ calcd. 287.1559 found 287.1152, $\Delta = -2.58$ ppm.

3,5-dibromophenyl acetate (4.9**)**

3,5-dibromophenol (2.50 g, 10.0 mmol) and DMAP (122 mg, 1.00 mmol) were added to a flask under N₂. Toluene (20 mL) and acetic anhydride (1.00 mL, 11.0 mmol) were added and the reaction stirred at room temperature overnight. The solvent was removed by rotary evaporation under reduced pressure to yield a brown oil. This oil was separated by flash chromatography (EtOAc:40-60 pet. ether, 1:9) to yield the desired compound **4.9** as a slightly yellow solid (2.73 g, 9.3 mmol, 93% yield).

TLC R_f: 0.70 (EtOAc:40-60 pet. ether, 1:9);

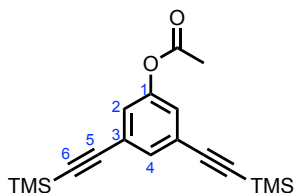
Melting Point: 57.2-59.1 °C;

¹H NMR (400 MHz, CDCl₃): δ 7.56 (t, J = 1.5 Hz, 1H, 4-H), 7.27 (d, J = 1.5 Hz, 2H, 2-H), 2.31 (s, 3H, OAc);

¹³C NMR (101 MHz, CDCl₃): δ 168.5 (C=O), 151.4 (1-C), 131.7 (4-C), 124.1 (2-C), 122.8 (3-C), 21.0 (OAc);

FT-IR (ATR): 3081, 1771, 1566, 1418, 1223, 933, 747 ν_{max}/cm⁻¹.

Matches previously reported spectral data.⁴

3,5-bis((trimethylsilyl)ethynyl)phenyl acetate (4.10**)**

4.9 (600 mg, 2.04 mmol), $\text{Pd}(\text{PPh}_3)_4$ (236 mg, 0.204 mmol) and CuI (39.0 mg, 0.204 mmol) were dissolved in toluene (6 mL) and Et_3N (6 mL). Nitrogen was bubbled through the solution for 20 min and TMSA (707 μL , 5.10 mmol) was added. The reaction was heated to 110 °C by microwave irradiation for 30 min. The reaction was filtered through celite and washed through with EtOAc (30 mL). The solution was washed with 1M HCl ($3 \times 30\text{mL}$), dried (MgSO_4) and the solvent was removed by rotary evaporation under reduced pressure to yield a brown solid (900 mg). This oil was separated by flash chromatography ($\text{EtOAc}:40\text{-}60$ pet. ether, 1:19) to yield the desired compound **4.10** as a white powder (576 mg, 1.75 mmol, 86% yield).

TLC R_f : 0.28 ($\text{EtOAc}:40\text{-}60$ pet. ether, 1:19);

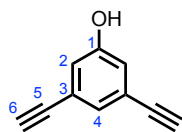
Melting Point: 95.0-96.6 °C;

$^1\text{H NMR}$ (400 MHz, CDCl_3): δ 7.43 (t, $J = 1.5$ Hz, 1H, 4-H), 7.14 (d, $J = 1.5$ Hz, 2H, 2-H), 2.27 (s, 3H, OAc), 0.23 (s, 18H, TMS);

$^{13}\text{C NMR}$ (101 MHz, CDCl_3): δ 168.9 (C=O), 150.1 (1-C), 132.9 (4-C), 125.1 (2-C), 124.6 (3-C), 103.0 (5-C), 95.9 (6-C), 21.0 (OAc), -0.2 (TMS);

FT-IR (ATR): 2960, 2159, 1773, 1195, 840 $\nu_{\text{max}}/\text{cm}^{-1}$;

Matches previously reported spectral data.⁴

3,5-diethynylphenol (**4.11**)

4.10 (116 mg, 0.350 mmol) and NaHCO₃ (148 mg, 1.77 mmol) were dissolved in MeOH (1 mL), THF (1 mL) and water (2 mL). The reaction was stirred overnight at 55 °C. The reaction was cooled to room temperature and water (10 mL) was added. The aqueous solution was extracted with Et₂O (6 × 10 mL). The combined organic extracted were dried (MgSO₄) and solvent removed by rotary evaporation under reduced pressure yielding a orange oil (99.5 mg). This oil was separated by flash chromatography (EtOAc:40-60 pet. ether, 1:4) to yield the desired compound **4.11** as an off-white powder (48.5 mg, 0.34 mmol, 97% yield).

TLC R_f: 0.17 (EtOAc:40-60 pet. ether, 1:4);

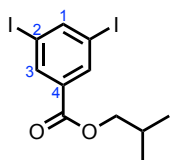
Melting Point: 83.7-84.7;

¹H NMR (400 MHz, CDCl₃): δ 7.23 (s, 1H, 4-H), 6.97 (s, 2H, 2-H), 5.13 (bs, 1H, OH), 3.09 (s, 2H, 6-H);

¹³C NMR (101 MHz, CDCl₃): δ 155.1 (1-C), 128.6 (4-C), 123.6 (2-C), 119.6 (3-C), 82.2 (5-C), 78.0 (6-C);

FT-IR (ATR): 3081, 1771, 1566, 933 ν_{max}/cm⁻¹;

Matches previously reported spectral data.⁴

Isobutyl 3,5-diiodobenzoate (4.13)

3,5-diiodobenzoic acid (200 mg, 0.530 mmol), EDC•HCl (113 mg, 0.588 mmol) and DMAP (6.50 mg, 53.5 μ mol) were dissolved in dry CH_2Cl_2 (5.3 mL) under N_2 . $i\text{BuOH}$ (0.101 μ L, 1.07 mmol) was added and reaction stirred for 2 h. The reaction was washed with 1M HCl (20 mL), water (20 mL) and brine (20 mL). The organic solution was dried (MgSO_4) and solvent was removed by rotary evaporation under reduced pressure yielding a pink solid (199 mg). This solid was separated by flash chromatography (EtOAc:40-60 pet. ether, 1:19) to yield the desired compound **4.13** as a white crystal plates (130 mg, 0.313 mmol, 58% yield).

TLC R_f : 0.78 (EtOAc:40-60 pet. ether, 1:9);

Melting Point: 56.5-57.8 °C;

$^1\text{H NMR}$ (400 MHz, CDCl_3): δ 8.31 (d, J = 1.5 Hz, 2H, 3-H), 8.22 (t, J = 1.5 Hz, 1H, 1-H), 4.10 (d, J = 6.5 Hz, 2H, $i\text{Bu}$), 2.16 – 1.85 (m, 1H, $i\text{Bu}$), 1.01 (d, J = 6.5 Hz, 6H, $i\text{Bu}$).

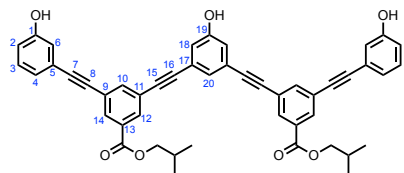
$^{13}\text{C NMR}$ (101 MHz, CDCl_3): δ 163.7 (C=O), 149.1 (1-C), 137.7 (3-C), 133.7 (4-C), 94.4 (2-C), 71.8 ($i\text{Bu}$), 27.8 ($i\text{Bu}$), 19.2 ($i\text{Bu}$);

FT-IR (ATR): 2961, 2363, 1723, 1546, 1416, 1254, 1120, 982 ν_{max} /cm⁻¹;

HRMS (ES+): $\text{C}_{18}\text{H}_{24}\text{OP}$ calcd. 429.8927 found 429.8911, Δ = -3.72 ppm.

Donor oligomerization (**4.14 - 4.17**)

4.1 (47.3 mg, 0.400 mmol), **4.11** (28.4 mg, 0.200 mmol) and **4.13** (172 mg, 0.400 mmol) were placed in a flask and degassed with N₂ for 30 min. Pd₂(dba)₃ (7.30 mg, 8.00 µmol) and CuI (1.50 mg, 8.00 µmol) and PPh₃ (10.5 mg, 40.0 µmol) were placed in a separate flask and degassed with N₂. Degassed Et₃N (167 µL, 1.20 mmol) was added and the contents of this flask transferred to the first using degassed toluene (8 mL). The reaction was stirred overnight at room temperature, in the dark under N₂. The solvent was removed by rotary evaporation under reduced pressure yielding a brown solid (186 mg). The sample was dissolved in DMSO and sonicated, before filtering. Preparative HPLC separation of the oligomerisation mixture was completed using a HIRBP-6988 prep column (250 × 25 mm, 5 µm particle size) with a water/THF solvent system (THF: 58% for 21 mins, 65% for 31 mins) at 15 mL min⁻¹.

Donor 3-mer (**4.14**)

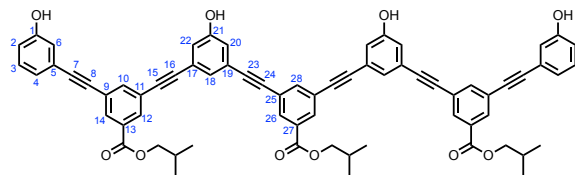
TLC R_f : 0.50 (MeOH:CH₂Cl₂ 1:9);

¹H NMR (500 MHz, THF-d₈): δ 9.36 (bs, 1H, 19-OH), 8.88 (bs, 2H, 1-OH), 8.14 – 8.11 (m, 4H, 12, 14-H), 7.90 (t, *J* = 1.5 Hz, 2H, 10-H), 7.28 (t, *J* = 1.5 Hz, 1H, 20-H), 7.18 (t, *J* = 8.0 Hz, 2H, 3-H), 7.06 – 6.99 (m, 4H, 6, 18-H), 6.99 – 6.96 (m, 2H, 4-H), 6.89 – 6.77 (m, 2H, 2-H), 4.15 (d, *J* = 6.5 Hz, 4H, *i*Bu), 2.14 – 2.10 (m, 2H, *i*Bu), 1.05 (d, *J* = 6.5 Hz, 12H, *i*Bu);

¹³C NMR (126 MHz, THF-d₈): δ 165.1 (C=O), 158.7 (19-C), 158.6 (1-C), 138.6 (10-C), 132.4 (Ar-C), 132.3 (Ar-C), 132.2 (Ar-C), 130.1 (3-C), 126.6 (20-C), 125.2 (9-C), 124.7 (Ar-C), 124.6 (Ar-C), 124.0 (5-C), 123.2 (4-C), 119.7 (18-C), 118.8 (6-C), 117.1 (2-C), 92.0 (-C≡), 90.7 (-C≡), 88.0 (-C≡), 87.1 (-C≡), 71.8 (*i*Bu), 28.7 (*i*Bu), 19.2 (*i*Bu);

FT-IR (ATR): 3412 (br), 2221, 1700, 1591, 1579, 1283, 1242 $\nu_{\text{max}}/\text{cm}^{-1}$;

HRMS (ES+): C₄₈H₃₈O₇ calcd. 727.2690 found 727.2658, Δ = -4.46 ppm.

Donor 4-mer (**4.15**)

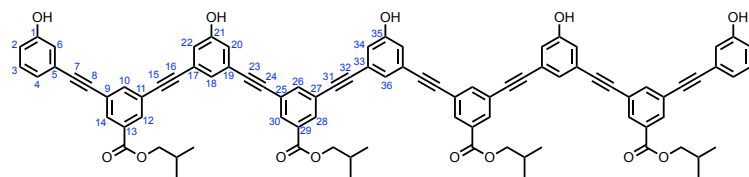
TLC R_f : 0.50 (MeOH:CH₂Cl₂ 1:9);

¹H NMR (500 MHz, THF-d₈): δ 9.80 (bs, 2H, 21-OH), 9.30 (bs, 2H, 1-OH), 8.15 (d, J = 1.5 Hz, 2H, 26-H) 8.13 – 8.10 (m, 4H, 12, 14-H), 7.94 (t, J = 1.5 Hz, 1H, 28-H), 7.90 (t, J = 1.5 Hz, 2H, 10-H), 7.28 (t, J = 1.5 Hz, 2H, 18-H), 7.18 (t, J = 8.0 Hz, 2H, 3-H), 7.06 – 6.99 (m, 6H, 6, 20, 22-H), 6.99 – 6.96 (m, 2H, 4-H), 6.89 – 6.77 (m, 2H, 2-H), 4.15 (d, J = 6.5 Hz, 6H, *i*Bu), 2.14 – 2.10 (m, 3H, *i*Bu), 1.05 (d, J = 6.5 Hz, 18H, *i*Bu);

¹³C NMR (126 MHz, THF-d₈): δ 165.1 (13-C=O), 165.0 (27-C=O), 159.0 (21-C), 158.8 (1-C), 138.7 (28-C), 138.6 (10-C), 132.5 (Ar-C), 132.4 (Ar-C), 132.4 (Ar-C), 132.3 (Ar-C), 132.2 (Ar-C), 130.0 (3-C), 126.4 (18-C), 125.3 (9-C), 124.8 (Ar-C), 124.7 (Ar-C), 124.5 (Ar-C), 124.5 (Ar-C), 124.0 (5-C), 123.0 (4-C), 119.9 (20, 22-C), 118.9 (6-C), 117.2 (2-C), 92.1 (-C≡), 90.9 (-C≡), 90.8 (-C≡), 87.9 (-C≡), 87.0 (-C≡), 71.8 (*i*Bu), 28.7 (*i*Bu), 19.2 (*i*Bu);

FT-IR (ATR): 3392 (br), 2925, 2226, 1721, 1591, 1560, 1282, 1239 $\nu_{\text{max}}/\text{cm}^{-1}$;

HRMS (ES+): C₆₉H₅₈O₁₀ calcd. 1046.4030 found 1046.4003, Δ = -2.58 ppm.

Donor 5-mer (**4.16**)

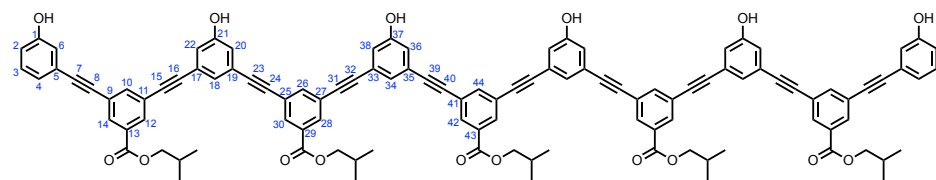
TLC R_f : 0.50 (MeOH:CH₂Cl₂ 1:9);

¹H NMR (500 MHz, THF-d₈): δ 9.03 (bs, 3H, 21, 35-OH), 8.65 (bs, 2H, 1-OH), 8.16 (d, *J* = 1.5 Hz, 4H, 28, 30-H) 8.13 – 8.10 (m, 4H, 12, 14-H), 7.94 (t, *J* = 1.5 Hz, 2H, 26-H), 7.90 (t, *J* = 1.5 Hz, 2H, 10-H), 7.32-7.29 (m, 3H, 18, 36-H), 7.18 (t, *J* = 8.0 Hz, 2H, 3-H), 7.06 – 6.99 (m, 8H, 6, 20, 22, 34-H), 6.99 – 6.96 (m, 2H, 4-H), 6.89 – 6.77 (m, 2H, 2-H), 4.15 (d, *J* = 6.5 Hz, 8H, *t*Bu), 2.14 – 2.10 (m, 4H, *t*Bu), 1.05 (d, *J* = 6.5 Hz, 24H, *t*Bu);

¹³C NMR (126 MHz, THF-d₈): δ 165.0 (13-C=O), 165.0 (29-C=O), 158.6 (21, 35-C), 158.5 (1-C), 138.7 (26-C), 138.6 (10-C), 132.6 (Ar-C), 132.5 (Ar-C), 132.4 (Ar-C), 132.3 (Ar-C), 132.3 (Ar-C), 130.1 (3-C), 126.8 (18-C), 125.2 (9-C), 124.8 (Ar-C), 124.7 (Ar-C), 124.7 (Ar-C), 124.1 (5-C), 123.4 (4-C), 119.7 (20, 22, 34-C), 118.9 (6-C), 117.1 (2-C), 91.9 (-C≡), 90.7 (-C≡), 90.7 (-C≡), 88.2 (-C≡), 88.1 (-C≡), 87.2 (-C≡), 71.8 (*t*Bu), 28.7 (*t*Bu), 19.2 (*t*Bu);

FT-IR (ATR): 3453 (br), 2958, 2269, 1720, 1703 1591, 1580, 1237 $\nu_{\text{max}}/\text{cm}^{-1}$;

MS (ES+): m/z (%) = 678.0 (100) [M-2H⁺], 1358.5 (50) [M-H⁺].

Donor 6-mer (**4.17**)

TLC R_f : 0.50 (MeOH:CH₂Cl₂ 1:9);

¹H NMR (500 MHz, THF-d₈): δ 9.03 (bs, 4H, 19-OH), 8.61 (bs, 2H, 1-OH), 8.16 (d, J = 1.5 Hz, 6H, 28, 30, 42-H) 8.13 – 8.10 (m, 4H, 12, 14-H), 7.94 (t, J = 1.5 Hz, 3H, 26, 44-H), 7.90 (t, J = 1.5 Hz, 2H, 10-H), 7.32-7.29 (m, 4H, 18, 34-H), 7.18 (t, J = 8.0 Hz, 2H, 3-H), 7.06 – 6.99 (m, 10H, 6, 20, 22, 36, 38-H), 6.99 – 6.96 (m, 2H, 4-H), 6.89 – 6.77 (m, 2H, 2-H), 4.15 (d, J = 6.5 Hz, 10H, *i*Bu), 2.14 – 2.10 (m, 5H, *i*Bu), 1.05 (d, J = 6.5 Hz, 30H, *i*Bu);

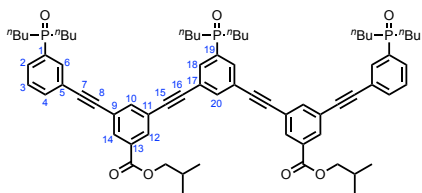
¹³C NMR (126 MHz, THF-d₈): δ 165.0 (13-C=O), 165.0 (29, 43-C=O), 158.6 (21, 37-C), 158.5 (1-C), 138.7 (26, 44-C), 138.6 (10-C), 132.6 (Ar-C), 132.5 (Ar-C), 132.4 (Ar-C), 132.3 (Ar-C), 132.3 (Ar-C), 130.1 (3-C), 126.8 (18-C), 125.2 (9-C), 124.8 (Ar-C), 124.7 (Ar-C), 124.7 (Ar-C), 124.7 (Ar-C), 124.1 (5-C), 123.4 (4-C), 119.7 (20, 22, 36, 38-C), 118.9 (6-C), 117.1 (2-C), 91.9 (-C≡), 90.7 (-C≡), 90.7 (-C≡), 88.2 (-C≡), 88.1 (-C≡), 87.2 (-C≡), 71.8 (*i*Bu), 28.7 (*i*Bu), 19.2 (*i*Bu);

FT-IR (ATR): 3411 (br), 2925, 2110, 1699, 1581, 1288 $\nu_{\text{max}}/\text{cm}^{-1}$;

MS (ES+): m/z (%) = 836.3 (100) [M-2H⁺], 1673.6 (20) [M-H⁺].

Acceptor oligomerization (**4.18 - 4.22**)

4.2 (105 mg, 0.400 mmol), **4.7** (57.3 mg, 0.200 mmol) and **4.13** (172 mg, 0.400 mmol) were placed in a flask and degassed with N₂ for 30 min. Pd₂(dba)₃ (7.30 mg, 8.00 µmol) and CuI (1.50 mg, 8.00 µmol) and PPh₃ (10.5 mg, 40.0 µmol) were placed in a separate flask and degassed with N₂. Degassed Et₃N (167 µL, 1.20 mmol) was added and the contents of this flask transferred to the first using degassed toluene (8 mL). The reaction was stirred overnight at room temperature, in the dark under N₂. The solvent was removed by rotary evaporation under reduced pressure yielding a brown solid (260 mg). The sample was dissolved in EtOH and sonicated, before filtering. Preparative HPLC separation of the oligomerisation mixture was completed using a HIRBP-6988 prep column (250 × 25 mm, 5 µm particle size) with a water/THF solvent system (THF: 60% for 42 mins, 65% for 33 mins) at 15 mL min⁻¹.

Acceptor 3-mer (**4.18**)

TLC R_f : 0.40 (MeOH:CH₂Cl₂ 1:9);

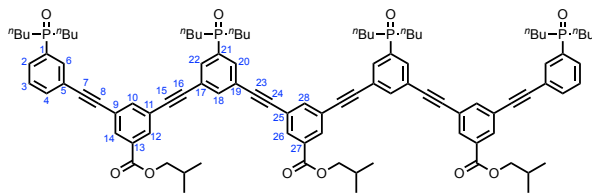
¹H NMR (500 MHz, CDCl₃): δ 8.19-8.15 (m, 4H, 12,14-H), 7.90 – 7.84 (m, 7H, 6, 10, 18, 20-H), 7.74-7.69 (m, 4H, 2, 4-H), 7.51 (td, *J* = 7.5, 2.5 Hz, 2H, 3-H), 4.16 (d, *J* = 6.5 Hz, 4H, *i*Bu), 2.14 – 2.10 (m, 2H, *i*Bu), 2.07-1.81 (m, 12H, ⁿBu), 1.71-1.55 (m, 6H, ⁿBu), 1.49-1.35 (m, 18H, ⁿBu), 1.06 (d, *J* = 6.5 Hz, 12H, *i*Bu), 0.91-0.87 (m, 18H, ⁿBu);

¹³C NMR (126 MHz, CDCl₃): δ 165.1 (C=O), 138.2 (10-C), 137.0 (d, *J* = 2.5 Hz, 20-C), 134.4 (4-C), 134.4 (d, *J* = 88.0 Hz, 19-C), 133.6 (d, *J* = 9.5 Hz, 6-C), 133.6 (d, *J* = 89.5 Hz, 1-C), 133.3 (d, *J* = 8.5 Hz, 18-C), 132.7 (12-C), 132.5 (14-C), 131.5 (13-C), 130.5 (d, *J* = 8.0 Hz, 2-C), 128.8 (d, *J* = 11.0 Hz, 3-C), 123.9 (9-C) 123.8 (d, *J* = 12.5 Hz, 17-C), 123.5 (11-C), 123.3 (d, *J* = 12.5 Hz, 5-C), 90.0 (-C≡), 89.6 (-C≡), 89.0 (-C≡), 88.8 (-C≡), 71.7 (*i*Bu), 29.7 (d, *J* = 68.5 Hz, ⁿBu), 27.9 (*i*Bu), 24.1 (d, *J* = 14.5 Hz, ⁿBu), 23.5 (d, *J* = 4.0 Hz, ⁿBu) 19.3 (*i*Bu), 13.6 (ⁿBu);

³¹P NMR (162 MHz, CDCl₃): δ 40.3 (1-P), 40.1 (19-P) (phosphine oxides);

FT-IR (ATR): 2957, 2220, 1718, 1594, 1440, 1221, 1169 $\nu_{\text{max}}/\text{cm}^{-1}$;

HRMS (ES+): C₇₂H₉₀O₇P₃ calcd. 1159.5894 found 1159.5886, Δ = -0.67 ppm.

Acceptor 4-mer (**4.19**)

TLC R_f : 0.40 (MeOH:CH₂Cl₂ 1:9);

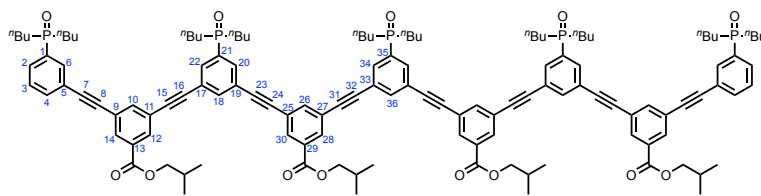
¹H NMR (500 MHz, CDCl₃): δ 8.20 (d, J = 1.5 Hz, 2H, 26-H), 8.19-8.15 (m, 4H, 12,14-H), 7.91 – 7.84 (m, 11H, 6, 10, 18, 20, 22, 28-H), 7.74-7.69 (m, 4H, 2, 4-H), 7.51 (td, J = 7.5, 2.5 Hz, 2H, 3-H), 4.16 (d, J = 6.5 Hz, 6H, *i*Bu), 2.14 – 2.10 (m, 3H, *i*Bu), 2.07-1.81 (m, 16H, ⁿBu), 1.71-1.55 (m, 8H, ⁿBu), 1.49-1.35 (m, 24H, ⁿBu), 1.06 (d, J = 6.5 Hz, 18H, *i*Bu), 0.91-0.87 (m, 24H, ⁿBu);

¹³C NMR (126 MHz, CDCl₃): δ 165.1 (13-C=O), 165.1 (27-C=O), 138.3 (10, 28-C), 137.0 (d, J = 2.5 Hz, 18-C), 134.4 (4-C), 134.4 (d, J = 88.0 Hz, 21-C), 133.6 (d, J = 9.5 Hz, 6-C), 133.6 (d, J = 89.5 Hz, 1-C), 133.3 (d, J = 8.5 Hz, 20, 22-C), 132.7 (26-C), 132.7 (12-C), 132.5 (14-C), 131.5 (27-C), 131.5 (13-C), 130.5 (d, J = 8.0 Hz, 2-C), 128.8 (d, J = 11.0 Hz, 3-C), 123.9 (9-C) 123.8 (d, J = 12.5 Hz, 17, 19-C), 123.6 (25-C), 123.5 (11-C), 123.3 (d, J = 12.5 Hz, 5-C), 90.0 (-C≡), 89.6 (-C≡), 89.5 (-C≡), 89.1 (-C≡), 89.0 (-C≡), 88.8 (-C≡), 71.7 (*i*Bu), 29.7 (d, J = 68.5 Hz, ⁿBu), 27.9 (*i*Bu), 24.1 (d, J = 14.5 Hz, ⁿBu), 23.5 (d, J = 4.0 Hz, ⁿBu) 19.3 (*i*Bu), 13.6 (ⁿBu);

³¹P NMR (162 MHz, CDCl₃): δ 40.3 (1-P), 40.1 (21-P) (phosphine oxides);

FT-IR (ATR): 2957, 2215, 1722, 1594, 1443, 1220, 1172 $\nu_{\text{max}}/\text{cm}^{-1}$;

HRMS (ES+): C₁₀₁H₁₂₃O₁₀P₄ calcd. 1642.7959 found 1642.7893, Δ = -4.00 ppm.

Acceptor 5-mer (**4.20**)

TLC R_f : 0.40 (MeOH:CH₂Cl₂ 1:9);

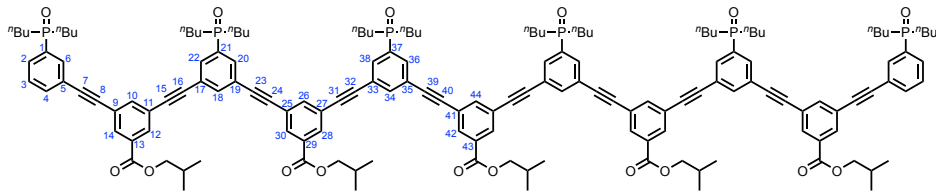
¹H NMR (500 MHz, CDCl₃): δ 8.20 (d, J = 1.5 Hz, 4H, 28, 30-H), 8.19-8.15 (m, 4H, 12, 14-H), 7.91 – 7.84 (m, 15H, 6, 10, 18, 20, 22, 26, 34, 36-H), 7.74-7.69 (m, 4H, 2, 4-H), 7.51 (td, J = 7.5, 2.5 Hz, 2H, 3-H), 4.16 (d, J = 6.5 Hz, 8H, ^tBu), 2.14 – 2.10 (m, 4H, ⁱBu), 2.07-1.81 (m, 20H, ⁿBu), 1.71-1.55 (m, 10H, ⁿBu), 1.49-1.35 (m, 30H, ⁿBu), 1.06 (d, J = 6.5 Hz, 24H, ⁱBu), 0.91-0.87 (m, 30H, ⁿBu);

¹³C NMR (126 MHz, CDCl₃): δ 165.1 (13-C=O), 165.1 (29-C=O), 138.3 (10, 26-C), 137.0 (d, J = 2.5 Hz, 18, 36-C), 134.4 (4-C), 134.4 (d, J = 88.0 Hz, 21, 35-C), 133.6 (d, J = 9.5 Hz, 6-C), 133.6 (d, J = 89.5 Hz, 1-C), 133.3 (d, J = 8.5 Hz, 20, 22, 34-C), 132.7 (28, 30-C), 132.7 (12-C), 132.5 (14-C), 131.5 (29-C), 131.5 (13-C), 130.5 (d, J = 8.0 Hz, 2-C), 128.8 (d, J = 11.0 Hz, 3-C), 123.9 (9-C) 123.8 (d, J = 12.5 Hz, 17, 19, 33-C), 123.6 (25, 27-C), 123.5 (11-C), 123.3 (d, J = 12.5 Hz, 5-C), 90.0 (-C≡), 89.6 (-C≡), 89.5 (bs, -C≡), 89.1 (bs, -C≡), 89.0 (-C≡), 88.8 (-C≡), 71.7 (ⁱBu), 29.7 (d, J = 68.5 Hz, ⁿBu), 27.9 (ⁱBu), 24.1 (d, J = 14.5 Hz, ⁿBu), 23.5 (d, J = 4.0 Hz, ⁿBu) 19.3 (ⁱBu), 13.6 (ⁿBu);

³¹P NMR (162 MHz, CDCl₃): δ 40.3 (1-P), 40.1 (21, 30-P) (phosphine oxides);

FT-IR (ATR): 2958, 2216, 1721, 1594, 1235, 1168, 726 $\nu_{\text{max}}/\text{cm}^{-1}$;

HRMS (ES+): C₁₃₀H₁₅₅O₁₃P₅ calcd. 2102.0048 found 2101.9944, Δ = -4.97 ppm.

Acceptor 6-mer (**4.21**)

TLC R_f : 0.40 (MeOH:CH₂Cl₂ 1:9);

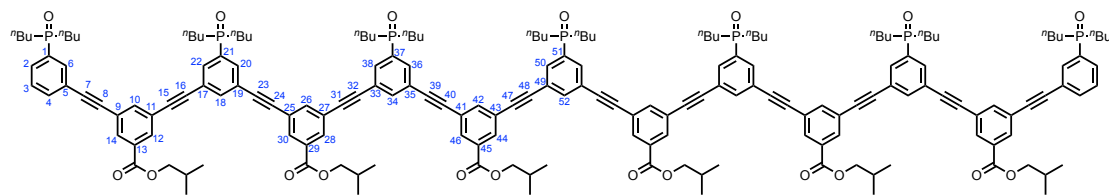
¹H NMR (500 MHz, CDCl₃): δ 8.20 (d, *J* = 1.5 Hz, 6H, 28, 30, 42-H), 8.19-8.15 (m, 4H, 12,14-H), 7.91 – 7.84 (m, 19H, 6, 10, 18, 20, 22, 26, 34, 36, 38, 44-H), 7.74-7.69 (m, 4H, 2, 4-H), 7.51 (td, *J* = 7.5, 2.5 Hz, 2H, 3-H), 4.16 (d, *J* = 6.5 Hz, 10H, *i*Bu), 2.14 – 2.10 (m, 5H, *i*Bu), 2.07-1.81 (m, 24H, ⁿBu), 1.71-1.55 (m, 12H, ⁿBu), 1.49-1.35 (m, 36H, ⁿBu), 1.06 (d, *J* = 6.5 Hz, 30H, *i*Bu), 0.91-0.87 (m, 36H, ⁿBu);

¹³C NMR (126 MHz, CDCl₃): δ 165.1 (13-C=O), 165.1 (29, 43-C=O), 138.3 (10, 26, 44-C), 137.0 (d, *J* = 2.5 Hz, 18, 34-C), 134.4 (4-C), 134.4 (d, *J* = 88.0 Hz, 21, 37-C), 133.6 (d, *J* = 9.5 Hz, 6-C), 133.6 (d, *J* = 89.5 Hz, 1-C), 133.3 (d, *J* = 8.5 Hz, 20, 22, 36, 38-C), 132.7 (28, 30, 42-C), 132.7 (12-C), 132.5 (14-C), 131.5 (29, 43-C), 131.5 (13-C), 130.5 (d, *J* = 8.0 Hz, 2-C), 128.8 (d, *J* = 11.0 Hz, 3-C), 123.9 (9-C) 123.8 (d, *J* = 12.5 Hz, 17, 19, 33, 35-C), 123.6 (25, 27, 41-C), 123.5 (11-C), 123.3 (d, *J* = 12.5 Hz, 5-C), 90.0 (-C≡), 89.6 (-C≡), 89.5 (bs, -C≡), 89.1 (bs, -C≡), 89.0 (-C≡), 88.8 (-C≡), 71.7 (*i*Bu), 29.7 (d, *J* = 68.5 Hz, ⁿBu), 27.9 (*i*Bu), 24.1 (d, *J* = 14.5 Hz, ⁿBu), 23.5 (d, *J* = 4.0 Hz, ⁿBu) 19.3 (*i*Bu), 13.6 (ⁿBu);

³¹P NMR (162 MHz, CDCl₃): δ 40.3 (1-P), 40.1 (21, 37-P) (phosphine oxides);

FT-IR (ATR): 2958, 2246, 1723, 1594, 1444, 1236, 1172 $\nu_{\text{max}}/\text{cm}^{-1}$;

MS (ES+): m/z (%) = 1271.0 (100) [M+2H⁺], 2540.2 (20) [M+H⁺].

Acceptor 7-mer (**4.22**)

TLC R_f : 0.40 (MeOH:CH₂Cl₂ 1:9);

¹H NMR (500 MHz, CDCl₃): δ 8.20 (d, *J* = 1.5 Hz, 8H, 28, 30, 44, 46-H), 8.19-8.15 (m, 4H, 12,14-H), 7.91 – 7.84 (m, 23H, 6, 10, 18, 20, 22, 26, 34, 36, 38, 42, 50, 52-H), 7.74-7.69 (m, 4H, 2, 4-H), 7.51 (td, *J* = 7.5, 2.5 Hz, 2H, 3-H), 4.16 (d, *J* = 6.5 Hz, 12H, ⁱBu), 2.14 – 2.10 (m, 6H, ⁱBu), 2.07-1.81 (m, 28H, ⁿBu), 1.71-1.55 (m, 14H, ⁿBu), 1.49-1.35 (m, 42H, ⁿBu), 1.06 (d, *J* = 6.5 Hz, 36H, ⁱBu), 0.91-0.87 (m, 42H, ⁿBu);

¹³C NMR (126 MHz, CDCl₃): δ 165.1 (13-C=O), 165.1 (29, 45-C=O), 138.3 (10, 26, 42-C), 137.0 (d, *J* = 2.5 Hz, 18, 34, 52-C), 134.4 (4-C), 134.4 (d, *J* = 88.0 Hz, 21, 37, 51-C), 133.6 (d, *J* = 9.5 Hz, 6-C), 133.6 (d, *J* = 89.5 Hz, 1-C), 133.3 (d, *J* = 8.5 Hz, 20, 22, 36, 38, 50-C), 132.7 (28, 30, 44, 46-C), 132.7 (12-C), 132.5 (14-C), 131.5 (29, 45-C), 131.5 (13-C), 130.5 (d, *J* = 8.0 Hz, 2-C), 128.8 (d, *J* = 11.0 Hz, 3-C), 123.9 (9-C) 123.8 (d, *J* = 12.5 Hz, 17, 19, 33, 35, 49-C), 123.6 (25, 27, 41, 43-C), 123.5 (11-C), 123.3 (d, *J* = 12.5 Hz, 5-C), 90.0 (-C≡), 89.6 (-C≡), 89.5 (bs, -C≡), 89.1 (bs, -C≡), 89.0 (-C≡), 88.8 (-C≡), 71.7 (ⁱBu), 29.7 (d, *J* = 68.5 Hz, ⁿBu), 27.9 (ⁱBu), 24.1 (d, *J* = 14.5 Hz, ⁿBu), 23.5 (d, *J* = 4.0 Hz, ⁿBu) 19.3 (ⁱBu), 13.6 (ⁿBu);

³¹P NMR (162 MHz, CDCl₃): δ 40.3 (1-P), 40.1 (21, 37, 51-P) (phosphine oxides);

FT-IR (ATR): 2932, 2184, 1723, 1595, 1444, 1236, 1129 $\nu_{\text{max}}/\text{cm}^{-1}$;

MS (ES+): m/z (%) = 1501.1 (100) [M+2H⁺], 3000.6 (5) [M+H⁺].

4.5.2 HPLC

The samples were analyzed by reverse phase HPLC using an Agilent LC-MSD ionTrap model XCT LCMS equipment in Electrospray mode. This system is composed of a modular Agilent 1200 Series HPLC system connected to an Agilent/Bruker ionTrap model XCT with MSMS capabilities. The modular Agilent 1200 Series HPLC system is composed of a HPLC high pressure binary pump, autosampler with injector programming capabilities, column oven with 6 μL heat exchanger and a Diode Array Detector with a semimicro flow cell (6 mm path length, 1.7 μl volume) to reduce peak dispersion when using short columns as in this case. The flow-path was connected using 0.12 mm ID stainless steel tubing to minimize peak dispersion. The outlet of the Diode Array Detector flowcell is connected via a switching valve to the IonTrap, the switching valve allowing directing the first segment of the chromatography corresponding to solvent front to waste. After removing the contamination ions associated with the solvent front, the switching valve directs the solvent to the electrospray ion source. While the solvent rate of the method is 1mL/min, the ion source has a dead volume passive splitting union installed which splits the flow rate entering the ion source to <100 $\mu\text{L}/\text{min}$, the rest of the flow rate is directed to waste. This reduction in flow rate enhances the electrospray signal and reduces the contamination in the ion source.

The Electrospray was set to +ve mode. The capillary needle has an orthogonal-flow sprayer design with respect to the ion transmission. The capillary needle voltage was set to +3500 V and the end plate offset was set to -500 V. The solvent eluting from the HPLC column entering the ESI capillary needle in the Ion Source Interface was nebulised with the assistance of N₂ at 15 psi. Drying N₂ gas heated to 325 °C and flowing at 5 L/min was used for the ESI desolvation stage. The ion transport and focusing region of the LC/MSD Trap is enclosed in the vacuum manifold, formed by a rough pump and two turbopumps. The ions formed on the Ion Source Interface enter and are guided through the glass capillary, where the capillary exit is set to -178 V. The bulk of the drying gas is removed by the rough pump before the skimmer which is set to -178 V. The ions then pass into an octopole ion guide (Octopole 1 set to -12 V DC followed by Octopole 2 set to -3 V

DC set to a radio frequency of 200 Vpp) that focuses and transports the ions from a relatively high-pressure position directly behind the skimmer to the focusing/exit lenses (Lens 1 set to +5 V followed by Lens 2 set to +60 V) coupling the ion transport to the ion trap. The selected ions entered the ion trap which had been set to a value of 109.9. For efficient trapping and cooling of the ions generated by the electrospray interface, helium gas is introduced into the ion trap.

The fractions were isolated using an Agilent HP-1100 preparative HPLC system. This is composed of a high pressure mixing binary pump capable of flow rates up to 50 mL/min at 400 bar back-pressure, with dual injector autosamplers loops (500 μ L and a 5 mL loop), a variable detector (190 nm to 600 nm) and a fraction collector. UV/vis absorption was measured at 290 nm (8 nm bandwidth) with reference 550 nm (100 nm bandwidth). The software for the fraction collector can be set to automatically collect on peak recognition.

4.5.3 Binding studies

A•D, AA•DD and D•DMSO complexes by NMR titration

Binding constants were measured by ^{31}P and ^1H NMR titrations in a Bruker 500 MHz AVIII HD Smart Probe spectrometer at 298 K. The host (phosphine oxide derivatives **3.18** or **3.20**, or phenol derivative **3.17**) was dissolved in toluene- d_8 at a known concentration ($[\text{3.18}] = 1.0 - 2.5 \text{ mM}$, $[\text{3.20}] = 0.15 \text{ mM}$, $[\text{3.17}] = 8.0 - 10 \text{ mM}$). The guest (phenol derivatives **3.17** or **3.19**, or DMSO) was dissolved in the host solution and made to a known concentration ($[\text{3.17}] = 20 - 30 \text{ mM}$, $[\text{3.19}] = 1.0 \text{ mM}$, $[\text{DMSO}] = 120 - 130 \text{ mM}$). A known volume of host was added to an NMR tube and the spectrum was recorded. Known volumes of guest in host solution were added to the NMR tube, and the spectra were recorded after each addition. The chemical shifts of the host spectra were monitored as a function of guest concentration and analysed using a purpose written software in Microsoft Excel. Errors were calculated as two times the standard deviation from the average value (95% confidence limit).

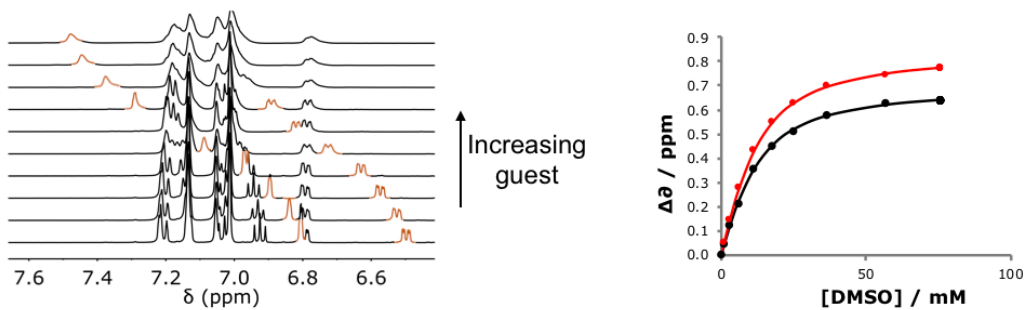


Figure 4.15: ^1H NMR data (500 MHz) for titration of DMSO into **3.17** (D, 9.6 mM), at 298 K in toluene- d_8 . Representative titration spectra and plots of complexation-induced change in chemical shift versus guest concentration (the line represents the best fit to a 1:1 binding isotherm).

AA•DD, AAA•DDD and AAAA•DDDD complexes by denaturation through competition

Binding constants were measured by ^{31}P NMR denaturation experiments in a Bruker 500 MHz AVIII HD Smart Probe spectrometer at 298 K. An equimolar solution of complementary homo-oligomers (phosphine oxide derivatives **3.20**,

4.18 or **4.19**, and phenol derivatives **3.19**, **4.14** or **4.15**) was produced at a concentration of 1 mM in toluene-d₈. A known volume of solution was added to an NMR tube and the spectrum recorded. Known volumes of DMSO-*d*₆ in toluene-d₈ and neat DMSO-*d*₆ were added and the spectrum recorded after each addition. The chemical shifts of the acceptor homo-oligomer spectra were monitored as a function of DMSO-*d*₆ concentration. Free ³¹P NMR shifts were monitored for a 1 mM solution of free A (**3.18**) in toluene-*d*₈ with the same concentrations of DMSO-*d*₆ to account for solvent effects. These were subtracted from the raw data and the corrected data analysed using a purpose written software in Microsoft Excel.

For all fittings, the association constants for certain species were fixed as explained in the discussion and **Figures 4.8-4.10**. For the AA•DD fitting, the ³¹P NMR shift of the phosphine oxide in the AA•DD•DMSO complex was fixed by equation 4.3 due to the formation of only one H-bond.

$$\delta_{\text{AA}\bullet\text{DD}\bullet\text{DMSO}} = \frac{(\delta_{\text{bound}} - \delta_{\text{free}})}{2} \quad 4.3$$

For the AAA•DDD fitting, the ³¹P NMR shifts of the phosphine oxides in the AAA•DDD•DMSO and AAA•DDD•(DMSO)₂ were fixed by equations 4.4 and 4.5.

$$\delta_{\text{AAA}\bullet\text{DDD}\bullet\text{DMSO}} = \frac{2(\delta_{\text{bound}} - \delta_{\text{free}})}{3} \quad 4.4$$

$$\delta_{\text{AAA}\bullet\text{DDD}\bullet(\text{DMSO})_2} = \frac{(\delta_{\text{bound}} - \delta_{\text{free}})}{3} \quad 4.5$$

For the AAAA•DDDD fitting the ³¹P NMR shifts of the phosphine oxides in the AAAA•DDDD•DMSO, AAAA•DDDD•(DMSO)₂, and AAAA•DDDD•(DMSO)₃ complexes were fixed by equations 4.6, 4.7 and 4.8.

$$\delta_{\text{AAAA}\bullet\text{DDDD}\bullet\text{DMSO}} = \frac{3(\delta_{\text{bound}} - \delta_{\text{free}})}{4} \quad 4.6$$

$$\delta_{\text{AAAA}\bullet\text{DDDD}\bullet(\text{DMSO})_2} = \frac{2(\delta_{\text{bound}} - \delta_{\text{free}})}{4} \quad 4.7$$

$$\delta_{\text{AAAA}\bullet\text{DDDD}\bullet(\text{DMSO})_3} = \frac{(\delta_{\text{bound}} - \delta_{\text{free}})}{4} \quad 4.8$$

4.6 References

- (1) Prince, R. B.; Okada, T.; Moore, J. S. *Angew. Chem. Int. Ed.* **1999**, *38* (1/2), 233–236.
- (2) Berendsen, H. J. C. In *A Student's Guide to Data and Error Analysis*; pp 84–111.
- (3) Zhao, W.; Huang, L.; Guan, Y.; Wulff, W. D. *Angew. Chem. Int. Ed.* **2014**, *53* (13), 3436–3441.
- (4) Ghosh, K.; Yang, H. B.; Northrop, B. H.; Lyndon, M. M.; Zheng, Y. R.; Muddiman, D. C.; Stang, P. J. *J. Am. Chem. Soc.* **2008**, *130* (15), 5320–5334.

Chapter 5

Mixed sequence oligomers

5.1 Introduction

Nucleic acids can fold into specific shapes, driven by the formation of intramolecular H-bonds.^{1,2} This tertiary structure allows the nucleotides to perform a range of functions, such as binding specific targets (aptamers), or catalysing reactions (ribozymes). Evaluating folding in potential synthetic information molecules is an important step in assessing their possible functionality.

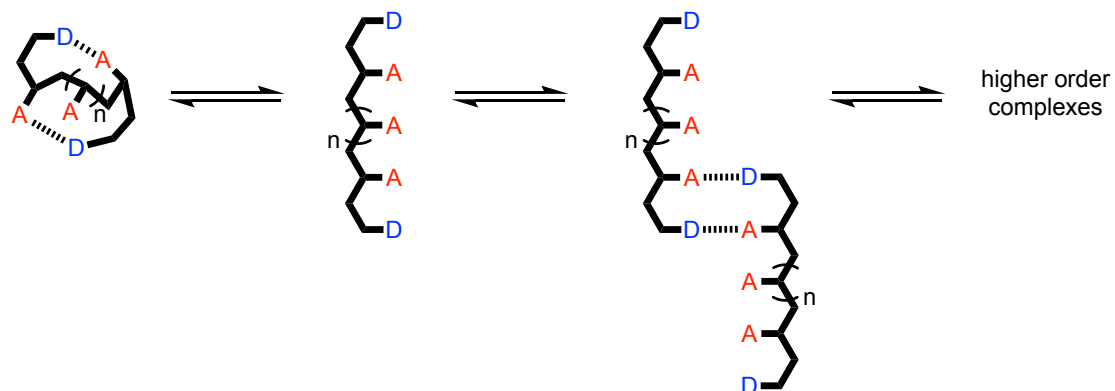
Moore and co-workers showed that phenylacetylene oligomers of greater than eight phenyl rings can fold into helices.³ In good solvents such as chloroform, the oligomers existed as random coils at all lengths. In acetonitrile, changes were observed in the ¹H NMR chemical shifts for aromatic protons (0.5 ppm), due to π-stacking between aromatic rings during folding. The folding is driven by solvophobic interactions. By changing solvent and temperature it was possible to denature folded oligomers. The stability of the folded structure increased linearly with oligomer length, due to the regular repeating structure of the helix formed. The folded conformation contains a cavity which can be used to bind substrates, such as (-)-alpha-pinene.⁴

No folding was observed in non-polar solvents (THF-*d*₈ and CDCl₃) for the molecules described in the previous chapter. These solvents were chosen due to the good solubility of the oligomers in them, but they are unlikely to promote folding. Oligomers bearing both H-bond donors and H-bond acceptors may fold in non-polar solvents, driven by the formation of intramolecular H-bonds.

5.2 Approach

To produce oligomers with a mix of sequence, oligomerisation followed by separation of the oligomeric product by preparative HPLC was used. Mono-functional chain stoppers that were complementary to the bifunctional recognition modules used in each oligomerisation gave oligomers capped with recognition groups complementary to the main oligomer chain (DA_nD and AD_nA oligomers).

In solution, flexible oligomers can fold to form intramolecular H-bonds, but this process competes with intermolecular H-bonding, forming dimers and supramolecular polymers (**Scheme 5.1**). The population of each species in equilibrium will be determined by their relative stabilities. NMR titration experiments were used to evaluate the extent of folding of the oligomers.

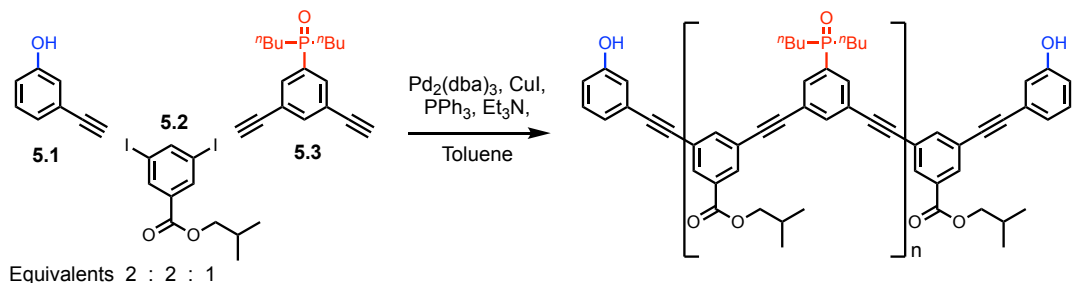


Scheme 5.1: Possible equilibria for flexible oligomers bearing both acceptor and donor recognition groups. These oligomers can fold and form intramolecular H-bonds as well as form duplexes and higher order complexes.

5.3 Results and discussion

5.3.1 Oligomer synthesis

Acceptor oligomers bearing donor capping groups were synthesised by oligomerisation of previously synthesised recognition modules (**5.1** and **5.3**) with the solubilising module (**5.2**) under Sonogashira conditions (**Scheme 5.2**). The ratio of starting materials was chosen to reflect the intended composition of the desired product, in this case the 3-mer. The product mixture was dissolved in ethanol and analysed by LCMS (**Figure 5.1a**). Oligomers up to the 8-mer were observed. The LCMS method was transferred to preparative HPLC, and the oligomers were separated (**Figure 5.1b**). Acceptor homo-oligomers from the 3-mer (**5.6**) to 6-mer (**5.9**) were isolated (Table 5.1). The 7-mer isolated was characterised by MS but the amount was too small to be characterised by any other technique. The overall yield of oligomers with respect to the solubilising module was 29%. The most abundant oligomer was the 3-mer, matching the initial stoichiometry of the starting materials used in the reaction.



Scheme 5.2: Oligomerisation of mono-acetylene phenol module and bis-acetylene phosphine oxide module to yield DA_nD oligomers.

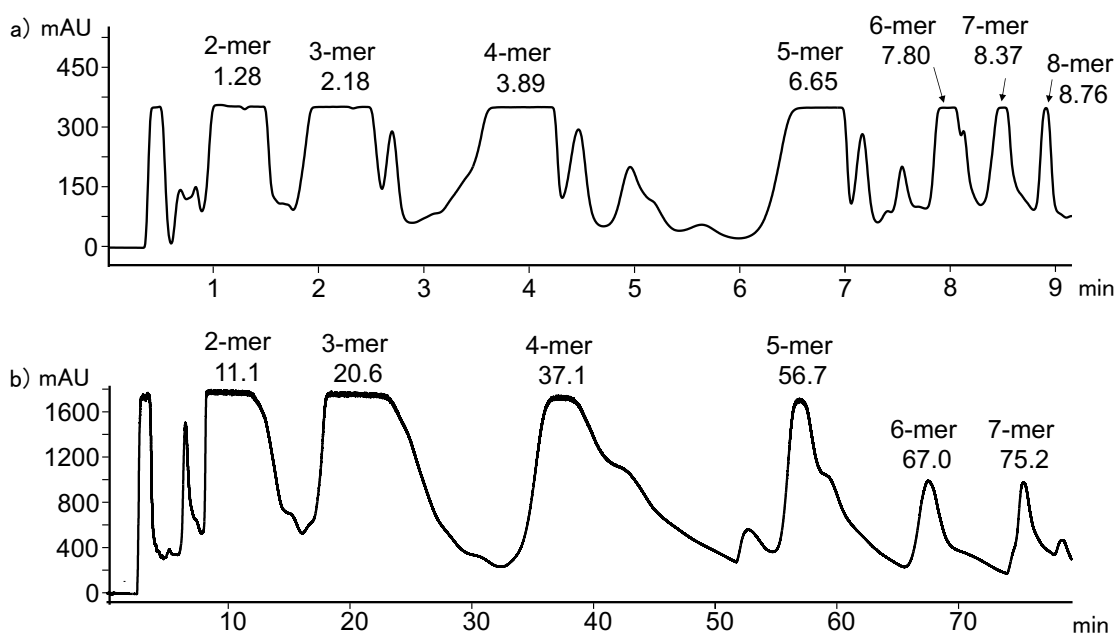
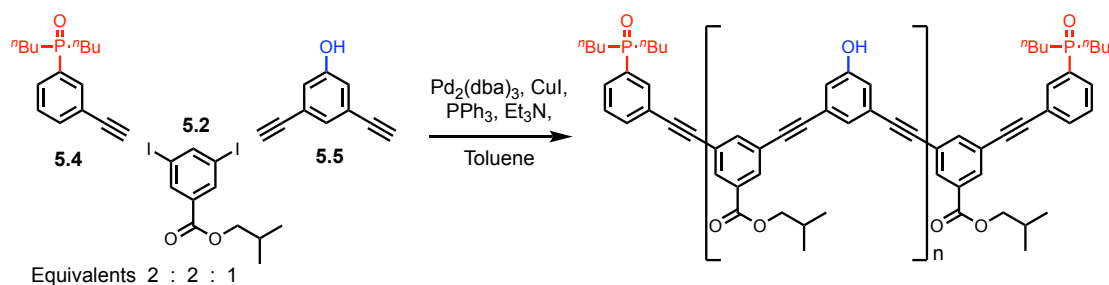


Figure 5.1: (a) LCMS analysis of DA_nD oligomerisation mixture using a Hichrom C₈C₁₈ column (50 × 4.6 mm, 5 µm particle size) with a water/THF (0.1% formic acid) solvent system (THF: 60% for 5 min, 60–70% over 2 min, 70% for 3 min) at a flow rate of 1 mL min⁻¹. (b) Preparative HPLC (bottom) separation of DA_nD oligomerisation mixture using a HIRBP-6988 prep column (250 × 25 mm, 5 µm particle size) with a water/THF solvent system (THF: 60% for 48 min, 65% for 31 min) at 15 mL min⁻¹. Both samples were prepared in EtOH. UV/vis absorption was measured at 290 nm. Peaks identified by MS are labelled with retention time in minutes.

Table 5.1: Isolated masses of DA_nD oligomers from oligomerisation reaction.

Product	Oligomer sequence	Mass / mg	mol / µmol	% by mol fraction
5.6 (3-mer)	DAD	17.2	19.8	50
5.7 (4-mer)	DAAD	11.9	8.9	22
5.8 (5-mer)	DAAAD	16.7	9.3	23
5.9 (6-mer)	DAAAAD	4.7	2.1	5

Donor oligomers bearing acceptor capping groups were synthesised by oligomerisation of previously synthesised recognition modules (**5.4** and **5.5**) with the solubilising module (**5.2**) under Sonogashira conditions (**Scheme 5.3**). The ratio of starting materials was chosen to reflect the intended composition of the desired product, in this case the 3-mer. The product mixture was dissolved in ethanol and analysed by LCMS (**Figure 5.2a**). Oligomers up to the 8-mer were observed. The LCMS method was transferred to preparative HPLC, and the oligomers were separated (**Figure 5.2b**). Acceptor homo-oligomers from the 3-mer (**5.10**) to 7-mer (**5.14**) were isolated (Table 5.2). The overall yield with respect to the solubilising module was 34%. The most abundant oligomer was the 3-mer, matching the initial stoichiometry of the starting materials used in the reaction.



Scheme 5.3: Oligomerisation of mono-acetylene phosphine oxide module and bis-acetylene phenol module to yield AD_nA oligomers.

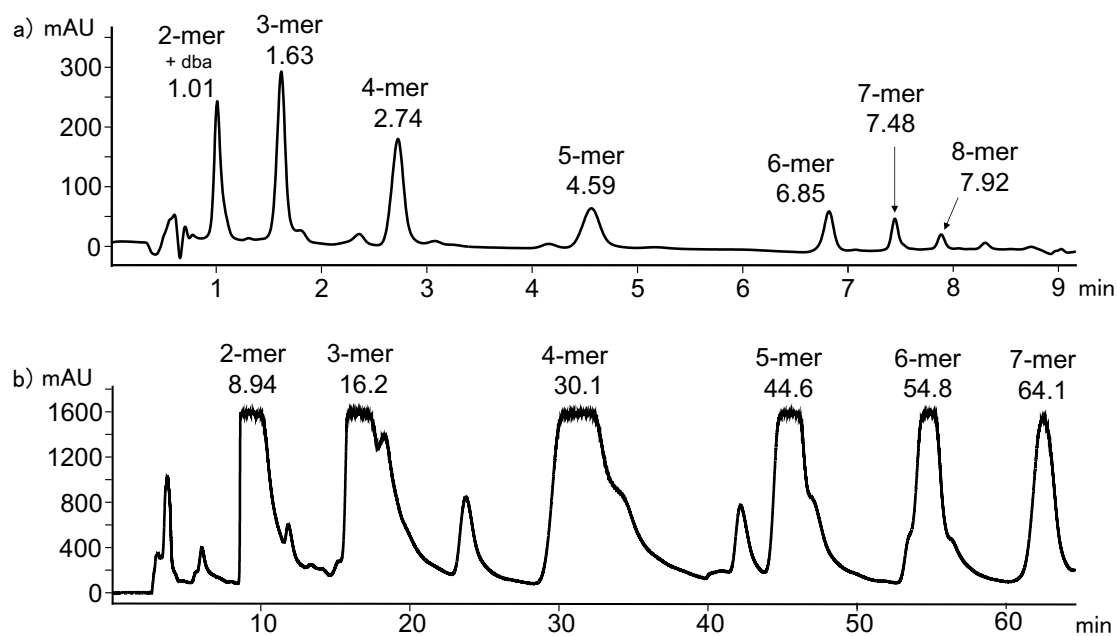


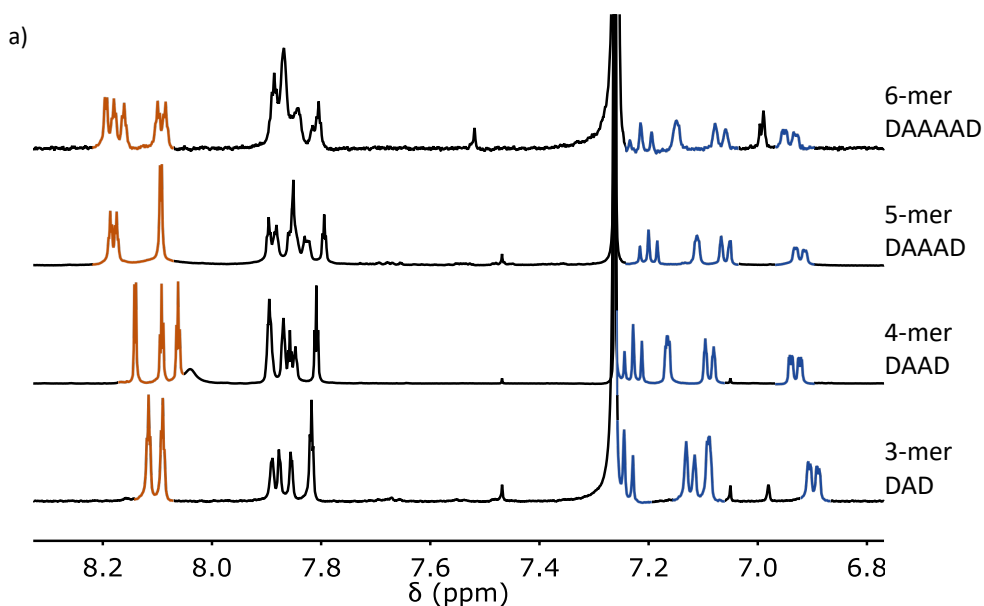
Figure 5.2: (a) LCMS analysis of AD_nA oligomerisation mixture using a Hichrom C₈C₁₈ column (50 × 4.6 mm, 5 µm particle size) with a water/THF (0.1% formic acid) solvent system (THF: 60% for 5 min, 60–70% over 1 min, 70% for 2 min) at a flow rate of 1 mL min⁻¹. (b) Preparative HPLC (bottom) separation of AD_nA oligomerisation mixture using a HIRBP-6988 prep column (250 × 25 mm, 5 µm particle size) with a water/THF solvent system (THF: 60% for 36 min, 65% for 28 min, 70% for 15 min) at 15 mL min⁻¹. Both samples were prepared in EtOH. UV/vis absorption was measured at 290 nm. Peaks identified by MS are labelled with retention time in minutes; dba = dibenzylideneacetone. At 24 mins and 42 mins peaks caused by impurities were observed but could not be identified.

Table 5.2: Isolated masses of AD_nA oligomers from oligomerisation reaction.

Product	Oligomer sequence	Mass / mg	mol / µmol	% by mol fraction
5.10 (3-mer)	ADA	24.2	23.8	50
5.11 (4-mer)	ADDA	18.1	13.6	28
5.12 (5-mer)	ADDDA	11.5	7.0	15
5.13 (6-mer)	ADDDDA	4.4	2.2	5
5.14 (7-mer)	ADDDDDA	2.8	1.2	2

5.3.2 Oligomer characterisation

The oligomers were initially identified by MS, and ^1H NMR spectroscopy was used to confirm the structures of the isolated products. The oligomers gave rise to distinct ^1H NMR signals which could be assigned to the terminal recognition modules, the internal recognition modules, and the solubilising modules. The ratios of integrals were used to confirm oligomer length. For the DA_nD oligomers, the ratio of the integrals of the ^1H NMR signals due to the terminal recognition groups (blue) compared with the signals due to the solubilising groups (red) allowed quantification of number of solubilising groups and therefore oligomer length (**Figure 5.3a**). These results were confirmed using the ratio of integrals of the ^{31}P NMR signals due to the terminal phosphine oxides (blue) compared with the signals due to the internal phosphine oxides (red) (**Figure 5.3b**). Similarly, for the AD_nA oligomers, the ratio of the integrals of the ^1H NMR signals due to the terminal recognition groups (blue) compared with the signals due to the solubilising groups (red) allowed quantification of the number of solubilising groups and therefore oligomer length (**Figure 5.4**).



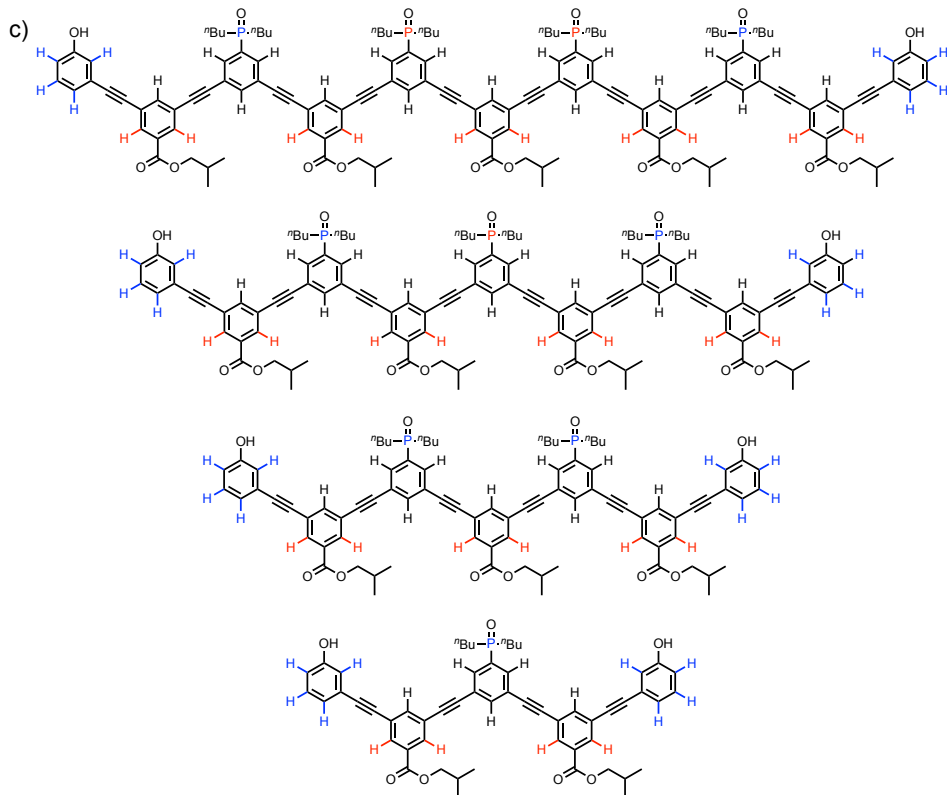
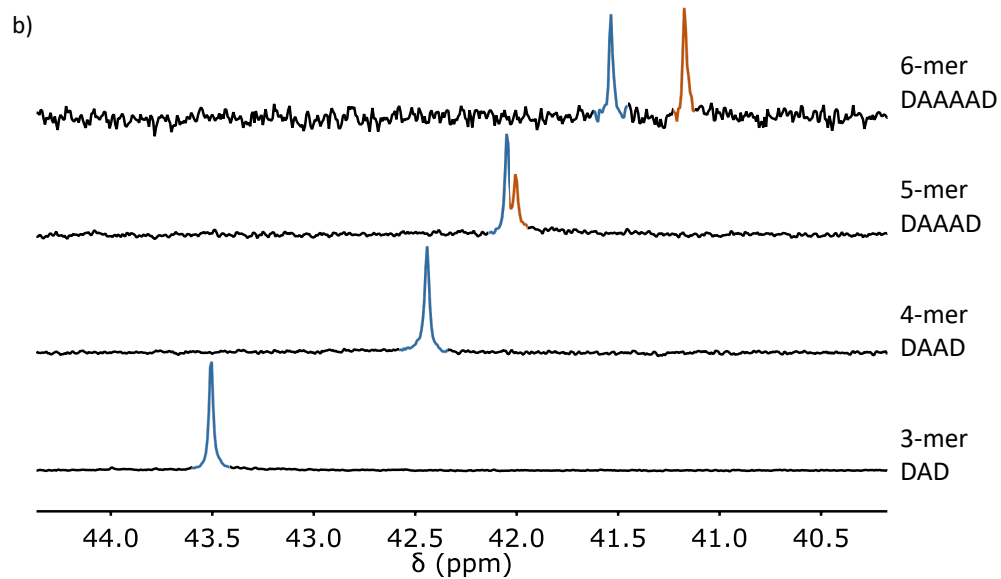


Figure 5.3: (a) Partial ^1H NMR spectra (500 MHz, CDCl_3), (b) ^{31}P NMR spectra (162 MHz, CDCl_3) and (c) chemical structures of DA_nD oligomers.

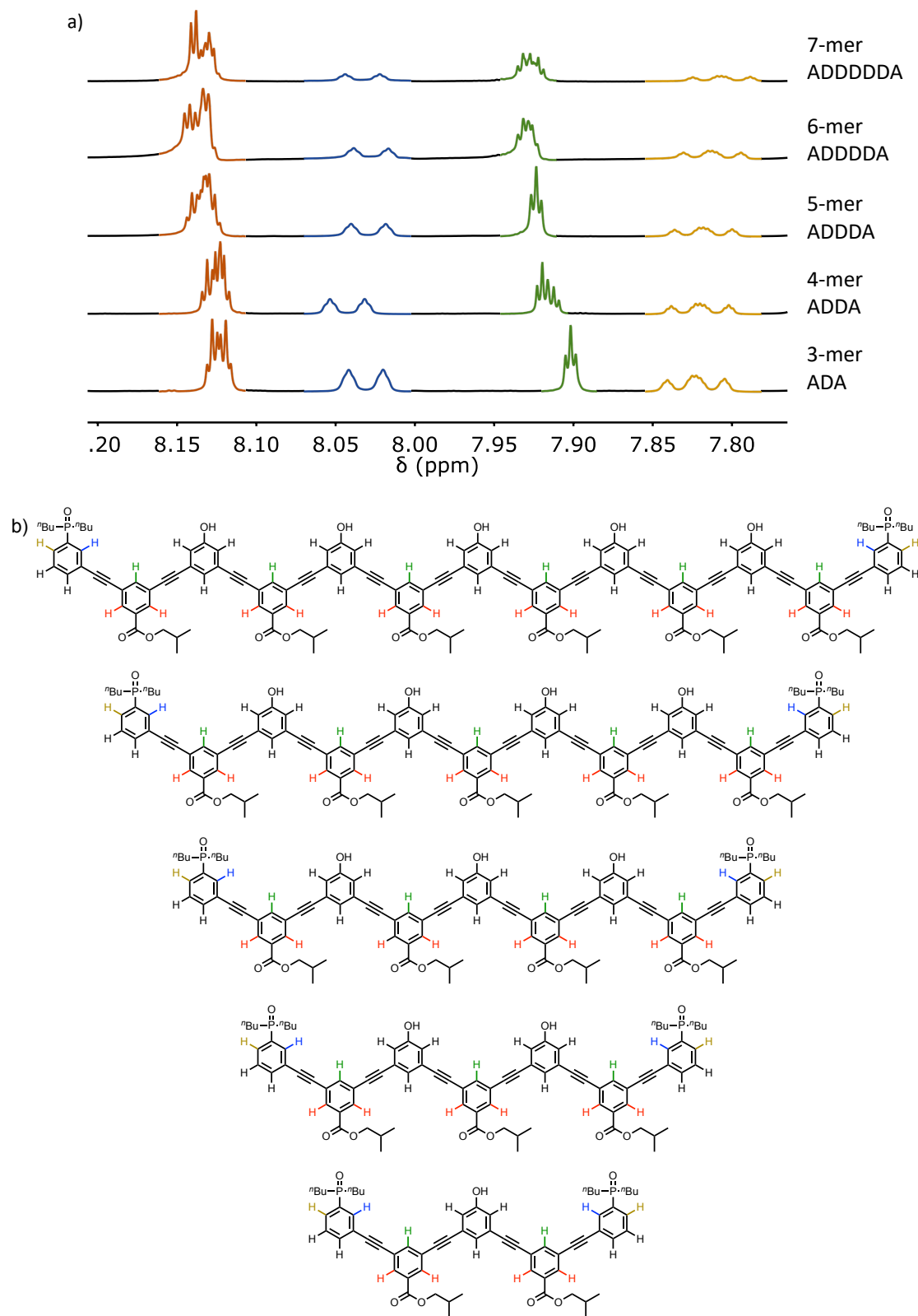
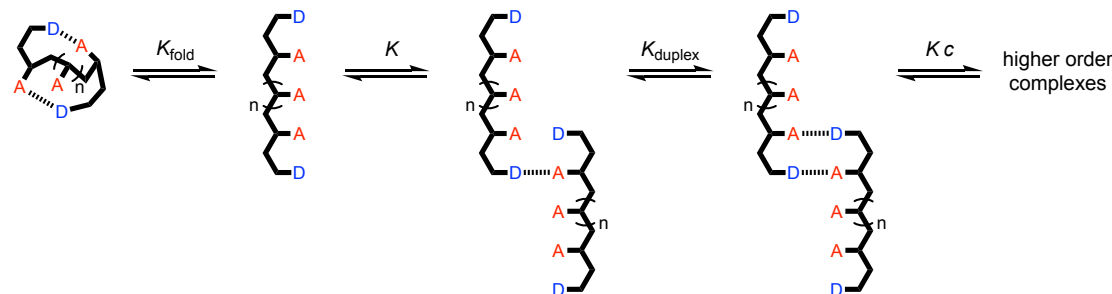


Figure 5.4: (a) Partial ^1H NMR spectra (500 MHz, THF- d_8) and (b) chemical structures of AD_nA oligomers.

For the AD_nA oligomers in $\text{THF}-d_8$ the chemical shifts of the signals due to equivalent protons from equivalent building blocks do not change as the length of the oligomers increases, showing no stacking of the aromatic rings that would be expected if they folded. For the DA_nD oligomers in CDCl_3 the spectra are similar, but some chemical shifts of the signals due to equivalent protons from equivalent building blocks change as the oligomer length increases (by up to 0.5 ppm). These systems are complicated by self-association in chloroform meaning it is not possible to determine if these changes are due to concentration changes or folding.

5.3.3 NMR dilution experiments

Scheme 5.4 shows the H-bonding equilibria that are possible for DA_nD oligomers. The observed self-association constant is the product of all association constants shown in **Scheme 5.4**. If there are no competing equilibria, then the observed self-association constant for the DA_nD oligomer would be similar to the association constant measured for the formation of the $\text{AD} \bullet \text{AD}$ duplex in chapter 3 (130 M^{-1} in CDCl_3). If the folding equilibrium competes with this process, it will lower the observed self-association constant for duplex formation and polymerisation.



Scheme 5.4: Possible equilibria for DA_nD oligomer assembly in solution. The equilibrium constants have additional statistical factors that are not shown.

The dimerization constants for DAD (**5.6**), DAAD (**5.7**) and DAAAD (**5.8**) were determined by NMR dilution experiments (**Figure 5.5**). In CDCl_3 the ^{31}P signals due to the phosphine oxides had limiting free chemical shifts of 40.0 – 41.6 ppm and limiting bound chemical shifts of 42.4 – 44.3. The dimerization constants

for the formation of self-associated complexes were determined to be in the range 210 – 575 M⁻¹ for all oligomers. These dimerization constants are the same order of magnitude as the AD•AD dimerization constant, suggesting that there is no 1,2-folding occurring. Folding would cause a decrease in dimerization constant due to a competing equilibrium. It was not possible to complete a NMR dilution experiment for DAAAAD due to the limited amount of material isolated. However, the chemical shifts measured at 0.05 mM for DAAAAD are the same as the free chemical shifts for the other oligomers, suggesting no folding occurs for this system either.

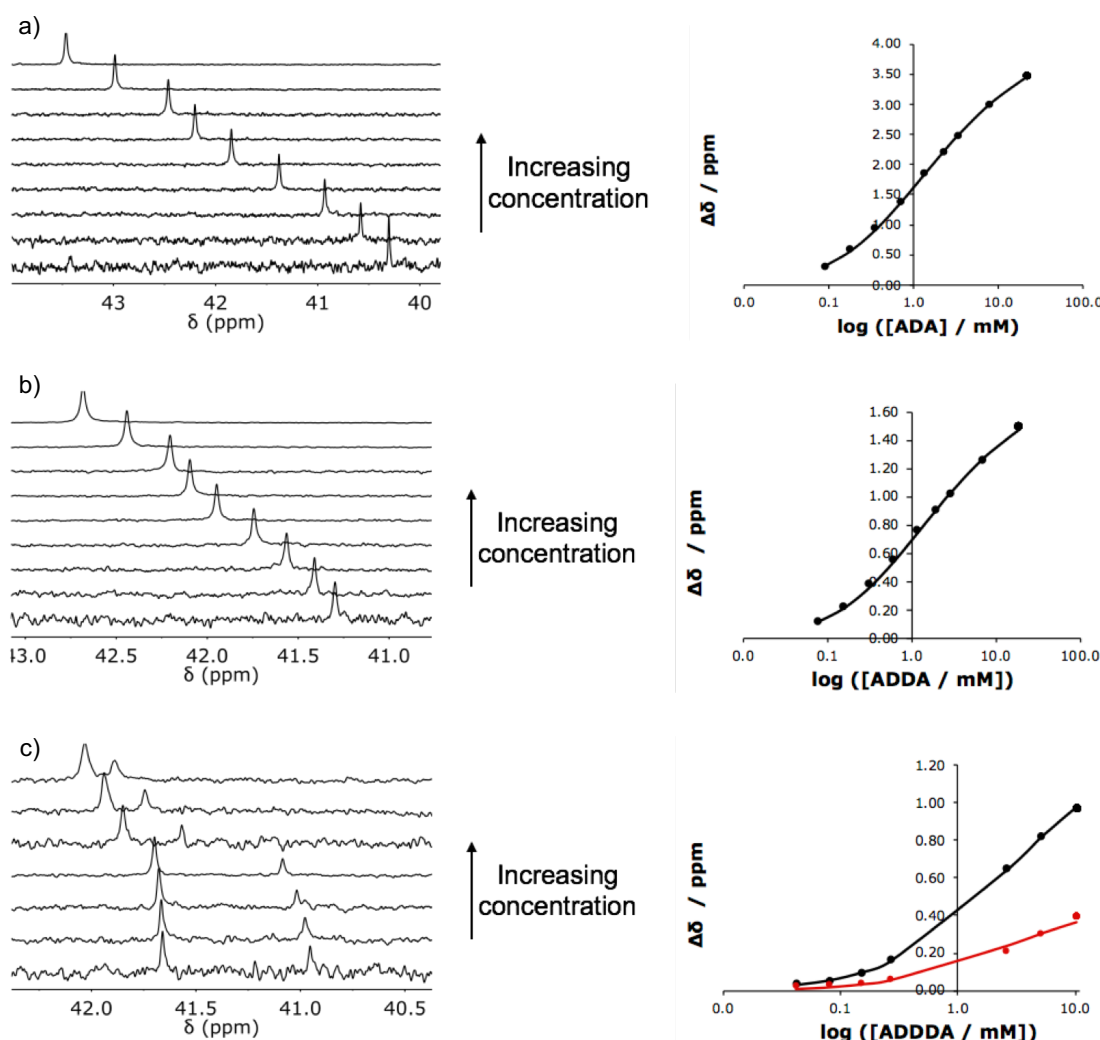


Figure 5.5: ^{31}P NMR data (202 MHz) for dilution of a) DAD 3-mer, **5.6** (0.09 – 21.9 mM), b) DAAD 4-mer, **5.7** (0.08 – 18.9 mM), and c) DAAAD 5-mer, **5.8** (0.04 – 10.3 mM) at 298 K in CDCl_3 . Representative dilution spectra and plot of complexation-induced change in chemical shift as a log function of guest concentration (the line represents the best fit to a dimerization isotherm).

The DAAAD spectra contain two inequivalent phosphorus signals, corresponding to the central phosphine oxide, with a δ_{free} of 40.9, and the external phosphine oxide, with a δ_{free} of 41.3. The DAAAAD spectrum also contains two inequivalent phosphorus signals, corresponding to the central and external phosphine oxides, with δ_{free} of 41.0 and 41.4 respectively.

Table 5.3: Association constants (K_{obs}) and ^{31}P chemical shifts (δ) measured by NMR dilutions in CDCl_3 at 298 K.

Oligomer	$K_{\text{obs}} / \text{M}^{-1}$	δ_{free}	δ_{bound}	$\Delta\delta / \text{PPM}$
AD	130 ± 30	40.2	44.1	3.9
DAD	490 ± 1	40.0	44.3	4.3
DAAD	575 ± 280	41.3	43.0	1.7
DAAAD	210 ± 70	40.9	42.2	1.5
		41.6	42.4	0.6
DAAAAD	nd	41.0 ^a	nd	nd
		41.4 ^a	nd	nd

nd = Not determined. a) chemical shifts recorded at 0.05 mM.

5.3.4 Crystal structure of DAD 3-mer

The structure of the DAD (**5.6**) 3-mer was investigated using X-ray crystallography. DAD was crystallised by slow evaporation from 10% CH_2Cl_2 in acetonitrile. In the crystal structure (**Figure 5.6**) there is no intramolecular H-bonding in the solid state, in agreement with the solution-phase NMR results. Instead, a duplex is observed.

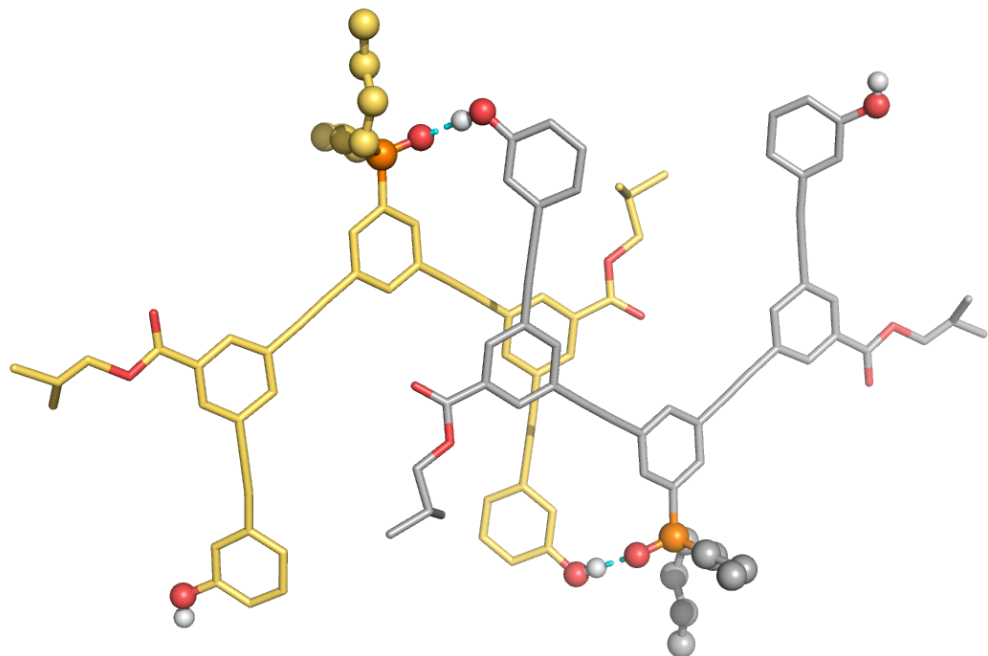


Figure 5.6: X-ray crystal structure of DAD 3-mer (**5.6**), which forms a H-bonded duplex in the solid state. Hydrogen atoms have been omitted for clarity. The recognition units are highlighted as balls, and the H-bonds are shown in light blue.

5.3.5 Modelling of DA_nD oligomers

Molecular mechanics calculations provide insight into the folding propensity of the DA_nD oligomers. A conformational search using the MMFFs force-field was performed for the DAD, DAAD, and DAAAD oligomers (**Figure 5.7**). The global minimum for the DAD 3-mer corresponds to an open conformation, in agreement with the experimental results. Molecular modelling suggests that the DAAD 4-mer and DAAAD 5-mer both fold into helices, each forming two intramolecular phenol-phosphine oxide H-bonds. This contradicts the results of the NMR experiments, suggesting that the modelling overestimates either the strength of the H-bonding or the flexibility of the backbone.

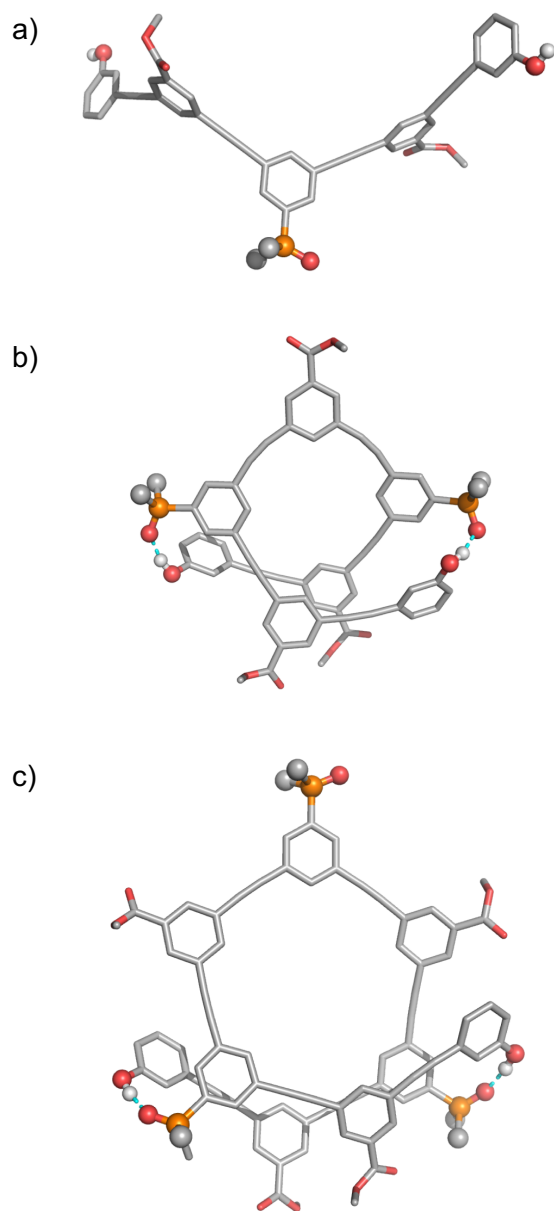


Figure 5.7: Lowest energy conformations of oligomers calculated using molecular mechanics conformational searches (MMFFs force-field and CHCl₃ solvation implemented in Macromodel) for (a) DAD, (b) DAAD, and (c) DAAAD with solubilising groups truncated to methyl esters. Hydrogen atoms have been omitted for clarity. The backbones are shown in grey, the recognition units are highlighted as balls, and the H-bonds are shown in light blue.

5.4 Conclusions

Mixed sequence oligomers were synthesised by oligomerisation and separation by reverse-phase preparative HPLC. Mass spectrometry and NMR spectroscopy were used to identify the products. DA_nD oligomers up to the 6-mer and AD_nA oligomers up to the 7-mer were synthesised, isolated and characterised.

NMR dilution experiments in chloroform were used to determine the extent of any intramolecular folding in the DAD, DAAD, and DAAAD oligomers, but none was observed. An X-ray crystal structure was obtained for the DAD 3-mer which confirmed the absence of intramolecular folding. Molecular mechanics calculations agreed with the absence of intramolecular folding in the DAD 3-mer. However, molecular modelling suggested that the DAAD and DAAAD oligomers fold into helices, contradicting the results of the NMR experiments.

These experiments show no folding in CDCl₃ and THF for mixed sequence oligomers up to the 6-mer. It may be possible to increase the likelihood of folding by changing the solvent: a more non-polar solvent would increase the strength of H-bonding (toluene), or a more polar solvent would increase solvophobic stacking of the aromatic rings (acetonitrile).

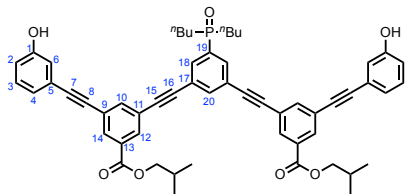
5.5 Experimental

5.5.1 Synthesis

All the reagents were obtained from commercial sources (Sigma-Aldrich, Alfa Aesar, Fisher Scientific and Fluorochem) and were used without further purification. Thin layer chromatography was carried out using silica gel 60F (Merck) on aluminium. ^1H and ^{13}C NMR spectra were recorded on either a Bruker AV3400 or AV3500 spectrometer at 298 K unless specifically stated otherwise. Residual solvent was used as an internal standard. All chemical shifts are quoted in ppm on the δ scale and the coupling constants expressed in Hz. Signal splitting patterns are described as follows: s (singlet), d (doublet), t (triplet), q (quartet), m (multiplet). ES+ mass spectra were obtained on a Waters LCT premier mass spectrometer. FTIR spectra were recorded on a PerkinElmer Spectrum One FT-IR spectrometer. Compound **5.4** was synthesised in chapter 3. Compounds **5.2**, **5.3** and **5.5** were synthesised in chapter 4.

DAD oligomerization (**5.6 - 5.9**)

5.1 (47.3 mg, 0.400 mmol), **5.3** (57.3 mg, 0.200 mmol) and **5.2** (172 mg, 0.400 mmol) were placed in a flask and degassed with N₂ for 30 minutes. Pd₂(dba)₃ (7.30 mg, 8.00 µmol) and CuI (1.50 mg, 8.00 µmol) and PPh₃ (10.5 mg, 40.0 µmol) were placed in a separate flask and degassed with N₂. Degassed Et₃N (167 µL, 1.20 mmol) was added and the contents of this flask transferred to the first using degassed toluene (8 mL). The reaction was stirred overnight at room temperature, in the dark under N₂. The solvent was removed by rotary evaporation under reduced pressure yielding a brown solid (465 mg). The sample was dissolved in EtOH and sonicated, before filtering. Preparative HPLC separation of the oligomerisation mixture was completed using a HIRBP-6988 prep column (250 × 25 mm, 5 µm particle size) with a water/THF solvent system (THF: 60% for 48 min, 65% for 31 min) at 15 mL min⁻¹.

DAD 3-mer (**5.6**)

TLC *R*_f: 0.40 (MeOH:CH₂Cl₂ 1:9);

¹H NMR (500 MHz, CDCl₃): δ 8.12 (t, *J* = 1.5 Hz, 2H, 12-H), 8.09 (t, *J* = 1.5 Hz, 2H, 14-H), 7.91 – 7.84 (m, 3H, 18, 20-H), 7.82 (t, *J* = 1.5 Hz, 2H, 10-H), 7.24 (t, *J* = 8.0 Hz, 2H, 3-H), 7.12 (dt, *J* = 7.5, 1.0 Hz, 2H, 4-H), 7.09 (dd, *J* = 2.5, 1.5 Hz, 2H, 6-H), 6.90 (ddd, *J* = 8.0, 2.5, 1.0 Hz, 2H, 2-H), 6.30 (bs, 2H, OH), 4.14 (d, *J* = 6.5 Hz, 4H, *i*Bu), 2.14 – 2.10 (m, 2H, *i*Bu), 2.07-1.81 (m, 4H, *n*Bu), 1.71-1.55 (m, 2H, *n*Bu), 1.49-1.35 (m, 6H, *n*Bu), 1.06 (d, *J* = 6.5 Hz, 12H, *i*Bu), 0.91 (t, *J* = 7.0 Hz, 6H, *n*Bu);

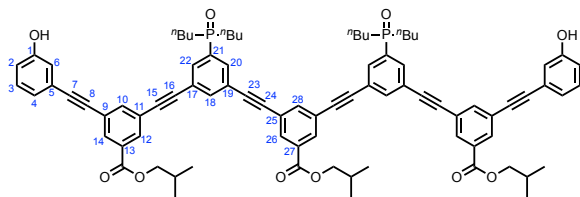
¹³C NMR (126 MHz, CDCl₃): δ 165.2 (C=O), 156.0 (1-C), 138.4 (10-C), 137.6 (20-C), 133.7 (d, *J* = 88.0 Hz, 19-C), 133.0 (18-C) 132.6 (12-C), 132.0 (14-C), 131.3 (13-C), 129.7 (3-C), 125.1 (5-C), 124.2 (4-C), 124.1 (17-C), 123.7 (11-C), 123.2 (9-C), 118.3 (6-C), 116.5 (2-C), 90.9 (-C≡), 90.4 (-C≡), 89.9 (-C≡), 87.2 (-C≡), 71.6 (*i*Bu), 29.2 (d, *J* = 68.5 Hz, *n*Bu), 27.9 (*i*Bu), 24.1 (d, *J* = 14.5 Hz, *n*Bu), 23.5 (d, *J* = 4.0 Hz, *n*Bu) 19.2 (*i*Bu), 13.6 (*n*Bu);

³¹P NMR (162 MHz, CDCl₃): δ 43.5 (phosphine oxide);

FT-IR (ATR): 3148 (br), 2923, 2224, 1722, 1591, 1232, 767 $\nu_{\text{max}}/\text{cm}^{-1}$;

HRMS (ES+): C₅₆H₅₆O₇P calcd. 871.3758 found 871.3719, Δ = -4.50 ppm.

DAAD 4-mer (5.7)



TLC R_f : 0.40 (MeOH:CH₂Cl₂ 1:9);

¹H NMR (500 MHz, CDCl₃): δ 8.14 (d, J = 1.5 Hz, 2H, 26-H), 8.09 (t, J = 1.5 Hz, 2H, 12-H), 8.06 (t, J = 1.5 Hz, 2H, 14-H), 8.04 (bs, 2H, OH), 7.92 – 7.82 (m, 7H, 18, 20, 22, 28-H), 7.81 (t, J = 1.5 Hz, 2H, 10-H), 7.24 (t, J = 8.0 Hz, 2H, 3-H), 7.17 (dd, J = 2.5, 1.5 Hz, 2H, 6-H), 7.09 (dt, J = 7.5, 1.0 Hz, 2H, 4-H), 6.93 (ddd, J = 8.0, 2.5, 1.0 Hz, 2H, 2-H), 4.15 (d, J = 6.5 Hz, 2H, ^tBu), 4.12 (d, J = 6.5 Hz, 4H, ^tBu), 2.14 – 2.10 (m, 3H, ^tBu), 2.07-1.81 (m, 8H, ⁿBu), 1.71-1.55 (m, 4H, ⁿBu), 1.49-1.35 (m, 12H, ⁿBu), 1.06 (d, J = 6.5 Hz, 18H, ⁱBu), 0.90 (t, J = 7.0 Hz, 12H, ⁿBu);

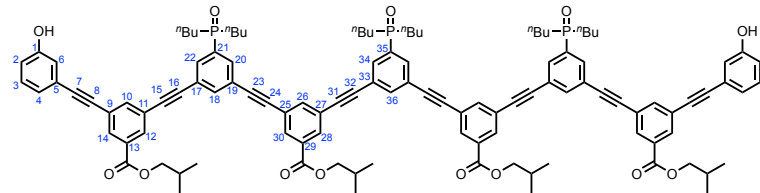
¹³C NMR (126 MHz, CDCl₃): δ 165.2 (13-C=O), 165.0 (27-C=O), 156.8 (1-C), 138.7 (28-C), 138.5 (10-C), 137.6 (18-C), 133.7 (d, J = 88.0 Hz, 21-C), 133.1 (22-C), 133.0 (20-C), 132.5 (12-C), 131.8 (14-C), 131.4 (26-C), 131.2 (13-C), 129.6 (3-C), 124.4 (4-C), 124.1 (17-C), 124.0 (19-C), 123.5 (11-C), 123.4 (25-C), 123.4 (5-C) 123.1 (9-C), 118.7 (6-C), 116.8 (2-C), 91.3 (-C≡), 90.0 (-C≡), 89.7 (-C≡), 89.1 (-C≡), 88.7 (-C≡), 87.0 (-C≡), 71.7 (ⁱBu), 71.6 (ⁱBu), 29.2 (d, J = 68.5 Hz, ⁿBu), 27.9 (ⁱBu), 24.1 (d, J = 14.5 Hz, ⁿBu), 23.5 (d, J = 4.0 Hz, ⁿBu) 19.3 (ⁱBu), 19.2 (ⁱBu), 13.6 (ⁿBu);

³¹P NMR (162 MHz, CDCl₃): δ 42.5 (phosphine oxide);

FT-IR (ATR): 3142 [br], 2926, 2226, 1720, 1592, 1234, 1156, 767 $\nu_{\text{max}}/\text{cm}^{-1}$;

HRMS (ES+): C₈₅H₈₈O₁₀P₂ calcd. 1330.5853 found 1330.5850, Δ = -0.20 ppm.

DAAAD 5-mer (**5.8**)



TLC R_f : 0.40 (MeOH:CH₂Cl₂ 1:9);

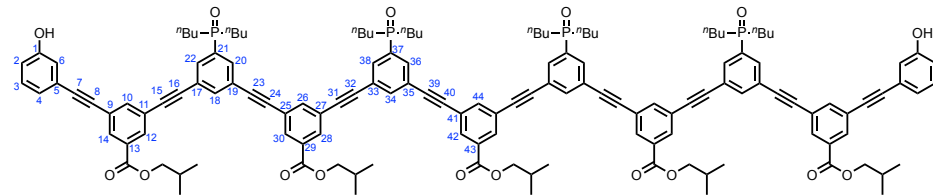
¹H NMR (500 MHz, CDCl₃): δ 8.18 (dt, J = 6.0, 1.5 Hz, 4H, 12, 14-H), 8.09 (d, J = 1.5 Hz, 4H, 28, 30-H), 7.97 – 7.81 (m, 11H, 18, 20, 22, 26, 34, 36-H), 7.79 (t, J = 1.5 Hz, 2H, 10-H), 7.20 (t, J = 8.0 Hz, 2H, 3-H), 7.11 (dd, J = 2.5, 1.5 Hz, 2H, 6-H), 7.06 (dt, J = 7.5, 1.0 Hz, 2H, 4-H), 6.92 (ddd, J = 8.0, 2.5, 1.0 Hz, 2H, 2-H), 4.16 (d, J = 6.5 Hz, 4H, ^tBu), 4.12 (d, J = 6.5 Hz, 4H, ^tBu), 2.14 – 2.10 (m, 4H, ^tBu), 2.07-1.81 (m, 12H, ⁿBu), 1.71-1.55 (m, 6H, ⁿBu), 1.49-1.35 (m, 18H, ⁿBu), 1.06 (d, J = 6.5 Hz, 12H), 1.03 (d, J = 6.5 Hz, 12H, ^tBu), 0.90 (t, J = 7.0 Hz, 18H, ⁿBu);

¹³C NMR (126 MHz, CDCl₃): δ 165.2 (13-C=O), 165.1 (29-C=O), 156.8 (1-C), 138.6 (26-C), 138.4 (10-C), 137.6 (18-C), 137.4 (38-C), 133.7 (d, J = 88.0 Hz, 21, 35-C), 133.1 (Ar-C), 133.0 (Ar-C), 132.5 (Ar-C), 132.0 (Ar-C), 131.5 (Ar-C), 131.2 (13-C), 129.6 (3-C), 124.4 (4-C), 124.1 (Ar-C), 124.0 (Ar-C), 124.0 (Ar-C), 123.5 (Ar-C), 123.5 (Ar-C), 123.4 (Ar-C), 123.4 (Ar-C), 123.1 (Ar-C), 118.7 (6-C), 116.9 (2-C), 91.3 (-C≡), 89.9 (-C≡), 89.6 (-C≡), 89.6 (-C≡), 89.1 (-C≡), 88.6 (-C≡), 86.9 (-C≡), 71.7 (^tBu), 71.6 (^tBu), 29.2 (d, J = 68.5 Hz, ⁿBu), 27.9 (^tBu), 24.1 (d, J = 14.5 Hz, ⁿBu), 23.5 (d, J = 4.0 Hz, ⁿBu) 19.3 (^tBu), 19.2 (^tBu), 13.6 (ⁿBu);

³¹P NMR (162 MHz, CDCl₃): δ 42.1, 42.0 (phosphine oxides);

FT-IR (ATR): 3129 (br), 2958, 2189, 1721, 1691 1594, 1235 $\nu_{\text{max}}/\text{cm}^{-1}$;

HRMS (ES+): C₁₁₄H₁₂₁O₁₃P₃ calcd. 1790.8020 found 1790.7977, Δ = -2.40 ppm.

DAAAAAD 6-mer (**5.9**)

TLC R_f : 0.40 (MeOH:CH₂Cl₂ 1:9);

¹H NMR (500 MHz, CDCl₃): δ 8.50 (bs, 2H, OH), 8.19 (d, J = 1.5 Hz, 2H, 42-H), 8.17 (dt, J = 6.0, 1.5 Hz, 4H, 12, 14-H), 8.09 (d, J = 1.5 Hz, 4H, 28, 30-H), 7.94 – 7.81 (m, 15H, 18, 20, 22, 26, 34, 36, 38, 44-H), 7.80 (t, J = 1.5 Hz, 2H, 10-H), 7.21 (t, J = 8.0 Hz, 2H, 3-H), 7.15 (dd, J = 2.5, 1.5 Hz, 2H, 6-H), 7.07 (dt, J = 7.5, 1.0 Hz, 2H, 4-H), 6.95 (ddd, J = 8.0, 2.5, 1.0 Hz, 2H, 2-H), 4.33 – 3.93 (m, 10H/^tBu), 2.14 – 2.10 (m, 5H, ⁱBu), 2.07–1.81 (m, 16H, ⁿBu), 1.71–1.55 (m, 8H, ⁿBu), 1.49–1.35 (m, 24H, ⁿBu), 1.08 – 1.01 (m, 30H, ⁱBu), 0.97 – 0.79 (m, 24H, ⁿBu);

¹³C NMR (126 MHz, CDCl₃): δ 165.2 (13-C=O), 165.1 (29, 43-C=O), 157.00 (1-C), 138.6 (26, 44-C), 138.4 (10-C), 137.5 (18-C), 137.3 (34-C), 133.1 (bs), 132.5 (Ar-C), 132.1 (Ar-C), 132.0 (Ar-C), 131.5 (Ar-C), 131.2 (13-C), 129.5 (3-C), 124.5 (4-C), 124.0 (bs), 123.5 (Ar-C), 123.5 (Ar-C), 123.1 (Ar-C), 118.7 (6-C), 116.9 (2-C), 91.4 (-C≡), 89.9 (-C≡), 89.6 (-C≡), 89.6 (-C≡), 89.1 (-C≡), 89.0 (-C≡), 88.7 (-C≡), 86.9 (-C≡), 71.7 (ⁱBu), 71.5 (ⁱBu), 29.2 (d, J = 68.5 Hz, ⁿBu), 27.9 (ⁱBu), 24.1 (d, J = 14.5 Hz, ⁿBu), 23.5 (d, J = 4.0 Hz, ⁿBu) 19.3 (ⁱBu), 19.2 (ⁱBu), 13.6 (ⁿBu);

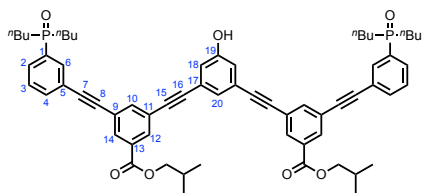
³¹P NMR (162 MHz, CDCl₃): δ 41.5, 41.2 (phosphine oxides);

FT-IR (ATR): 3187 (br), 2958, 2172, 1722, 1594, 1236 $\nu_{\text{max}}/\text{cm}^{-1}$;

HRMS (ES+): C₁₄₃H₁₅₄O₁₆P₄ calcd. 2251.0187 found 2251.0203, Δ = -0.70 ppm.

ADA oligomerization (**5.10 - 5.14**)

5.4 (105 mg, 0.400 mmol), **5.5** (28.4 mg, 0.200 mmol) and **5.2** (172 mg, 0.400 mmol) were placed in a flask and degassed with N₂ for 30 minutes. Pd₂(dba)₃ (7.30 mg, 8.00 µmol) and CuI (1.50 mg, 8.00 µmol) and PPh₃ (10.5 mg, 40.0 µmol) were placed in a separate flask and degassed with N₂. Degassed Et₃N (167 µL, 1.20 mmol) was added and the contents of this flask transferred to the first using degassed toluene (8 mL). The reaction was stirred overnight at room temperature, in the dark under N₂. The solvent was removed by rotary evaporation under reduced pressure yielding a brown solid (415 mg). The sample was dissolved in EtOH and sonicated, before filtering. Preparative HPLC separation of the oligomerisation mixture was completed using a HIRBP-6988 prep column (250 × 25 mm, 5 µm particle size) with a water/THF solvent system (THF: 57% for 100 min, 100% for 5 min) at 15 mL min⁻¹.

ADA 3-mer (**5.10**)

TLC R_f : 0.40 (MeOH:CH₂Cl₂ 1:9);

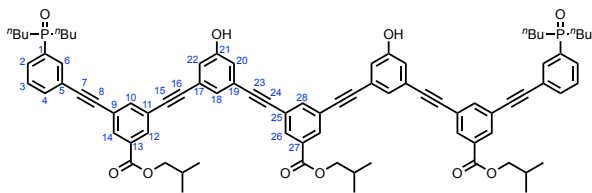
¹H NMR (500 MHz, THF-d₈): δ 10.10 (bs, 1H, OH), 8.15 (s, 4H, 12, 14-H), 8.05 (d, J = 10.5 Hz, 6-H), 7.92 (s, 2H, 10-H), 7.85 (dd, J = 10.0, 7.5 Hz, 2H, 2-H), 7.79 – 7.73 (m, 2H, 4-H), 7.59 (td, J = 7.5, 2.5 Hz, 2H, 3-H), 7.31 (d, J = 1.5 Hz, 1H, 20-H), 7.17 (d, J = 1.5 Hz, 2H, 18-H), 4.17 (d, J = 6.5 Hz, 4H, *t*Bu), 2.14 – 2.10 (m, 2H, *t*Bu), 2.07–1.81 (m, 8H, *n*Bu), 1.71–1.55 (m, 4H, *n*Bu), 1.49–1.35 (m, 12H, *n*Bu), 1.06 (d, J = 6.5 Hz, 12H, *t*Bu), 0.91 (t, J = 7.0 Hz, 12H, *n*Bu);

¹³C NMR (126 MHz, THF-d₈): δ 164.1 (C=O), 158.5 (19-C), 138.0 (10-C), 134.9 (d, J = 88.5 Hz, 1-C), 134.0 (4-C), 133.7 (d, J = 9.0 Hz, 6-C), 131.8 (Ar-C), 131.6 (12-C), 131.6 (14-C), 130.8 (d, J = 8.5 Hz, 2-C), 128.6 (d, J = 11.0 Hz, 3-C), 125.5 (20-C), 124.1 (Ar-C), 123.8 (Ar-C), 123.7 (Ar-C), 123.0 (d, J = 12.0 Hz, 5-C), 119.3 (18-C), 90.3 (-C≡), 90.0 (-C≡), 88.2 (-C≡), 87.1 (-C≡), 71.1 (*t*Bu), 29.3 (d, J = 68.5 Hz, *n*Bu), 27.9 (*t*Bu), 24.1 (d, J = 14.5 Hz, *n*Bu), 23.5 (d, J = 4.0 Hz, *n*Bu) 19.3 (*t*Bu), 13.6 (*n*Bu);

³¹P NMR (202 MHz, THF-d₈): δ 38.0 (phosphine oxide);

FT-IR (ATR): 3060 (br), 2958, 2164, 1722, 1594, 1159, 768 $\nu_{\text{max}}/\text{cm}^{-1}$;

HRMS (ES+): C₆₄H₇₃O₇P₂ calcd. 1015.4826 found 1015.4798, Δ = -2.82 ppm.

ADDA 4-mer (**5.11**)

TLC R_f : 0.40 (MeOH:CH₂Cl₂ 1:9);

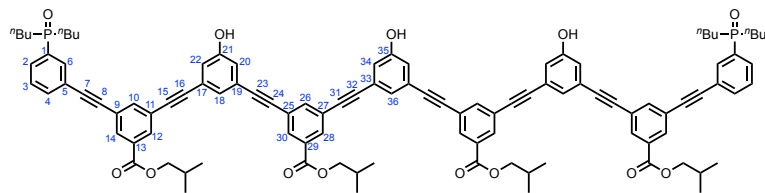
¹H NMR (500 MHz, THF-*d*₈): δ 9.85 (bs, 2H, OH), 8.15 (d, *J* = 2.0 Hz, 6H, 12, 14, 26-H), 8.07 (d, *J* = 11.0 Hz, 2H, 6-H), 7.94 (d, *J* = 2.0 Hz, 3H, 10, 28-H), 7.84 (dd, *J* = 10.0, 7.5 Hz, 2H, 2-H), 7.80 – 7.74 (m, 2H, 4-H), 7.59 (td, *J* = 7.5, 2.5 Hz, 2H, 3-H), 7.32 (d, *J* = 1.5 Hz, 2H, 18-H), 7.12 (d, *J* = 1.5 Hz, 4H, 20, 22-H), 4.17 (d, *J* = 6.5 Hz, 6H, *t*Bu), 2.14 – 2.10 (m, 3H, *t*Bu), 2.07-1.81 (m, 8H, *n*Bu), 1.71-1.55 (m, 4H, *n*Bu), 1.49-1.35 (m, 12H, *n*Bu), 1.07 (d, *J* = 6.5 Hz, 6H, *t*Bu), 1.06 (d, *J* = 6.5 Hz, 12H, *t*Bu), 0.91 (t, *J* = 7.0 Hz, 12H, *n*Bu);

¹³C NMR (126 MHz, THF-*d*₈): δ 166.1 (27-C=O), 166.0 (13-C=O), 160.2 (21-C), 140.0 (10-C), 136.6 (d, *J* = 88.5 Hz, 1-C), 135.9 (4-C), 135.6 (d, *J* = 9.0 Hz, 6-C), 133.6 (Ar-C), 133.4 (12-C), 133.4 (14-C), 132.6 (d, *J* = 8.5 Hz, 2-C), 130.5 (d, *J* = 11.0 Hz, 3-C), 127.7 (Ar-C), 126.0 (Ar-C), 125.9 (Ar-C), 125.7 (Ar-C), 125.6 (Ar-C), 125.6 (Ar-C), 125.0 (d, *J* = 12.0 Hz, 5-C), 121.0 (18-C), 92.1 (-C≡), 92.0 (-C≡), 91.9 (-C≡), 90.1 (-C≡), 89.1 (-C≡), 89.0 (-C≡), 73.0 (*t*Bu), 29.3 (d, *J* = 68.5 Hz, *n*Bu), 27.9 (*t*Bu), 24.1 (d, *J* = 14.5 Hz, *n*Bu), 23.5 (d, *J* = 4.0 Hz, *n*Bu) 20.3 (*t*Bu), 14.9 (*n*Bu);

³¹P NMR (202 MHz, THF-*d*₈): δ 39.2 (phosphine oxide);

FT-IR (ATR): 3074 (br), 2961, 2222, 1722, 1594, 1256, 1236 $\nu_{\text{max}}/\text{cm}^{-1}$;

HRMS (ES+): C₈₅H₈₉O₁₀P₂ calcd. 1331.5926 found 1331.5880, Δ = -3.39 ppm.

ADDDA 5-mer (**5.12**)

TLC R_f : 0.40 (MeOH:CH₂Cl₂ 1:9);

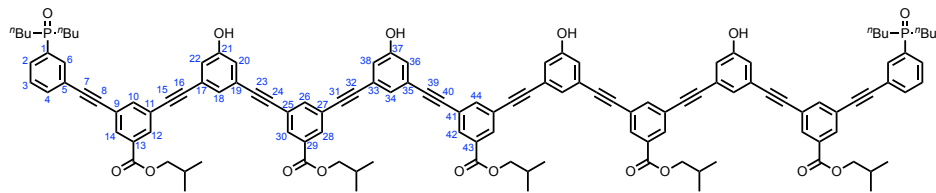
¹H NMR (500 MHz, THF-d₈): δ 9.56 (bs, 3H, OH), 8.16 – 8.11 (m, 8H, 12, 14, 28, 30-H), 8.03 (dt, *J* = 11.0, 1.5 Hz, 2H, 6-H), 7.92 (t, *J* = 1.5 Hz, 4H, 10, 26-H), 7.82 (ddt, *J* = 10.5, 7.5, 1.5 Hz, 2H, 2-H), 7.75 (d, *J* = 8.0 Hz, 2H, 4-H), 7.57 (td, *J* = 7.5, 2.5 Hz, 2H, 3-H), 7.28 (dt, *J* = 2.5, 1.5 Hz, 4H, 18, 36-H), 7.07 (m, 6H, 20, 22, 34-H), 4.15 (d, *J* = 6.5 Hz, 4H, *i*Bu), 4.14 (d, *J* = 6.5 Hz, 4H, *i*Bu), 2.14 – 2.10 (m, 4H, *i*Bu), 2.07-1.81 (m, 8H, ⁿBu), 1.71-1.55 (m, 4H, ⁿBu), 1.49-1.35 (m, 12H, ⁿBu), 1.06 (d, *J* = 6.5 Hz, 12H, *i*Bu), 1.04 (d, *J* = 6.5 Hz, 12H, *i*Bu), 0.91 (t, *J* = 7.0 Hz, 12H, ⁿBu);

¹³C NMR (126 MHz, THF-d₈): δ 166.1 (29-C=O), 166.0 (13-C=O), 160.1 (21-C), 160.0 (35-C), 140.0 (10-C), 139.9 (26-C), 136.3 (d, *J* = 88.5 Hz, 1-C), 135.9 (4-C), 135.6 (d, *J* = 9.0 Hz, 6-C), 133.7 (Ar-C), 133.6 (Ar-C), 133.6 (Ar-C), 133.4 (Ar-C), 133.4 (Ar-C), 132.6 (d, *J* = 8.5 Hz, 2-C), 130.5 (d, *J* = 11.0 Hz, 3-C), 127.7 (20-C), 127.6 (Ar-C), 126.0 (Ar-C), 125.9 (Ar-C), 125.7 (Ar-C), 121.1 (36-C), 121.0 (18-C), 92.1 (-C≡), 92.0 (-C≡), 91.9 (-C≡), 90.1 (-C≡), 89.1 (-C≡), 89.0 (-C≡), 73.0 (*i*Bu), 29.3 (d, *J* = 68.5 Hz, ⁿBu), 27.9 (*i*Bu), 24.1 (d, *J* = 14.5 Hz, ⁿBu), 23.5 (d, *J* = 4.0 Hz, ⁿBu) 20.3 (*i*Bu), 14.9 (ⁿBu);

³¹P NMR (162 MHz, CDCl₃): δ 39.5 (phosphine oxide);

FT-IR (ATR): 3013 (br), 2961, 2203, 1723, 1593, 1236, 768 $\nu_{\text{max}}/\text{cm}^{-1}$;

HRMS (ES+): C₁₀₆H₁₀₆O₁₃P₂ calcd. 1648.7103 found 1648.7030, Δ = -4.47 ppm.

ADDDDA 6-mer (**5.13**)

TLC R_f : 0.40 (MeOH:CH₂Cl₂ 1:9);

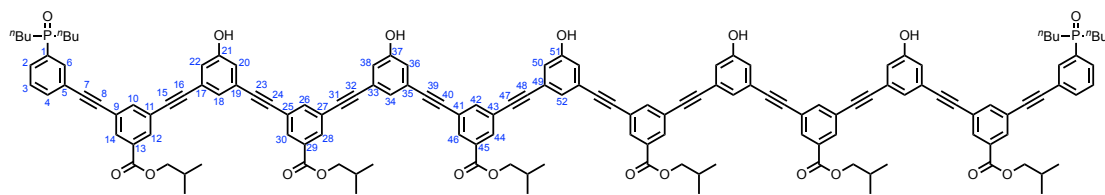
¹H NMR (500 MHz, THF-d₈): δ 9.51 (bs, 4H, OH), 8.16 – 8.12 (m, 10H, 12, 14, 28, 30, 42-H), 8.02 (dt, *J* = 11.0, 1.5 Hz, 2H, 6-H), 7.95 – 7.91 (m, 5H, 10, 26, 44-H), 7.81 (ddt, *J* = 10.5, 7.5, 1.5 Hz, 2H, 2-H), 7.74 (d, *J* = 8.0 Hz, 2H, 4-H), 7.56 (td, *J* = 7.5, 2.5 Hz, 2H, 3-H), 7.30 – 7.27 (m, 4H, 18, 34-H), 7.07 – 7.02 (m, 8H, 20, 22, 36, 38-H), 4.15 (d, *J* = 6.5 Hz, 4H, *i*Bu), 4.14 (d, *J* = 6.5 Hz, 6H, *i*Bu), 2.14 – 2.10 (m, 5H, *i*Bu), 2.07 – 1.81 (m, 8H, ⁿBu), 1.71-1.55 (m, 4H, ⁿBu), 1.49-1.35 (m, 12H, ⁿBu), 1.06 – 1.03 (m, 30H, *i*Bu), 0.91 (t, *J* = 7.0 Hz, 12H, ⁿBu);

¹³C NMR (126 MHz, THF-d₈): δ 166.1 (29, 43-C=O), 166.0 (13-C=O), 160.1 (21-C), 160.0 (37-C), 140.0 (10-C), 139.9 (26, 44-C), 136.3 (d, *J* = 88.5 Hz, 1-C), 135.9 (4-C), 135.6 (d, *J* = 9.0 Hz, 6-C), 133.7 (Ar-C), 133.6 (Ar-C), 133.6 (Ar-C), 133.6 (Ar-C), 133.4 (Ar-C), 133.4 (Ar-C), 132.0 (d, *J* = 8.5 Hz, 2-C), 130.5 (d, *J* = 11.0 Hz, 3-C), 127.7 (20-C), 127.6 (Ar-C), 126.0 (Ar-C), 126.1 (Ar-C), 125.9 (Ar-C), 125.7 (Ar-C), 121.1 (34-C), 121.0 (18-C), 92.1 (-C≡), 92.0 (-C≡), 91.9 (-C≡), 90.1 (-C≡), 89.1 (-C≡), 89.0 (-C≡), 73.0 (*i*Bu), 29.3 (d, *J* = 68.5 Hz, ⁿBu), 27.9 (*i*Bu), 24.1 (d, *J* = 14.5 Hz, ⁿBu), 23.5 (d, *J* = 4.0 Hz, ⁿBu) 20.3 (*i*Bu), 14.9 (ⁿBu);

³¹P NMR (162 MHz, CDCl₃): δ 39.4 (phosphine oxide);

FT-IR (ATR): 3030 (br), 2960, 2199, 1722, 1583, 1236, 768 $\nu_{\text{max}}/\text{cm}^{-1}$;

MS (ES+): m/z (%) = 825.1 (100) [M+2H⁺], 1648.8 (10) [M+H⁺].

ADDDDDA 7-mer (**5.14**)

TLC R_f : 0.40 (MeOH:CH₂Cl₂ 1:9);

¹H NMR (500 MHz, THF-*d*₈): δ 9.36 (bs, 5H, OH), 8.15 – 8.12 (m, 12H, 12, 14, 28, 30, 44, 46-H), 8.03 (dt, *J* = 11.0, 1.5 Hz, 2H, 6-H), 7.94 – 7.91 (m, 6H, 10, 26, 42-H), 7.82 (ddt, *J* = 10.5, 7.5, 1.5 Hz, 2H, 2-H), 7.75 (d, *J* = 8.0 Hz, 2H, 4-H), 7.57 (td, *J* = 7.5, 2.5 Hz, 2H, 3-H), 7.31 – 7.27 (m, 5H, 18, 34, 52-H), 7.08 – 7.02 (m, 10H, 20, 22, 36, 38, 50-H), 4.15 (d, *J* = 6.5 Hz, 4H, *i*Bu), 4.14 (d, *J* = 6.5 Hz, 8H, *i*Bu), 2.14 – 2.10 (m, 6H, *n*Bu), 2.07 – 1.81 (m, 8H, *n*Bu), 1.71-1.55 (m, 4H, *n*Bu), 1.49-1.35 (m, 12H, *n*Bu), 1.06 – 1.03 (m, 36H, *i*Bu), 0.91 (t, *J* = 7.0 Hz, 12H, *n*Bu);

¹³C NMR (126 MHz, THF-*d*₈): δ 166.1 (29, 45-C=O), 166.0 (13-C=O), 160.1 (21-C), 160.0 (37, 51-C), 140.0 (10-C), 139.9 (26, 42-C), 136.3 (d, *J* = 88.5 Hz, 1-C), 135.9 (4-C), 135.6 (d, *J* = 9.0 Hz, 6-C), 133.7 (Ar-C), 133.6 (Ar-C), 133.6 (Ar-C), 133.6 (Ar-C), 133.4 (Ar-C), 133.4 (Ar-C), 132.0 (d, *J* = 8.5 Hz, 2-C), 130.5 (d, *J* = 11.0 Hz, 3-C), 127.7 (20-C), 127.6 (Ar-C), 126.0 (Ar-C), 126.1 (Ar-C), 125.9 (Ar-C), 125.7 (Ar-C), 121.1 (34, 52-C), 121.0 (18-C), 92.1 (-C≡), 92.0 (-C≡), 91.9 (-C≡), 90.1 (-C≡), 89.1 (-C≡), 89.0 (-C≡), 73.0 (*i*Bu), 29.3 (d, *J* = 68.5 Hz, *n*Bu), 27.9 (*i*Bu), 24.1 (d, *J* = 14.5 Hz, *n*Bu), 23.5 (d, *J* = 4.0 Hz, *n*Bu) 20.3 (*i*Bu), 14.9 (*n*Bu);

³¹P NMR (162 MHz, CDCl₃): δ 39.4 (phosphine oxide);

FT-IR (ATR): 3144 (br), 2963, 2199, 1722, 1583, 1237, 770 $\nu_{\text{max}}/\text{cm}^{-1}$;

MS (ES+): m/z (%) = 983.4 (100) [M+2H⁺], 1965.2 (5) [M+H⁺]

5.5.2 HPLC

The samples were analyzed by reverse phase HPLC using an Agilent LC-MSD ionTrap model XCT LCMS equipment in Electrospray mode. This system is composed of a modular Agilent 1200 Series HPLC system connected to an Agilent/Bruker ionTrap model XCT with MSMS capabilities. The modular Agilent 1200 Series HPLC system is composed of a HPLC high pressure binary pump, autosampler with injector programming capabilities, column oven with 6 μL heat exchanger and a Diode Array Detector with a semimicro flow cell (6 mm path length, 1.7 μl volume) to reduce peak dispersion when using short columns as in this case. The flow-path was connected using 0.12 mm ID stainless steel tubing to minimize peak dispersion. The outlet of the Diode Array Detector flowcell is connected via a switching valve to the IonTrap, the switching valve allowing directing the first segment of the chromatography corresponding to solvent front to waste. After removing the contamination ions associated with the solvent front, the switching valve directs the solvent to the electrospray ion source. While the solvent rate of the method is 1mL/min, the ion source has a dead volume passive splitting union installed which splits the flow rate entering the ion source to <100 $\mu\text{L}/\text{min}$, the rest of the flow rate is directed to waste. This reduction in flow rate enhances the electrospray signal and reduces the contamination in the ion source.

The Electrospray was set to +ve mode. The capillary needle has an orthogonal-flow sprayer design with respect to the ion transmission. The capillary needle voltage was set to +3500 V and the end plate offset was set to -500 V. The solvent eluting from the HPLC column entering the ESI capillary needle in the Ion Source Interface was nebulised with the assistance of N₂ at 15 psi. Drying N₂ gas heated to 325 °C and flowing at 5 L/min was used for the ESI desolvation stage. The ion transport and focusing region of the LC/MSD Trap is enclosed in the vacuum manifold, formed by a rough pump and two turbopumps. The ions formed on the Ion Source Interface enter and are guided through the glass capillary, where the capillary exit is set to -178 V. The bulk of the drying gas is removed by the rough pump before the skimmer which is set to -178 V. The ions then pass into an octopole ion guide (Octopole 1 set to -12 V DC followed by Octopole 2 set to -3 V

DC set to a radio frequency of 200 Vpp) that focuses and transports the ions from a relatively high pressure position directly behind the skimmer to the focusing/exit lenses (Lens 1 set to +5 V followed by Lens 2 set to +60 V) coupling the ion transport to the ion trap. The selected ions entered the ion trap which had been set to a value of 109.9. For efficient trapping and cooling of the ions generated by the electrospray interface, helium gas is introduced into the ion trap.

The fractions were isolated using an Agilent HP-1100 preparative HPLC system. This is composed of a high pressure mixing binary pump capable of flow rates up to 50 mL/min at 400 bar back-pressure, with dual injector autosamplers loops (500 μ L and a 5 mL loop), a variable detector (190 nm to 600 nm) and a fraction collector. UV/vis absorption was measured at 290 nm (8 nm bandwidth) with reference 550 nm (100 nm bandwidth). The software for the fraction collector can be set to automatically collect on peak recognition.

5.5.3 Binding studies

NMR dilutions

^{31}P NMR dilution experiments for all oligomers were performed in a Bruker 500 MHz AVIII HD Smart Probe spectrometer at 298 K. Known volumes of the oligomers in solution at known concentrations were added to NMR tubes and the spectra were recorded ($[5.6] = 0.09 - 21.9 \text{ mM}$, $[5.7] = 0.08 - 18.9 \text{ mM}$, $[5.8] = 0.04 - 10.3 \text{ mM}$). The chemical shifts of the phosphine oxide peaks in the ^{31}P NMR spectra were monitored as a function of guest concentration and analysed using a purpose written software in Microsoft Excel. Errors were calculated as two times the standard deviation from the average value (95% confidence limit).

5.5.4 X-ray crystal structure of 5.6

Pure compound **5.6** (5 mg) was dissolved in 10% CH₂Cl₂ in MeCN (0.5 mL), and the mixture was filtered to a vial and sealed with a plastic cap with a small hole, resulting in crystallization after 10 days at room temperature. Crystals suitable for X-ray crystallography were selected using an optical microscope and examined at 180 K on a Nonius KappaCCD diffractometer using Mo K α radiation ($\lambda = 0.7107 \text{ \AA}$). All non-hydrogen atoms were refined anisotropically. Hydrogen atoms were placed in idealized positions.

Formula	C ₅₆ H ₅₅ O ₇ P		
Temperature / K	180		
Space group	C2/c		
Cell lengths / Å	a 24.5550 (0.0007)	b 11.5883 (0.0003)	c 37.9435 (0.0010)
Cell angles / °	α 90	β 108.3188 (0.0014)	γ 90
Cell volume / Å³	10249.7 (0.5)		
Z	8		
R factor	0.14		

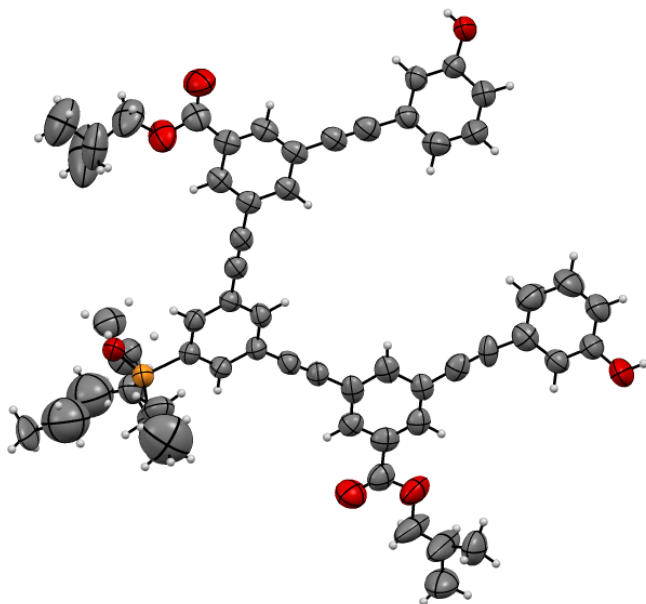


Figure 5.8: X-ray structure of **5.6** in ORTEP view (ellipsoids are drawn at 50% probability level).

5.5.5 Molecular Mechanics

Molecular mechanics calculations were performed using MacroModel version 9.8 (Schrödinger Inc.).⁵ All structures were minimized first and the minimized structures were then used as the starting molecular structures for all MacroModel conformational searches. The force field used was MMFFs as implemented in this software (CHCl₃ solvation). The charges were defined by the force field library and no cut off was used for non-covalent interactions. A Polak-Ribiere Conjugate Gradient (PRCG) was used and each minimisation was subjected to 10,000 iterations. The minima converged on a gradient with a threshold of 0.1. The sampling method was selected to be large scale low mode sampling. Conformational searches were performed from previously minimized structures using 10,000 steps. Images were created using PyMol.⁶ Calculations were performed on simplified oligomers in which the solubilising groups were changed to methyl groups in order to reduce the computational cost. The conformations shown are the lowest energy structures. Calculations were repeated three times from different starting conformations. For the DAD 3-mer, the 50 lowest energy structures were all within 0.5 kJ mol⁻¹ with none forming H-bonds. For the DAAD 4-mer, the 50 lowest energy structures were all within 3.0 kJ mol⁻¹ with the same backbone conformation forming two H-bonds in each structure. For the DAAAD 5-mer, the 50 lowest energy structures were all within 6.0 kJ mol⁻¹ with the same backbone conformation forming two H-bonds in each structure.

5.6 References

- (1) Huizenga, D. E.; Szostak, J. W. *Biochemistry* **1995**, *34* (2), 656–665.
- (2) Johnston, W. K.; Unrau, P. J.; Lawrence, M. S.; Glasner, M. E.; Bartel, D. P. *Science (80-.)* **2001**, *292* (5520), 1319–1325.
- (3) Hill, D. J.; Mio, M. J.; Prince, R. B.; Hughes, T. S.; Moore, J. S. *Chem. Rev.* **2001**, *101* (12), 3893–4012.
- (4) Stone, M. T.; Moore, J. S. *Org. Lett.* **2003**, *6* (4), 469.
- (5) MacroModel, version 9.8, Schrödinger, LLC, New York, NY, 2014..
- (6) The PyMOL Molecular Graphics System, Version 1.6 Schrödinger, L. .

5.7 Acknowledgements

I would like to thank Giulia who developed the LCMS method for the DAD oligomerisation, completed the NMR dilution experiments and modelling for the ADA 3-mer (**5.6**), ADDA 4-mer (**572**) and ADDDA 5-mer (**5.8**), and for allowing me to include the crystal structure of **5.6**.

Chapter 6

Template oligomerisation

6.1 Introduction

An important property of nucleic acids is their ability to transfer sequence information during DNA replication, transcription, and translation. Template oligomerisation is a key property of an information molecule. Homo-oligomers of this system have been shown to form duplexes with length complementary homo-oligomers bearing complementary recognition groups. Binding between oligomers and monomer units bearing complementary recognition units can be used for template oligomerisation experiments. First it is necessary to consider the theoretical aspects of the factors that will determine the efficiency of template reactions.

In an ideal situation, two molecules of a substrate **S** can react together to yield a product **P** as shown in equation 6.1. The bimolecular rate constant for this untemplated reaction is k_2 , so at an initial concentration of substrate $[S]_0$, the initial rate of the reaction without a template is given by equation 6.2.



$$\text{Rate}_{\text{Untemp}} = k_2 [S]_0^2 \quad 6.2$$

This reaction can be templated if the template **T** binds two substrate molecules and accelerates the intramolecular reaction between them. If the two binding sites are identical, both sites bind the substrate with the association constant K , to give a binary complex **S•T** and ternary complex **S•T•S**. For simplicity, statistical factors are ignored in this discussion.



For each of these equilibria, the equilibrium constant can be written as a function of the concentration of unbound substrate $[S]_{\text{free}}$, unbound template $[T]_{\text{free}}$ and the concentration of the complexes, $[S \bullet T]$ and $[S \bullet T \bullet S]$.

$$K = [S \bullet T]/([S]_{\text{free}}[T]_{\text{free}}) \quad 6.5$$

$$K^2 = [S \bullet T \bullet S]/([S]_{\text{free}}^2[T]_{\text{free}}) \quad 6.6$$

If the concentration of template used is half of the initial concentration of substrate ($2[T]_0 = [S]_0$), then the ternary complex $S \bullet T \bullet S$ becomes the dominant species when $[S]_0 \gg 1/K$.

The reaction of ternary complex $S \bullet T \bullet S$ to form the templated product $T \bullet P$ (equation 6.7) occurs with a unimolecular rate constant of k_1 . The initial rate of this intramolecular reaction ($\text{Rate}_{\text{Intra}}$) is given in equation 6.8. Rearrangement of equation 6.6 to substitute $[S \bullet T \bullet S]$ gives the rate in terms of the initial concentrations of substrate and template.



$$\text{Rate}_{\text{Intra}} = k_1[S \bullet T \bullet S] = K^2 k_1 [S]_{\text{free}}^2 [T]_{\text{free}} \quad 6.8$$

Assuming binding of the substrate to the template has no effect on the rates of any intermolecular reactions between bound or unbound substrate molecules, the overall rate of reaction with the template is the sum of the untemplated reaction and the intramolecular reaction.

$$\text{Rate}_{\text{Temp}} = \text{Rate}_{\text{Untemp}} + \text{Rate}_{\text{Intra}} \quad 6.9$$

When $[S]_0 \gg 1/K$, the substrate is fully bound to the template and the rate of the intramolecular reaction levels off at a value of $0.5k_1[S]_0$. The rate of the untemplated bimolecular reaction increases with concentration and becomes

greater than the maximum rate of the intramolecular reaction when $k_2[S]_0 > 0.5k_1$. When $[S]_0 = 0.5k_1/k_2$, the template doubles the rate of reaction, and as the reaction concentration increases, the effect of the template becomes increasingly less significant. The ratio k_1/k_2 is important when considering the effectiveness of a template and this parameter is known as the effective molarity for the templated intramolecular reaction.

$$EM^\ddagger = k_1/k_2 \quad 6.10$$

The reaction concentration must be below the effective molarity for the increase in rate due to the template to be significant. The rate enhancement can be defined as the rate of the templated reaction divided by the rate of the untemplated reaction (equation 6.11). Anderson and Anderson calculated this is equal to equation 6.12.¹

$$\text{Rate Enhancement} = \frac{\text{Rate}_{\text{Temp}}}{\text{Rate}_{\text{Untemp}}} = \frac{k_2[S]_0^2 + K^2 k_1 [S]_{\text{free}}^2 [T]_{\text{free}}}{k_2[S]_0^2} \quad 6.11$$

$$= 1 + \frac{EMK^2 [S]_{\text{free}}^4}{2[S]_0^3} \quad 6.12$$

Equation 6.12 predicts a maximum template effect at a concentration of $[S]_0 = 3/(4K)$, where the rate enhancement is $1 + 2KEM/27$. At very low concentrations, the $S \cdot T \cdot S$ complex will not be significantly populated, and very little templated reaction will occur. At very high concentrations the untemplated reaction will out-compete the templated reaction. The case described above is an ideal situation and does not consider an important factor: the template and substrates can bind to themselves, introducing additional equilibria. However, the model gives the general principles of templating reactions and can be used as a starting point to select appropriate condition for templating experiments.

According to equation 6.12, the optimum concentration for templating experiments depends only on the binding constant K , and for the phenylacetylene based information oligomers in toluene it will be approximately 1 mM ($K = 760$

M^{-1}). Assuming the kinetic EM is the same as the thermodynamic EM measured previously, the rate enhancement will be approximately a factor of 3 for this system ($KEM = 29$). For oligomerisation reactions, there are a number of possible products from intermolecular reactions in solution. A H-bonding template will bind to the growing oligomer chain fragments, increasing the rate of reaction between them. Under the correct conditions, the rate of templated reaction will be much greater than the untemplated reaction, increasing the rate of formation of the complementary product relative to the untemplated products.

6.2 Approach

Nucleic acid template oligomerisation allows sequence information to be copied, however, to simplify analysis of the product mixtures of the templating experiments on the phenylacetylene oligomers, no sequence information will be involved, and only length templating will be attempted. The oligomerisation reactions in chapters 4 and 5 resulted in a distribution of products over a range of oligomer lengths. Addition of an appropriate template to the reaction mixture should accelerate the formation of the complementary product, resulting in a change of the product distribution (**Figure 6.1**).

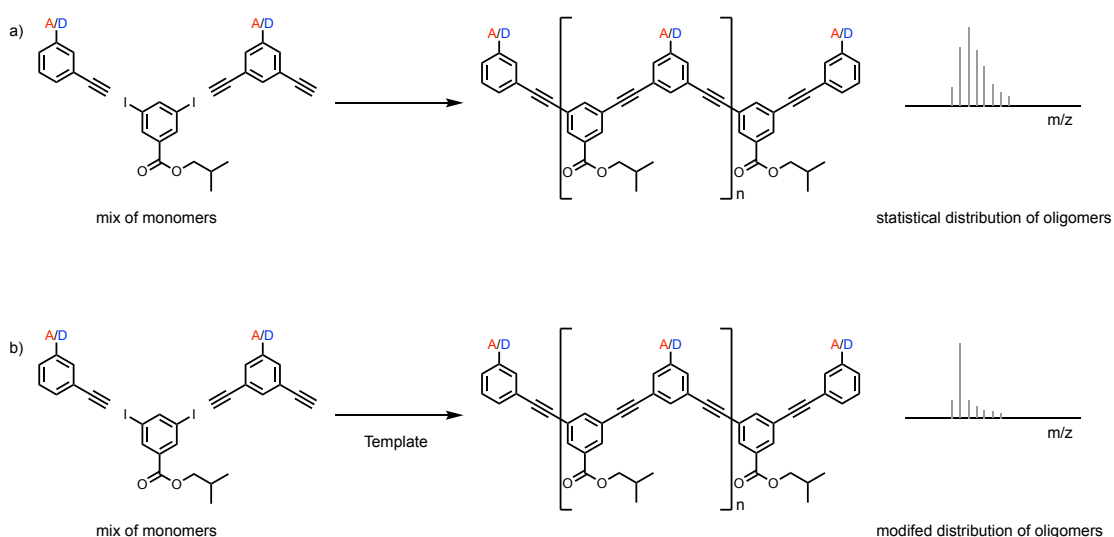


Figure 6.1: (a) Oligomerisation leads to a statistical distribution of products, b) addition of an appropriate template can alter this distribution to increase the formation of the complementary product.

The oligomerisations to produce DA_nD oligomers were used for the first templating experiment. With homo-oligomer templates, there would be no selectivity for locating chain stoppers at the terminal recognition groups of the template. This would template the formation of all products up to and including the length of the template (**Figure 6.2a**). Using a template with terminal recognition groups that are different to the internal recognition groups should template termination of the product at the correct length (**Figure 6.2b**).

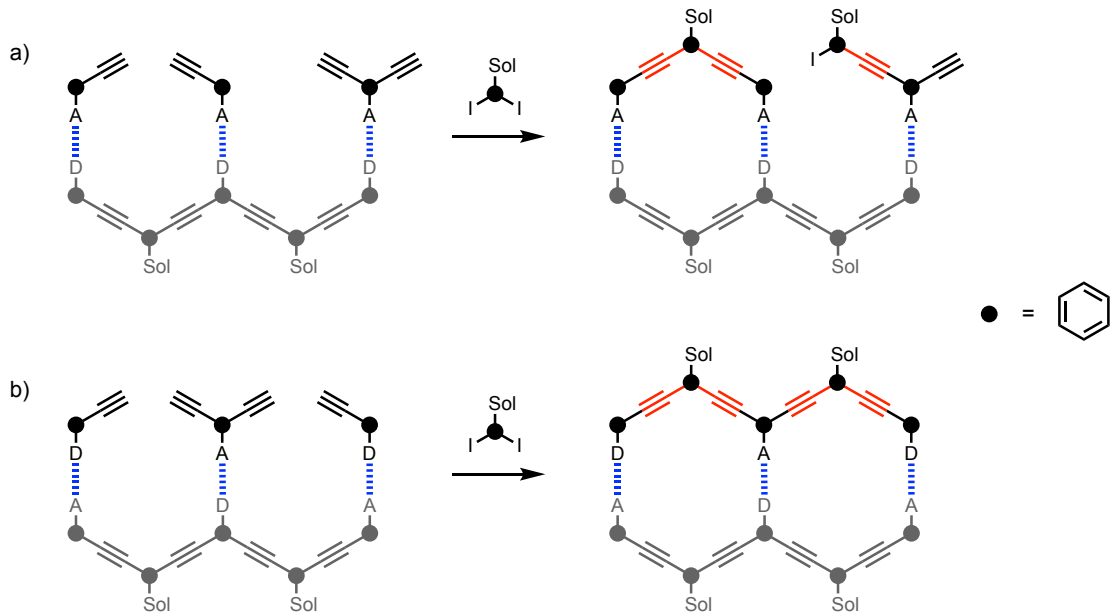
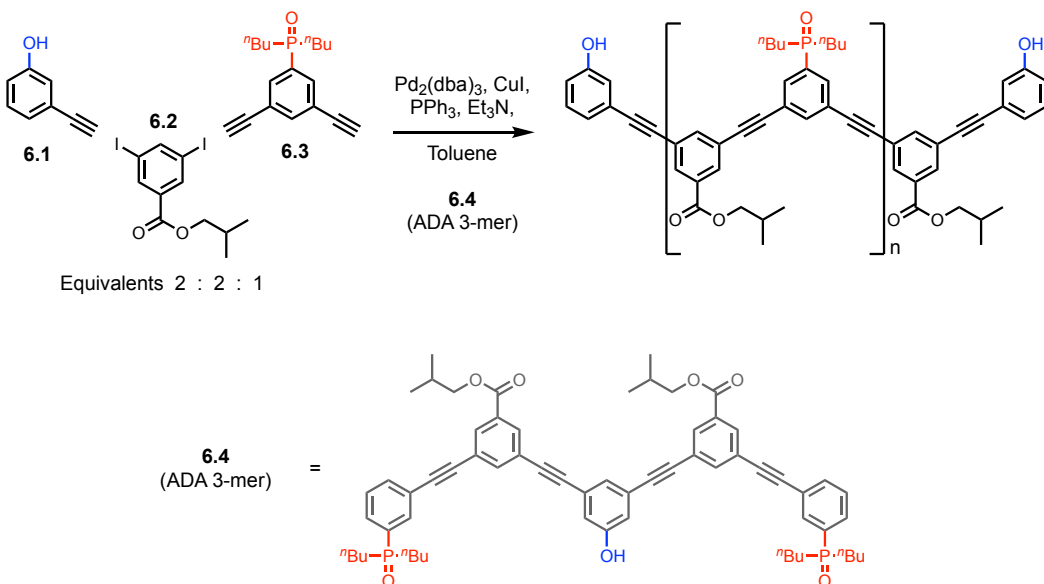


Figure 6.2: Homo-oligomer templates (grey) are likely to promote undesired side reactions by templating the coupling of two terminal recognition groups. b) Mixed sequence templates (grey) allow precise alignment of the recognition modules and should template formation of a single product.

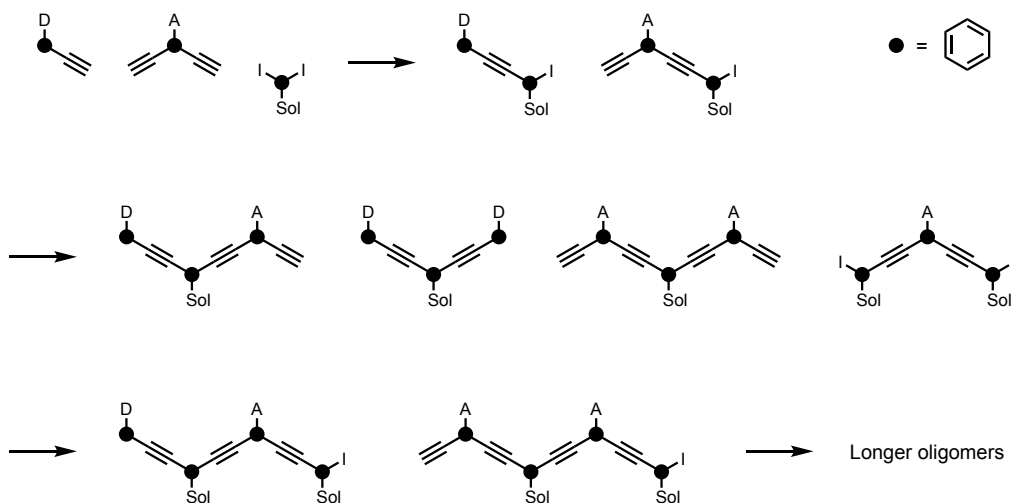
6.3 Results and discussion

6.3.1 Template reaction using mixed sequence oligomers

The ADA 3-mer (**6.4**) was chosen as the template for the DA_nD oligomerisation reaction (**Scheme 6.1**). With this experiment the first reaction that must occur is intermolecular (**Scheme 6.2**). The calculated concentration for maximum rate enhancement was 1 mM, but this may limit the background reaction rate. A reaction concentration of 10 mM was used as a compromise. This concentration is lower by a factor of 10 when compared to previously completed oligomerisation reactions. Throughout this chapter, the concentration used in the oligomerisation reactions will be defined as the maximum concentration of bonds that could be formed if the reaction went to completion. For example, for 50 mM of solubilising module, 100 mM of bonds would be formed. The catalyst loading is defined relative to the total number of bonds that could be formed if the reaction went to completion. The recognition modules (**6.1** and **6.3**), must first react with the solubilising module (**6.2**) via an intermolecular process. The products can react with more modules or with each other to form longer oligomers. The limited amount of the template available from the preparative oligomerisation reaction in chapter 5 placed limits on the scale at which the reaction was carried out.



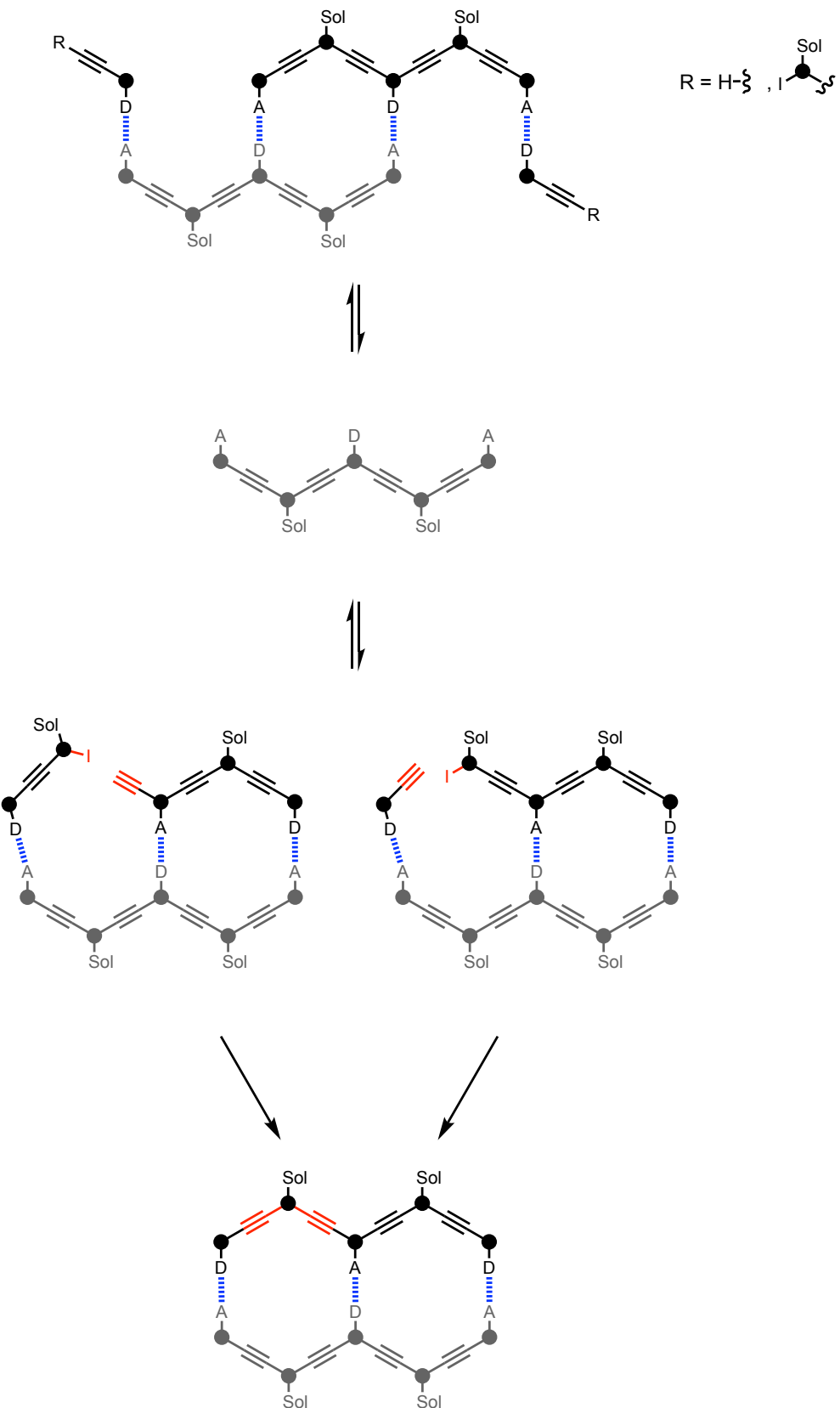
Scheme 6.1: Template oligomerisation of phosphine oxide recognition modules with terminal phenol recognition modules using ADA (**6.4**) as a template.



Scheme 6.2: Intermolecular reactions in solution form the oligomers required for the templating reaction to occur.

In solution, the ADA template will self-associate with an association constant similar to the 2-mer binding constants in toluene measured in chapter 4 ($K \sim 10^4 \text{ M}^{-1}$) (**Scheme 6.3**). For a 10 mM reaction, the template is used at a concentration of 2.5 mM. At this concentration the self-associated state will be highly populated. Under these conditions the template dimer will also form complexes with the donor module ($K \sim 10^3 \text{ M}^{-1}$). Any DA 2-mers that are formed in the oligomer reaction illustrated in **Scheme 6.2** will be able to disrupt the

template self-association through competition. The **DA•T** association constant should be very similar to the template self-association constant since both complexes have two phenol-phosphine oxide H-bonds. The free A recognition site in the **DA•T** complex can form a H-bond to a D module, and with correct Sonogashira functionalities in place, the templated reaction would form the **DAD•T** complex. Other equilibria and reaction pathways that could lead to unwanted products are possible but are not shown.



Scheme 6.3: Template synthesis of DAD on an ADA template (grey). Non-covalent template dimerisation competes with formation of the key ternary complex, where the intramolecular coupling reaction takes place.

The previous preparative DA_nD oligomerisation described in chapter 5 which was carried out with a reaction concentration of 100 mM bonds formed, and LCMS analysis identified products up to the 6-mer (**Figure 6.3a**). When the oligomerisation was repeated at 10 mM bonds formed, no products were observed (**Figure 6.3b**). The reaction mixture was analysed every 24 hours for 72 hours, and no changes were observed even with longer reaction times. Some small peaks were observed by UV detection at 290 nm, but these could not be identified by MS even with high injection volumes. The retention times for these small peaks matched impurities also observed in the 100 mM bonds formed oligomerisation (**Figure 6.3a**), suggesting they may be decomposition products or undesired side-products. The 10 mM bonds formed reaction containing the template looked very similar to without the template (**Figure 6.3c**). The template peak was very large and confirmed by MS. More impurity peaks were observed, matching those in the 100 mM bonds formed oligomerisation (**Figure 6.3a**). It was not possible to determine if the lack of reaction was caused by the low concentration or practical difficulties in performing the reaction on such a small scale.

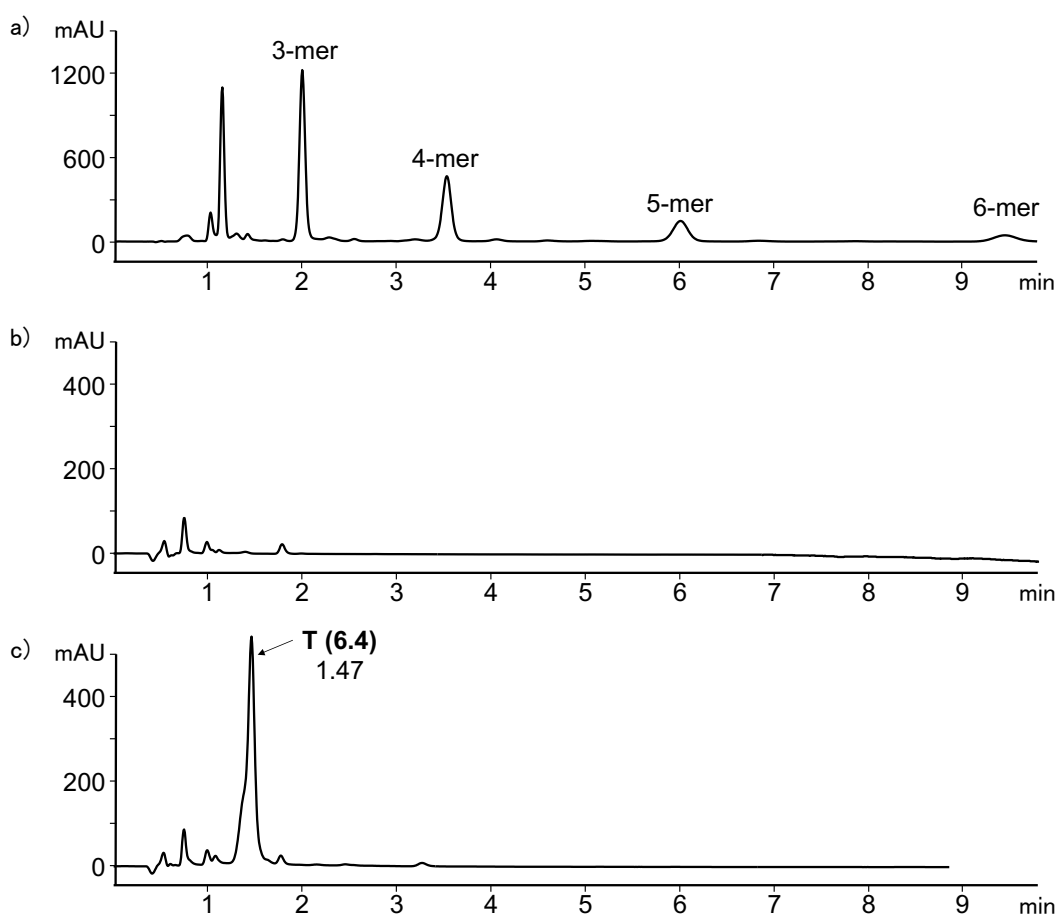
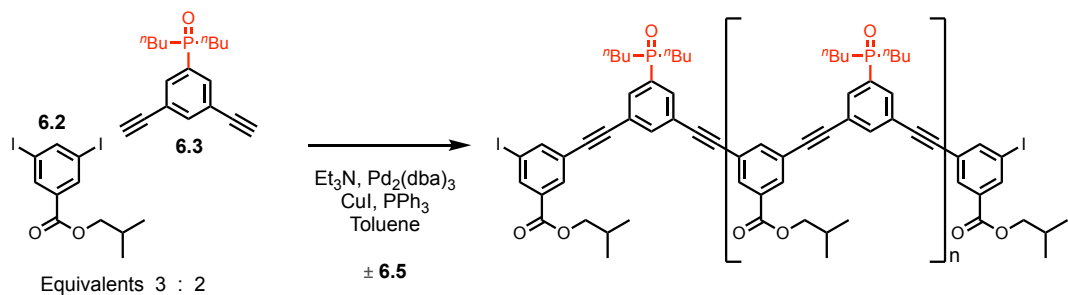


Figure 6.3: LCMS analysis of DA_nD oligomerisations in toluene after 72 hours. (a) Preparative oligomerisation carried out at 100 mM bonds formed and catalyst loading of 2%, (b) Untempered reaction carried out at 10 mM bonds formed and a catalyst loading of 4%, and (c) template reaction carried out at 10 mM bonds formed and a catalyst loading of 4% with ADA 3-mer (**6.4**) as a template at 2.5 mM, using a Hichrom C₈C₁₈ column (50 x 4.6 mm, 5 µm particle size) with a water/THF (0.1% formic acid) solvent system (THF: 60% 3 mins, 60-65% 1 min, 65% 2 mins, 65-70% 2 mins, 100% 2 mins) at a flow rate of 1 mL min⁻¹. UV/vis absorption was measured at 290 nm. Template peak labelled with retention time in minutes.

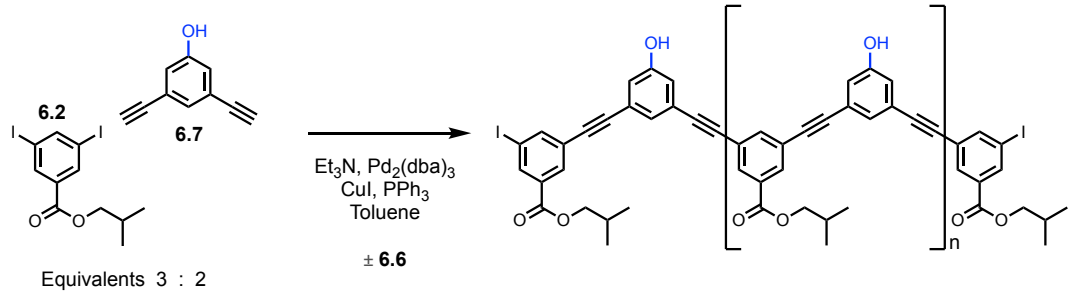
6.3.2 Template reaction using homo-oligomers

To allow an increase in reaction concentration, the template was changed to either the DD 2-mer (**6.5**) or the AA 2-mer (**6.6**). These compounds were synthesised stepwise in chapter 3 on a larger scale than the longer oligomers

synthesised in chapter 4. It should be possible to use these compounds to template the oligomerisation of the bis-acetylene recognition modules by using an excess of the solubilising module as chain stoppers. Oligomerisation reactions were set up, each with and without a template. Oligomerisation of the phosphine oxide recognition module was carried out with 1.5 equivalents of the solubilising module at a concentration of 30 mM bonds formed and catalyst loading of 4% (**Scheme 6.4**). Oligomerisation of the phenol recognition module was carried out using the same conditions (**Scheme 6.5**). With 1.5 bonds formed per solubilising module, and a concentration of 40 mM bonds formed.



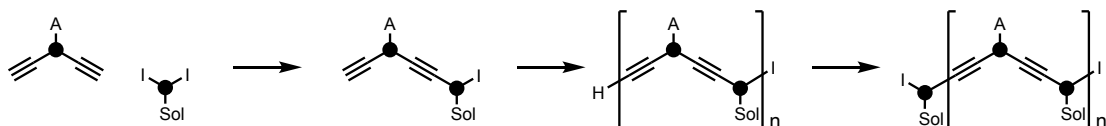
Scheme 6.5: Template oligomerisation of the phosphine oxide recognition module using the DD 2-mer (**6.5**) as a template.



Scheme 6.6: Template oligomerisation of the phenol recognition module using the AA 2-mer (**6.6**) as a template.

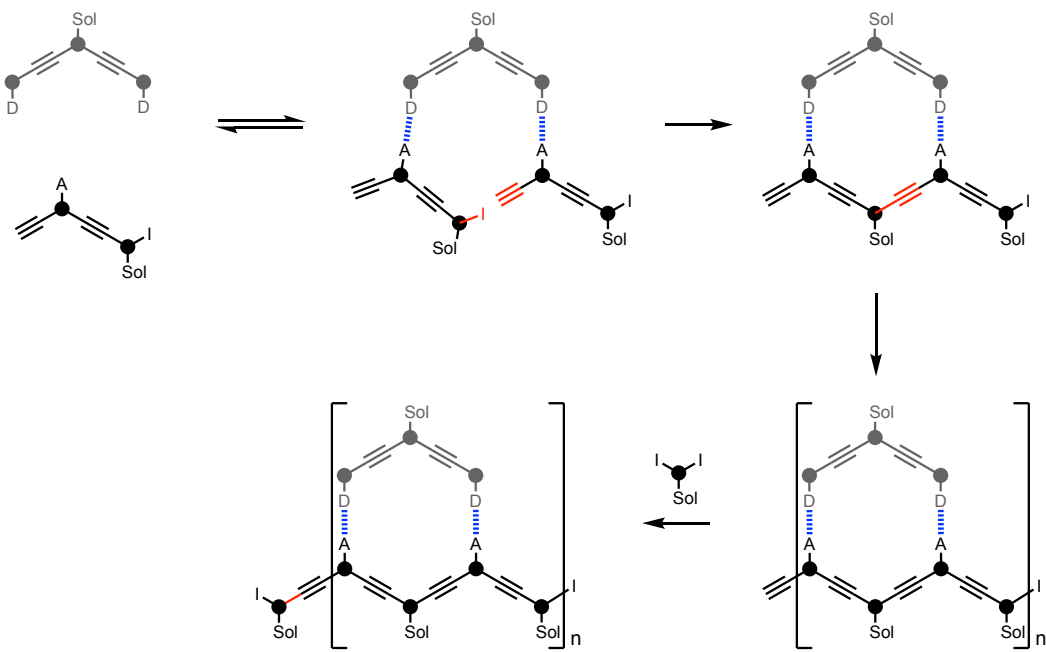
These reactions have the advantage of more template being available, allowing the reaction to be carried out at a higher concentration. A higher concentration should increase the rate of the intermolecular reactions required for the formation of precursor oligomers, but a higher reaction concentration would also increase the background reaction rate relative to the templated rate, reducing any template effect.

In solution, the recognition module must first react with the solubilising module (**Scheme 6.7**). The product can then react to form oligomers, which will react with the excess solubilising module to form oligomers with terminal solubilising modules. The average length will be defined by the stoichiometry, so with a 3:2 ratio of modules the major product should be the 2-mer.



Scheme 6.7: Intermolecular reactions in solution between the modules form the oligomers required for the templating reaction to occur.

When the reaction is completed with the DD template in solution, the acceptor recognition modules should bind strongly to it (**Scheme 6.8**). The alignment of reaction sites will increase the reaction rate of 2-mer formation. Finally, reaction with excess solubilising module will form the 2-mer with terminal solubilising modules.



Scheme 6.8: The DD template (grey) can form a complex with two acceptor 1-mers, leading to template formation of the AA 2-mer. The terminal acetylene can react with a solubilising module to form the final templated product.

The results are shown in **Figure 6.4**. Other than the starting materials and catalyst, no other species were identified by LCMS. The peaks at 2.9 minutes and 4.3 minutes in the acceptor oligomerisation with the DD 2-mer template (**6.5**) (**Figure 6.4b**) match the retention times for undesired products observed in preparative 100 mM bonds formed oligomerisations (**Figure 6.3a**). The only difference between the reactions with and without the template is the large peak due to the template. The reactions were monitored over 72 hours, and no changes observed with longer reaction times.

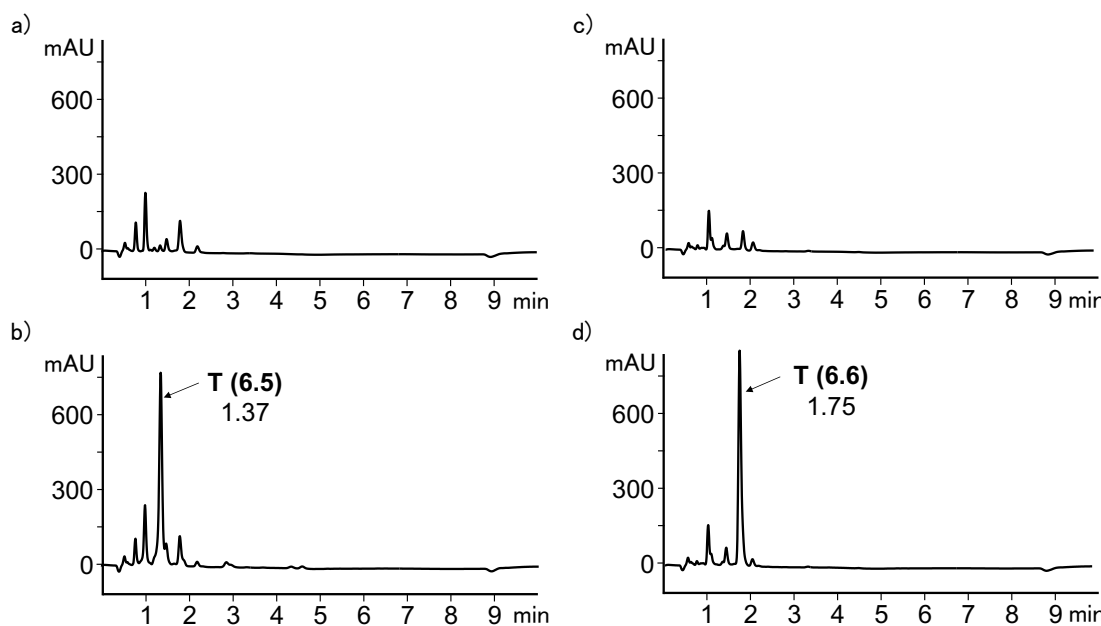


Figure 6.4: LCMS analysis of template oligomerisations after 72 hours performed at 40 mM bonds formed in toluene with a 4% catalyst loading: (a) untemplated acceptor oligomerisation, (b) acceptor oligomerisation with 10 mM DD 2-mer (**6.5**) as a template, (c) untemplated donor oligomerisation and (d) donor oligomerisation with 10 mM AA 2-mer (**6.6**) as a template, using a Hichrom C₈C₁₈ column (50 x 4.6 mm, 5 µm particle size) with a water/THF (0.1% formic acid) solvent system (THF: 60% 3 mins, 60-65% 1 min, 65% 2 mins, 65-70% 2 mins, 100% 2 mins) at a flow rate of 1 mL min⁻¹. UV/vis absorption was measured at 290 nm. Template peaks are labelled with retention times in minutes.

The concentration of catalyst was increased by a factor of ten to a 40% catalyst loading in an attempt to increase the extent of oligomerisation. The only change to the LCMS trace was an increase in the sizes of the peaks due to the catalyst (**Figure 6.5**). In the donor oligomerisation reactions, there were small peaks at 3.4 minutes and 4.6 minutes. These compounds could not be identified by MS, and there was no difference between the untemplated and templated reactions. These reactions were completed at a concentration just below half of preparative 100 mM bonds formed oligomerisations and with a higher catalyst concentration. This would suggest the problem is caused by practical difficulties, most likely performing the reaction in anaerobic conditions on a 1 mL scale. Oxygen can cause Glaser couplings and oxidise the catalysts, preventing the desired reaction.

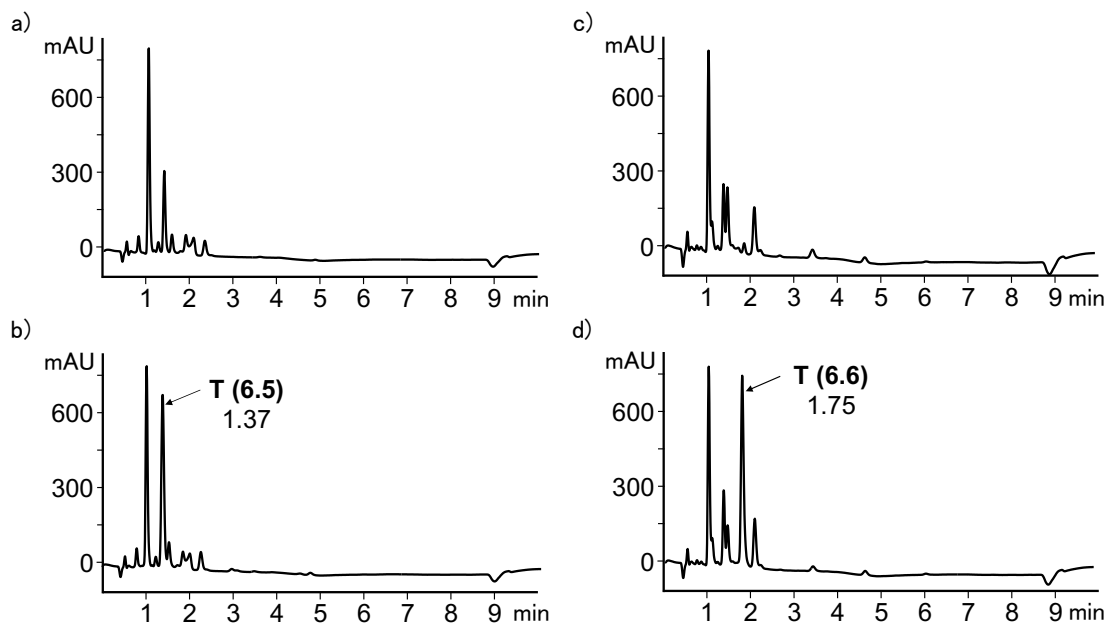


Figure 6.5: LCMS analysis of template oligomerisations after 72 hours performed at a concentration of 40 mM bonds formed in toluene with a 40% catalyst loading: (a) untemplated acceptor oligomerisation, (b) acceptor oligomerisation with 10 mM DD 2-mer (**6.5**) as a template, (c) untemplated donor oligomerisation and (d) donor oligomerisation with 10 mM AA 2-mer (**6.6**) as a template, using a Hichrom C₈C₁₈ column (50 x 4.6 mm, 5 µm particle size) with a water/THF (0.1% formic acid) solvent system (THF: 60% 3 mins, 60-65% 1 min, 65% 2 mins, 65-70% 2 mins, 100% 2 mins) at a flow rate of 1 mL min⁻¹. UV/vis absorption was measured at 290 nm. Template peaks are labelled with retention times in minutes.

6.4 Conclusions

Two types of template oligomerisation reactions were completed using the ADA 3-mer, AA 2-mer or DD 2-mer as a template. The ADA 3-mer was used to template length in an oligomerisation at a concentration of 10 mM on a 1 mL scale, but no reaction was observed by LCMS analysis. This oligomerisation was previously completed successfully at 100 mM. The reaction concentration and volume were limited by the amount of template, and it was not possible to determine the reason for lack of reaction.

The AA and DD 2-mers were used as templates in oligomerisations at concentrations of 40 mM on a 1 mL scale, and again no oligomerisation was observed. Considering the reaction concentration was just below half the concentration of successful oligomerisations, it is likely the problems stem from keeping the small-scale reactions anaerobic.

6.5 Experimental

6.5.1 Template reactions

All the reagents were obtained from commercial sources (Sigma-Aldrich, Alfa Aesar, Fisher Scientific and Fluorochem) and were used without further purification. Thin layer chromatography was carried out using with silica gel 60F (Merck) on aluminium. Compounds **6.5** and **6.6** were synthesised in chapter 3. Compounds **6.2** and **6.3** were synthesised in chapter 4. Compound **6.4** was synthesised in chapter 5.

DA_nD oligomerisation with an ADA 3-mer (5.6) template

Reactant solution

6.1 (4.73 mg, 40.0 µmol), **6.3** (5.73 mg, 20.0 µmol) and **6.2** (17.2 mg, 40.0 µmol) were placed in a flask and degassed with N₂ for 30 minutes. Degassed toluene (5 mL) was added.

Catalyst solution

Pd₂(dba)₃ (14.7 mg, 16.0 µmol) and CuI (3.00 mg, 16.0 µmol) and PPh₃ (21.0 mg, 80.0 µmol) were placed in a flask and degassed with N₂ for 30 minutes. Degassed Et₃N (167 µL, 1.20 mmol) and degassed toluene (50 mL) were added.

Non-templated reaction

Reactant solution (0.5 mL) and catalyst solution (0.5 mL) were transferred to a degassed flask and the reaction was stirred overnight at room temperature, in the dark, under N₂.

Templated reaction

6.4 (2.06 mg, 2.00 µmol) was placed in a flask and degassed with N₂ for 15 minutes. Reactant solution (0.5 mL) and catalyst solution (0.5 mL) were transferred to a degassed flask and the reaction was stirred overnight at room temperature, in the dark, under N₂.

An aliquot of each reaction solution (50 µL) was diluted with EtOH up to 1 mL, filtered and analysed by HPLC using a Hichrom C₈C₁₈ column (50 x 4.6 mm, 5 µm particle size) with a water/THF (0.1% formic acid) solvent system (THF: 60% 3 mins, 60-65% 1 min, 65% 2 mins, 65-70% 2 mins, 100% 2 mins) at a flow rate of 1 mL min⁻¹. UV absorption measured as 290 nm.

Acceptor oligomerisation with DD (**6.5**) as a template

Catalyst solution

Pd₂(dba)₃ (7.33 mg, 80.0 µmol) and CuI (1.50 mg, 80.0 µmol) and PPh₃ (10.5 mg, 40.0 µmol) were placed in a flask and degassed with N₂. Degassed Et₃N (83.2 µL, 1.20 mmol) and degassed toluene (10 mL) were added.

Non-templated reaction

6.3 (5.73 mg, 20.0 µmol) and **6.2** (12.9 mg, 30.0 µmol) were placed in a flask and degassed with N₂ for 30 minutes. Catalyst solution (1 mL) was transferred to the flask and the reaction was stirred overnight at room temperature, in the dark, under N₂.

Templated reaction

6.3 (5.73 mg, 20.0 µmol) and **6.2** (12.9 mg, 30.0 µmol) and **6.5** (4.64 mg, 10.0 µmol) were placed in a flask and degassed with N₂ for 30 minutes. Catalyst solution (1 mL) was transferred to the flask and the reaction was stirred overnight at room temperature, in the dark, under N₂.

An aliquot of each reaction solution (50 µL) was diluted with EtOH up to 1 mL, filtered and analysed by HPLC using a Hichrom C₈C₁₈ column (50 x 4.6 mm, 5 µm particle size) with a water/THF (0.1% formic acid) solvent system (THF: 60% 3 mins, 60-65% 1 min, 65% 2 mins, 65-70% 2 mins, 100% 2 mins) at a flow rate of 1 mL min⁻¹. UV absorption measured as 290 nm.

Donor oligomerisation with AA (**6.6**) as a template

Catalyst solution

Pd₂(dba)₃ (7.33 mg, 80.0 µmol) and CuI (1.50 mg, 80.0 µmol) and PPh₃ (10.5 mg, 40.0 µmol) were placed in a flask and degassed with N₂. Degassed Et₃N (83.2 µL, 1.20 mmol) and degassed toluene (10 mL) were added.

Non-templated reaction

6.7 (5.73 mg, 20.0 µmol) and **6.2** (12.9 mg, 30.0 µmol) were placed in a flask and degassed with N₂ for 30 minutes. Catalyst solution (1 mL) was transferred to the flask and the reaction was stirred overnight at room temperature, in the dark, under N₂.

Templated reaction

6.7 (2.84 mg, 20.0 µmol) and **6.2** (12.9 mg, 30.0 µmol) and **6.6** (7.53 mg, 10.0 µmol) were placed in a flask and degassed with N₂ for 30 minutes. Catalyst solution (1 mL) was transferred to the flask and the reaction was stirred overnight at room temperature, in the dark, under N₂.

An aliquot of each reaction solution (50 µL) was diluted with EtOH up to 1 mL, filtered and analysed by HPLC using a Hichrom C₈C₁₈ column (50 x 4.6 mm, 5 µm particle size) with a water/THF (0.1% formic acid) solvent system (THF: 60% 3 mins, 60-65% 1 min, 65% 2 mins, 65-70% 2 mins, 100% 2 mins) at a flow rate of 1 mL min⁻¹. UV absorption measured as 290 nm.

6.5.2 HPLC

The samples were analyzed by reverse phase HPLC using an Agilent LC-MSD ionTrap model XCT LCMS equipment in Electrospray mode. This system is composed of a modular Agilent 1200 Series HPLC system connected to an Agilent/Bruker ionTrap model XCT with MSMS capabilities. The modular Agilent 1200 Series HPLC system is composed of a HPLC high pressure binary pump, autosampler with injector programming capabilities, column oven with 6 µL heat exchanger and a Diode Array Detector with a semimicro flow cell (6 mm pathlength, 1.7 µl volume) to reduce peak dispersion when using short columns as in this case. The flow-path was connected using 0.12 mm ID stainless steel tubing to minimize peak dispersion. The outlet of the Diode Array Detector flowcell is connected via a switching valve to the IonTrap, the switching valve allowing to direct the first segment of the chromatography corresponding to solvent front to waste. After removing the contamination ions associated with the solvent front, the switching valve directs the solvent to the electrospray ion source. While the solvent rate of the method is 1mL/min, the ion source has a dead volume passive splitting union installed which splits the flowrate entering the ion source to <100 µL/min, the rest of the flowrate is directed to waste. This reduction in flow rate enhances the electrospray signal and reduces the contamination in the ion source.

The Electrospray was set to +ve mode. The capillary needle has an orthogonal-flow sprayer design with respect to the ion transmission. The capillary needle voltage was set to +3500 V and the end plate offset was set to -500 V. The solvent eluting from the HPLC column entering the ESI capillary needle in the Ion Source Interface was nebulised with the assistance of N₂ at 15 psi. Drying N₂ gas heated to 325 °C and flowing at 5 L/min was used for the ESI desolvation stage. The ion transport and focusing region of the LC/MSD Trap is enclosed in the vacuum manifold, formed by a rough pump and two turbopumps. The ions formed on the Ion Source Interface enter and are guided through the glass capillary, where the capillary exit is set to -178 V. The bulk of the drying gas is removed by the rough pump before the skimmer which is set to -178 V. The ions then pass into an

octopole ion guide (Octopole 1 set to -12 V DC followed by Octopole 2 set to -3 V DC set to a radio frequency of 200 Vpp) that focuses and transports the ions from a relatively high pressure position directly behind the skimmer to the focusing/exit lenses (Lens 1 set to +5 V followed by Lens 2 set to +60 V) coupling the ion transport to the ion trap. The selected ions entered the iontrap which had been set to a value of 109.9. For efficient trapping and cooling of the ions generated by the electrospray interface, helium gas is introduced into the ion trap.

6.6 References

- (1) Anderson, S.; Anderson, H. In *Templated Organic Synthesis*; Diederich, F., Stang, P. J., Eds.; Wiley-VCH, 2000; pp 1–38.

Appendix I

Fitting analysis

I.1 Fitting from chapter 3

The titration data was used to determine the association constant, K_a , using the following equations:

$$K_a = \frac{[H \bullet G]}{[H][G]}$$

$$[H]_{total} = [H] + [H \bullet G]$$

$$[G]_{total} = [G] + [H \bullet G]$$

$$\frac{[H \bullet G]}{[H]_{total}} = \frac{\partial_{\text{measured}} - \partial_{\text{free}}}{\partial_{\text{bound}} - \partial_{\text{free}}}$$

I.1.1 Titration 1:1 fitting for complex 3.18•3.17 (CDCl₃, 298 K)

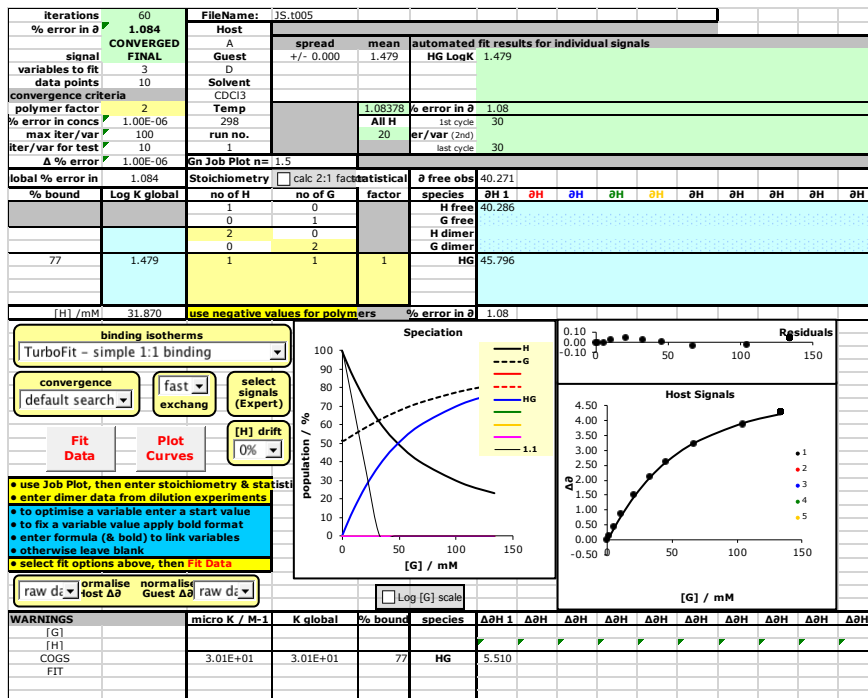


Figure I.1: H = 31.9 mM, G = 229 mM

I.1.2 Titration 1:1 fitting for complex 3.20•3.19 (CDCl₃, 298 K)

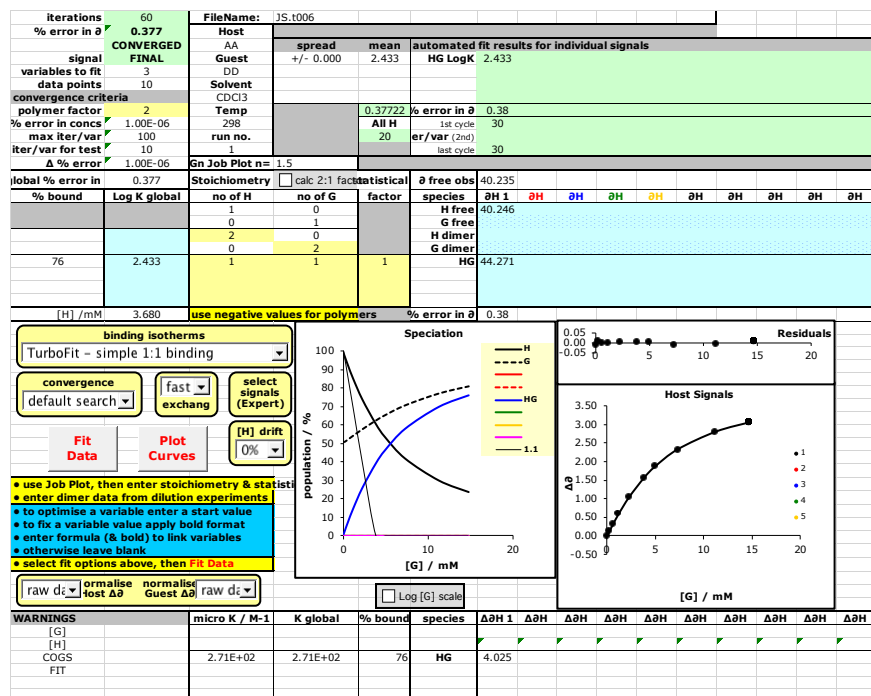


Figure I.2: H = 3.68 mM, G = 24.7 mM

I.1.3 Dilution dimerization fitting for complex 3.22•3.22 (CDCl₃, 298 K)

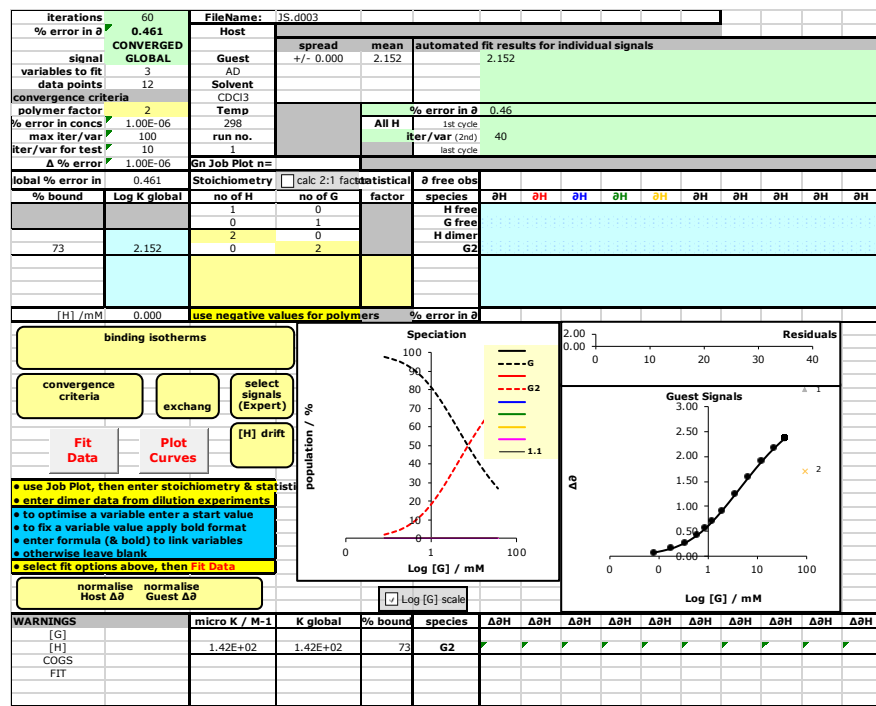


Figure I.3

I.2 Fitting from chapter 4

I.2.1 Titration 1:1 fitting for complex 3.18•3.17 (toluene-*d*₈, 298 K)

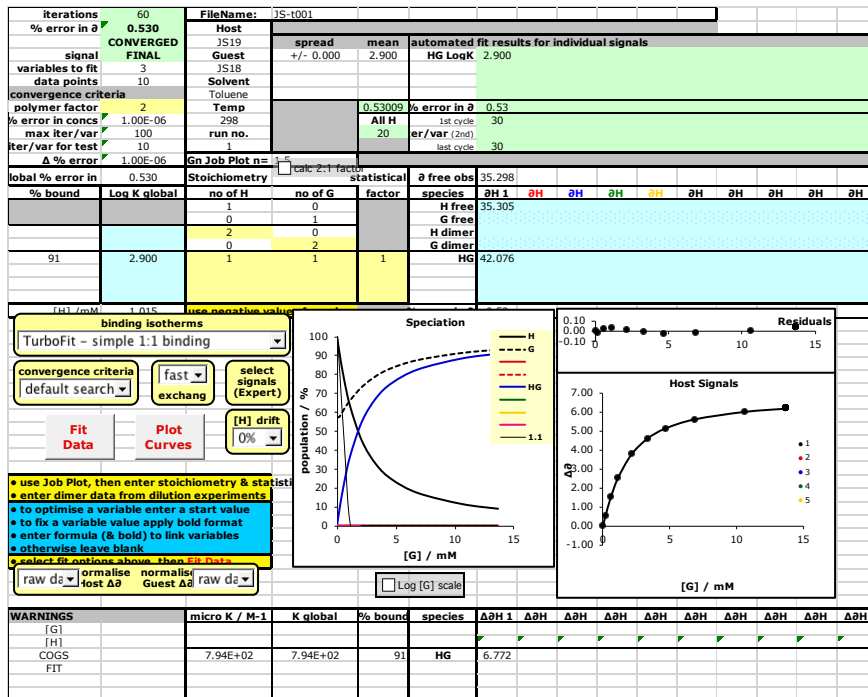


Figure I.4: H = 1.02 mM, G = 23.2 mM

I.2.2 Titration 1:1 fitting for complex 3.20•3.19 (toluene-*d*₈, 298 K)

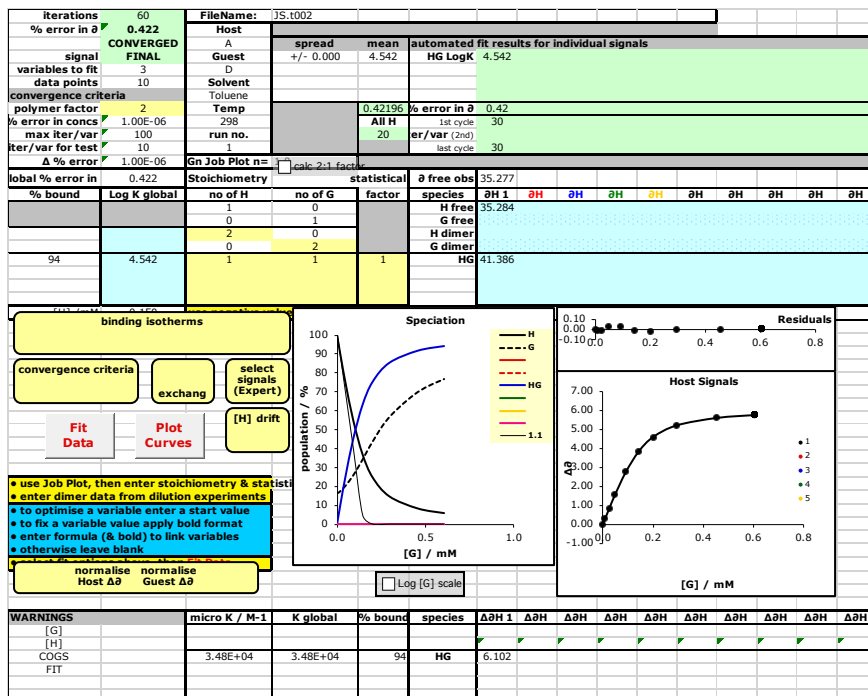


Figure I.5: H = 0.15 mM, G = 1.00 mM

I.2.3 Denaturation fitting for complex 3.20•3.19 (toluene- d_8 , 298 K)

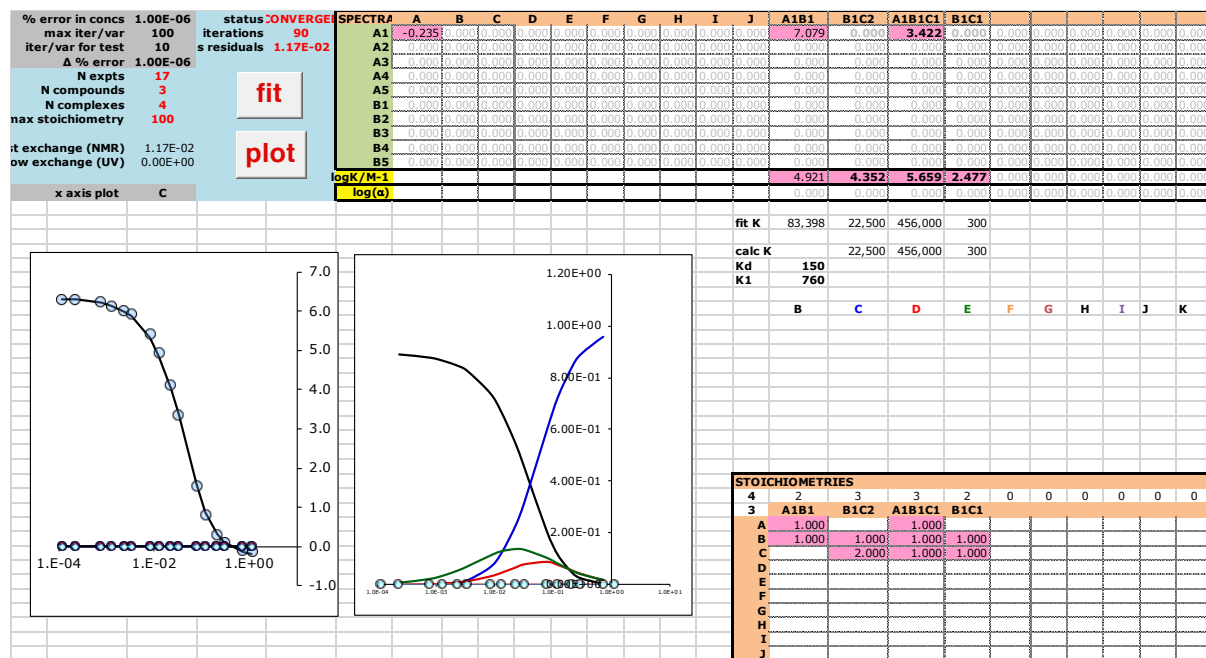


Figure I.5: H = 1.0 mM, G = 1.0 mM

I.2.4 Denaturation fitting for complex 4.11•3.15 (toluene- d_8 , 298 K)

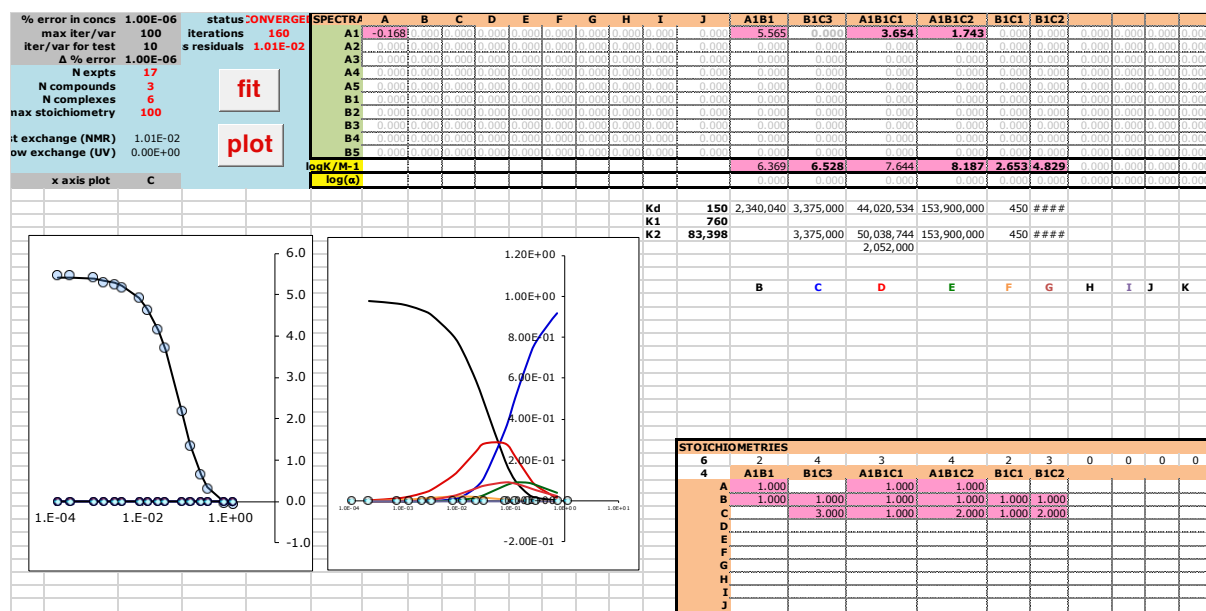


Figure I.7: H = 1.0 mM, G = 1.0 mM

I.2.5 Denaturation fitting for complex 4.12•3.16 (toluene- d_8 , 298 K)

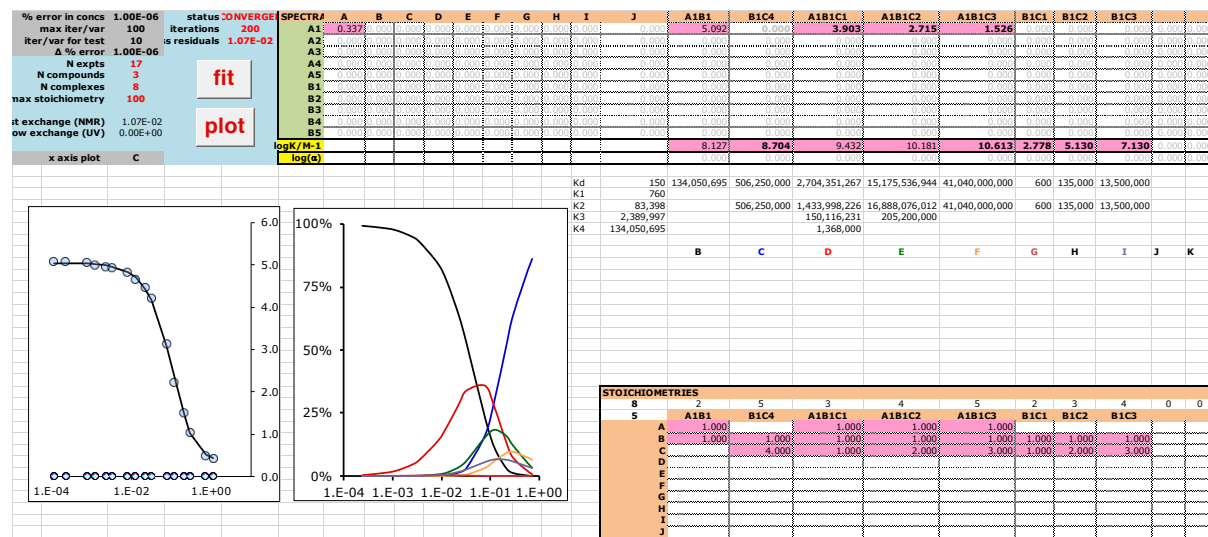


Figure I.8: H = 1.0 mM, G = 1.0 mM

I.3 Fitting from chapter 5

I.3.1 Dilution dimerization fitting for complex 5.6•5.6 (CDCl₃, 298 K)

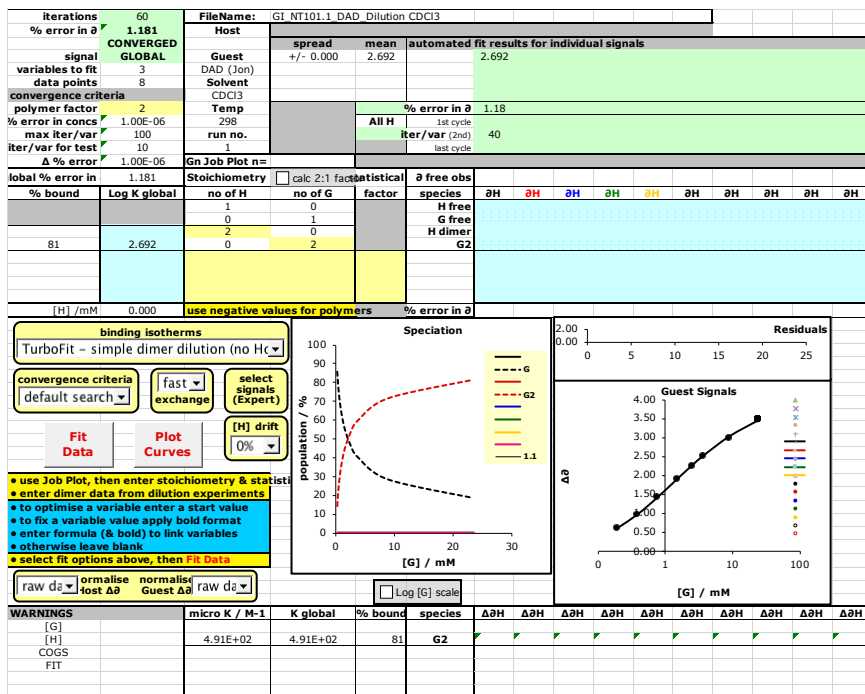


Figure I.9

I.3.1 Dilution dimerization fitting for complex 5.7•5.7 (CDCl₃, 298 K)

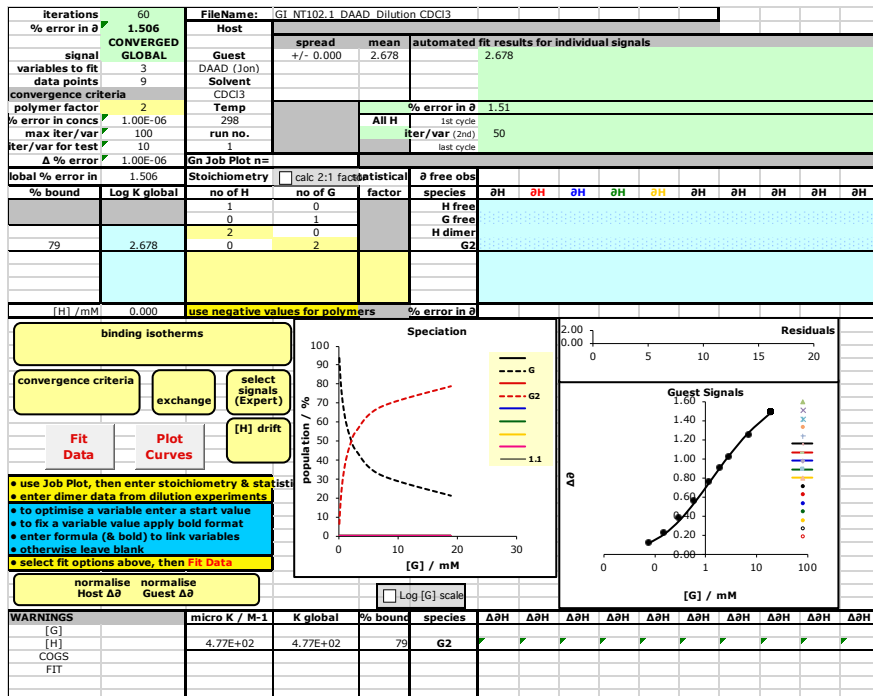


Figure I.10

I.3.1 Dilution dimerization fitting for complex 5.8•5.8 (CDCl_3 , 298 K)

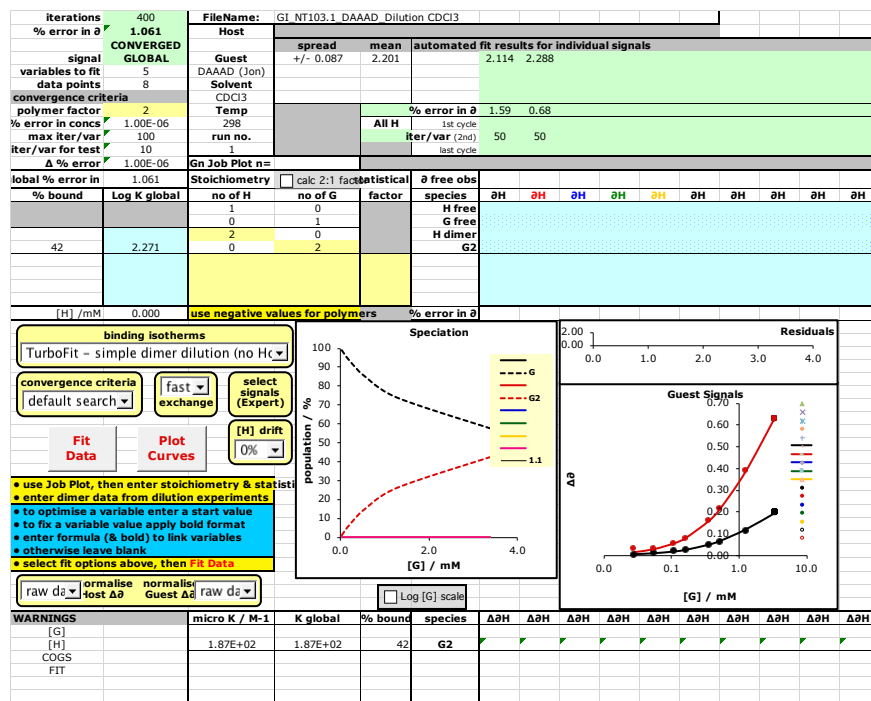


Figure I.11